BMR JOURNAL

OF AUSTRALIAN GEOLOGY & GEOPHYSICS

VOLUME 13 NUMBER 2

1992

BMR JOURNAL

OF AUSTRALIAN GEOLOGY & GEOPHYSICS

VOLUME 13 NUMBER 2 JULY 1992

CONTENTS

Editor, BMR Journal: Bernadette Hince

Cover design by Saimonne Bissett

Figures prepared by BMR Cartographic Services Unit unless otherwise indicated.

AUSTRALIAN GOVERNMENT PUBLISHING SERVICE CANBERRA 1992

ISSN 0312-9608

Month of issue: July

Subscriptions to the BMJ Journal are available through the BMR (GPO Box 378, Canberra ACT 2601; tel. (06) 249 9642, fax (06) 257 6466) or through the Australian Government Publishing Service (Mail Order Sales, GPO Box 84, Canberra ACT 2601; tel. (06) 295 4485).

Other matters concerning the Journal should be sent to the Editor, BMR Journal.

Typeset in Australia by MultiMedia Typesetting and Graphic Design, Fyshwick, A.C.T.

Printed for AGPS by National Capital Printing, Fyshwick, A.C.T.

BMR Journal of Australian Geology & Geophysics, 13, 87-92

Glacially grooved surfaces in the Grant Group, Grant Range, Canning Basin and the extent of Late Palaeozoic Pilbara ice sheets

P.E. O'Brien[1] & N. Christie-Blick[2]

Grooved surfaces in Late Palaeozoic Grant Group rocks in the central Grant Range were cut by glacial ice. The orientation of the grooves and small step-like sedimentary structures on the surfaces indicate ice motion from the south-southeast. Pebbles of banded iron formation in marine diamictites associated with the surfaces suggest that the ice originated in the Pilbara Block and extended 400 km into the Canning Basin. The geometry of facies associated with the grooves indicates that they were cut at or near the grounding line of an ice shelf in a marine embayment occupying the Fitzroy Trough. These surfaces confirm the existence of large continental ice sheets in Western Australia during the Late Palaeozoic glaciation.

Introduction

The Canning Basin of Western Australia (Fig. 1) contains extensive deposits formed during the Permo-Carboniferous glaciation. As with many glacially fed basins, the bulk of the Grant Group is not diamictite deposited directly by glacial ice, but is predominantly thick sandstone units variously described as glaciofluvial, glaciomarine or glaciolacustrine (Towner & Gibson, 1983). Diamictites resting on glacially striated pavements are known only from the laterally equivalent Paterson Formation on the southern edge of the basin (Fig. 1; Towner & others, 1976; Jackson & van der Graaff, 1981). Bedded mudstone, with striated boulders and pebbles, is more widespread (Crowe & others, 1978). Previous field work has produced no evidence of grounded ice in the major depocentres, hence workers reconstructing Late Palaeozoic palaeogeography have inferred that grounded glacial ice extended only a short distance from the southern basin margin (Fig. 1; Crowell & Frakes, 1971a,b; BMR Palaeogeographic Group, 1990). However, Redfern (1991) argued that glacial ice eroded Palaeozoic carbonates and deposited subglacial and supraglacial diamictites on the Barbwire Terrace, raising the possibility that thick ice extended 400 km north from the Pilbara or that local ice masses grew on the Broome Arch and adjoining terraces (Fig. 1).

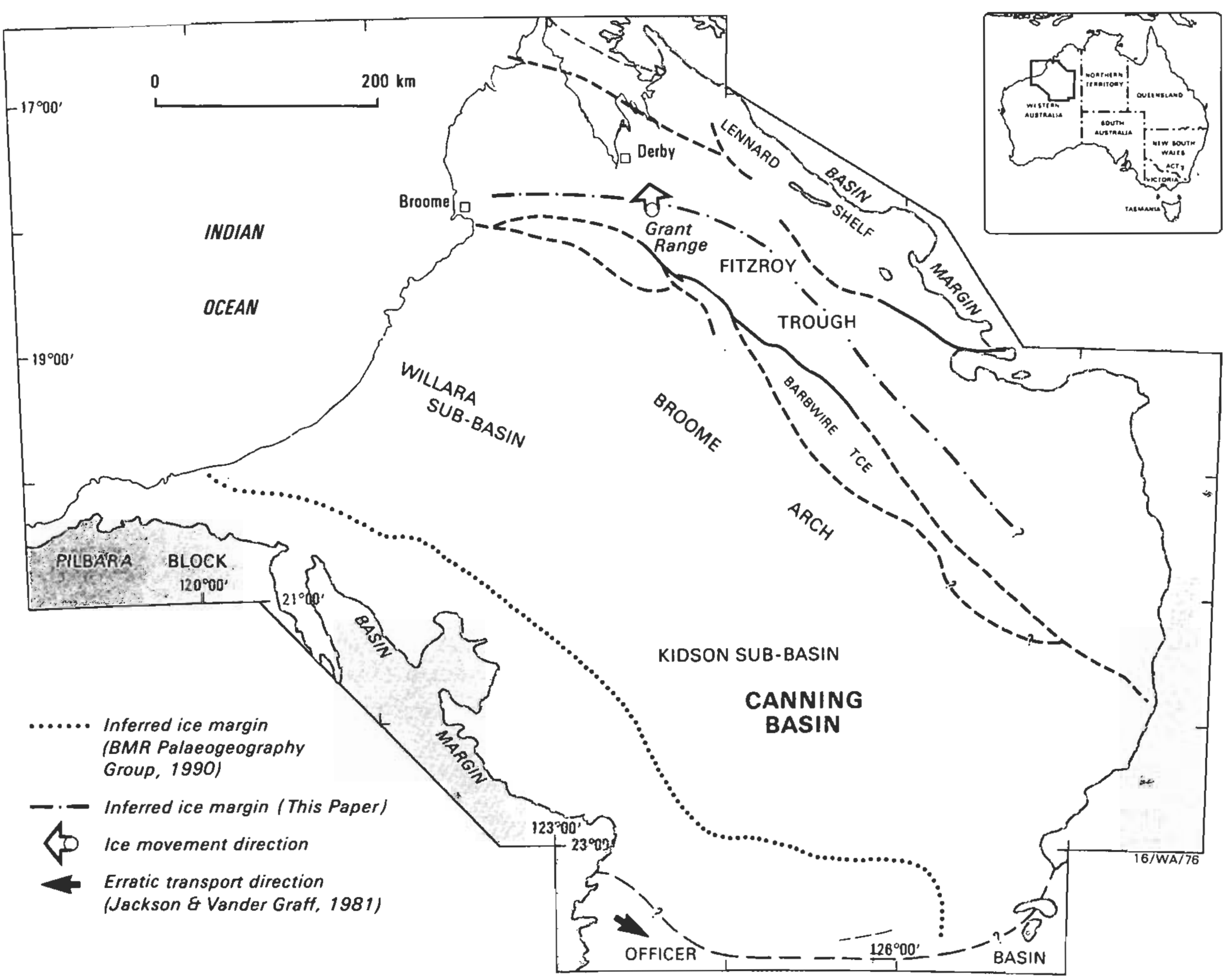

Figure 1. Canning Basin, Western Australia showing the major structural elements and the Grant Range outcrops.
Also shown are ice transport directions inferred by Jackson & van der Graaff (1981) and this study, and maximum ice margin limits from BMR Palaeogeographic Group (1991) and this study.

[1] Bureau of Mineral Resources, Geology & Geophysics, GPO Box 378, Canberra ACT 2601
[2] Department of Geological Sciences and Lamont-Doherty Geological Observatory of Columbia University, Palisades, New York 10964 USA

In July 1990, we discovered sediments containing glacially-cut grooves in the upper part of the Grant Group in Grant Range near the northern basin margin, confirming that glacial ice extended much further north than the southern Canning Basin margin.

Location and stratigraphic setting

The Grant Range is a roughly elliptical range of strike ridges of Grant Group and overlying Poole Sandstone some 90 km south-southeast of Derby (Fig. 1). The rocks are part of the succession deposited in the Fitzroy Trough, a major northwest-trending graben that forms the deepest part of the Canning Basin (Fig. 1). The range, and others like it to the east, are formed by resistant rocks brought to the surface in the cores of anticlines formed by strike slip movement along the southwestern boundary faults of the Fitzroy Trough (Figs 1, 2). The interval containing the grooved surfaces crops out in the central Grant Range (Fig. 2).

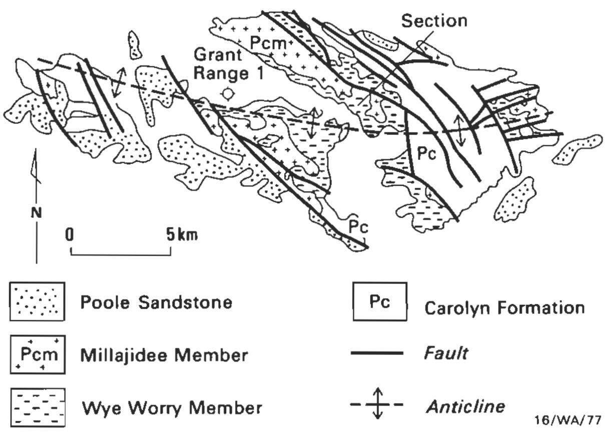

Figure 2. Map of the Grant Group outcrops in the Grant Range showing location of the section described.

In the Fitzroy Trough, the Grant Group is divided into three formations: the Betty, Winifred and Carolyn Formations (Table 1; Towner & Gibson, 1983) of which only the upper part of the Carolyn is exposed. Crowe & others (1978) recognised two members overlying massive sandstones of the Carolyn Formation in the St Georges Range. The lower Wye Worry Member features diamictite, bedded to massive mudstone with striated pebbles and boulders and marine fossils and poorly sorted, bedded fine sandstone. The overlying Millajidee Member is dominated by moderately sorted fine to medium sandstone with common cross beds.

Table 1. Stratigraphy of the Grant Group after Towner & Gibson (1983) and Crowe & others (1978).

Formation	*Member*	*Maximum thickness (m)*	*Lithology*
Carolyn	Millajidee	75	Medium sandstone
	Wye Worry	110	Mudstone, diamictites
		415	Coarse to fine sandstone
Winifred		278	Siltstone, fine sandstone
Betty		1714	Fine to coarse sandstone, minor siltstone & conglomerate

Our preliminary work suggests that these two members are mappable through the St Georges and Grant Ranges, though variation in outcrop expression has led to some difficulties in mapping them on air photos. We recognised three units in the Carolyn Formation outcrops (Table 1):

1. Massive to cross-bedded fine sandstone of the undifferentiated Carolyn Formation;
2. Wye Worry Member — bedded to massive diamictites and mudstones containing far-travelled and striated clasts and marine fossils (bryozoa, bivalves and brachiopods) accompanied by a variety of fine to medium sandstone facies and minor conglomerate.
3. Millajidee Member — a variety of facies associations ranging from fluvial to deltaic and shallow marine shoreface deposits but all predominantly composed of fine sandstone. An erosion surface with tens of metres of relief in places separates the Millajidee Member from the underlying Wye Worry Member.

Facies association

The section containing the grooved surfaces is part of the Wye Worry Member in the central Grant Range (Fig. 3). It contains two facies associations, called M and S (Table 2). Association M consists of green-grey sandy diamictites with basement pebbles and boulders (M1), crudely bedded silty fine sandstone (M2), massive, dolomite-cemented fine sandstone lenses with erosional bases (M3), and beds and lenses of poorly sorted pebbly medium sandstone (M4). M1 diamictite and M3 sandstone in the St Georges Range contain marine fossils. Basement pebbles include granitoids, gneisses, quartzite and banded iron formation. The banded iron formation pebbles were probably derived from the Pilbara Block to the south.

Table 2. Facies associated with the grooved surfaces in the Grant Group, central Grant Range.

Facies	*Description*	*Interpretation*
M1	Greenish grey sandy diamictite, basement pebbles to boulders. Marine fossils present in other outcrops	Glaciomarine diamictite deposited by ice rafting and from suspension
M2	Grey silty fine sandstone, cudely bedded, scattered pebbles	Glaciomarine outwash, sands and silts deposited by overflows, pebbles by ice rafting
M3	Fine sandstone, massive with dolomite cement, occupies erosionally-based lenses	Glaciomarine outwash, lenses cut and filled by underflow currents
M4	Poorly sorted, pebbly medium sandstone in tabular beds and lenses	Glaciomarine outwash, higher energy flows than M3
S1	Medium sandstone, moderately sorted, climbing ripples	Proximal glaciomarine outwash. Underflow deposits, high suspended sediment deposition rate
S2	Medium sandstone, moderately sorted, trough cross sets	Proximal outwash, channel or upper fan deposits
S3	Medium sandstone, moderately sorted, planar parallel laminae	Proximal outwash deposited under upper plane bed conditions
S4	Medium sandstone, massive with mudstone clasts & deformed masses of fine sandstone	Sediment gravity flows deposited on delta or fan front
S5	Massive silty mudstone <0.2m thick separating sandstone facies and directly overlying grooved pavements	Mud deposited from suspension during periods of low meltwater flow just after flotation of ice or retreat of grounding line

Association S consists of moderately sorted, medium sandstone facies in tabular beds up to 1.4 m thick with a range of internal structures including climbing ripples (Facies S1), large-scale trough cross-lamination (Facies S2), and planar parallel lamination (Facies S3). There are also structureless beds containing mudstone clasts (Facies S4) (Table 2, Fig. 4). Some laminated beds are convoluted; some massive beds

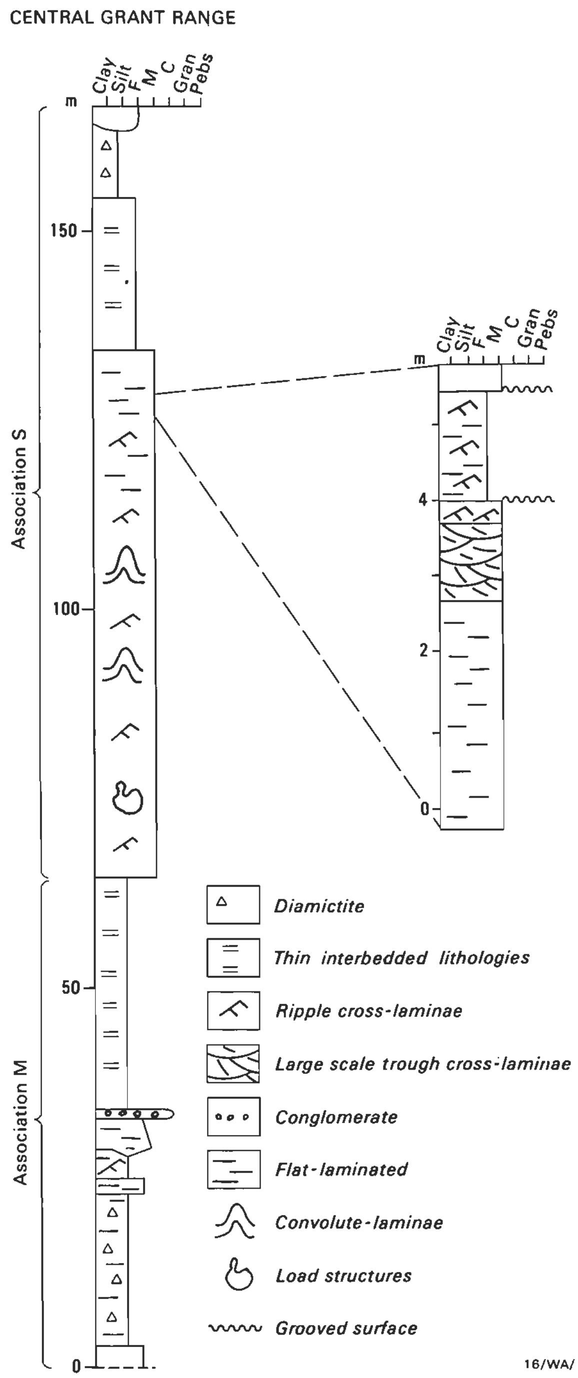

Figure 3. Generalised section through the central Grant Range succession and a detailed section through part of the interval containing the grooved surfaces.
Association S consists of incompletely exposed, thinly interbedded sandstone facies. Grooved surfaces are cut in fine to medium sandstone and overlain by thin mudstone beds.

contain deformed bodies of fine sandstone floating in medium sandstone. Cross laminae indicate palaeocurrents flowing towards the northwest. Wood impressions are scattered through some sandstone beds. Massive red-brown mudstone beds (S5) up to 0.2 m separate the sandstone beds.

Description of grooves

Grooved surfaces form the upper boundary of some of the Association S sandstone beds where they are now exhumed by selective weathering of Facies S5 mudstone beds and very thin drapes (Fig. 4). Though the exposures are not continuous, these surfaces can be traced for more than 200 m on the same bedding planes. Most of the grooved surfaces feature straight, parallel ridges and grooves 3 to 4 mm across and high that extend for more than 1 m (Fig. 5). Grooves begin and end as low angle bifurcations of ridges or end in steps a few millimetres high (Fig. 5). These steps are steeply sloping segments of featureless sandstone approximately at the angle of repose that are either normal, subparallel or oblique to the grooves (Fig. 5). Accompanying the grooves and steps are some large flat-sided ridges up to 5 cm across and 3 cm high, some of which have smaller grooves cut in their crest, and areas of unaligned depressions and ridges in the surface (Fig. 5). The train of small domes seen on the surface in Figure 5 is probably a secondary cementation feature. Groove alignment is very strong. Three surfaces display grooves trending towards 343°, two towards 341° and one towards 338°. These directions are maintained in outcrops over 200 m.

Facies interpretation

The massive to crudely bedded diamictite containing marine fossils and striated dropstone of Association M is typical of glaciomarine sediments (Anderson & Molnia, 1989); the coarse grainsize fraction is deposited by ice-rafting and the fine fraction by settling of suspended fines from meltwater plumes (Powell, 1981). The sandstone facies are all poorly sorted, suggesting deposition from currents laden with fine suspended sediment. The abundant sand fraction reflects deposition from density currents closer to the ice front than the diamictites (Powell, 1981). Thinly bedded facies may represent overflow or interflow deposits (Powell & Molnia, 1989), whereas the lenticular units were deposited by bottom-hugging currents capable of eroding the substrate.

Association S sandstone beds contain structures indicating unidirectional current flow ranging from lower to upper flow regimes. Massive beds containing sandstone bodies probably formed by mass flow (Frakes & Crowell, 1969). Their tabular bed geometry suggests sheet flows and the interbedded thin mudstones indicate episodes of quiet water sedimentation. Convolute lamination suggests high sedimentation rates. This combination of facies is consistent with deposition on the foresets of glaciolacustrine or glaciomarine deltas or subaqueous outwash fans (Gustavson & others, 1975; Rust & Romanelli, 1975; Shaw, 1975). In such a setting, massive sandstone with mud and sandstone clasts probably represents mass flow deposits formed by failure of the delta front (Postma & others, 1983) and the parallel laminated, ripple and large-scale cross sets were probably deposited by meltwater streams. They are better sorted than Association M sandstones, as a result of silt and clay being swept out into more distal environments (Powell, 1981). The thin mudstone beds probably formed as drapes during periods of low flow caused by winter freezing (Church & Gilbert, 1975) or by abandonment of the depositional site by the meltwater streams.

Interpretation of grooves

Grooved sediment surfaces can originate by sliding of sediment masses (Pickering, 1987), drifting sea ice (Barnes & others, 1987) or icebergs (Barnes, 1987) or beneath grounded glacial ice (Boulton & others, 1974). The surface features of the grooved surfaces rule out a sediment slide origin and suggest some characteristics of the ice that made them. The dip on the steps suggests that they are slip faces formed by loose sand being bulldozed into cavities. Cavities would not form at the base of a sediment slide.

Figure 4. Sandstone beds separated by thin mudstones and grooved surfaces.
The hammer rests against trough cross-bedded medium sandstone; the lower of the sandstone beds shown is massive medium sandstone. Grooved surfaces are indicated by arrows.

Figure 5. Features of a grooved surface.
Ice movement was from right to left (towards the northwest) as indicated by the transverse steps (arrowed) that formed as slip faces as the ice bulldozed the loose sand bed.

Side scan sonar images of sea bed gouged by drifting ice (Barnes & others, 1987, fig. 5a,b) suggest that sets of gouges may vary in orientation by up to 90° within a few tens of metres. Likewise, superimposed sets of gouges also typically diverge significantly (Barnes & others, 1987). Drifting sea ice or icebergs are unlikely to cut grooves with such little stratigraphic or spatial variation as those in the Grant Range, so the grooves were probably cut by glacial ice. The transverse steps formed by projections in the glacier sole pushing the sand into cavities in front of them, whereas the longitudinal steps developed by sand being pushed sideways into longitudinal cavities (Fig. 6). The slip faces themselves indicate an unconsolidated bed and ice motion towards the northwest.

The large flat-sided ridges probably formed between bumps in the ice or represent cavity fillings on the downstream side of bed obstacles (cf. Boulton & others, 1974). The upstream ends of grooves represent points at which small projections such as pebbles in the base of the ice lost contact with the bed.

The existence of subglacial cavities on an unconsolidated sand bed could indicate fast ice motion and cavitation about bed obstacles (Lliboutry, 1968) or low effective pressure on the glacier bed (Boulton, 1975). Cavitation about bed obstacles is a feature of glaciers sliding on consolidated rock beds rather than unconsolidated basin sediments, therefore low effective pressure is the more likely explanation. Effective pressure is the weight of the ice minus the subglacial water pressure (Boulton, 1975). Low effective pressure can develop because ice thins, because subglacial meltwater cannot percolate through the bed as fast as it is produced, or because the ice is about to float in standing water. In the Grant Range case, the glacier bed was fine sand so meltwater would have escaped easily. The setting of the grooves within glaciomarine outwash suggests that the cavities developed because the ice was close to floating. Thus, the grooves were cut by repeated grounding of glacial ice on a glaciomarine outwash fan. The presence of cavities suggests that the grounding line never advanced far past this area. The six successive grooved surfaces probably developed because of episodic minor advances of the grounding line.

Discussion

The grooved surfaces in the Grant Range indicate the presence of glacial ice moving north to north-northwest across the Canning Basin in the Late Palaeozoic. Clasts of granitic and metamorphic rocks and especially of banded iron formation imply that the ice originated at least 410 km to the south (Fig. 1). The basement clasts could not have been derived from any closer area because thick older Palaeozoic sedimentary rocks extend 390 km south of the Grant Range. Clearly a continental-scale ice sheet was present, probably centred on the Pilbara Block to the south with an ice thickness of several thousand metres at its centre. Ice sheets of this dimension were not unusual during the Pleistocene glaciation (Denton & Hughes, 1981).

Evidence for subglacial erosion on the Barbwire Terrace which forms the southern flank of the Fitzroy Trough to the southeast of the Grant Range (Redfern, 1991) suggests that the ice was firmly grounded along the edge of the Trough. Therefore, evidence for near floating ice in the Grant Range suggests that an ice shelf may have developed in the Fitzroy Trough during glacial maxima. Dropstone laminites and marine fossils in the Grant Group southwest of the Fitzroy Trough (Towner & Gibson, 1983; Foster & Waterhouse, 1988) indicate that the ice grounding line retreated across the southwestern Canning Basin as the ice decayed.

Acknowledgements

Jim Jackson, John Kennard, Peter Southgate, John Lindsay, Annie Holmes and Mike Sexton provided valuable discussion in the field and read the manuscript. Prof. L.A. Frakes and Dr V.A. Gostin provided helpful reviews. Bruno Zimmerman, Inge Zielinger and Christian Thun provided field support. Terry Brown drafted the figures. Christie-Blick's Canning Basin research is supported by the National Science Foundation of the USA.

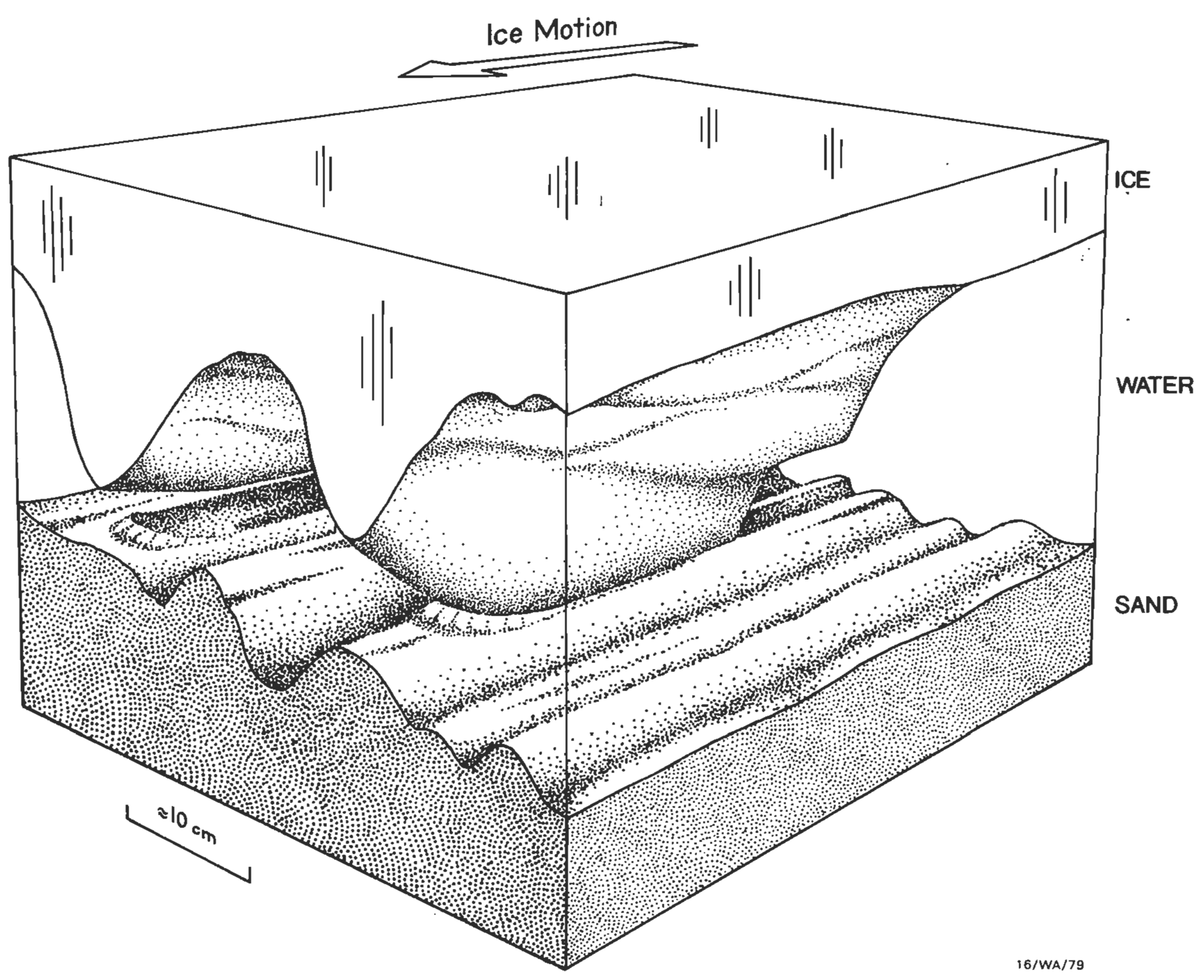

Figure 6. Formation of the grooved surfaces.
Irregularities in the glacier sole skimmed the unconsolidated sand bed cutting the grooves and pushing sand into cavities, where it formed small slip faces in front of and flanking the protuberances.

References

Anderson, J.B. & Molnia, B.F., 1989 — Glacial-marine sedimentation. *American Geophysical Union, Short Course in Geology*, 9, 127 pp.

Barnes, P.W. 1987 — Morphological studies of the Wilkes Land continental shelf, Antarctica — glacial and iceberg effects. *In* Eittreim, S.L. & Hampton, M.A. (editors), The Antarctic continental margin: geology and geophysics of offshore Wilkes Land. *Circum-Pacific Council for Energy and Mineral Resources Earth Science Series*, 5A, Houston, Texas, 175—194.

Barnes, P.W., Asbury, J.L, Rearic, D.M. & Ross, C.R., 1987 — Ice erosion of a sea-floor knickpoint at the inner edge of the Stamukhi Zone, Beaufort Sea, Alaska. *Marine Geology*, 76, 207—222.

BMR Palaeogeographic Group, 1990 — Australia — evolution of a continent. *Bureau of Mineral Resources, Australia*, 97 pp.

Boulton, G.S., 1975 — Processes and patterns of subglacial sedimentation: a theoretical approach. *In* Wright, A.E. & Moseley, F. (editors), Ice Ages: ancient and modern. *Geological Journal Special Publication*, 6, 7—42.

Boulton, G.S., Dent, D.L. & Morris, E.M., 1974 — Subglacial shearing and crushing and the role of water pressures in tills from Southeast Iceland. *Geografiska Annaler*, 56A, 135—158.

Church, M. & Gilbert, R., 1975 — Proglacial fluvial and lacustrine environments. *In* Jopling, A.V. & McDonald, B.C. (editors), Glaciofluvial and glaciolacustrine sedimentation. *Society of Economic Paleontologists and Mineralogists, Special Publication*, 23, 22—100.

Crowe, R.W.A., Towner, R.R. & Gibson, D.L., 1978 — Permian and Mesozoic geology of the Derby and Mount Anderson 1:250 000 Sheet areas, Western Australia. *Bureau of Mineral Resources, Australia, Record* 1978/8, 160 pp.

Crowell, J.C. & Frakes, L.A., 1971a — Late Palaeozoic glaciation of Australia. *Journal of the Geological Society of Australia*, 17, 115—155.

Crowell, J.C. & Frakes, L.A., 1971b — Late Paleozoic glaciation Part IV, Australia. *Bulletin of the Geological Society of America*, 82, 2515—2540.

Denton, G.H. & Hughes, T.J., 1981 — The last great ice sheets. *John Wiley & Sons, New York.*

Foster, C.B. & Waterhouse, J.B., 1988 — The *Granulatisporites confluens* Oppel-zone and Early Permian marine faunas from the Grant Formation on the Barbwire Terrace, Canning Basin, Western Australia. *Australian Journal of Earth Sciences*, 35, 135—158.

Frakes, L.A. & Crowell, J.C., 1969 — Late Paleozoic glaciation: I, South America. *Geological Society of America, Bulletin*, 80, 1007—1042.

Gustavson, T.C., Ashley, G.M. & Boothroyd, J.C., 1975 — Depositional sequences in glaciolacustrine deltas. *In* Jopling, A.V. & McDonald, B.C. (editors), Glaciofluvial and glaciolacustrine sedimentation. *Society of Economic Paleontologists and Mineralogists Special Publication*, 23, 264—280.

Jackson, M.J. & van der Graaff, W.J.E., 1981 — Geology of the Officer Basin, Western Australia. *Bureau of Mineral Resources, Bulletin* 206, 102 pp.

Lliboutry, L., 1968 — General theory of subglacial cavitation and sliding of temperate ice. *Journal of Glaciology*, 7, 21–58.

Pickering, K., 1987 — Wet-sediment deformation in the Upper Ordovician Point Leamington Formation: an active thrust-imbricate system during sedimentation, Notre Dame Bay, north-central Newfoundland. *In* Jones, M.E. & Preston, R.M.F. (editors), Deformation of sediments and sedimentary rocks. *Geological Society Special Publication*, 29, 213–240.

Postma, G., Roep, T.B. & Ruegg, G.H.J., 1983 — Sandy-gravelly mass-flow deposits in an ice-marginal lake (Saalian, Leuvenumsche Beek Valley, Veluwe, The Netherlands), with emphasis on plug-flow deposits. *Sedimentary Geology*, 34, 59–82.

Powell, R.D., 1981 — A model for sedimentation by tidewater glaciers. *Annals of Glaciology*, 2, 129–134.

Powell, R.D. & Molnia, B.F., 1989 — Glaciomarine sedimentary processes, facies and morphology of the south—southeast Alaska shelf and fjords. *Marine Geology*, 85, 359–390.

Redfern, J., 1991 — Subsurface facies analysis of Permo-carboniferous glaciogenic sediments, Canning Basin, Western Australia. *In* Ulbrich, H. & Rocha-Campos, A.C. (editors), Gondwana Seven Proceedings: papers presented at the Seventh International Gondwanan Symposium, Sao Paulo, 1988. *Instituto de Geosciencias, Universidade de Sao Paulo*, 349–363.

Rust, B.R. & Romanelli, R., 1975 — Late Quaternary outwash deposits near Ottawa, Canada. *In* Jopling, A.V. & McDonald, B.C. (editors), Glaciofluvial and glaciolacustrine sedimentation. *Society of Economic Paleontologists and Mineralogists Special Publication*, 23, 177–192.

Shaw, J., 1975 — Sedimentary successions in Pleistocene ice-marginal lakes. *In* Jopling, A.V. & McDonald, B.C. (editors), Glaciofluvial and glaciolacustrine sedimentation. *Society of Economic Paleontologists and Mineralogists Special Publication*, 23, 281–303.

Towner, R.R. & Gibson, D.L., 1983 — Geology of the onshore Canning Basin, Western Australia. Bureau of Mineral Res*ources, Australia, Bulletin* 215, 51 pp.

Towner, R.R., Crowe, R.W.A. & Yeates, A.N., 1976 — Notes on the geology of the southern part of the Canning Basin. *Bureau of Mineral Resources, Australia, Record* 1976/95.

BMR Journal of Australian Geology & Geophysics, 13, 93–105

Salinity of deep formation water in the Canning Basin, Western Australia

James Ferguson[1], Hashem Etminan[1] & Fereidoun Ghassemi[2]

Salinity of deep formation water in the Canning Basin, estimated from well log data or measured on water samples from oil-production wells and drill stem tests, ranges from almost fresh water (<1000 mg/L TDS) to brines which contain >300 000 mg/L TDS. Salinity is generally below 10 000 mg/L and rarely above 100 000 mg/L, partly because most wells have been drilled near the margins of the Canning Basin or its sub-basins and/or they intersect only the top few km of sedimentary sections. Most very high salinity water (>100 000 mg/L) was found in the south of the Canning Basin, particularly in the Willara and Kidson Sub-Basins, which were the sites of sabkhas (e.g. the Mellinjerie Limestone) and extensive deposition of evaporites (e.g. the Carribuddy Formation) in the Ordovician and Silurian. Salinity depends strongly on depth and sometimes increases from the top to the base of a stratigraphic unit or group of units before abruptly decreasing at the top of the underlying unit and then rising again. This type of pattern is most evident where the stratigraphic units are relatively thick, and the profiles are best preserved in low to moderate permeability sediments located in present-day low recharge areas of the basin. The pattern is probably formed by 'stacking' of a series of palaeo-salinity profiles, produced during a marine—continental or other depositional cycle in which the relatively high-salinity marine or non-marine water in the upper parts of the aquifer was partly replaced by low-salinity terrigenous groundwater. Average salinity of individual stratigraphic units within the basin increases linearly with increasing depth of burial, which suggests that the more saline deeper water interacts with the nearer-surface meteoric systems, probably via molecular diffusion of salt. Salinity is abnormally high in those parts of the Grant Group where re-solution of evaporites from the underlying Carribuddy Formation can occur, and in the low-permeability Mellinjerie Limestone where original highly saline pore water is retained and/or there is dissolution of associated evaporites. Higher than expected salinity also occurs in the Devonian Reef Complex and the Nita Formation, where water may contain remnants of palaeo-brines which entered the sediments before their permeability was reduced by cementation and compaction.

Introduction

The present-day distribution of saline water in deep aquifers and low-permeability sediments in the Canning Basin (Figs 1a–d) is pertinent to questions of petroleum generation and migration, and to genetic models for the Mississippi-Valley style Zn-Pb deposits which occur in the Lennard Shelf and near the Admiral Bay Fault (Fig. 1a). The major Palaeozoic aquifers in the Canning Basin are the Permian Poole and Grant Sandstones and the Devonian Tandalgoo Formation (Fig. 1b), and the maximum salinity in these aquifers is close to that of seawater (Ghassemi & others, 1990). The Liveringa Formation, the Laurel Formation (which is part of the Fairfield Group) and the Poulton Formation are also permeable, although they are less extensive than the major aquifers. The northern Canning Basin is predominantly low in salinity, particularly on the Lennard Shelf, although the maximum is about 70 000 mg/L Total Dissolved Solids (TDS), but highly saline formation water (up to 250 000 mg/L TDS) occurs in the Admiral Bay Fault area of the Willara Sub-Basin.

In this investigation, information on salinity-depth relationships for the Canning Basin has been obtained by supplementing the existing salinity data with about 250 salinity values calculated from well logs from 40 oil exploration wells (Fig. 1a). Hanor and his co-workers (e.g. Hanor & Bailey, 1983; Hanor, 1987) have shown that the nature of salinity versus depth profiles can be particularly useful in identifying recent and palaeo-hydrodynamic processes in sedimentary basins. Ranganathan & Hanor (1987) have discussed the origins of different types of profile and shown that the salinity profiles predicted for large scale molecular diffusion in subsiding sedimentary basins are linear or have gradients which increase downwards. They noted that this type of profile occurs in areas of northern Louisiana and southern Arkansas (Dickey, 1966, 1969; Hanor, 1984), but that the salinity change with depth is usually more complex (Fig. 2a). Salinity may rise gradually and non-linearly and reach a maximum (e.g. in the Michigan and Alberta Basins), or it may reach maximum values part way down the sedimentary sequence, decrease sharply, and then increase again (e.g.the Gulf Coast Basin). The origins of these more complex types of salinity profile are not well understood, but could be affected by advection, expulsion of fluids from geopressured zones and, during basin compaction, expulsion of saline water into aquifers from adjacent clay layers.

[1] Groundwater Program, Bureau of Mineral Resources, Geology & Geophysics, GPO Box 378, Canberra ACT 2601

[2] Centre for Resource and Environmental Studies, Australian National University, GPO Box 4, Canberra ACT 2601

Methods

Availability of data

The salinity of most formation water in the Canning Basin (Tables 1—6) was calculated from well logs (Tables 1, 4), because only a few direct measurements on water samples obtained from oil-production wells (Table 3) and drill stem tests (DSTs) (Tables 2, 4) could be made.

The producing oil wells in the Canning Basin occur in the Blina, Sundown, West Terrace and Lloyd oil fields on the Lennard Shelf (Fig. 1a). Water samples were obtained from ten wells in these fields, and in all cases the salinity was <5000 mg/L (Table 3). Salinity data from DSTs are available from exploration wells within most of the major structural subdivisions of the Basin (Fig. 1c) but, after elimination of obviously contaminated samples, only 44 measurements remain (Tables 2, 4). Considerably more data have been obtained from the well log calculations. For formation water within sediments of onshore wells 266 salinity values have been calculated (Table 1), and for offshore sediments 18 salinity values have been obtained (Table 4).

Salinity measurements and calculations

Salinity of water samples from oil-production wells and from DSTs was measured with an optical refractometer accurate to ±1000 mg/L.

Estimates of salinity from well logs were obtained using the Archie method of calculation. As a guide to the reliability of the data, a number of calculations were repeated using the SP and Ratio methods. Details of these calculation procedures are described by Schlumberger (1972).

All of the calculation methods require a good estimate of the formation temperatures. Burne & Kantsler (1977) have delineated regional thermal trends in the Canning Basin. They noted that for a large number of wells only bottom hole temperatures were available, and that there were usually insufficient data to correct these temperatures to actual formation temperatures. They estimated that individual bottom hole maximum temperatures were 2—32°C too low. Consequently, they adopted a

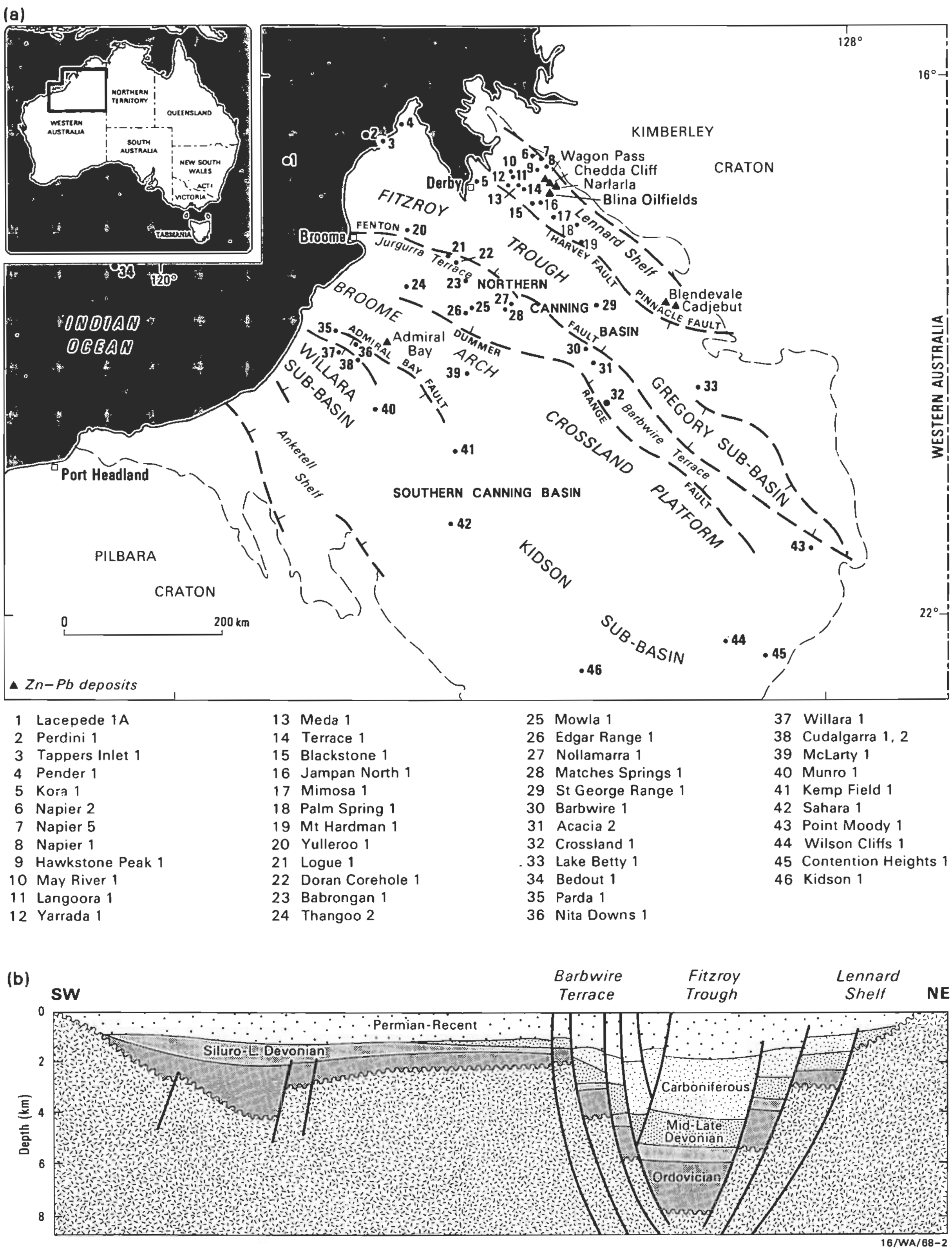

Figure 1 a. Main structural units of the Canning Basin, showing location of Zn—Pb prospects and deposits, the producing oil wells at and near Blina on the Lennard Shelf, and oil exploration wells for which salinity data have been derived. **1 b. Schematic cross-section (after Purcell, 1984).** Recent BMR seismic results have confirmed that the Fitzroy Trough is more asymmetric than shown here.

pragmatic approach and used the maximum bottom-hole temperatures as an indicator of the formation temperatures.

The correction factors for bottom-hole temperatures considered by Burne & Kantsler (1977) included those by Dowdle & Cobb (1975). This method and others (Whittaker, 1985; Hearst & Nelson, 1985) need time-dependent data, but Kehle (1971) has presented an empirical curve for correcting measured bottom hole temperatures. In the present investigation the data which have been used are the Kehle-corrected maximum bottom-hole temperatures, interpolated where necessary between the top and bottom temperatures by using depth versus temperature relationships obtained by linear regression. The temperature corrections range up to about 18°C (Table 7), but differences between salinity calculated using corrected and uncorrected bottom hole temperatures (BHTs) are small (with

Table 1. Calculated salinity of deep formation water in the onshore Canning Basin.

Age and formation	*Well name*	*Depth[1] (m)*	*Salinity (mg/L) ($NaCl_{eq}$)*
Late Carboniferous and Permian			
Poole Sandstone	Langoora 1	563	550
	May River 1	448	2500
	Mimosa 1	605	1550
	Mt Hardman 1	353	400
	Point Moody 1	431	4 000
		547	19 000
		648	9 000
	Babrongan 1	274	1 400
	Wilson Cliffs 1	468	2 000
	Palm Spring 1	158	1 500
Grant Group	Pender 1	566	9 700
		782	9 000
		855	8 500
	May River 1	642	3 700
		790	1 150
		1037	460
	Blackstone 1	919	2 000
		1313	2 700
		1434	3 000
	Hawkestone Peak 1	128	270
		184	270
	Langoora 1	688	1 400
		941	2 000
		1038	4 000
		1218	7 900
	Mimosa 1	857	2 000
		1037	4 500
	St George Range 1	713	2 900
		963	45 000
		1224	3 800
	Lake Betty 1	855	6 500
		1130	16 000
		1373	17 000
		1495	9 000
	Mt Hardman 1	620	750
		810	1 600
		1055	1 200
	Point Moody 1	791	17 000
		883	19 000
		931	15 000
		1087	11 000
		1192	16 000
		1436	39 000
		1563	18 000
		1620	26 000
		1895	37 000
		1966	43 000
	Tappers Inlet 1	1003	9 800
		1229	1 500
		1500	24 000
	Yulleroo 1	602	3 500
	Logue 1	643	2 250
		796	1 800
		925	2 700
		1192	3 500
		1299	3 600
	Doran Corehole 1	276	550
		367	800
		480	1 250
		674	1 100
	Babrongan 1	401	1 000
		611	4 500
	Mowla 1	306	7 500
		415	49 000
	Matches Springs 1	274	1 000
		505	9 000
		580	6 000
	Parda 1	680	6 800
		877	15 000
		959	15 000
	Munro 1	1084	14 000
		1160	37 000
	Sahara 1	672	3 100
		811	7 400
	Kidson 1	750	1 600
		907	9 000
		1224	9 000
	Contention Heights 1	479	1 720
		702	14 000
		806	15 000
	Wilson Cliffs 1	796	2 300
		925	2 500
		956	1 900
	Palm Spring 1	125	1 100
		301	700
		451	1 670
	Nollamarra 1	675	1 100
		858	900
	Kennedia 1	753	800
		863	1 500
	McLarty 1	300	6 000
		303	3 900
	Edgar Range 1	323	27 000
		474	26 000
Laurel Formation	Napier 2	114	750
	Blackstone 1	1544	2 600
	Langoora 1	1316	5 500
		1465	7 700
	St George Range 1	2973	15 800
	Lake Betty 1	1928	14 000
		2355	22 000
		2474	19 000
	Mt Hardman	2150	19 500
	Logue 1	1556	9 500
Devonian			
Poulton Formation	Lake Betty 1	3095	25 000
	Tappers Inlet 1	2012	11 000
Tandalgoo Formation	Matches Springs 1	1739	8 500
	Sahara 1	1267	6 900
		1421	6 900
		1648	13 000
	Kidson 1	1909	5 500
		2337	26 000
		2532	27 000
	Contention Heights 1	886	2 800
	Wilson Cliffs 1	1284	2 000
		1405	2 400
		1639	4 500
	Barbwire 1	401	7 700
Carboniferous			
Anderson Formation	St George Range 1	1510	5 000
		2639	3 500
		2843	15 000
	Yulleroo 1	1040	1 800
		1079	9 000
		1756	5 400
		2232	10 100
		2418	31 000
		2672	10 900
		2866	36 000
		3355	44 000
		3404	30 000
		3877	1 300
		4093	5 800
	Point Moody 1	2126	18 000
Devonian			
Napier Formation Reef Complex	Napier 2	245	700
		337	5 000
		450	2 000
		520	19 000
		748	3 900
		889	3 500
		951	2 200
		1099	3 500
		1172	3 000
		1407	7 000
	Napier 1	314	8 000
		739	18 000
		837	12 000
		916	37 000
		1007	27 000
		1130	40 000
		1218	10 500
		1390	12 000
		1561	7 500
		1720	4 600
Fairfield Formation	May River 1	1225	4 700
		1444	4 600
		1526	10 100
	Blackstone 1	1663	27 000
		1765	32 000
		1831	44 000

Age and formation	*Well name*	*Depth*[1] *(m)*	*Salinity (mg/L)* ($NaCl_{eq}$)
Blackstone Formation		2059	19 000
		2227	30 000
Napier Formation	Napier 5	543	7 800
		826	7 200
Van Emerick Conglomerate		1040	10 500
Station Creek Formation		1207	4 400
		1434	2 300
		1610	6 600
Fairfield Formation	Hawkestone Peak 1	497	69 000
		561	10 000
Devonian Reef		674	2 900
		736	2 400
		870	2 900
		948	750
		1055	3 500
		1131	1 500
Fairfield Formation	Langoora 1	1526	1 100
		1587	7 000
Luluigui Formation	Mimosa 1	1260	2 800
Clanmeyer Formation		1572	22 000
Devonian Reef		2623	65 000
		2875	64 000
		3065	40 000
		3368	37 000
		3593	70 000
		3965	50 000
Luluigui Formation	Lake Betty 1	2703	27 000
		2826	14 000
		2995	18 000
	Mt Hardman 1	2675	24 000
		2895	20 000
		3303	17 000
Pillara Formation	Tapper Inlet 1	1823	5 000
Clanmeyer Formation	Logue 1	2197	2 200
Pillara Formation	Barbwire 1	160	35 000
		276	5 300
Clanmeyer Formation	Babrongan 1	1543	1 300
Virgin Hills Formation		1805	2 700
Devonian Reef	Mowla 1	521	32 000
		611	23 000
		703	70 000
	Matches Springs 1	733	2 500
		1007	5 500
		1129	25 000
		1434	2 250
	Crossland 1	582	3 600
		643	4 500
		704	5 300
		826	16 500
Mellingerie Limestone	Sahara 1	997	37 000
		1038	190 000
		1087	120 000
	Kidson 1	1666	35 000
		1757	16 000
	Wilson Cliffs 1	1029	6 000
		1052	8 500

Age and formation	*Well name*	*Depth*[1] *(m)*	*Salinity (mg/L)* ($NaCl_{eq}$)
Fairfield Formation	Yulleroo 1	4377	1 800
		4503	4 400
Mellingerie Limestone	Kemp Field 1	581	105 000
Silurian—Early Devonian			
Carribuddy Formation	McLarty 1	1662	122 000
	Willara 1	1834	13 000
	Sahara 1	1726	24 000
		1958	55 000
	Kidson 1	2671	85 000
		3029	12 000
	Contention Heights 1	1285	8 000
	Wilson Cliffs 1	1979	3 600
		2172	7 300
		2381	5 500
Ordovician			
Nambeet Formation	Tappers Inlet 1	2524	13 500
		2756	22 000
Nita Formation	Barbwire 1	764	27 000
Goldwyer Formation		828	5 400
Nita Formation	Matches Springs 1	2120	138 000
		2203	69 000
Goldwyer Formation		2623	25 000
	McLarty 1	1773	23 000
		1861	23 000
		2084	54 000
Willara Formation		2224	24 000
		2317	33 000
L. Ordovician Sandstone		2503	250 000
		2523	>300 000
Goldwyer Formation	Parda 1	1221	25 000
Willara Formation		1512	5 500
		1680	9 200
		1724	15 000
Nita Formation	Munro 1	1538	38 000
Willara Formation		1846	30 000
		1953	30 000
		2096	160 000
	Willara 1	2654	13 800
		2773	5 500
		3050	7 500
		3276	2 000
Nambeet Equivalent		3477	17 000
Goldwyer Formation	Contention Heights 1	1404	4 000
Willara Formation		1586	14 000
		1648	55 000
Goldwyer Formation	Wilson Cliffs 1	2607	10 000
Nambeet Formation		2980	6 900
		3258	4 400
		3495	8 500
Nita Formation	Blackstone 1	2322	14 000
		2508	12 000
	Edgar Range 1	1181	5 200
		1921	6 000

[1]Midpoint of the range over which salinity was calculated.

one exception, Table 8). Overall, the uncertainties in the estimation of the BHTs do not appear likely to be a significant source of error in the salinity calculations.

Salinity obtained by calculation from well log data is in NaCl equivalents (expressed as mg/L). Some Canning Basin DST water is very high in Ca and the equivalent NaCl value can be up to about 15—20% lower than the real TDS value (Table 9).

Accuracy of salinity data

The descending order of reliability of the salinity data is (a) formation water from producing oil wells; (b) DST waters; (c) calculated salinities. DST water samples were assessed using chemical criteria for contamination by drilling fluids before being included in the data set. The accuracy of the calculated values was assessed by comparing the results of calculations by the three methods (Archie, SP and Ratio) and, where possible, also comparing the calculated values to those of DST water from the same or similar depths. A detailed comparison of the results of the Archie and SP methods for the well Point Moody 1 was made (Table 10), as well as a more general comparison of DST, Archie and SP data (Table 11).

The data from Point Moody 1 (Table 10) indicate that the calculated salinity values are reliable for permeable Canning Basin sediments of Late Carboniferous/Early Permian age or younger (i.e. from the base of the Grant Group upwards). For this well, the Archie and SP methods give similar results and agreement between the calculated data and DST measurements is excellent at 547 m and good at 1436 m (Table 10). Calculated salinity also appears to be reliable for the offshore wells (which have intersected mainly Cretaceous, Jurassic and Permian sediments; Table 4) because the salinity values calculated for shallow (Cretaceous) sediments approach that of seawater as the sediment—seawater interface is approached.

Calculated salinity for rocks older than Carboniferous is probably less reliable. Although a detailed comparison of the Archie and SP data for a number of wells in the Canning Basin indicates no systematic difference between the two methods, there is a large scatter, particularly at higher salinity. Also,

(c)

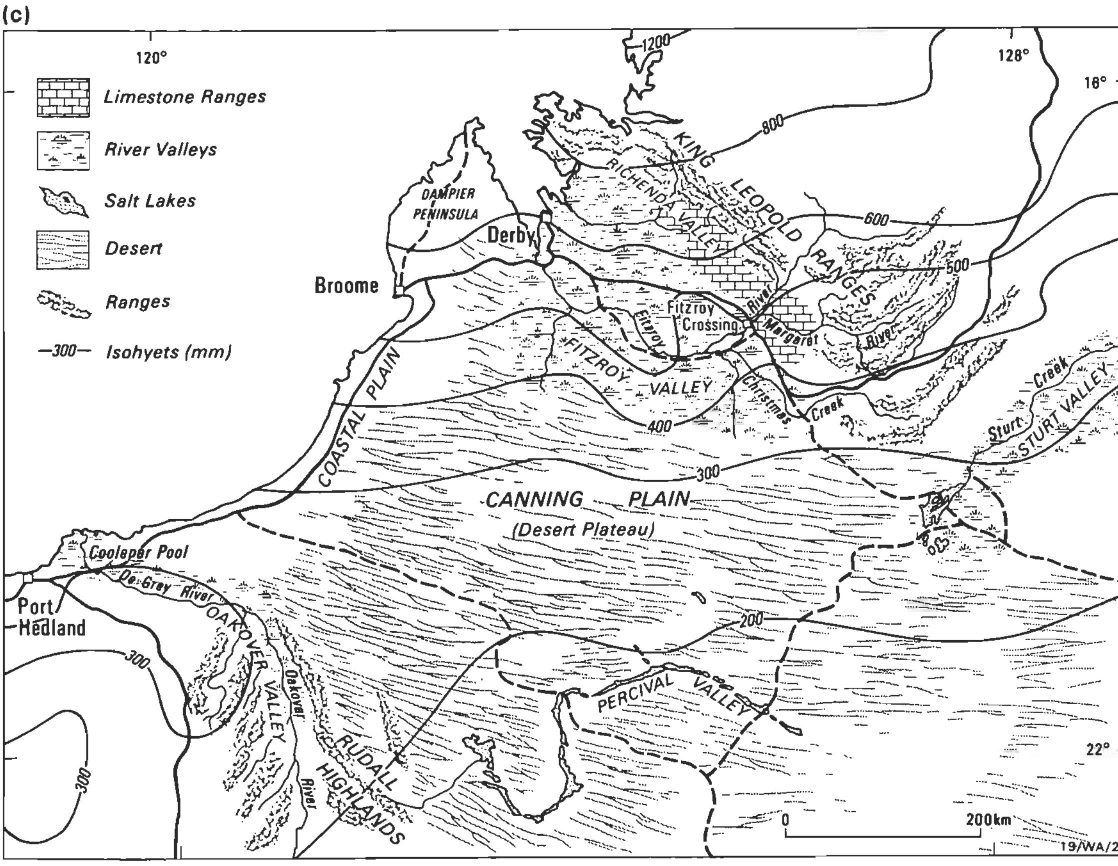

Figure 1 c. Physiography of the Canning Basin, showing the major river systems in the northern areas of the Basin, and the arid, desert areas of the south.

Table 2. Salinity of Drill Stem Test (DST) samples of deep formation water from the onshore Canning Basin.

Age and formation	*Well name*	*Depth (m)*	*Salinity (mg/L)*
Late Carboniferous and Permian			
Poole Sandstone	Point Moody 1	541	10 000
	Mt Hardman 1	320	500
Grant Group	Point Moody 1	1420	41 000
	Mowla 1	472	22 800
Laurel Formation	Meda 1	1572	37 000
		1570	40 000
Carboniferous			
Anderson Formation	Yulleroo 1	3350	129 000
	St George Range 1	2797	32 100
Devonian			
Poulton Formation	Napier 2	1473	3 000
	Napier 5	1610	1 500
Tandalgoo (equivalent)	Matches Springs 1	1739	8 000
Mellingerie (equivalent)	Mowla 1	487	22 800
	Kemp Field 1	859	8 000
Fairfield Formation	Nollamarra 1	1045	4 000
Pillara (equivalent)	Kennedia 1	2543	9 000
	Terrace 1		16 000
			6 000
	Jampan North 1	1987	9 000
(Devonian Reef)	Meda 1	2087	3 000
		2326	34 000
Fairfield Formation	May River 1	1445	7 900
	Blackstone 1	1689	25 800
		1851	5 600
	Kora 1	1780	1 380
		1609	4 428
	Yarrada 1	2024	58 070
	Acacia 2	1174	141 700
		1102	102 500
Devonian Reef	Hawkestone Peak 1	646	3 720
		779	600
Silurian-Early Devonian			
Carribuddy Formation	Wilson Cliffs 1	1979	17 700
Ordovician			
Willara/Goldwyer	Thangoo 2	896	10 000
	Nita Downs 1	1525	120 000
Nita Formation		1488	251 800
		1488	248 600
	Cudalgarra 1	1280	90 000
		1245	90 560
		1280	21 180
		1376	135 200
		1376	142 400
	Cudalgarra 2	(DST 2)	194 200
Nambeet	Wilson Cliffs 1	3422	17 780

[1]Midpoint of the range over which the salinity was calculated or the Drill Stem Test water obtained.
DST data is that for samples showing no obvious signs of contamination by drilling fluids (see *Methods* in text).

Table 3. Salinity of deep formation water from producing oil wells in the onshore Canning Basin.

Age and formation	*Well name*	*Depth (m)*	*Salinity (mg/L)*
Devonian			
Yellow Drum Formation	Blina 1	1160—1254	4 000
Nullala Limestone		1402—1478	
	Blina 2	1470—1490	4 000
	Blina 3	1456—1485	4 000
	Blina 5	1457—1472	4 000
Yellow Drum Formation	Blina 6	1207—1225	3 000
L. Grant Formation	West Terrace 1	1147—1159	145
	West Terrace 2	~1150	160
	Sundown 1	~1098	180
	Sundown 4	~1090	180
Anderson Formation	Lloyd 1	1512—1522	155

some low to moderate permeability sediments have considerably different calculated salinity and these calculated values differ considerably from DST data (Table 11). For example, in

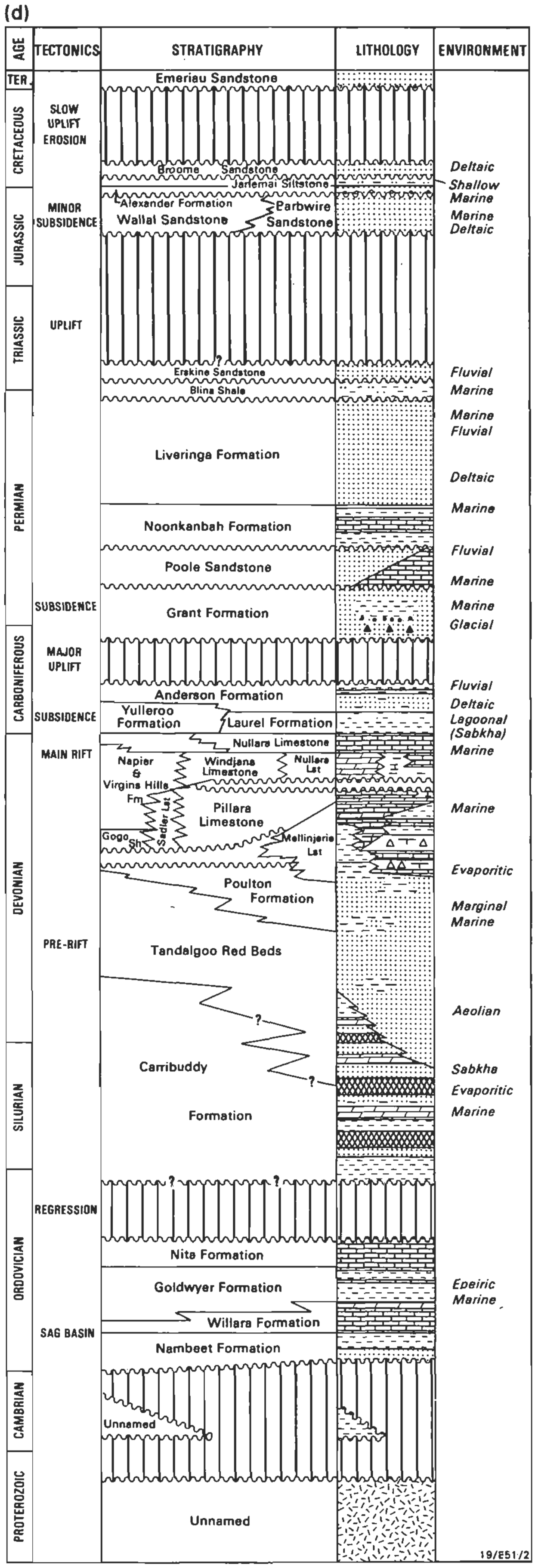

Figure 1 d. Generalised stratigraphy, tectonics and lithologic units of the Canning Basin (after Brown & others, 1984).

Table 4. Calculated and Drill Stem Test salinity of deep formation water in the offshore Canning Basin.

Age and formation	*Well name*	*Depth (m)*	*Salinity[1] (mg/L)*
Post-Grant			
Cretaceous—Jurassic	Bedout 1	1504	40 000
		1816	81 000
		1950	64 000
		2151	120 000
		2349	110 000
		2645	75 000
		2714	100 000
		2963	30 000
Cretaceous—Permian	Lacepede 1	702	34 000
		803	38 000
		977	36 000
		1038	35 000
		1313	50 000
		1465	55 000
		1617	49 000
		1770	38 000
		1938	51 000
		2212	160 000
	Perdini 1	876	15 000[2]
	Perdini 1		16 000[2]

[1]Calculated value unless otherwise stated
[2]DST

the Anderson Formation (Carboniferous), intersected by Yulleroo-1 over a depth of about 3 km, the maximum calculated salinity is about 40 000 mg/L, whereas DST water from about the same depth has an NaCl equivalent of 116 000 mg/L. Similarly, in several holes in the Willara Sub-Basin (Cudalgarra-1 and -2; Nita Downs-1; and Great Sandy-1), the calculated values are considerably lower than the DST salinity (Table 10). However, underestimation of salinity is unlikely to be a general problem because calculated salinity values of about 300 000 mg/L have been obtained for 'Lower Ordovician Sands' in the Nambeet Formation (McLarty-1), the Middle Devonian Mellinjerie Limestone (190 000 mg/L; Sahara-1) and the Ordovician Nita Formation (140 000 mg/L; Matches Springs-1). These differences could be real if the water obtained from DSTs came from fractures and the calculations give pore water values. More likely, they are caused by the presence of clayey sands, 'shoulder effects' on the resistivity logs, and/or hydrocarbons in the sediments which affect the calculated values.

Results

Canning Basin formation water salinity ranges widely, from almost fresh water with <1000 mg/L TDS to brines which contain >300 000 mg/L TDS and are probably saturated with halite (Tables 5, 6). More than one-third of the salinity values are below 10 000 mg/L and only a few are above 100 000 mg/L. This salinity distribution partly reflects a sampling bias towards shallow depths and/or areas of low-salinity water at the basin margin. Even in the Fitzroy Trough the oil-exploration wells intersect only the top few kilometres of a sedimentary section which is over 18 km thick in places.

Table 5. Range and average salinity values for deep formation water in major Palaeozoic aquifers in the Canning Basin.

Age, formation/ number of samples	*Average depth (m)*	*Salinity range (mg/L) Minimum*	*Maximum*	*Average salinity (mg/L)*
Late Carboniferous and Permian				
Poole Sandstone (12)	446	400	19 000	4 400
Grant Group (86)	851	270	49 000	9 900
Grant Group (7) (directly overlying Carribuddy Formation)	766	3 900	37 000	18 970
Fairfield Group (16)	1 783	4 000	69 000	16 200
Fairfield Group — Laurel Formation (12)	1 751	750	40 000	16 100
Devonian				
Poulton Formation (4)	2 047	1 500	25 000	10 100
Tandalgoo Formation (13)	1 554	2 000	27 000	11 000

Low-salinity water is most evident at the northeast margin of the Basin, where relatively high rainfall recharges the groundwater systems and produces a strong basinwards flow of meteoric water through the Lennard Shelf. There, salinity is low in the Grant Formation (Fig. 3) but significantly higher in the underlying Devonian carbonates. Salinity in the Devonian carbonates increases basinwards towards the Fitzroy Trough, but is unusually high in some wells drilled near the Pinnacle Fault System (e.g. ~70 000 mg/L in the Devonian Reef Complex in Mimosa-1; Table 1).

Salinity in the major Paleozoic aquifers, which are not restricted to the northern area of the Basin, is generally higher than at the northeast margin. Groundwater in the Poole—Grant sequence flows from the margin of the basin towards the centre and from the southeast to northwest, where it discharges into the Indian Ocean (Ghassemi & others, 1990). The aquifer is recharged directly through its outcrops and indirectly from overlying Mesozoic sediments. Salinity is 270—49 000 mg/L, and averages 9900 mg/L (Table 5). Salinity in the shallow parts of the aquifer is lower than average. Basin-wide maps (Ghassemi & others, 1990) show patterns which are consistent with the

Table 6. Salinity range and average for deep formation water in minor aquifers and low permeability strata in the Canning Basin.

Age, formation/ number of samples	*Average depth (m)*	*Salinity range (mg/L) Minimum*	*Maximum*	*Average salinity (mg/L)*
Post-Grant				
Offshore Cretaceous to Permian (22)	1840	15 000	160 000	73 100
Offshore Cretaceous (5)	1005	34 000	40 000	36 600
Offshore Jurassic (8)	2050	50 000	120 000	81 900
Offshore Triassic (1)	2963			30 000
Offshore Upper Permian (4)	1884	38 000	160 000	74 500
Carboniferous				
Anderson Formation (17)	2590	1300	129 000	23 000
Devonian				
Van Emerick Conglomerate (1)	1040			10 500
Station Creek Formation (3)	1417	2 300	6 600	4 400
Blackstone Formation (2)	2143	19 000	30 000	24 500
Luluigui Formation (7)	2665	2 800	27 000	17 500
Clanmeyer Formation (3)	1771	1 300	22 000	8 500
Reef Complex - incl. Pillara (56), Virgin Hills and Napier Formation	1227	600	70 000	15 600
Mellingerie Limestone (10)	1055	1 800	190 000	54 800
Silurian-Devonian				
Carribuddy Formation(11)	1933	3 600	122 000	32 700
Ordovician				
Nita Formation (8)	1588	5 200	251 800	88 300
Goldwyer Formation (8)	1800	4 000	54 000	21 200
Willara Formation (16)	2082	5 500	160 000	33 400
Nambeet Formation (7)	3130	4 400	22 000	12 900
Lower Ordovician Sandstone (2)	2513	250 000	>300 000	~275 000

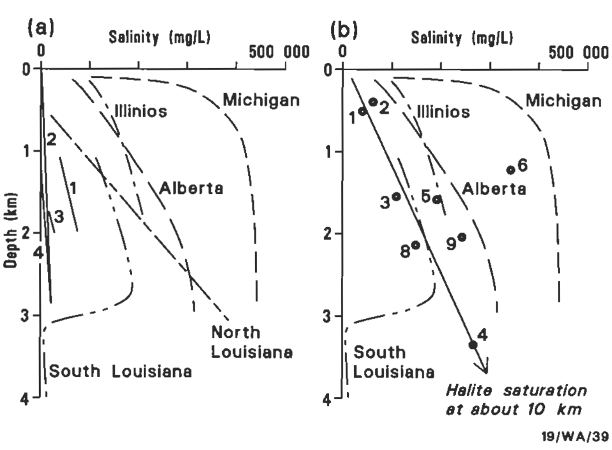

Figure 2. Salinity against depth profiles for the Canning Basin and various sedimentary basins in the USA.

The linear relationship for the North Louisiana Basin (Ranganathan & Hanor, 1987) is considered to be a result of molecular diffusion between low salinity meteoric recharge water near the surface and halite saturated water formed by dissolution of buried evaporites (the Louann Salt).

a. Average salinity for the Canning Basin shows a linear relationship with depth. The sampling bias in the Canning Basin towards lower salinity water means that maximum salinity of each Canning Basin formation should be used in inter-basin comparison. (1) Canning Basin offshore. (2—4) Canning Basin onshore (see text for sub-groupings).

b. Maximum salinity of formation water from the Grant Group and the northern Canning Basin increases approximately linearly with depth; the rate of increase is lower than in the USA basins. Halite saturation would be reached at about 10 km depth. Salinity in the southern Canning Basin changes erratically with depth but is relatively high, probably because of the low rainfall and the presence of evaporites at shallow depths.

1, Poole Sandstone; 2, Grant Group; 3, Laurel Formation; 4, Anderson Formation; 5, Carribuddy Formation; 6, Mellinjerie Limestone; 7, Nambeet Formation (Lower Ordovician Sandstone); 8, Goldwyer Formation; 9, Willara Formation.

Note : Salinity against depth profiles for individual wells are not usually linear, and in some profiles the salinity reaches a maximum and then decreases, as occurs in the Gulf Coast (see Fig. 5).

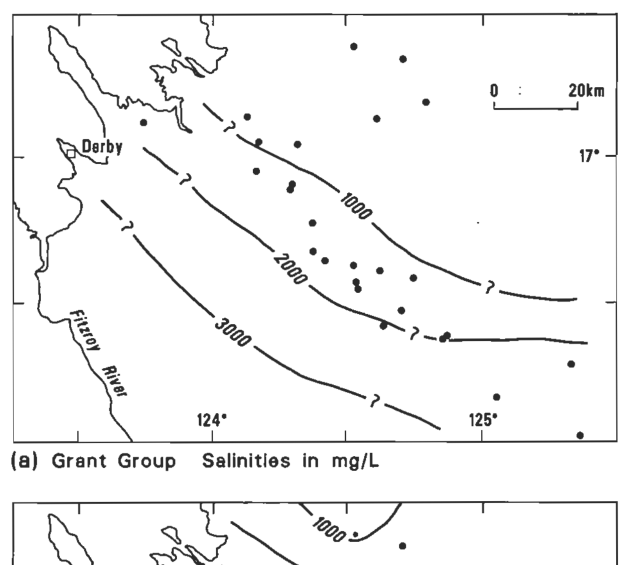

Figure 3. Salinity contours for the Lennard Shelf and adjacent areas of the Fitzroy Trough (after unpublished figures from Home Energy Pty Ltd).

a. Salinity contours in the Grant Group showing the gradual increase in salinity from the margin towards the Fitzroy Trough. This salinity trend is consistent with the Lennard Shelf being a site of high recharge.

b. Salinity in the Devonian Carbonates increases basinwards and is significantly higher than in the overlying Grant Group. The origins of the anomalously high salinity in parts of the area are not known.

present-day groundwater flow, i.e. salinity is low at the basin margins and increases along the flow lines. In the eastern part of the Basin where the Grant Group is directly underlain by the Carribuddy Formation there is an area of relatively high salinity water, presumably caused by dissolution of the underlying evaporites. The Permian—Carboniferous Tandalgoo Sandstone aquifer is recharged from the Grant Group in the south and southeast, and discharges towards the northwest (Ghassemi & others, 1990). Salinity is 2000—27 000 mg/L, and averages 11 000 mg/L (Table 5). In the shallower parts of the aquifer it increases from the south and southeast to the northwest, as indicated by the hydrologic data.

Most very high salinity water (>100 000 mg/L) has been encountered in the southern Canning Basin, particularly the Willara and Kidson Sub-Basins, which is consistent with the present-day desert climate and the presence of Silurian and Ordovician sabkha deposits (e.g. the Mellinjerie Limestone) and evaporites (Carribuddy Formation) in many of the wells. Strangely, the highest salinity is not in the Carribuddy, but in the underlying Nita Formation (250 000 mg/L) and the 'Lower Ordovician Sand' of the Nambeet Formation (>300 000 mg/L). The latter deposits may be fluvial, strandline or shallow marine (Conolly & others, 1984).

Salinity in three wells in sediments currently buried beneath the Indian Ocean (Perdini-1, Lacepede-1 and Bedout-1) averages about 75 000 mg/L for the Permian and declines to close to the seawater salinity value for the Cretaceous sediments. The maximum calculated value is 160 000 mg/L (Tables 4 & 6). In the more offshore wells (Lacepede-1 and Bedout-1), seawater directly overlies this brine (in Lacepede-1 the salinity is almost constant from 702 to 1038 m, in the range 34 300–38 000 mg/L). Nearer the shore (Perdini-1), the shallower sediments contain mixtures of seawater and low-salinity meteoric water (16 000 mg/L TDS). Seawater/meteoric water mixtures also occur in the onshore coastal areas (e.g. Tapers Inlet-1) where seawater has intruded into those parts of the Grant Group where the hydraulic heads are below sea level (Ghassemi & others, 1990).

Table 7. Correction of Bottom Hole Temperatures and comparison with actual formation temperatures for the well Yulleroo 1.

Depth (m)	*BHT (°C)*[1]	*Corrected BHT (°C)*[2]
916	60	67
2309	71	87
2983	83	101
3155-3307		actual formation temperature 83°C[3]
3225	84.5	101
3346-3357		actual formation temperature 88°C[3]
3395-3408		actual formation temperature 93°C[3]
3699	96	114
4079	109	126
4456	112	129
4576	121	138

[1]Measured Bottom Hole Temperature (BHT) taken from well logs.
[2]Corrected BHT. Corrections made using Kehle's (1971) chart for estimating values for equilibrium BHT.
[3]Burne & Kantsler (1977)

Table 8. Comparison of salinity values calculated by the Archie Method using corrected and measured BHTs for the well Yulleroo 1.

	Salinity (mg/L)	
Measured Depth (m)	*BHT*[1]	*Corrected BHT*[2]
602	3 700	3 700
1040	11 000	10 000
1079	8 500	8 000
1756	5 400	4 700
2232	10 100	9 400
2418	30 000	27 000
2672	13 000	12 000
2866	36 000	31 000
3355	22 000	19 000
3404	45 000	40 000
3877	14 000	13 000
4093	5 800	5 000
4377	1 800	1 600
4503	4 400	4 000

[1]Measured temperature
[2]Measured temperature corrected by Kehle's method (1971)
Interpolations from linear regression analysis of temperature v depth relationships.

Table 9. Measured salinity and NaCl equivalent.

Well name	*Depth (m)*	*Measured salinity (mg/L)*	*NaCl equivalent (mg/L)*
Yulleroo No. 1	3342	125 000[1]	116 000
Nita Downs No. 1	1457–1460 and 1439—1442	225 000[1]	198 000
Wilson Cliffs No. 1	1975	17800[2]	16600

[1]Ca-rich brine
[2]NaCl-dominated water

Table 10. Calculated salinity in Late Carboniferous/Early Permian or younger sediments encountered in the well Point Moody-1.

Depth (m)	*Archie*[1] *(mg/L)*	*Archie*[2] *(mg/L) BHT corrected*	*SP*[3] *(mg/L) Nomographs*	*SP*[4] *(mg/L) BHT corrected Formula value*
431	4 000	3 800	—	—
547	11 000	10 000	7 500	9 300
(DST 10 000)[5]				
648	9 000	85 000	6 100	6 200
791	17 000	16 000	16 000	15 900
883	19 000	18 000	25 000	22 900
931	15 000	14 000	—	—
1087	—	—	11 000	9 700
1192	39 000	35 000	32 000	25 000
1372	—	33 000	—	29 000
1436	39 000	37 000	38 000	30 600
(DST 41 000)[5]				
1563	32 000	28 000	35 000	26 000
1620	26 000	23 000	24 000	21 400
1734	—	12 500	—	14 000
1861	—	28 000	—	27 000
1966	43 000	36 000	65 000	48 300
2126	18 000	15 000	10 000	8 200

[1]Salinity calculated using the Archie method; BHTs not temperature corrected.
[2]Salinity calculated using the Archie method. BHTs corrected by Kehle's (1971) method.
[3]Salinity calculated using the Schlumberger Nomograph SP method; BHTs not temperature corrected.
[4]Salinity calculated using the Schlumberger Nomograph SP method. BHTs corrected by Kehle's (1971) method.
[5]Salinity of DST water.

Salinity—depth relationships

Salinity of deep formation water in the Canning Basin is strongly depth dependent, both basin-wide and within individual stratigraphic units. Basin-wide trends have been examined by comparing average salinity over a number of wells for each stratigraphic unit, and second-order and more localised trends by examining the types of profiles which occur in individual wells.

Local salinity—depth relationships. In areas of the Basin which are not subject to extensive flushing by low-salinity meteoric water, a salinity against depth pattern is common to a number of wells. This pattern can be best seen where individual stratigraphic units are thick or, under some circumstances, in a group of several adjacent thin units. In this type of pattern, the salinity within each stratigraphic unit or group of units fluctuates but generally increases with depth till it reaches a maximum, after which it abruptly decreases before gradually rising again (Figs 4a—c). The resulting appearance is that of a series of stacked sub-patterns (Figs 4a—c). For the northern Canning Basin the best developed patterns are those for the Poole Sandstone—Grant Group in Point Moody-1 (Fig. 4a), the Anderson Formation in Yulleroo-1 (Fig. 4b) and the Fairfield Formation in Blackstone-1 (Fig. 4b). In the southern Canning Basin, Parda-1 provides the best example (Fig. 4c). Offshore,

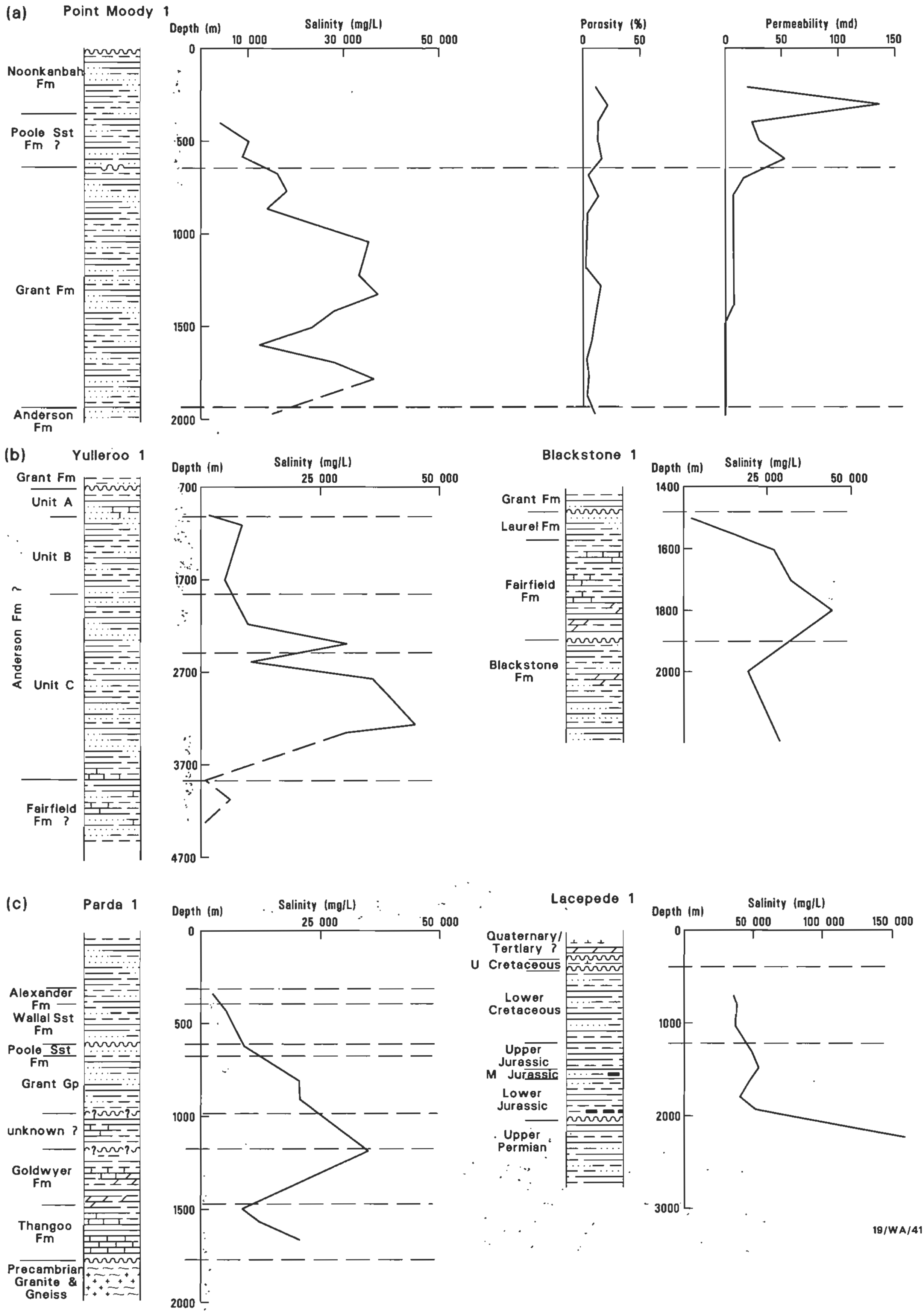

Figure 4. Salinity against depth profiles in individual wells in the Canning Basin.
a. An example from the Northern Canning Basin (Point Moody-1) of a common salinity profile in which salinity increases with depth, reaches a maximum and then abruptly decreases, usually at a stratigraphic boundary. Changes in porosity and permeability with depth are shown for the Poole Sandstone and Grant Group in Point Moody-1. This is the most complete data set available for the Canning Basin wells. Low salinity and high permeability correspond in the top part of the section but not elsewhere. Salinity changes in the bottom part of the section correspond to some extent with possible fluctuations between marine and continental conditions during the deposition of the Grant Group, but they are more likely to be related to subsequent groundwater regimes. **b.** Similar salinity profiles from the Northern Canning Basin (Yulleroo-1 and Blackstone-1). **c.** Salinity profiles from the Southern Canning Basin (Parda-1) and the offshore Canning Basin (Lacepede-1).

Table 11. Measured and calculated salinity of DST water from the Canning Basin.

Well name	*Depth (m)*	*Salinity DST samples (mg/L)*	*Calculated salinity[1] (mg/L)*
Point Moody 1	1420—1440	41 000	39 000
	543—546	10 000	19 000
Yulleroo 1	3342—3357	125 000	44 000
Kemp Field 1[2]	845—874	8 000	
	581		105 000
McLarty 1	296—307	6 000	3 900
Mimosa 1	1033	30 000	
	1073		4 500
	734—3736		17 000
	605		1 555
Mowla 1	487—3600	23 000	
	415		49 000
	611		23 000
Hawkestone Peak 1	638—3655	3 720	
	674		290
Wilson Cliffs 1	1975—1985	17 780	
	1979		3 600
May River 1	1445	7 900	
	1444		4 600
Blackstone 1	1689	25 800	
	1663		27 000
	1851	5 600	
	1831		44 000
St George Range 1	2797	32 000	
	2843		15 000
Cudalgarra 1	1238—252	91 000	38 0003
	1273—1286	21 000	24 000[3]
	1350—1402	132 000	5 000–75 000[3]

[1]Calculated by Archie method unless otherwise indicated.
[2]Calculation is for the Mellinjerie Limestone. The DST may have been in the Tandalgoo Formation.
[3]Calculated by SP method.

this type of profile occurs in Lacepede-1 (Figure 4c) and in Bedout-1 (Table 4).

Detailed information from the Grant Group in Point Moody-1 gives clues to the origins of these stacked sub-patterns. The general increase in salinity with depth is not smooth (Fig. 4a); salinity increases with depth in the upper part of the aquifer and then decreases by a factor of up to 3 before increasing again. The low but fluctuating salinity in the shallower parts of the aquifer probably reflects permeability differences in the sediments, because the shallow zone is relatively permeable (Fig. 4a), and would be selectively highly flushed by recharging low-salinity groundwater. Support for this view comes from calculations by Ghassemi & others (1990) indicating that travel times in the Poole—Grant Group aquifers are ~1–4 5 10^6 year. This suggests that original connate water is unlikely to remain in the sandy parts of the aquifer to the present day. In contrast, salinity in the lower parts of the aquifer is relatively high and the fluctuations do not correlate with present-day permeability or porosity (Fig. 4). The maximum salinity of about 50 000 mg/L is not greatly different from that of sea water (35 000 mg/L) and indicates these sediments could have retained some original marine or saline non-marine (connate) porewater.

The abrupt salinity decreases usually coincide with stratigraphic boundaries (some of which are also unconformities or disconformities), which are not necessarily the sites of aquicludes. This supports the proposition that original depositional conditions influence salinity. The pattern would be most easily explained if each upwards decreasing salinity profile were set in place before the next depositional cycle commenced. Long retention times in the low permeability clayey and/or cemented parts of the aquifer would strongly limit the mobility of the connate waters.

The stacked palaeo-salinity profiles are, in general, less obvious if the stratigraphic units are thin. However, if recharge is low, interplay of the effects of low salinity groundwater flushing and permeability and depositional environment controls of salinity can become more obvious. For example, in the southern Canning Basin a strong permeability and depositional environment control on salinity is evident in a low permeability sabkha/intertidal unit, the Mellinjerie Limestone, which has a much higher salinity than the adjacent permeable Grant Group and Tandalgoo Sandstone (Sahara-1 and Kidson-1; Figs 5a, b). However, some displacement of saline water by low salinity meteoric flushing has occurred because the salinity in the Mellinjerie Limestone is considerably lower in Kidson-1, which is nearer the basin margin than Sahara-1.

The profiles also become less evident if flushing by present-day low-salinity meteoric water is strong. In the Fitzroy Valley, for example, salinity is low to considerable depths (Fig. 5c). There is an overall increase in salinity with depth, but the increased low-salinity meteoric influence overprints any cyclical fluctuations within stratigraphic units and changes at strata boundaries. The Lennard Shelf appears to lie between the southern Canning Basin and the Fitzroy Valley and a combination of moderately high recharge, thin sedimentary units and highly variable permeabilities produces apparently erratic salinity changes with depth.

Regional salinity-depth relationships. The data from individual wells indicate that hydrodynamic processes, such as flushing by low salinity meteoric waters, influence groundwater salinity on at least a regional basis. However, vertical movement of saline water is likely to be severely inhibited by the effectively low large-scale vertical permeability of the basin sediments. Under these conditions large-scale advective vertical movement of brine is unlikely, and diffusion may be important in transferring salt across stratigraphic boundaries. To determine whether large-scale vertical diffusion is effective in the Canning Basin, the salinity data have been averaged for wells grouped according to the following combination of regional and stratigraphic similarities:

(i) Offshore sediments, which are Cretaceous to Permian (Fig. 6a);
(ii) Basin-wide, Late Carboniferous and Permian sediments, mainly the Poole—Grant Group aquifer, but including the low-permeability Anderson Formation and the permeable but not extensive Laurel Formation (Fig. 6b);
(iii) Lennard Shelf Devonian sediments, which consist mainly of carbonate-reef and other deposits centred on the Lennard Shelf and adjacent areas of the Fitzroy Trough, and including the Devonian Reef complex and the Station Creek, Clanmeyer, Poulton, Blackstone and Luluigui Formations (Fig. 6c);
(iv) Willara and Kidson Sub-Basins Devonian and Ordovician sediments, which include the Devonian Tandalgoo Formation and Mellingerie Limestone and the Ordovician Goldwyer, Nita and Nambeet Formations (Fig. 6d).

For each group the salinity and the depth at which the salinity measurements were taken have been averaged and graphed as 'average salinity against average depth' (Figs 6a—d) allowing a reasonable *comparison* of stratigraphic units if every unit is encountered in all the wells averaged. However, the *absolute* value of these 'average' salinity values depends strongly on the location of the wells used in the averaging process. For example, most wells used are located near the Basin margins which, as mentioned previously, biases the average towards low salinity.

In all four groups of wells there is a linear relationship between average salinity and average depth, which is consistent with upwards diffusion of salt towards lower salinity near-surface waters. The slope of the average depth-salinity lines is ~50 000

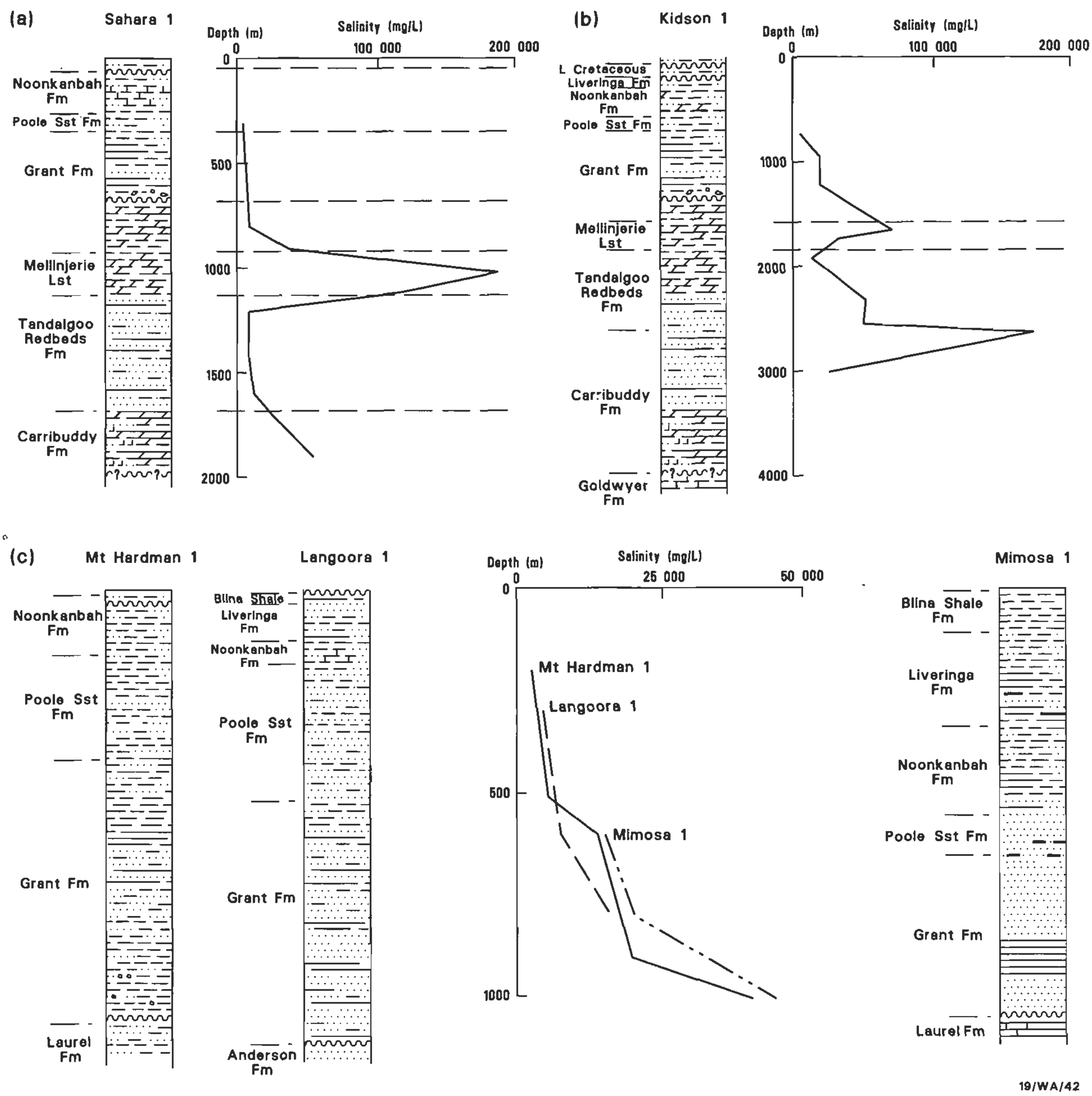

Figure 5. Recharge/depositional environment/low permeability control on salinity.

a. High salinity in the sabkha/lagoonal Mellinjerie Limestone in Sahara-1. High salinity may have been produced by re-solution of evaporites formed during deposition or early diagenesis, and preserved because of the low permeability of the sediments (Ghassemi & others., !990).

b. Salinity in the Mellinjerie Limestone in Kidson-1. This is higher than in the adjacent strata but the difference is smaller than in Sahara-1. The position of Kidson-1 nearer the basin margin probably results in higher recharge and removal of higher salinity porewater.

c. Strongly recharge-influenced salinity profiles from the Fitzroy Valley area of the Northern Canning Basin. The recharge appears to have been sufficient to smooth out any palaeo-salinity fluctuations which might have been present in the upper strata, and produces a relatively gradual increase in salinity with depth.

mg/L/km for the offshore sediments (i) and 45 000 mg/L/km for the Devonian and Ordovician sediments of Willara and Kidson Sub-Basins (iv), and ~10,000 mg/L/km for the Late Carboniferous and Permian sediments (ii) and Lennard Shelf Devonian sediments (iii). In the southern Canning Basin this probably reflects the presence of the evaporites of the Carribuddy Formation at shallow depths.

In each group the average salinity of some stratigraphic units plots significantly away from the line. For the offshore sediments the near-shore well Perdini-1 clearly plots below the salinity/depth trend line (Figure 6a) because seawater is the normal shallow low salinity water, but Perdini-1 has also been influenced by meteoric water and shallow sediment salinity is as low as 16 000 mg/L.

In the onshore Canning Basin, deviations from the average salinity—depth lines are usually towards higher salinity. The salinity of the Grant Group plots slightly above the line (Fig. 6b), but if it is subdivided into those areas which directly overlie the Carribuddy Formation and those which do not, then it is apparent that higher salinity results from the dissolution of evaporites. When these evaporite-influenced salinity values are deleted, the remainder plot closer to the line.

For the Devonian carbonates of the Lennard Shelf, high salinity occurs in the Devonian Reef Complex and possibly the Blackstone Formation (Fig. 6c). In the Devonian and Ordovician sediments in the Willara and Kidson Sub-Basins, the Nita Formation (average 88 300 mg/L, maximum 250 000 mg/L) and the Mellinjerie Limestone (average 54 000 mg/L) are highly saline. As discussed before, high salinity in the Mellinjerie

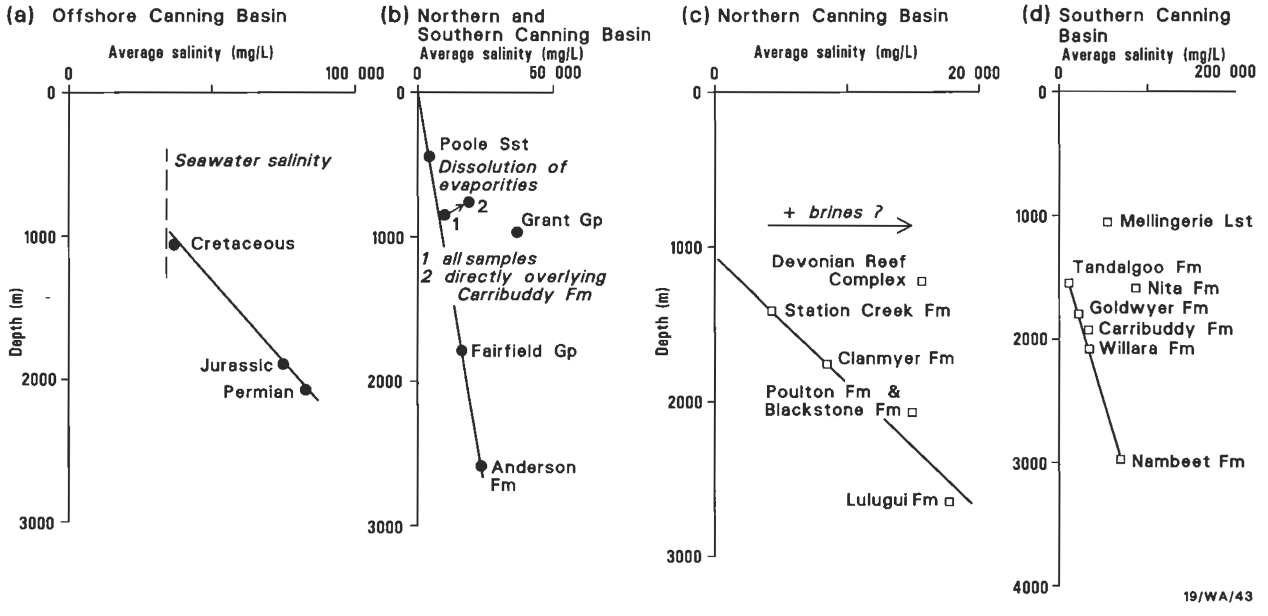

Figure 6. Relationship of salinity and depth, showing relationship of the average salinity measurements for each Formation (or Group) to the average depth at which salinity was determined.
Formations and Groups have been assembled into the following four classes:
a. Offshore Canning Basin. Because of the limited stratigraphic information in some of the well logs salinity has been arranged by age of the sediments. The relationship is linear, and probably extrapolates to the present-day seawater value. However, as indicated by the single sample from Perdini-1, in near-shore areas lower than seawater salinity values in shallow sediments may result from seawater—meteoric water mixing.
b. Onshore Canning Basin, including the extensive Poole Sandstone and Grant Group aquifers, and the Fairfield Group and Anderson Formation, which occur mainly in the Northern Canning Basin. Relationship of average salinity to depth is linear. The small displacement of the Grant Group to higher salinity is almost eliminated if wells in which the Grant Group directly overlies the evaporite-containing Carribuddy Formation are considered separately.
c. Onshore Canning Basin, including data from the Lennard Shelf area at the northern margin of the Northern Canning Basin. The displacement of Devonian Reef salinity to higher values is consistent with geochemical evidence that small quantities of marine bitterns may have entered some strata on the Lennard Shelf.
d. Onshore Canning Basin, including data mainly from the Willara and Kidson Sub-basins in the Southern Canning. High salinity in the Mellingerie Limestone may reflect the combination of evaporites formed during the original sabkha/lagoonal conditions of deposition and low permeabilities.

Limestone probably reflects its sabkha origins and low permeability. The origin of high salinity in the Nita Formation is not clear, but could be remnants of brines which originated elsewhere in the Basin.

Comparison with other sedimentary basins

The Canning Basin has been subject to to several depositional cycles; our data come from sediments back to Ordovician in age. The investigation is therefore more extensive but less comprehensive than salinity data on deep formation water in the Alberta, Illinois, and Michigan Basins, and the Gulf Coast in the USA (Ranganathan & Hanor, 1987).

The Canning Basin salinity can be made more comparable with those in the USA basins if maximum rather than average salinity for each stratigraphic unit is used to help overcome the sampling bias towards the Canning Basin margins. The Canning Basin plots of the maximum salinity against depth are approximately linear for the northern areas (Fig.. 2b) but there is a much lower increase in salinity with depth than in the USA basins. In the southern Canning Basin the maximum salinity is scattered widely, but some values are comparable with those in the USA basins (except for the Michigan Basin) (Fig. 2b).

In general, Canning Basin deep formation water salinity is comparatively low, but the major processes which produce the water are probably similar to those which generate high salinity water in other basins. High salinity water (~250 000 mg/L) in the southern Canning Basin is a mixture of bittern water and meteoric water which has re-dissolved halite and calcium sulphate minerals. Other water is a mixture of low salinity meteoric water, the meteoric water containing re-dissolved evaporites and, in some cases, a minor proportion of bitterns. Water formed by dissolution of evaporites can approach halite saturation in some USA basins, but in the Canning Basin salinity of this type of water is typically about 50 000 mg/L (e.g. in those parts of the Grant Formation overlying the Carribuddy Formation). However, geological evidence from the southern Canning (Bentley, 1984) suggests that highly saline water formed by dissolution of evaporite minerals should be more extensive than is indicated by the few instances of highly saline water encountered in this investigation. Bentley (1984) has noted that the northern edge of the Carribuddy Salt has been gradually eroded since its deposition, probably in two separate phases. Salt has also been mobilised into domes and pillow structures, which should increase the potential for dissolution by removing the salt from the protection of enclosing shales.

The linear increase in average salinity-depth in both the onshore and offshore areas of the Canning Basin is similar to the linear relationships observed in areas of northern Louisiana and southern Arkansas (Dickey, 1966, 1969; Hanor, 1984; Ranganathan & Hanor, 1987). Hanor (1984) suggested that in North Louisiana the linear trends were caused by steady-state diffusion of NaCl from the Louann Salt, which occurs at about 3 km depth, combined with active meteoric recharge at the surface. Extrapolation of the salinity data to the depth at which the Louann Salt occurs, gave a salinity close to that expected for halite saturation. For the Canning Basin, extrapolation of the average salinity-depth lines to basement gives salinity values well below halite saturation. However, use of maximum rather than average salinity values for the northern Canning Basin gives a gradient which extrapolates to that of halite saturation at 10 km depth (Fig. 2b). There is evidence to suggest that evaporites are present at considerable depths in the Fitzroy Trough, which contains up to 18 km of sediment (Drummond

& others, 1991).

The Canning Basin stacked salinity sub-profiles in individual wells also have similar counterparts in the USA basins. Significant reversals of salinity increases with depth have been found in Cainozoic sands and shales of the Gulf coast, USA (Schmidt, 1973; Hanor & others, 1986). Hanor & others (1986) noted that in Tertiary sediments in Southern Louisiana the base of the salinity maximum is coincident with the overpressured or geopressured section. Hanor (1984) has suggested that dissolution of salt diapirs in the hydropressured section and the subsequent large-scale dynamic dispersion of dissolved salt away from the domes is the most likely explanation of the salinity profiles. An alternative explanation of the salinity reversals (Omaston, 1975) is that the lower salinity water may simply have been originally less saline than that above. In the Canning Basin, formation pressures are close to hydrostatic (Ghassemi & others, 1990), and there is no obvious spatial association of the salinity maxima with evaporites.

Conclusions

1. Salinity in the Canning Basin deep aquifers shows the effects of large-scale regional or semi-regional processes, particularly meteoric recharge and vertical diffusion of salt, and more localised effects including re-solution of evaporites, retention of connate water and residual mobilised palaeobrines.

2. Recharge by low-salinity meteoric water has a major influence on groundwater salinity at the Basin margins, particularly in the Lennard Shelf area of the northern Canning Basin. In the major Phanerozoic aquifers, the Poole Sandstone—Grant Group, and the Tandalgoo Formation, salinity is low at the Basin margins and generally increases down the flow lines.

3. Upwards diffusion of salt from deep saline groundwater towards the lower salinity surface water occurs across stratigraphic boundaries, producing linear salinity against depth gradients over several kilometre thick sedimentary sequences.

4. Brines occur at depth in the Basin. The most saline water occurs in the southern Canning Basin, but highly diluted examples of these brines are also evident in some parts of the Lennard Shelf.

5. Saline water formed by re-solution of evaporites is evident, particularly in those areas of the Grant Group which are directly underlain by the evaporite-containing Carribuddy Formation. Salinity is considerably lower than halite saturation although geological evidence of extensive dissolution of the Carribuddy Formation evaporites indicates that halite-saturated water should occur in the Basin.

6. In some areas of the Basin, restricted present-day meteoric recharge has allowed the preservation of salinity profiles representing original saline depositional conditions and superimposed low-salinity palaeo-hydrologic regimes.

Acknowledgements

The authors thank BHP Co. Ltd, Billiton Australia Ltd, Command Petroleum N.L., CRA Exploration Pty Ltd, Kufpec Australia Pty Ltd, Eromanga Energy, Esso Australia, and Santos Ltd and the Geological Survey of Western Australia for the provision of water and rock samples and access to well completion and internal reports.

References

Bentley, J., 1984 — Petroleum geology of Central Broome Platform. *In* Purcell, P.G. (editor), The Canning Basin, W.A. *Proceedings of the Geological Society of Australia/Petroleum Exploration Society of Australia Symposium, Perth, 1984.*

Brown, S.A., Boserio, I.M., Jackson, K.S. & Spence, K.W., 1984 — The geological evolution of the Canning Basin. *In* Purcell, P.G. (editor), The Canning Basin, W.A. *Proceedings of the Geological Society of Australia/Petroleum Exploration Society of Australia Symposium, Perth, 1984.*

Burne, R. V. & Kantsler, A.J., 1977 — Geochemical constraints on the hydrocarbon potential of the Canning Basin, Western Australia. *BMR Journal of Australian Geology & Geophysics*, 2, 271–288.

Conolly, J., Falvey, M., Kingsley, D., Melton, B. & Russell, T., 1984 — Geology and petroleum potential of the southern Canning Basin. *In* Purcell, P.G. (editor), The Canning Basin, W.A. *Proceedings of the Geological Society of Australia/Petroleum Exploration Society of Australia Symposium, Perth, 1984.*

Dickey, P.A., 1966 — Patterns of chemical composition of deep subsurface waters. *AAPG Bulletin*, 50, 2472–2478.

Dickey, P.A., 1969 — Increasing concentration of subsurface brines with depth. *Chemical Geology*, 4, 361–370.

Dowdle, W.L. & Cobb, W.H., 1975 — Static formation temperature from well logs — an empirical method. *Journal of Petroleum Technology*, 27, 1326–30.

Drummond, B.J., Sexton, M.J., Barton, T.J. & Shaun, R.D., 1991 — The nature of faulting along the margins of the Fitzroy Trough, Canning Basin, and complications for the tectonic development of the trough. *Exploration Geophysics*, 22, 111–116.

Ghassemi, F., Etminan, H & Ferguson, James, 1990 — Hydrogeology of deep aquifers in the Canning Basin, Western Australia. *In* Proceedings of the International Conference on groundwater in large sedimentary basins, Perth, Western Australia, 9–13 July 1990. *Australian Water Resources Council Conference Series* No. 20. *Department of Primary Industries and Energy, Australian Government Publishing Service, Canberra*, 558 pp.

Hanor, J.S., 1984 — Variation in the composition of oilfield brines with depth in Northern Louisiana and Southern Arkansas: implications for mechanisms and rates of mass transport and diagenetic reaction. *Gulf Coast Association of Geological Societies, Transactions*, 24, 55–61.

Hanor, J.S. 1987 — Origin and migration of subsurface sedimentary brines. *Society of Economic Palynologists and Mineralogists Short Course* No. 21. *SEPM, Tulsa Oklahoma*, 247 pp.

Hanor, J.S. & Bailey, J.E., 1983 — Use of hydraulic head and hydraulic gradient to characterise geopressured sediments and the direction of fluid migration in the Louisiana Gulf coast. *Gulf Coast Association of Geological Societies, Transactions*, 33, 115–122.

Hanor, J.S., Bailey, J.E., Rodgers, M.C. & Milner, L.R., 1986 — Regional variations in physical and chemical properties of South Louisiana oilfield brines. *Gulf Coast Association of Geological Societies, Transactions*, 36, 143–149.

Hearst, J.R. & Nelson, P.H., 1985 — Well logging for physical properties. *McGraw-Hill, New York*, 571 pp.

Kehle, R.C., 1971 — Geothermal survey of North America; 1971 annual progress report. *AAPG unpublished report*, 37 pp.

Omaston, M.F., 1975 — Discussion: Interstitial water composition and geochemistry of deep Gulf Coast shales and sandstones. *AAPG Bulletin*, 56, 2022–2028.

Purcell, P.G., 1984 — The Canning Basin, W.A. — an introduction. *In* Purcell, P.G. (editor), The Canning Basin, W.A. *Proceedings of the Geological Society of Australia/Petroleum Exploration Society of Australia Symposium, Perth, 1984.*

Ranganathan, V. & Hanor, J.S., 1987 — A numerical model for the formation of saline water due to diffusion of dissolved NaCl in subsiding sedimentary basins with evaporites. *Journal of Hydrology*, 92, 97–120.

Schlumberger Ltd, 1972 — Log Interpretation: Volume I— Principles. *Schlumberger Ltd, New York.*

Schmidt, G.W., 1973 — Interstitial water composition and geochemistry of deep Gulf Coast shales and sands. *AAPG Bulletin*, 57, 321–327.

Whittaker, A., 1985 — Theory and evaluation of formation pressures, a pressure detection reference handbook: *IHRDC Publishers, Boston* 231 pp.

BMR Journal of Australian Geology & Geophysics, 13, 107–111

The Regional Seismographic Network and seismicity of central Queensland

William V Cooper[1], Byron McKavanagh[1], Bruce Boreham[1], Kevin McCue[2,1], Russell Cuthbertson[3] & Gary Gibson[4]

The Central Queensland Seismographic Network consisting of four short-period seismographs was established between May 1990 and March 1991 by the University of Central Queensland, the Bureau of Mineral Resources and the Queensland Department of Resource Industries. These stations have been located to provide coverage over approximately 70 000 km^2 of central Queensland where the earthquake hazard and risk are above average for continental Australia. The network has enabled discriminants to be devised to distinguish local earthquakes from large blasts at the coal mines and quarries in the region; travel times from blasts are being used for studies of local crustal structure. Several small local and regional earthquakes have been detected in the short period of network operation; their relationship to the region's tectonic history is being assessed. The intensity in Rockhampton of the June 1918 Bundaberg earthquake, the largest known earthquake along the eastern seaboard of Australia, is re-evaluated. The area of strong shaking was larger than originally supposed and alluvial areas of downtown Rockhampton were subject to significant amplification of ground motion.

Introduction

Since 1981, the Queensland Department of Resource Industries (then the Queensland Department of Mines) has operated a single short period vertical component seismograph for the Gladstone Area Water Board near the Awoonga High Dam. With the installation of an additional three seismographs near Rockhampton in 1990, two recorders bought by the Applied Physics Department of the University of Central Queensland (UCQ) and another lent by the Australian Seismological Centre, Bureau of Mineral Resources, the Central Queensland Regional Seismographic Network was born. The Applied Physics Department, University of Central Queensland, Rockhampton, operates the network.

Establishment of the Central Queensland Regional Seismographic Network has provided coverage of major population and industrial centres at Rockhampton and Gladstone and data acquisition for a research program in earth sciences at the University of Central Queensland.

This paper reviews the historical seismicity of the area, the tectonic setting, details of the network and the potential to evaluate the crustal structure of central Queensland with the network using large regional coalmine blasts to the west of the network and Australian Defence Force ordinance testing to the northeast.

Seismicity of central Queensland

Epicentres of earthquakes recorded over the last 30 years show that Rockhampton and Gladstone are within the intersection region of two intraplate seismicity zones: a 500 km wide, north—northeast-trending belt extending from southwest Tasmania to the vicinity of Fraser Island, Queensland, and an apparently narrower, less active belt trending north—northwest from about Fraser Island to the tip of York Peninsula. A recent study of the seismicity of a small part of this zone in central and southeast Queensland (Cuthbertson, 1990) indicates that, since 1977, most earthquakes in central Queensland have occurred offshore or south of the Mount Morgan lineament. The area north of this line may be undergoing a period of quiescence, but it is more likely that small earthquakes in this area have not previously been detected, due to the lack of local seismographs.

Various studies have been made of the effects of earthquakes that were widely felt in central Queensland during the last 100 years, from which it would appear there are two distinct subzones of seismic activity (Fig. 1). The first is east of Heron Island, mostly within the Capricorn Basin, and encompasses epicentres of the earthquakes of 1918, 1922, 1974 and 1978; the other, near Gayndah, encompasses epicentres of the earthquakes of 1883, 1910, 1935 and 1953.

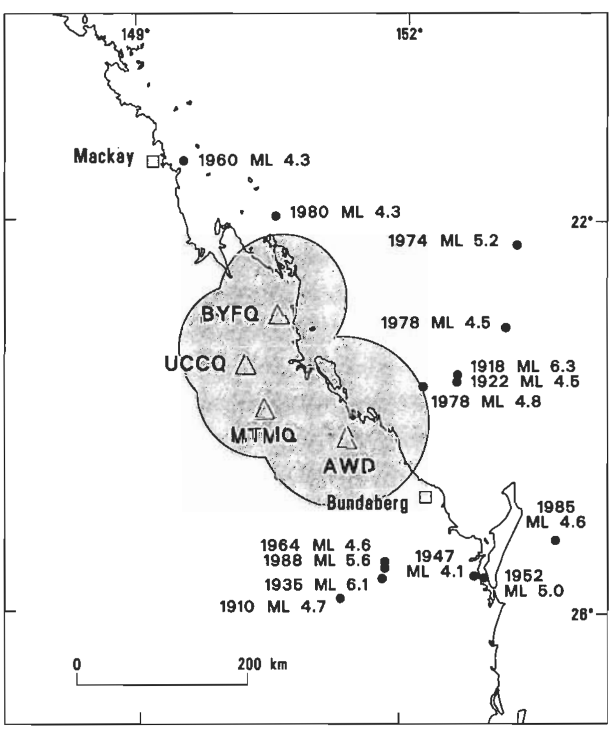

24/Q/22

Figure 1. Central Queensland historic earthquakes greater than magnitude ML 4, and Central Queensland Regional Network detection capability for earthquakes of magnitude ML 2 and greater.

The central Queensland area has been shaken by at least fourteen earthquakes greater than Richter magnitude ML 4 in the last 110 years (Table 1). Two of them were potentially very destructive with magnitudes of about 6: the 1883 Gayndah and 1918 Bundaberg earthquakes (Bryan & Whitehouse, 1938; Everingham & others, 1982). Several of the earthquakes have had large aftershocks. The 1883 Gayndah earthquake was followed by an ML 5.0 aftershock. Aftershocks of the 1918 Bundaberg earthquake were felt in and around Rockhampton until 20 August 1918, over two months after the main shock; six of them, all occurring within two hours of the main shock, had magnitudes in the range ML 5.1—5.6. The ML 5.0 Heron Island earthquake in 1978 had a relatively large ML 4.5 after-

[1] Department of Applied Physics, School of Science, University of Central Queensland, Rockhampton, QLD 4702
[2] Australian Seismological Centre, Bureau of Mineral Resources, Geology & Geophysics, GPO Box 378, Canberra ACT 2601
[3] Queensland Department of Resource Industries, GPO Box 194, Brisbane QLD 4001
[4] Seismology Research Centre, Phillip Institute of Technology, Bundoora VIC 3083

shock. This apparent pattern is quite different from that at Newcastle after the December 1989 ML 5.6 earthquake, where only a single small aftershock was recorded.

Table 1. Central Queensland earthquakes, ML ≥4.0.

Date	*Time (UTC)*	*Location Latitude ° S*	*Location Longitude ° E*	*Place*	*Magnitude (ML)*
28.8.1883	16:55	25.5	151.7	Gayndah	5.9
24.11.1910	23:00	25.7	151.2	Munduberra	5.2
6.6.1918	18:15	23.5	152.5	Bundaberg	6.0
7.3.1922	16:54	23.5	152.5	Bundaberg	4.5
12.4.1935	01:32	25.5	151.7	Gayndah	5.2
11.6.1947	10:03	25.5	152.7	Maryborough	4.1
24.6.1952	01:44	25.5	152.8	Maryborough	5.0
3.12.1953	15:42	24.5	151.4	Manypeaks	4.4
19.10.1960	11:37	21.2	149.5	Mackay	4.3
3.3.1964	06:13	25.4	151.7	Gayndah	4.5
24.12.1974	02:25	22.1	153.2	Coral Sea	5.2
28.11.1978	17.33	23.4	152.4	Off Heron Island	5.0
8.2.1980	04:42	21.8	150.5	Nothumberland Island	4.3
08.02.1985	08:23	25.1	153.6	Off Indian Head	4.6

A review was conducted of central Queensland newspaper reports of the earthquakes listed in Table 1. The assessed intensities for the 1883, 1910, 1953, 1960 and 1978 earthquakes were in agreement with the published isoseismal maps for those earthquakes (Everingham & others, 1982; Rynn & others, 1987). No newspaper reports were found of the 1922, 1947, 1952, 1964, 1974, 1980 or 1985 earthquakes.

1918 earthquake. Newspaper reports of the 1918 earthquake were assigned intensities on the Modified Mercalli (MM) scale. The reports indicate that most people felt three separate shocks. The first was only slightly felt, with intensities of MM III—V. This was followed in less than a minute by the major shock. The intensities for the major shock have been used to redraft an isoseismal map (Fig. 2). Where there was more than one intensity for a particular area, the mean has been used for the plotted value. This map shows that the earthquake was felt more intensely and over a wider area than indicated by a previous isoseismal map (Hedley, 1925; Everingham & others, 1982).

In the Rockhampton area, intensities of MM VII and VIII were observed on Quaternary flood plain alluvium consisting of unconsolidated sand, gravel, silt and clay, while those located on or near bedrock were MM VI and lower. The difference in intensity shows that the ground motion was amplified by the underlying alluvial sediments in those areas of higher intensity, by a factor of 2 to 4. A similar increase in intensity was observed in alluvial areas of downtown Newcastle, New South Wales, during the 1989 earthquake (McCue & others, 1990) and also in the suburbs of San Francisco underlain by bay muds, 100 km from the epicentre of the October 1989 Loma Prieta California earthquake (Hough & others, 1990).

1935 earthquake. Newspaper reports of the 1935 earthquake indicate that intensities of at least MM III—IV were experienced in and around Rockhampton. The *Rockhampton Morning Bulletin* reported that the earthquake was felt rather severely in the railway administration block, at the corner of Denison and Stanley Streets. Here furniture was displaced and large presses rocked in the top story offices, from which a hurried exit was made. The published isoseismal map (Bryan & Whitehouse, 1938; Everingham & others, 1982) indicates that the average intensity in Rockhampton was between MM II and III. The railway administration block is on alluvial sediments, so this second earthquake clearly illustrates that ground motion amplification has occurred again and highlights a potentially serious problem for town planners in Rockhampton.

Tectonic setting

Bell & Adams (1990) proposed that in eastern Canada, which like central Queensland is quite distant from plate boundaries, the current regional stress field is produced by modern plate tectonic processes and not relict or locked-in stresses from past tectonic cycles. If they are correct, it may be more useful to map faults, measure extant crustal stresses and establish the link to present plate tectonic processes to explain the current high stress and seismicity, rather than unravel the ancient geological record. A condensed history of the tectonic setting is therefore provided here.

The east coast of Queensland has been described as a tectonically passive subsiding continental margin (Falvey & Mutter, 1981) over the last 50 Ma. Before then, a brief period of seafloor spreading opened the Tasman Sea, 57—95 Ma, and Coral Sea, 57—65 Ma (Hayes & Ringis, 1973; Jenkin, 1984; Veevers, 1984). The Capricorn Basin developed at this time as a failed rift. The late Cretaceous basaltic and trachytic lava flows and plugs found just north of Rockhampton and dated at 67 Ma (Wellman, 1978) are evidence of hot spots which were related to this episode of seafloor spreading. However, as recently as 0.6 to 1.1 Ma, three volcanoes erupted in the Bundaberg area (Johnson, 1989), a clear sign that intraplate crustal and possibly upper mantle deformation is continuing today.

The predominant trend of inherited surface lineaments in the central Queensland region is northwesterly and epicentres might be expected to align in this direction. The northwest-trending Parkhurst and east—southeast-trending Bajool faults intersect near the town of Bajool between Rockhampton and Gladstone (Wilmott & others, 1986), and recent small earthquakes there were felt quite strongly in the locality. Their relationship to the major faults is still being assessed.

Listric faults on current models (Fergusson & others, 1988) may be exposed by foci progressively deepening from west to east or by detection of seismic phase reflections or conversions from surface explosions. Some seismicity may also be related to the failed rift in the Capricorn Basin in a similar way to that of the New Madrid area of the United States (Johnston, 1982), especially offshore earthquakes such as those of 1918, 1922, 1974 and 1978 (Table 1).

From limited focal mechanism studies and crustal stress measurements, it appears that at present central Queensland is subject to horizontal compression oriented northeast or north—northeast (Cuthbertson, 1990; Denham & Windsor, 1991). This is perpendicular to the direction of prominent regional surface lineaments such as the Parkhurst fault, making their reactivation difficult (except for the reactivation of normal faults as thrust faults). The direction of the principal stress is parallel to that through the islands of New Guinea, Bougainville and the Solomon Islands straddling the plate boundary in the northeast quadrant. We consider it distinctly possible that the crustal stress and subsequent intraplate earthquakes such as that at Bundaberg in 1918 resulted from distant edge plate processes, but it is not yet known how or indeed whether the stress release is influenced by existing faults.

Station distribution, instrumentation, and data analysis

The Central Queensland Regional Seismographic Network consists of four short period seismographs, two analogue recorders with 1 hertz vertical transducers and two digital recorders with triaxial 2 hertz transducers. The analogue recorder near the Awoonga High Dam (AWD) is operated by the Queensland Department of Resource Industries (DRI) for the Gladstone

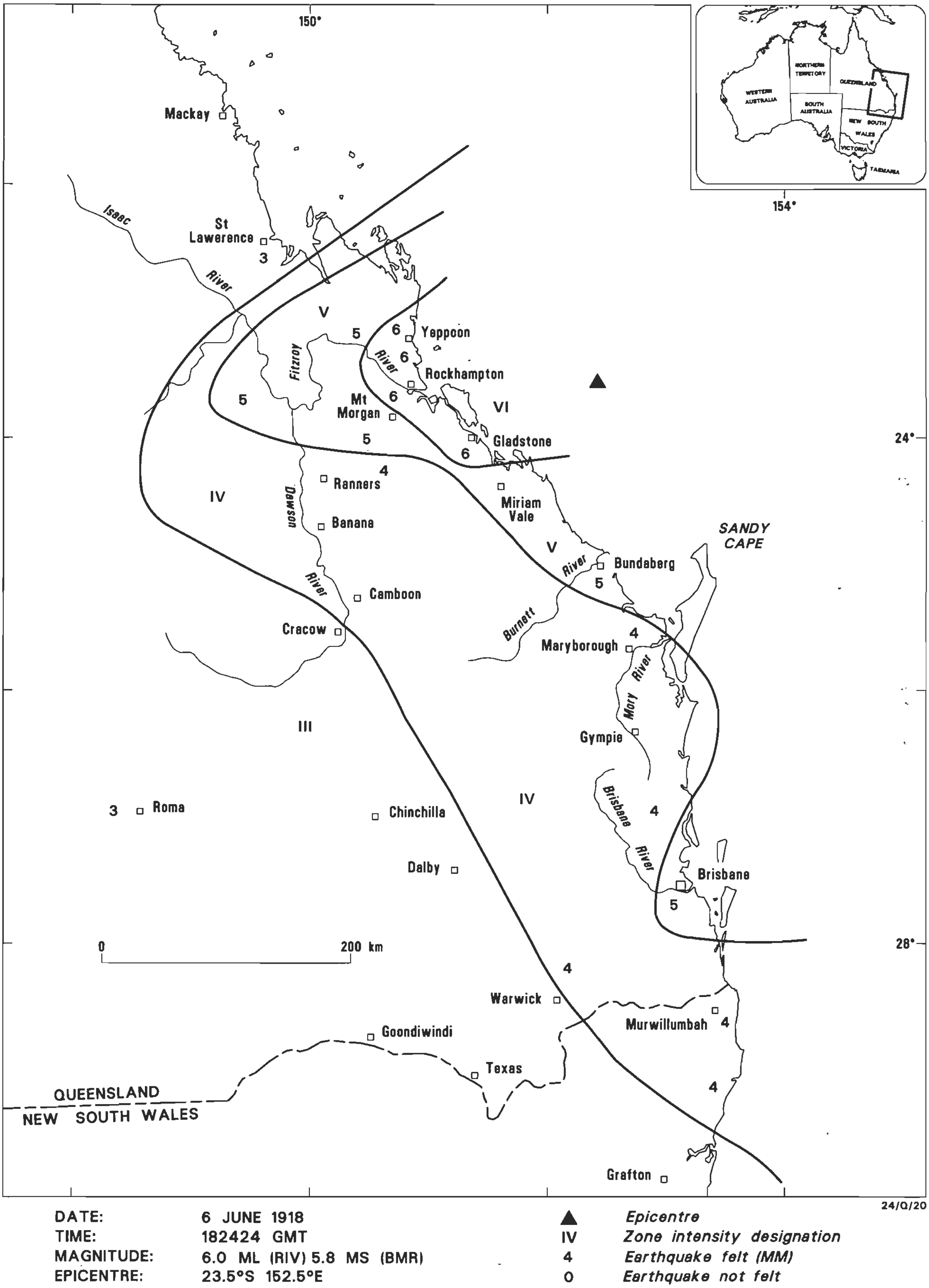

Figure 2. Revised isoseismal map, Bundaberg earthquake 6 June 1918.

Area Water Board and the seismograms are forwarded each week to the University of Central Queensland, Rockhampton, for interpretation. The digital recorder at the Fletcher Creek Reservoir (MTMQ) near Mt Morgan is owned by the Bureau of Mineral Resources (BMR). The remaining two seismographs are owned by the Applied Physics Department of the University of Central Queensland. The analogue recorder is installed on campus (UCQ), and the digital recorder is located near Byfield (BYFQ). Figure 1 illustrates the location of the seismographs and the detection capability provided by the network for magnitude ML 2 and greater earthquakes. Figure 3 shows response curves for each instrument in the network (Table 2).

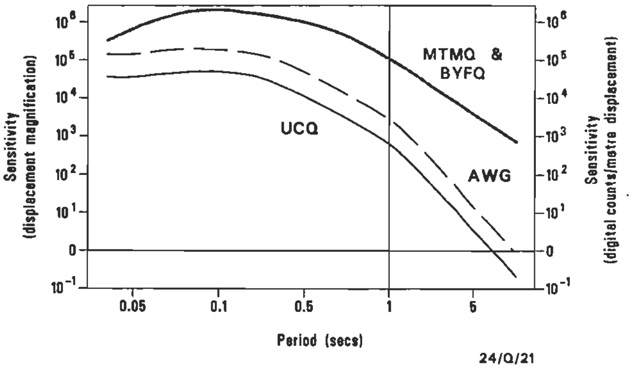

Figure 3. Central Queensland Regional Network analogue and digital recorders response curves.

Data from the seismographs are analysed and interpreted at the University of Central Queensland using a Webster minicomputer and a series of programs written at the Seismology Research Centre, Phillip Institute of Technology, Melbourne. The programs allow data manipulation, analysis and cataloguing as well as location of hypocentres. A three layer crustal model is used to locate hypocentres (Cuthbertson, 1986, 1990). The model has boundaries at 10 and 30 km, with P and S wave velocities of 5.55 km/s and 3.3 km/s in the top layer, and 6.67 km/s and 3.8 km/s in the lower crust. A local earthquake catalogue is compiled at the University of Central Queensland, and copied to the Department of Resource Industries, Brisbane and the Australian Seismological Centre, Canberra.

A small local offshore earthquake with a magnitude of approximately ML 2.4 was recorded on the network at 04:29 UTC on 15 March, 1991. Its location 100 km east of Gladstone was near the presumed epicentre of the 1918 Bundaberg earthquake. Two small earthquakes on 10 June 1991 near Bajool, 35 km south of Rockhampton, were also recorded and felt widely around the epicentre. The larger had a magnitude of ML 2.8. Portable seismographs were installed in the epicentral region and recorded several aftershocks.

Central Queensland blasting

Most seismic events recorded by the network have been explosions, either quarry blasts or coal mine blasts (Table 3). In the central Queensland area, both open cut mining and underground long-wall mining methods are used. We have learnt to differentiate the blasts from earthquakes by their near constant location, coda shape, time of day, and ultimately by confirmation of the blast times with the operators of the quarries and mines.

Table 3. Mines whose blasts are recorded on the Central Queensland regional seismographic network.

Locations given for open-cut mines are approximate, as the mines may be up to 20 km long.

	Location			
Name	*Latitude ° S*	*Longitude ° E*	*Operator*	*Type*
Blackwater	23.77	148.83	BHP, Utah, Curragh	Open cut
Boundary Hill	24.30	150.59	Callide Coal	Open cut
Callide	24.32	150.63	Callide Coal	Open cut
German Creek	22.98	148.55	Capcoal	Open cut & long wall
Goonyella	21.78	147.92	BHP Utah	Open cut
Gregory	23.90	148.17	BHP Utah	Open cut
Marmor	23.68	150.72	Wells Lime Works	Surface quarry blasting
Moura	24.61	150.09	BHP Utah TDM	Open cut & long wall
Mt Etna	23.16	150.45	Central Qld Cement	Surface quarry blasting
Nerimbera	23.40	150.60	Sellars Quarry	Surface quarry blasting
Norwich Park	22.70	148.42	BHP Utah	Open cut
Peak Downs	22.23	148.17	BHP Utah	Open cut
Saraji	22.39	148.27	BHP Utah	Open cut
Taralgoola	24.10	151.24	Frost Enterprises	Surface quarry blasting

The blasts always have large surface wave amplitudes relative to the P or S wave amplitudes, and sometimes surprisingly large shear wave amplitudes compared with those of the P wave. The coda shape of blast seismograms depends on several variables: the quantity of explosives, orientation of the hole spread in relation to the azimuth of the seismograph, and the blast delay interval. It is illegal to blast at night, and the daytime blasts are often timed to coincide with shift breaks; these are two important discriminants for establishing the origin of seismic events on the seismograms.

Ordinance blasts at the Australian Defence Force reserve are usually much smaller than the mine blasts and usually at or near the surface. This makes for smaller seismogram signatures, except for the airblast which travels at the velocity of sound in air (approximately 330 m/s), and is clear evidence of non-earthquake origin.

A database of these blasts and their known signatures is being maintained for future investigations into the crustal structure of central Queensland.

Conclusion

The Central Queensland Regional Seismographic Network has been established to monitor an area of above average seismicity in a densely populated region of central Queensland. The area was identified by a meeting of State, Commonwealth and Territory representatives in May 1990 at the BMR in Canberra following the Newcastle earthquake, as one urgently requiring more intense monitoring for better earthquake hazard evaluation, so that steps can be taken to minimise the probability of structural collapse, injuries and mortalities.

Table 2. Central Queensland Seismographic Network stations.

		Location		Elevation			
Name	*Code*	*Latitude ° S*	*Longitude ° E*	*(m)*	*Foundation*	*Instrument*	*Start date*
UCQ	UCQ	23.323	150.517	35	mudstone	MEQ-800	20.5.90
Byfield	BFYQ	22.820	150.626	80	granite	Kelunji	15.3.91
Awoonga Dam	AWD	24.078	151.316	110	mudstone	MEQ-800	22.9.81
Fletcher Ck	MTMQ	23.763	150.390	170	welded tuff	Kelunji	27.8.90

A database of local earthquakes has been compiled to establish whether any correlation exists between the present day seismicity and the geological structure of the central Queensland region, and to determine the stress field by constructing composite fault mechanism solutions.

Examination of historical records has demonstrated that significant amplification of ground motion has occurred in areas underlain by alluvium in central Rockhampton, relative to those areas situated on firm foundations. A microzonation and geotechnical study should be undertaken to delineate the extent, depth, soil characteristics, relative ground motion amplification and predominant site period of those areas most at risk.

Characteristic signatures of local explosions have been identified to differentiate them from earthquakes, and a database of blasts established to improve the crustal model, and identify and map any listric faults which may underlie the region.

Acknowledgements

Substantial funding for this network has been provided by a research grant from the University of Central Queensland. Col Greensill assisted with the preparation of the seismograph sites, built the field enclosures, and assisted with data collection. Jenny Hafner aided with data collection. Their assistance is gratefully acknowledged.

References

Bell, J.S. & Adams, J., 1990 — Do the rocks remember? How contemporary are regional stresses in Canada? *In* Proceedings of conference *Stresses in Underground structures, October 2–3, 1990, Ottawa, Canada.*

Bryan, W.H. & Whitehouse, F.W., 1938 — The Gayndah earthquake of 1935. *Proceedings of the Royal Society of Queensland*, 49, 106–119.

Cuthbertson, R.J., 1986 — Seismological studies by the Geological Survey of Queensland. *Queensland Government Mining Journal*, Dec. 1986, 495–497.

Cuthbertson, R.J., 1990 — The seismo-tectonics of southeast Queensland. *In* Finlayson, D.M. (editor), The Eromanga—Brisbane geoscience transect. *Bureau of Mineral Resources, Australia, Bulletin* 232, 67–81.

Denham, D. & Windsor, C.R., 1991 — The crustal stress pattern in the Australian continent. *Exploration Geophysics*, 22, 101–105.

Everingham, I.B., Mc Ewan, A.J. & Denham, D., 1982 — Atlas of isoseismal maps of Australian earthquakes. *Bureau of Mineral Resources, Australia, Bulletin* 214.

Falvey, D.A. & Mutter, J.C., 1981 — Regional plate tectonics and the evolution of Australia's passive continental margins. *BMR Journal of Australian Geology & Geophysics*, 6, 1–29.

Fergusson, C.L., Henderson, R.A. & Leitch, E.C., 1988 — Tectonostratigraphic terranes and subduction complex melange, Northern New England orogen. *Central Queensland New England Orogen — tectonics and metallogenesis. Symposium Proceedings, University of New England, Armidale*, 32–41.

Hayes, D.D. & Ringis, J., 1973 — Seafloor spreading in the Tasman Sea. *Nature*, 243, 454–458.

Hedley, C., 1925 — The Queensland earthquake of 1918. *Transactions of the Royal Geographical Society of Australia (Qld). Report of the Great Barrier Reef Committee*, 1, 151–156.

Hough, S.E., Friberg, P.A., Busby, R., Field, E.F., Jacob, K.H. & Borcherdt, R., 1990 — Sediment induced amplification and the collapse of the Nimitz Freeway. *Nature*, 344, 853–855.

Jenkin, J.J., 1984 — Evolution of the Australian coast and continental margin. Coastal geomorphology in Australia. *Academic Press, San Diego*, 23–42.

Johnson, R.W. (editor), 1989 — Intraplate volcanism in eastern Australia and New Zealand. *Cambridge University Press, Cambridge.*

Johnston, A.C., 1982 — A major earthquake zone on the Mississippi. *Scientific American*, 245(4), 52–60.

McCue, K., Wesson, V. & Gibson, G., 1990 — The Newcastle, New South Wales, earthquake of 28 December 1989. *BMR Journal of Australian Geology & Geophysics*, 11, 559-567.

Rynn, J.M.W., Denham, D., Greenhalgh, S., Jones, T., Gregson, P.J., McCue, K.F. & Smith, R.S., 1987 — Atlas of isoseismal maps of Australian earthquakes. *Bureau of Mineral Resources, Australia, Bulletin* 222.

Veevers, J.J., 1984 — Phanerozoic earth history of Australia. *Clarendon Press, Oxford.*

Wellman, P., 1978 — Potassium-argon ages of Cainozoic volcanic rocks from the Bundaberg, Rockhampton and Clermont areas of Central Queensland. *Proceedings of the Royal Society of Queensland*, 89, 59–64.

Willmott, W.F., O'Flynn, M.L. & Trezise, D.L., 1986 — 1:100,000 Geological map commentary, Rockhampton region, Queensland. *Government Printer, Queensland, Brisbane.*

BMR Journal of Australian Geology & Geophysics, 13, 113–129

Stratigraphy and palynology of Mesozoic sediments from the Great Australian Bight area, southern Australia

Neville F. Alley[1] & Jonathan D.A. Clarke[2]

The offshore Mesozoic Bight and Duntroon Basins formed through rifting and separation of the Australian and Antarctic plates. Palynological investigation of samples dredged from the continental slope and submarine canyon walls in these basins during BMR *Rig Seismic* Cruise 66 showed that the bulk of the palynofloras correlate with the Maastrichtian to possibly earliest Paleocene *Forcipites* (al. *Tricolpites*) *longus* spore/pollen Zone and the *Manumiella druggii* microplankton Zone. The zones are characteristic of the upper Potoroo Formation, thus this part of the Formation is widespread in the Bight and Duntroon Basins. Environments of deposition ranged from paralic to marine. Two samples from each of the Bight and western Duntroon Basins contain palynofloras ranging in age from Santonian to Maastrichtian, indicating a lower Potoroo/Wigunda Formation source, and one sample from the Duntroon Basin with an Early Cretaceous palynoflora points to a Ceduna Formation source. Recycled Permian, Neocomian—Aptian and Albian—Cenomanian palynomorphs are common in the Potoroo and Wigunda Formations. These imply the provenance of the Maastrichtian sequences was via streams flowing from the east and north into the Great Australian Bight area. Palynological evidence indicates that lowland temperate rainforests were widespread on the Australian side of the rift at least during the Campanian—Maastrichtian.

Introduction

The sedimentary basins flanking the southern margin of the Australian continent were formed through rifting of the Australian and Antarctic plates (Veevers, 1984, 1987; Stagg & others, 1990). Three structural and morphological sectors of the rift basins consist of the Bremer Basin in the west, the Bight Basin and Duntroon Basin in the central sector and the Otway and West Tasmanian basins in the east (Fig. 1). There is no onshore exposure of the Maastrichtian sediments in the Bight and Duntroon Basins, and there is poor offshore well control.

The Bureau of Mineral Resources (BMR) cruises 65 and 66 were designed to gather more data on the Bight and Duntroon Basins. Cruise 65 collected seismic data; cruise 66 collected geological and geophysical data. Preliminary results of the cruises were published by Willcox & others (1988) and Davies & others (1989). This paper presents the palynology and palynostratigraphy of dredged samples collected on cruise 66 (Fig. 2), correlates these with the known stratigraphy and provides evidence for the vegetation and climate prevailing during Campanian—Maastrichtian times. The work complements foraminiferal and nannofossil biostratigraphic information derived during the same cruise (Shafik, 1990; McGowran, 1991).

Sample processing

Palynological processing in the initial stages followed a standard laboratory procedure involving crushing, boiling in concentrated HCl followed by concentrated HF and heavy liquid separation with $ZnBr_3$ (SG 2). Many of the palynofloras at this stage were found to have undergone significant thermal alteration and preservation was poor. In these cases the oxidation stages (Schulze solution followed by a wash in a dilute solution of K_2CO_3) were omitted or reduced, and in some cases only sieving (129 µ followed by 10 µ) was undertaken after heavy liquid separation.

Microscope analyses and photography were undertaken on a Zeiss Photomicroscope III. Initially counts were attempted on the palynofloras to establish relative frequencies of species and the ratio between pollen/spores and microplankton. Because of

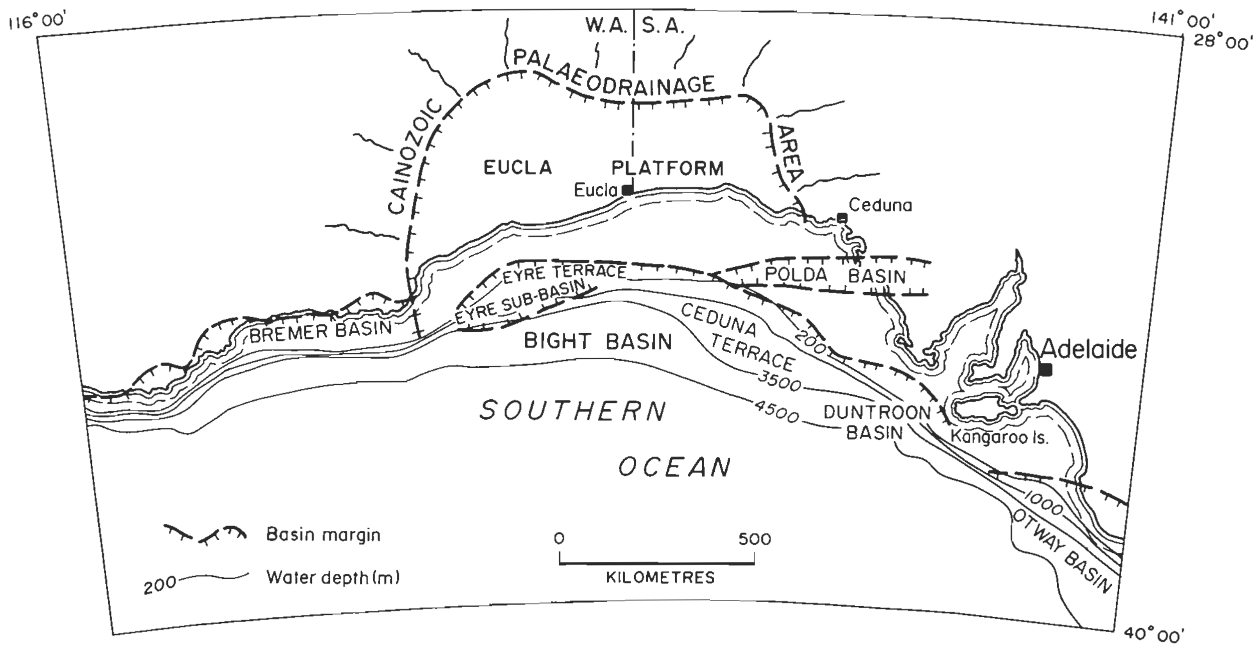

Figure 1. Major Cretaceous and Tertiary basins referred to in the text, and bathymetry of the southern Australian continental margin.

[1] South Australia Department of Mines and Energy, 191 Greenhill Road, Parkside SA 5063
[2] Western Mining Corporation, Preston, VIC 3072

the generally poor preservation and low yields of palynomorphs from the samples, counting was abandoned and only the presence of species and an assessment of their relative abundance were recorded. Detailed records of the palynofloras are available through the South Australian Department of Mines and Energy.

Age determinations are made on the basis of the presence/absence of key species and the general composition of the palynofloras. Some samples contain a mixture of palynomorphs ranging in age from Late Cretaceous to Eocene. Such mixtures are probably a result of contamination during dredging and/or submarine downslope movement of younger materials to be incorporated with older sediment on the continental slope and canyon walls. There is, however, clear evidence of recycling of older palynomorphs into younger sediments, as seen by the presence of low frequencies of Permian, Jurassic and Early Cretaceous palynomorphs in most of the Late Cretaceous palynofloras. In these cases the age determinations were made on the basis of the dominant makeup of the palynofloras.

Citations for fossil taxa used in the text are given in Appendix 1.

Regional setting

The southern Australian continental margin is a divergent passive margin developed during Jurassic and Cretaceous times by extension and rifting between the Australian and Antarctic plates. Seafloor spreading began in the Cenomanian and continues today (Candé & Mutter, 1982; Veevers, 1986; Stagg & others, 1990). The zone affected by the rifting and spreading is referred to as the Southern Rift System (Stagg & others, 1990).

The Great Australian Bight area forms the central part of the Southern Rift System and consists of two superimposed structural systems: an early series of narrow ENE—WSW trending grabens and half grabens and a later, more extensive series of normal faults that define the main basins (Fig. 1; Stagg & others, 1990).

The locations of offshore wells that provide the basis for the stratigraphy are shown in Figure 2 and the stratigraphy is summarised in Figure 3. The Great Australian Bight area developed on a substrate of Precambrian rocks, the Archaean Yilgarn craton and Proterozoic Albany—Fraser Mobile Belt in the west and the Archaean—Proterozoic Gawler Craton in the east (Stagg & others, 1990). Pre-rift cover sediments of Late Proterozoic and Palaeozoic age are locally present beneath the northern part of the Great Australian Bight (Lowry, 1970), representing outliers of the Officer Basin (Jackson & van de Graaff, 1981) or locally preserved Permian sediments such as in the Denman Basin.

The first Mesozoic depositional sequence comprises Jurassic sediments, which have been intersected only in the Polda Basin, but are known to occur over a wide area of the Great Australian Bight in graben and half graben structures. Sedimentation was non-marine, resulting in fluviolacustrine, lacustrine and coal deposits (Bein & Taylor, 1981; Gatehouse & Cooper, 1982).

The second sequence is of Cretaceous age and unconformably overlies the Jurassic sequence. It is made up of the Duntroon and Bight Groups which include sandstone, coal, shale, carbonaceous siltstone and marl (Fig. 3; Cockshell 1990). These sediments were deposited in lacustrine deltas, marine deltas and shallow marine shelf environments.

The third and youngest sequence comprises the carbonates of the Eucla Group (Whyte, 1978; Fraser & Tilbury, 1979) and the largely terrestrial clastic equivalent of the Immarna Group. These sediments disconformably overlie Cretaceous strata largely of the Bight Group and locally the Duntroon Group.

Stratigraphy and palynology of the *Rig Seismic* Cruise 66 samples

Stratigraphic relationships

The interpreted stratigraphic context of the samples from Cruise 66 is given in Appendix 2. Original biostratigraphic and tentative palynological information is recorded in Davies & others (1989); nannofossil assemblages were described by Shafik (1990).

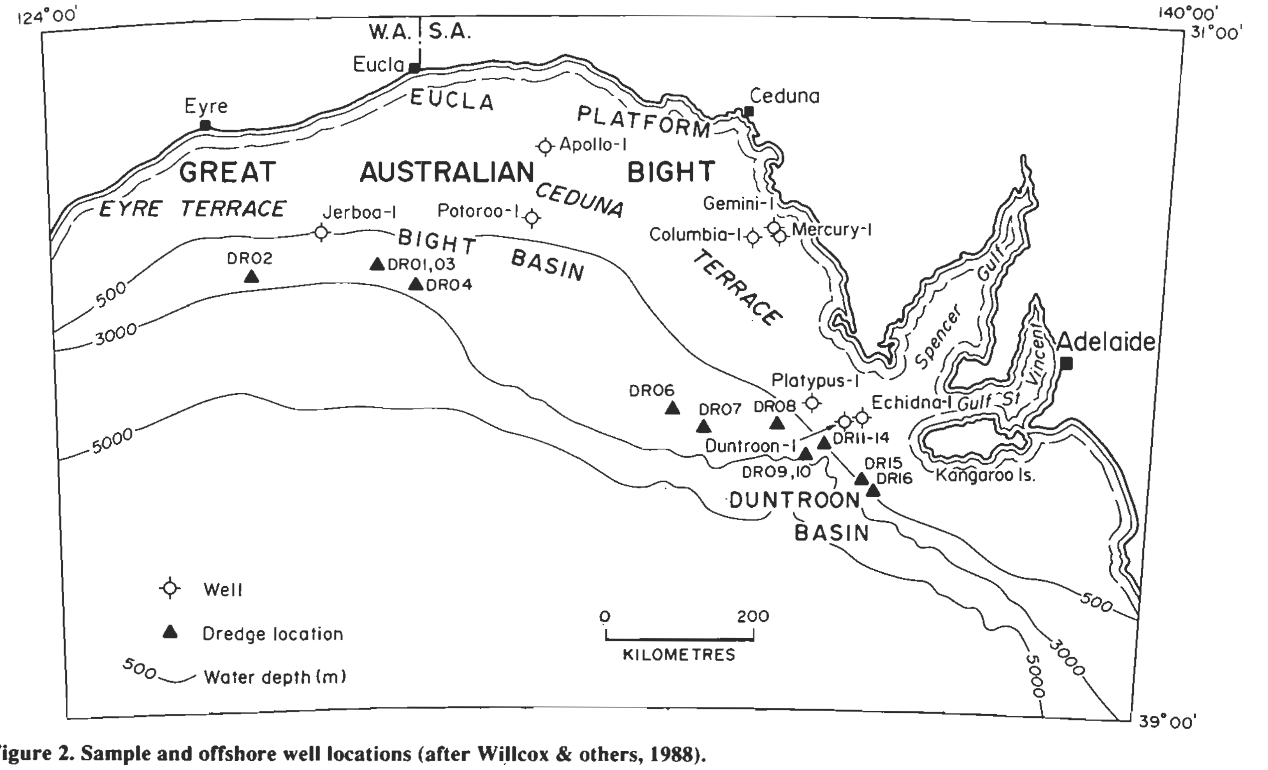

Figure 2. Sample and offshore well locations (after Willcox & others, 1988).

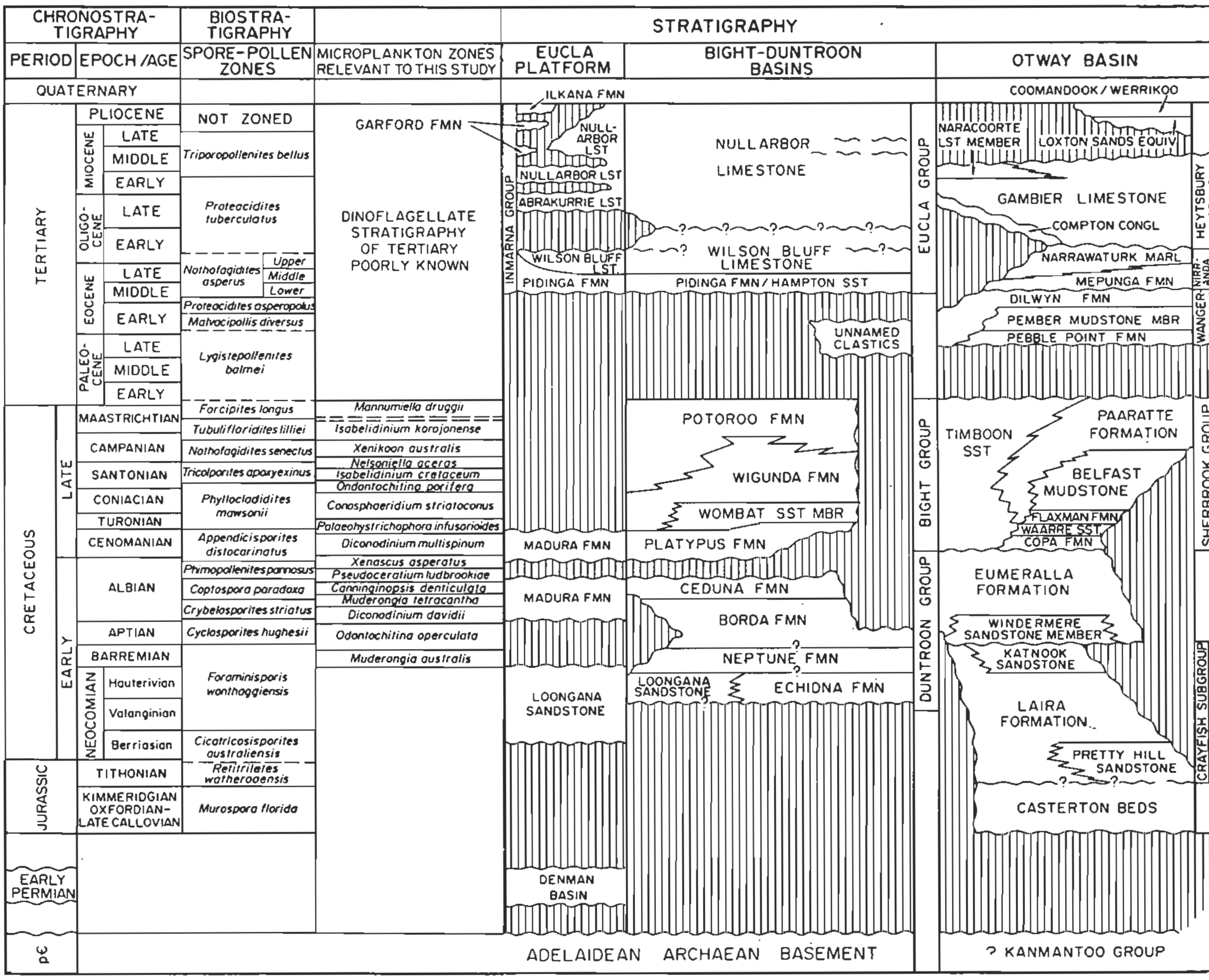

Figure 3. Stratigraphy and palynological zones for the Mesozoic and Tertiary basins of the southern Australian continental margin. Stratigraphy modified from Morton (1990).

The Late Cretaceous samples are mainly glauconitic and calcareous sandstone and conglomerate together with brown-black organic-rich mudstone and siltstone. Most were deposited in a shallow marine environment and are correlated with the estuarine and deltaic facies of the Potoroo and Wigunda Formations. Minor dolomitic sediments, probably deposited in a peritidal environment, are correlated with the dolomite bands in the Wigunda Formation described by Robertson & others (1979).

Palynostratigraphy

The dating and correlation undertaken in this study are based on the Australian Mesozoic palynological zonal scheme developed by Helby & others (1987) with additional information from Morgan (1979). Palynological zonation, age, source unit and interpreted environment of deposition for individual samples are given in Appendix 2.

1. Early Cretaceous. One sample (DR16B) contains only microplankton, a number of which range either from the Aptian or the Albian onwards or range from Aptian to Albian. These include *Callaiosphaeridium asymmetricum, Florentinia deanei, Gonyaulacysta cassidata, Heterosphaeridium heteracanthum, Litosphaeridium siphoniphorum, Protoellipsodinium densispinum, Spiniferites wetzeli* and *Tanyosphaeridium salpinx*. This assemblage is probably Albian in age but lacks the zonal fossils diagnostic of the microplankton zones within this interval.

The Aptian to Albian age and the relatively high diversity of the microplankton assemblage indicate a source in the marine Ceduna Formation.

2. *Odontochitina porifera* to *Nelsoniella aceras* microplankton zones. Sample DR04 contains a sparse assemblage of dinoflagellates including *Odontochitina porifera* and *Palaeohystrichophora infusorioides*, indicating a correlation with either of the above zones.

A marine environment of deposition is indicated on the basis of the presence of the microplankton. The range in age (Coniacian to Campanian) suggests that the sample came from either Potoroo Formation or Wigunda Formation.

3. *Xenikoon australis* to *Isabelidinium korojonense* microplankton zones. Sample DR03C contains a sparse assemblage of pollen and spores of no value in zonation, but the sparse assemblage of dinoflagellates contains *Xenikoon australis* and *Palaeostomocystis reticulata*. The ranges of these two taxa are believed not to overlap (Helby & others, 1987), *P. reticulata* first appearing near the base of the *I. korojonense* Zone and the youngest occurrence of *X. australis* at the base of the same zone. Due to this, the zonation is uncertain and a range in age (Campanian to Maastrichtian) is assigned to the assemblage.

The presence of the microplankton indicates deposition in marine conditions. The sample appears to have come from the lower Potoroo Formation or the Wigunda Formation.

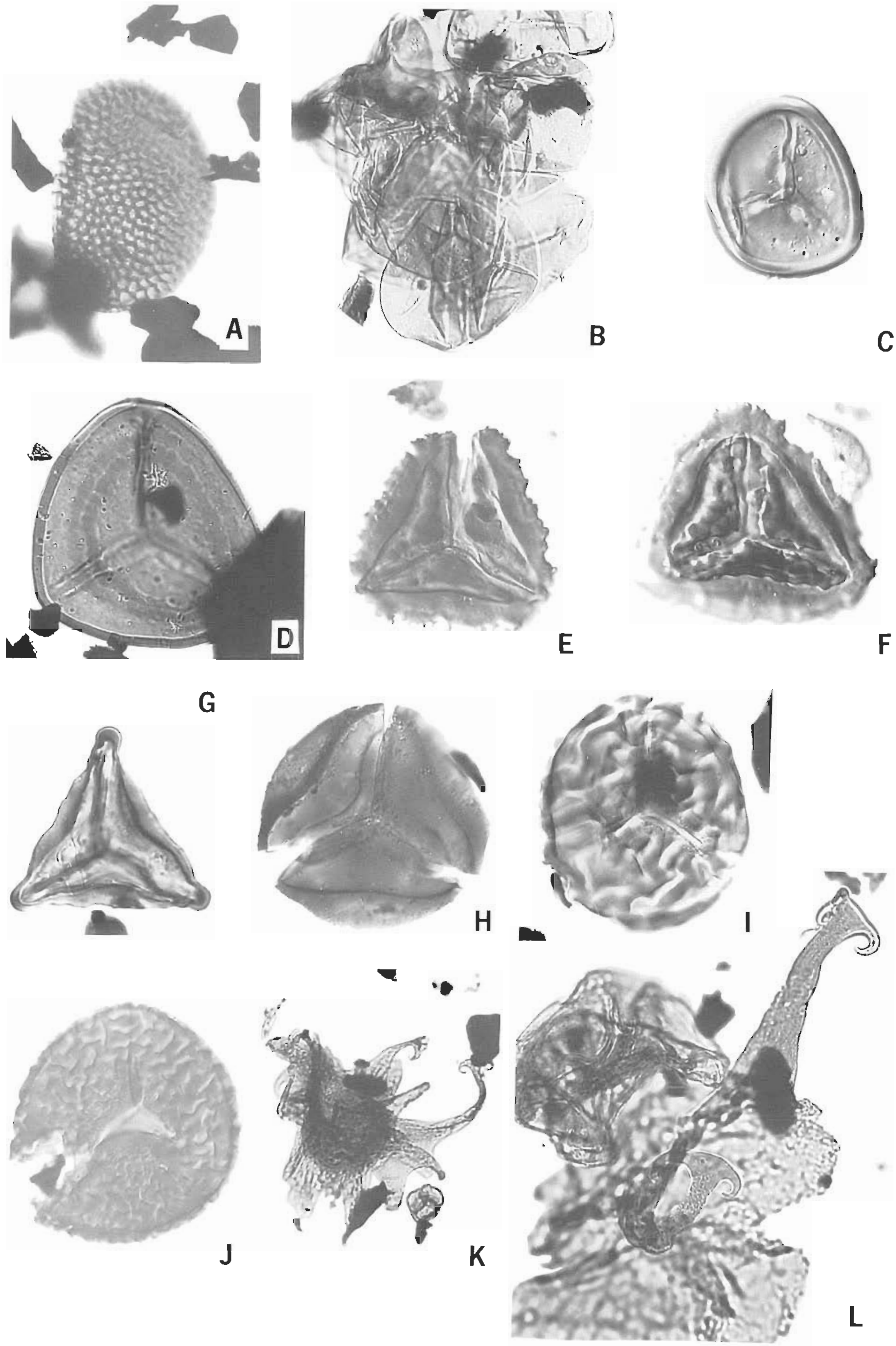
A
B
C
D
E
F
G
H
I
J
K
L

4. Upper *Nothofagidites senectus* to *Forcipites* (al. *Tricolpites*) *longus* spore/pollen zones. An assemblage of pollen and spores from sample DR07H contains *Gambierina rudata*, *Lygistepollenites balmei*, *Nothofagidites endurus* and *Tricolporites apoxyexinus*, indicating at least the above zonal range. This is supported by the presence of a few specimens of *Beaupreaidites orbiculatus* which ranges between these two zones (Dettmann & Jarzen, 1988).

The possible range in age of the sample (Campanian to Maastrichtian) indicates that it has come from either the Potoroo or the Wigunda Formation. The presence of a very sparse microplankton assemblage suggests a paralic environment of deposition.

5. *Isabelidinium korojonense* to *Manumiella druggii* microplankton zones. Sample DR09C contains a diverse spore/pollen assemblage lacking zonal fossils, but contains a diverse microplankton assemblage that includes *Manumiella druggii*, *Isabelidinium belfastense*, *I. bakeri* and *I. pellucidum*. The ranges of *M. druggii* and *I. belfastense* do not overlap (Helby & others, 1987); the range of *I. pellucidum* lies between the ranges of these two species, but does not overlap with either of them. In view of the problems of recycling of palynomorphs the sample cannot be dated precisely. A Campanian—Maastrichtian age is supported by the occurrence of the pollen *Nothofagidites senectus* and *Tricolporites apoxyexinus* and the spores *Ornamentifera sentosa* and *Stereisporites* (*Tripunctisporis*) sp.

The range in age of the sample (Campanian to Maastrichtian) indicates a source from either the Potoroo Formation or upper Wigunda Formation. An open marine setting is suggested by the presence of the diverse microplankton assemblage.

6. *Forcipites longus* spore/pollen Zone and *Manumiella druggii* microplankton Zone. Most of the samples contain palynofloras that allow a correlation with either of these Maastrichtian to possibly early Danian zones (Appendix 1). Many of these samples contain pollen, spores and microplankton and thus it is possible to assign both zones to individual samples, providing a high degree of confidence with the determinations.

Spore/pollen assemblages assigned to the *Forcipites longus* Zone may contain *F. longus* in association with *F.* (al. *Tricolpites*) *sabulosus*, *Grapnelispora evansii*, *Quadraplanus brossus*, *Ornamentifera sentosa*, *Tubulifloridites* (al. *Tricolporites*) *lilliei*, *Gambierina rudata*, *Tetracolporites verrucosus* and *Peninsulapollis* (al. *Tricolpites*) *gillii*. A number of other taxa are also sporadically present, including *Proteacidites scaboratus*, *Stereisporites viriosus*, *Triporopollenites sectilis*, *Nothofagidites endurus*, *N. senectus*, *Anacolosidites* sp., *Microfoveolatosporis* sp., *Tricolpites reticulatus* and *Beaupreaidites orbiculatus*. The consistent occurrence of the spore *Stereisporites* (*Tripunctisporis*) sp. in many of the samples suggests that these palynofloras may be from the upper part of the *F. longus* Zone.

Microplankton assemblages assigned to the *Manumiella druggii* Zone contain, in association with the nominate species, *Manumiella conorata*, *Alisocysta circumtabulata* and *Palaeostomocystis reticulata*, which can be the dominant taxa, and *Fromea chytra*. The consistent occurrence of *Isabelidinium cretaceum*, *I. belfastense*, *I. pellucidum*, *Microdinium ornatum* (which is common in a few samples) and *Dinogymnium nelsonense* suggests that recycling of dinoflagellates ascribed to preceding zones has occurred.

The lithology of the sediments and age of the palynofloras indicates that these samples from the Bight and Duntroon Basins were dredged from the upper part of the Potoroo Formation. The frequency and diversity of the microplankton assemblages suggests that the conditions of deposition ranged from paralic to marine, although no pattern could be discerned from the areal distribution of these environments.

Recycled palynomorphs

Recycled palynomorphs are common in the Potoroo and Wigunda Formations (Appendix 3). Although many of these fossils are long ranging, they can be divided into broad age groups which are useful in inferring the provenance of the sediments in which they were transported.

1. Permian recycled palynomorphs. The oldest fossils are of Permian age and were recovered only from sediments in the Duntroon Basin (Appendix 3). The source for these palynomorphs is probably the Early Permian Cape Jervis Formation in the Troubridge Basin to the east and northeast of the sample sites. The nearest Permian sediments are on Kangaroo Island. It is possible, however, that some of the palynomorphs occurring in samples in the western part of the Duntroon Basin may have been derived from the Permian in the Polda Basin to the north or perhaps even the Denman Basin to the west.

The occurrence of *Dulhuntyispora* cf. *D. omasi* in the sample DR12G about 150 km due west of Kangaroo Island is intriguing. This genus does not occur below Stage 5 palynofloras in the Australian Permian palynofloral zonal system (Evans, 1969; Price, 1983) and is indicative of Late Kungurian or younger Permian assemblages. Sediments of this age are not known from Permian basins nearby, including the Denman, Polda, Arckaringa, Troubridge and Nadda (sub Murray Basin) basins. The source is either a now eroded younger unit in these basins or is much more distant, from the Perth, Cooper, Springfield or Oakland basins where younger Permian sediments occur.

The nearest Kungurian or younger Permian sediments are found at depth in the small Permian—Triassic Springfield Basin in the southern Flinders Ranges of South Australia. However, there is no evidence of Mesozoic channels draining southwards from the Springfield area to the Duntroon Basin, nor have recycled specimens of *Dulhuntyispora* spp. yet been found in Mesozoic and Tertiary sediments adjacent to this basin.

Rare specimens of recycled *Dulhuntyispora* spp. are encountered in the Early Cretaceous strata underlying the Murray Basin. It is thus possible that a sediment source for the Duntroon Basin could have been as far away as the Permian in the Oaklands Basin of southwestern New South Wales. In view of the position of the Cretaceous sediments on the northern side of the rift and their progradational aspect from the east and north, an Antarctic source for the recycled Permian palynomorphs is unlikely.

Figure 4. Magnification ×500 unless otherwise stated.
A, *Microfoveolatosporites* cf. *M. fromensis*, equatorial view of ornamentation that is more strongly developed than usually found on this species, ×200, S6444/1. **B,** *Cyathidites minor*, group of spores, S6421/1. **C,** *Stereisporites* (*Tripunctisporis* sp.), proximal surface, ×790, S6443/1. **D,** *Stereisporites viriosus*, proximal surface with focus on the amb, S6443/2. **E, F,** *Ornamentifera sentosa*. e, Proximal view of well developed, ragged cingulum, ×790, S6412/2; f, proximal polar surface showing rugula developed on the contact areas, S6446/2. **G,** *Clavifera triplex*, equatorial view of undulating cingulum, ×790, S6412/1. **H,** *Camarozonosporites bullatus*, proximal surface showing thickened labra and broad cingulum, S6444/2. **I, J,** *Camarozonosporites amplus*. i, specimen with large ridges emanating from laesura, S6443/1; j, View of ruptured distal surface with granulae about the distal pole, S6443/1. **K, L,** *Grapnelispora evansii*. k, Specimen with only two appendages intact, ×200, S6415/2. l, Closer view of appendages, S6446/1.

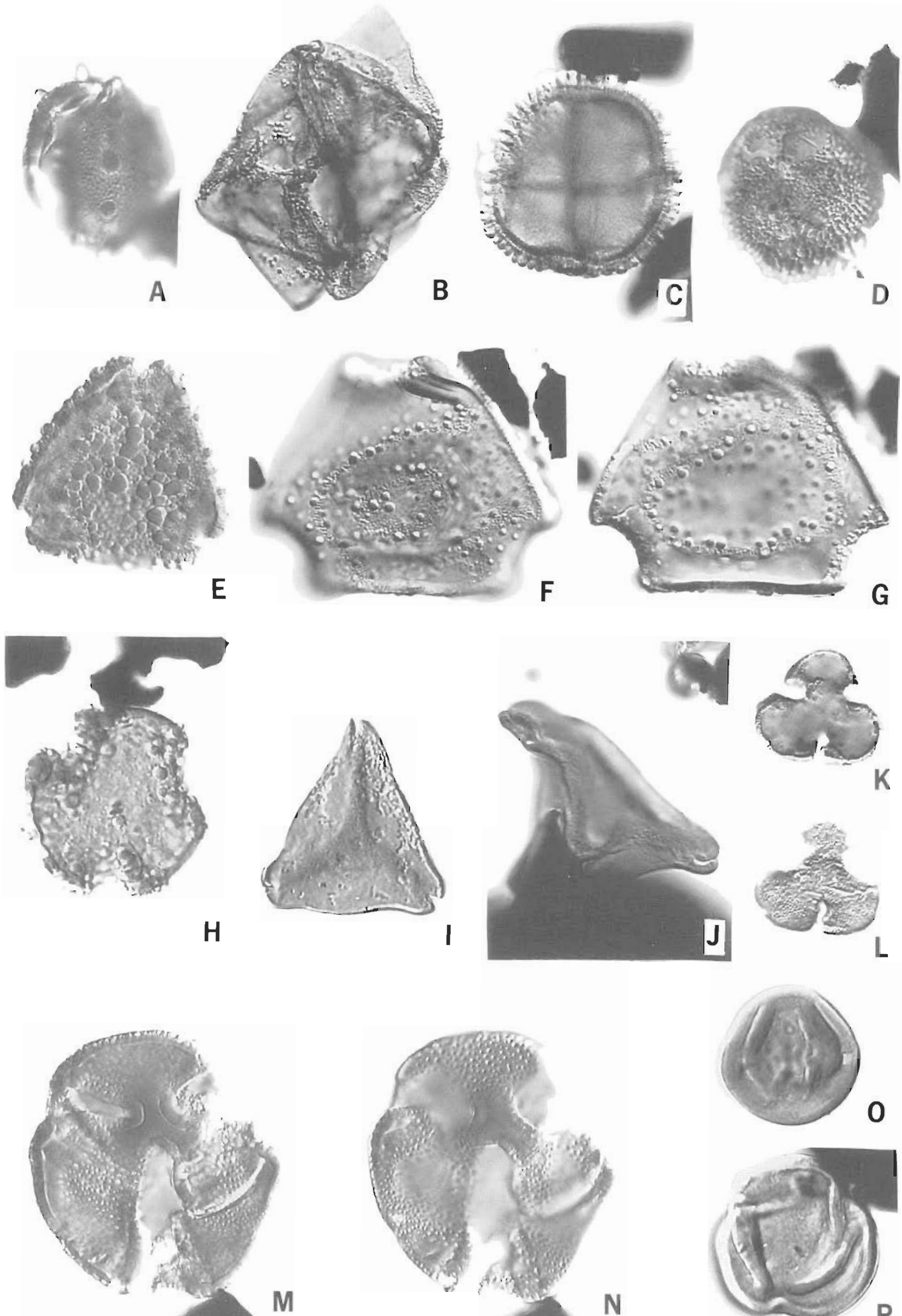
A
B
C
D
E
F
G
H
I
J
K
L
M
N
O
P

2. Late Jurassic—Early Cretaceous recycled palynomorphs. The largest proportion of recycled palynomorphs in the Potoroo and Wigunda Formations ranges in age from Late Jurassic to Early Cretaceous (Appendix 3). The most likely source for these is the Duntroon Group. A few Aptian—Albian dinoflagellates in the lower Potoroo Formation and/or the Wigunda Formation can only have come from the Borda Formation or the marine facies of the Platypus Formation in the Bight Basin. The presence of the Late Jurassic—Early Cretaceous palynomorphs in the Bight Group indicates that a measure of erosion of the Duntroon Group occurred before deposition of the Late Cretaceous sequence. This interpretation is in agreement with a hiatus between the Ceduna and Platypus Formations in the Bight Basin.

A number of pollen and spore species which are relatively common, or at least occur consistently in the Jurassic and infrequent in the Early Cretaceous, are well represented in the recycled palynomorphs. These include *Callialasporites* spp., *Classopollis* spp. and *Murospora florida*. This may indicate that some of the Potoroo and Wigunda Formations were sourced from the Jurassic Polda Formation in the Polda Basin.

3. Albian—Cenomanian recycled palynomorphs. Palynomorphs with this age range are well represented in the Potoroo and Wigunda Formations and have probably been reworked from the upper Duntroon Group. The presence of the dinoflagellate *Diconodinium psilatum* implies a source from either the Ceduna Formation or the marine facies of the Platypus Formation in the Bight Basin.

The zonal pollen *Phimopollenites pannosus* is reworked into the Potoroo and Wigunda Formations in the Bight and Duntroon Basins. In view of the absence of sediments containing the *P. pannosus* Zone palynofloras in the Bight Basin (Fig. 3, represented by the hiatus in the late Albian section), it is compelling to argue for some erosion of the upper part of the Ceduna Formation.

Regional correlation

Otway Basin

The Mesozoic Otway Basin is separated from the Duntroon Basin by a basement high consisting predominantly of Late Proterozoic—Ordovician sediments, granites and metasediments of the Adelaide Geosyncline and Kanmantoo Trough.

The oldest sequence in the Otway Basin is represented by the Otway Group, composed predominantly of mudstone, siltstone and volcanoclastic sandstone with minor coal deposited in a non-marine rift environment. The lower part of the Group, which includes Pretty Hill Sandstone, Laira Formation and Katnook Sandstone, has been placed in the Crayfish Subgroup (Morton, 1990).

Palynofloras from the Pretty Hill Sandstone and lower Laira Formation in the lower Otway Group correlate with the *Cicatricosisporites australiensis* and *Foraminisporis wonthaggiensis* zones, indicating a Neocomian age and time equivalence with the Loongana/Echidna and Neptune formations of the Bight Basin (Fig. 3). The upper Otway Group, comprising Katnook Sandstone and Eumeralla Formation, contains palynofloras indicating that the sediments range from the upper *F. wonthaggiensis* Zone to the *Phimopollenites pannosus* Zone (Aptian to Albian). The *P. pannosus* Zone is of limited areal extent within the Eumeralla Formation.

The Late Cretaceous sequence (Sherbrook Group) unconformably overlies the Otway Group. This clastic sequence was deposited in marine and deltaic environments, with progradation of non-marine coal-bearing deposits in the upper part of the section.

The Sherbrook Group contains a number of units with markedly time transgressive boundaries (Morton, 1990). The Timboon Sandstone contains palynofloras ranging from the *Appendicisporites distocarinatus* Zone to the *Forcipites longus* Zone (Morton, 1990), indicating an age range from Cenomanian to Maastrichtian and perhaps even earliest Paleocene (Fig. 3). A similar age range applies to the Paaratte Formation although its base is a little younger than that of the Timboon Sandstone. Palynofloras from the Copa, Waarre and Flaxman formations correlate with the *A. distocarinatus* Zone of Cenomanian age. Belfast Mudstone palynofloras range from the *A. distocarinatus* Zone through to the *Tricolporites apoxyexinus* Zone (Cenomanian to Santonian), and the sediments are time equivalents of the Platypus and Wigunda Formations in the Bight Basin.

Eastern Antarctic basins

The stratigraphy and depositional history of the eastern Antarctic margin is poorly known. An overview of the marginal basins of Antarctica was given by Quilty (1986), while the conjugate Australian and Antarctic margins were compared by Veevers (1987). The seismic stratigraphy of the Adelie coast (Wannesson, 1990) can be closely compared with the Bight and Otway Basins.

The seismic reflection data show many similarities to the southern Australian margin. Synrift sedimentation along the eastern Antarctic continental margin began in the Jurassic and continued until the Early Cretaceous. Post rift sedimentation has occurred since the Early Cretaceous. Synrift and early post rift sediments of Jurassic, Cretaceous and earliest Tertiary ages are probably very similar to those of the southern margin of Australia.

The palynological record of eastern Antarctica is scanty. The only *in situ* Mesozoic sediment is a non-marine clay in George V Basin (Dormack & others, 1980; Dormack & Anderson, 1983), although recycled Mesozoic palynomorphs are common in offshore Pleistocene sediments. Three suites are present, including Permian assemblages found only in the Shackleton Ice Shelf area, and Late Jurassic to Early Cretaceous and Late Cretaceous to early Tertiary assemblages elsewhere (Truswell, 1982, 1983).

Non-marine Late Jurassic/Early Cretaceous recycled palynofloras have been tentatively correlated with Loongana/

Figure 5. Magnification ×790 unless otherwise stated.
A, *Spinozonocolpites* cf. *S. prominatus*, spines thicker and lower in amplitude than characteristic of the species, S6412/1. **B,** *Amosopollis cruciformis*, showing granulate surface of the cells, S6443/1. **C, D,** *Quadraplannus brossus*. c, View showing the junction between individual pollen grains and baculate ornamentation around amb, 5500, S6444/1; d, view of surface ornamentation, S6415/2. **E,** *Beaupreaidites verrucosus*, S6412/1. **F–H,** *Beaupreaidites orbiculatus*. f, View of gemmate ornamentation, S6422/1; g, Ragged characteristics of the colpi, S6422/1; h, Clustering of gemma around colpi and the development of a faint ora, S6413/1. **I, J,** *Forcipites longus*. i, Corroded specimen lacking ornamentation, S6413/2; j, Folded specimen with scabrate ornamentation preserved, S6446/1. **K, L,** *Tricolpites reticulatus*, S6413/1. k, View of equator showing deeply incised colpi and characteristic trilobate form; l, Polar view of finely reticulate ornamentation. **M, N,** *Tricolporites* sp., S6447/1. m, Oblique polar view showing lack of ornamentation at the poles and nexinal thickening adjacent to the colpi; n, Optical section and surface view of ornamentation showing expanded clava heads, partly fused to form a perforate tectum. **O, P,** *Tricolporites apoxyexinus*. o, Equatorial view, S6444/1; p, Oblique polar view, S6444/2.

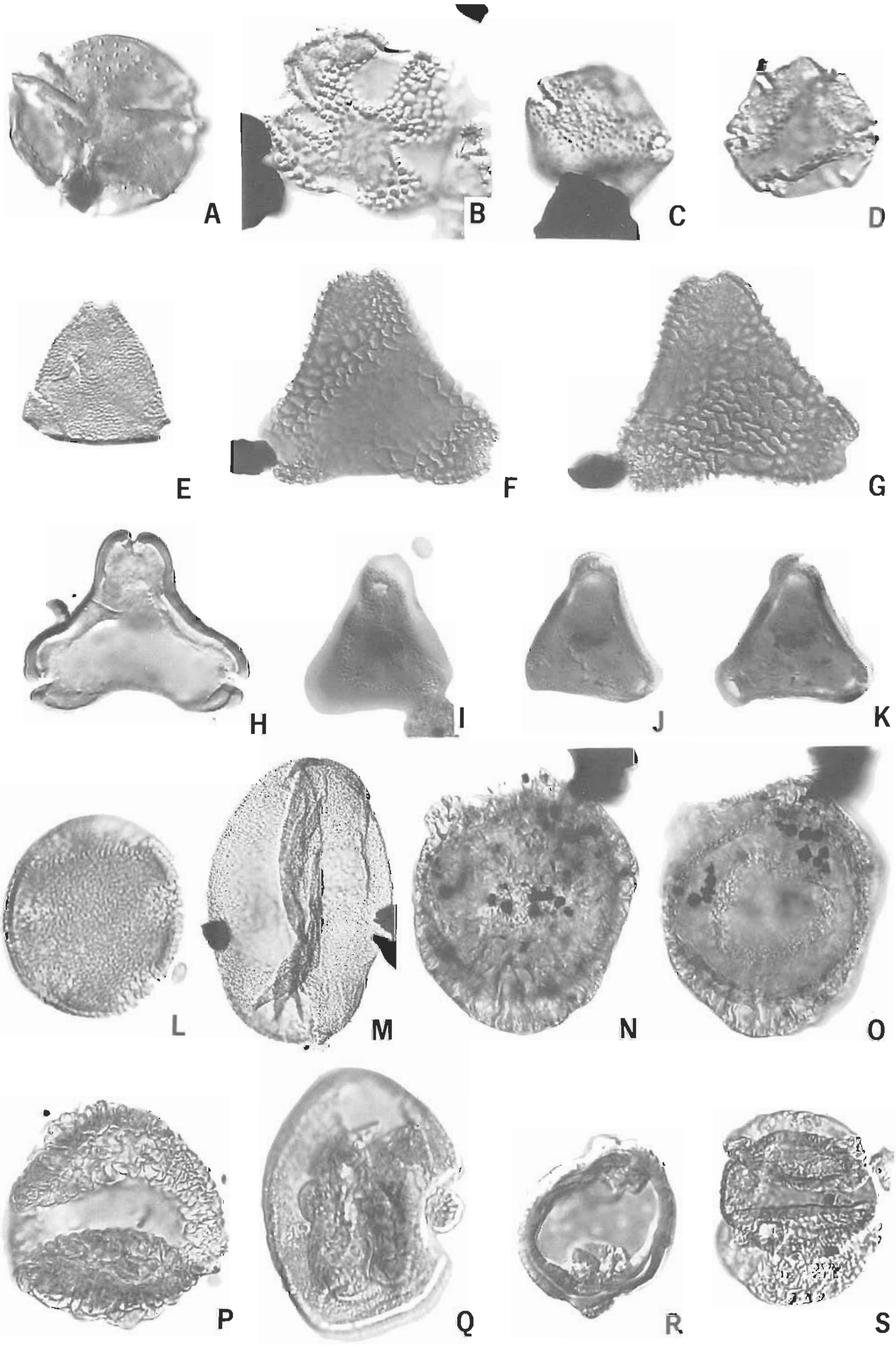
A
B
C
D
E
F
G
H
I
J
K
L
M
N
O
P
Q
R
S

Madura and Platypus Formations of the Bight Basin (Truswell, 1982). However, based on the recycled taxa present, they could fall into two palynological zones. The older correlate with the *Cicatricosisporites australiensis* Zone of latest Jurassic to early Neocomian age and the younger the Albian *Coptospora paradoxa* Zone. This suggests that the older palynofloras may have been derived from rocks equivalent to the Loongana/ Echidna Formation in the Bight Basin and the younger from the Ceduna Formation.

The composition of the Late Cretaceous/early Tertiary pollen and spore assemblages along with the dinoflagellates (Truswell, 1982) suggests an age range from Maastrichtian to perhaps Eocene. Thus equivalents of the Potoroo and Pidinga Formations may be present along eastern Antarctica.

Phytogeographic implications of the Maastrichtian palynofloras

Studies of the southern Australian and Antarctic vegetation during the Late Cretaceous (Campanian—Maastrichtian) show that podocarp-rich coniferous forests, including *Podocarpus*, *Dacrydium* and *Lagarostrobus*, and the araucarians were widespread (Dettmann, 1981, 1989; Dettmann & Jarzen, 1988, 1990; Dettmann & Thomson, 1987). These elements also dominate palynofloras from the Bight and Duntroon Basins. They are represented by common to abundant *Podocarpidites ellipticus* (*Podocarpus*), *Lygistepollenites florinii* (*Dacrydium*), *Phyllocladidites mawsonii* (*Lagarostrobus*) and *Araucariacites australis* (*Araucaria*), but *Dacrycarpus* is absent. The araucarians are probably also seen in the form of *Dilwynites granulatus* and *D. tuberculatus* which occur consistently in the palynofloras.

Such a forest association has modern analogues in the temperate and tropical rainforests fringing the western and southeastern Pacific. One anomaly in the Great Australian Bight palynofloras, however, is the common occurrence of the trisaccate pollen of *Microcachryidites antarcticus* which is comparable to pollen of extant *Microcachrys tetragona* Hooker (J.D. Hooker, 1845), a species restricted to the subalpine areas of montane Tasmania.

The presence of plants normally associated with montane rainforest is supported by the consistent occurrences of the pollen of *Beaupreaidites elegansiformis*, *B. verrucosus* and *B. orbiculatus*. These pollen taxa are allied to extant *Beauprea* which often occurs as a shrub or understorey tree in montane rainforests and upland heathlands in New Caledonia (Dettmann & Jarzen, 1990).

Other arboreal rainforest taxa present in the palynofloras are occasional occurrences of *Nothofagidites senectus* and *N. endurus*, representing the ancestral forms of the extant genus *Nothofagus* (southern beech), and rare specimens of *N. brachyspinulosus* and *N. flemingii* which are comparable to pollen of living species within subgenera *Nothofagus* and *Fuscospora*. All of these records are from the Duntroon Basin. The extant subgenera today grow in the cool temperate rainforests of Tasmania, New Zealand and Chile (Dettmann & others, 1990).

A pollen group well represented in the Great Australian Bight palynofloras is that indicative of the Proteaceae, some taxa of which have palaeoclimatic implications. *Macadamia* pollen is present as rare occurrences of *Propylipollis* (al. *Proteacidites*) *scaboratus*. The extant genus grows in the rainforests of Queensland and New Caledonia. More frequent records of *Gevuina* and/or *Hicksbeachia* pollen are present as *Proteacidites tripartitus* and *Propylipollis* (al. *Proteacidites*) *reticuloscabratus*. The modern genera are distributed in the rainforests of Queensland, Papua New Guinea and Chile. Dettmann & Jarzen (1990) note the strong similarity between the pollen of *Proteacidites amolosexinus* and the extant genus *Knightia*, which is an emergent rainforest tree in New Zealand and New Caledonia. Of all the above Proteaceae pollen, *P. amolosexinus* is the most consistently occurring species in the Great Australian Bight palynofloras.

Ilex, a genus which in Australia is currently restricted to humid tropical areas, occurs consistently in the palynofloras as *Ilexpollenites anguloclavatus* and occasionally as *I. megagemmatus*. Elsewhere the extant genus is widely spread in cool temperate to tropical humid montane to lowland locations as a tree, shrub or creeper.

More than half the samples from the Great Australian Bight contain low frequencies of *Australopollis obscurus* which is believed to have strong affinities to the pollen produced by *Trimenia* (Dettmann & Jarzen, 1990) or *Callitriche* (Partridge & Macphail, 1990). The former genus is restricted to warm humid areas of the central to western Pacific; in New Caledonia one species grows in association with *Nothofagus* and araucarian rainforest. On the other hand, *Callitriche* is an aquatic herb widely distributed in eastern and southeastern Australia, New Zealand, Chile, Asia, southern Europe and North America.

Tricolpites reticulatus, a rare species in the Great Australian Bight palynofloras, is very closely allied to the pollen of extant *Gunnera*. The latter genus is currently distributed in Southern Hemisphere tropical to temperate rainforests. This group of herbs is a strong coloniser of open areas such as stream banks, and could have been established along the river channels upstream of deltas during deposition of the Potoroo and Wigunda Formations.

The forest association was complemented by abundant ferns and mosses. Tree ferns are well represented as *Cyathidites australis* and *C. minor*, a number of ferns as *Baculatisporites comaumensis*, *B. disconformis*, *Osmundacidites wellmanii*, and the Polypodiaceae as *Laevigatosporites major* and *L. ovatus*. Sphagnum (peat) moss is common as *Stereisporites antiquasporites* and clubmoss as *Retitriletes austroclavatidites*. *Gleichenia* spores are very common in some samples as *Gleicheniidites circinidites* and *G. senonicus* and more rarely as *Clavifera triplex* and *Ornamentifera sentosa*, all indicating relatively warm conditions.

Although most of the above extant taxa are found in tropical areas, they are usually associated with more temperate, montane forests. Thus, the phytogeographic implications of the palynofloras are that either these were temperate montane rainforests existing within a general tropical climate, or that the

Figure 6. Magnification ×790 unless otherwise stated.
A, *Tubulifloridites lilliei*, polar view, S6447/1. **B**, *Tetracolporites verrucosus*, polar view, S6444/2. **C, D**, *Nothofagidites senectus*. c, View of evenly distributed spinose ornamentation, S6413/1; d, Polar view of folded specimen showing u-shaped terminations to the colpi, S6447/1. **E**, *Proteacidites amolosexinus*, polar view, S6413/2. **F, G**, *Proteacidites* sp., different polar views of the ornamentation, S6442/1; superficially resembles *Proteacidites kopiensis* Harris, 1972, except that the ornamentation remains coarse in the polar areas, the exine curves in and the nexine thickens slightly near the pores. **H**, *Gambierina rudata*, S6446/2. **I–K**, *Anacolosidites* sp., S6412/1. i, View of pore located very close to apices of pollen; j, Optical section showing exine stratication and fine columellae of the sexine; k, Equatorial view showing pores located close to apices. **L**, *Australopollis obscurus*, S6415/2. **M**, *Araucariacites australis*, ×500, S6442/2. **N, O**, *Lygistepollenites balmei*, ×500, S6430/1. n, View of proximal cap; o, Optical section showing rod-like ornamentation. **P**, *Lygistepollenites florinii*, S6415/2. **Q**, *Phyllocladidites mawsonii*, view of folded in sacci, S6444/1. **R**, *Phyllocladidites verrucosus*, S6446/2. **S**, *Podocarpidites ellipticus*, S6422/1.

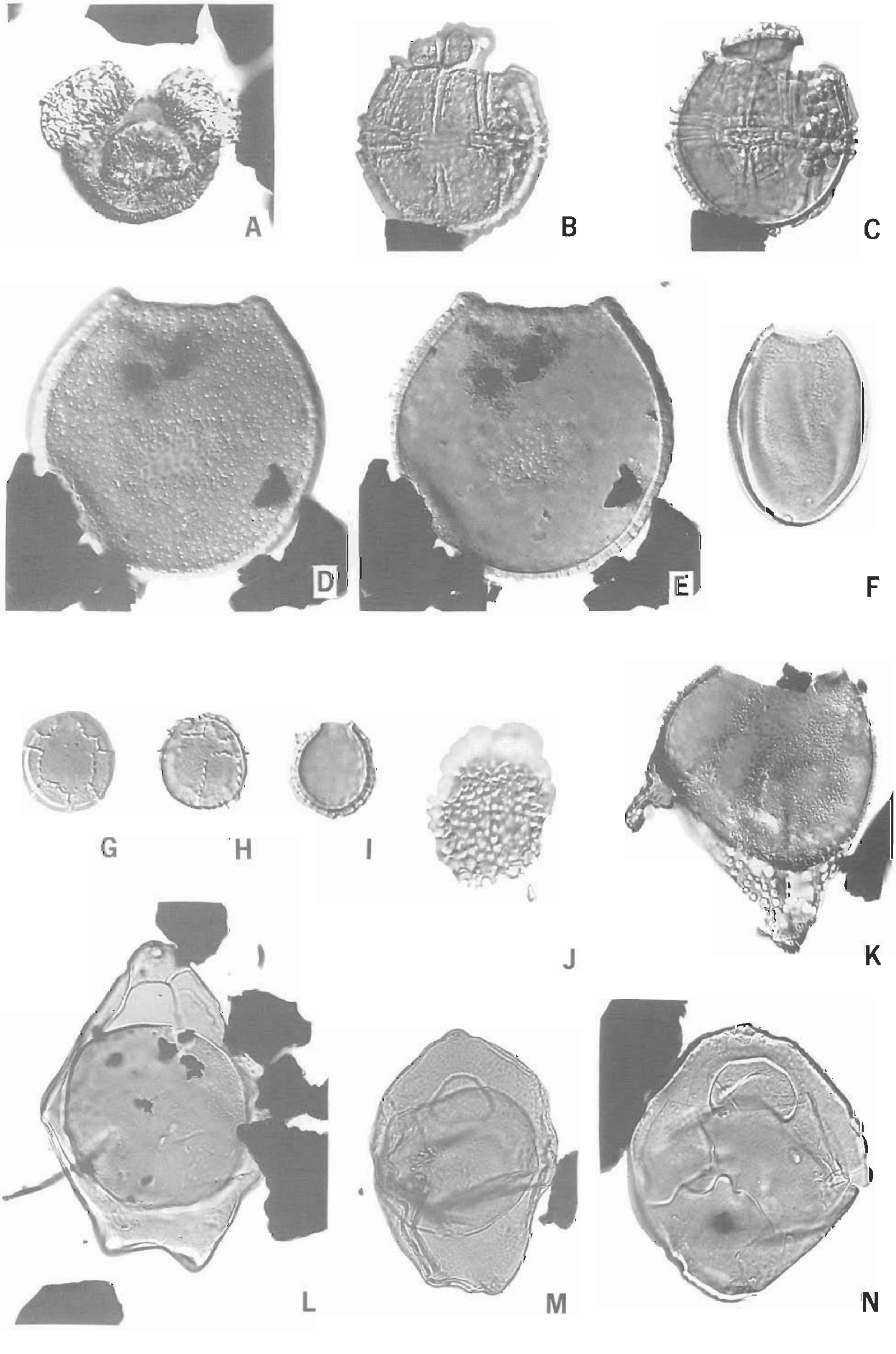
A
B
C
D
E
F
G
H
I
J
K
L
M
N

rift area experienced lower temperatures, allowing temperate rainforests to prevail in lowland areas. The latter probably applies because there is no evidence to support the presence of significant uplands adjacent to the Great Australian Bight on the Australian side of the rift in Maastrichtian times.

The difficulties in determining the modern affinities for the above Late Cretaceous taxa are readily acknowledged. The mixture of apparently tropical through to subalpine taxa growing in a lowland plain environment poses a dilemma in palaeoecological interpretation. It should be borne in mind that the ecological tolerances of a number, or all, of the species may have changed with time and that there may be no simple modern analogue for the fossil spectra.

However, in general the palaeoclimatic interpretations are similar to other biostratigraphic and isotopic evidence from the Maastrichtian sediments along the southern Australian margin and Antarctica. For example, nannofossil data from the Bight Basin and south Perth Basin contain faunas indicative of relatively high latitudes or cool to cold surface water temperatures (Davies & others, 1989; Shafik, 1990, 1991). Estimates of surface water temperatures near the coast of Antarctica from an oxygen isotope study of benthic foraminifera indicate temperate climatic conditions during the Maastrichtian (Barrera & others, 1987).

Conclusions

The *Rig Seismic* Cruise 66 obtained samples mainly of Late Cretaceous (Campanian—Maastrichtian) and Tertiary age. Most of the samples analysed for palynology are Maastrichtian to possibly earliest Paleocene in age and have come from the Potoroo Formation and to a lesser extent from Wigunda Formation. This indicates that the prograding shallow water to paralic Potoroo Formation is widespread on the continental shelf and slope.

The data agree with the nannofossil and foraminiferal evidence (Shafik, 1990, 1991; McGowran, 1991) that show marine influence along the southern Australian margin during the Maastrichtian to be more widespread than previously thought (Frakes & others, 1987). The transgression is named 'Ceduna Ingression' and dated as Late Maastrichtian (McGowran, 1991) which is consistent with the palynological correlations of upper *Forcipites longus* Zone for a number of samples from the Great Australian Bight.

There seem to have been two sources of sediment for the Campanian—Maastrichtian units. Major rivers draining from the east eroded Permian rocks in the upper reaches of the present River Murray and the St Vincent Gulf area and redeposited them along the eastern and northern margins of the Duntroon Basin. Other sediment may have been transported by southerly flowing streams providing sources of sediment from Permian and Jurassic rocks on Eyre Peninsula and areas further west.

The other major source of sediment for the latest Cretaceous sequences appears to have been from erosion of the Duntroon Group and, to a lesser extent, the lower part of the Bight Group. A significant phase of exposure of the Early Cretaceous units, in particular the Ceduna Formation, is indicated by the late Albian hiatus in the Bight Basin and the presence of recycled palynofloras of this age in the overlying strata. The hiatus, which is widespread in the Great Australian Bight and partly in the Otway Basin, may represent a major rifting phase between Australia and Antarctica.

During the Maastrichtian, the southern continental margin of Australia lay between 60°S and 70°S latitude. The presence of widespread podocarp—araucarian-dominated temperate rainforest in this area and adjacent Antarctica and southern South America (Dettmann, 1989) indicates lack of the latitudinal climatic zonation that currently exists. The implication also is that the global climate was significantly warmer than present.

Acknowledgements

We greatly appreciate the comments of D.I. Gravestock and A.J. Hill on the stratigraphy of the Bight and Duntroon Basins and N.G. Marshall for invaluable advice on the Late Cretaceous microplankton assemblages. Suggestions made by the referees, M.E. Dettmann and S. Shafik, greatly improved the text. Drafting was undertaken by the Drafting Branch, South Australian Department of Mines and Energy. N.F. Alley publishes with the permission of the Director-General, South Australia Department of Mines and Energy.

References

Barrera, E., Huber, B.T., Savin, S.M. & Webb, P., 1987 — Antarctic marine temperatures: Late Campanian through Early Paleocene. *Palaeoceanography*, 2, 21—47.

Bein, J. & Taylor, M.J. 1981 — The Eyre Sub-basin: recent exploration results. *The APEA Journal*, 21, 91—98.

Cande, S.C. & Mutter, J.C., 1982 — A revised identification of the oldest sea-floor spreading anomalies between Australia and Antarctica. *Earth and Planetary Science Letters*, 58, 151—160.

Cockshell, C.D., 1990 — A seismic study of the Duntroon Basin. *South Australia Department of Mines and Energy, Report Book* 90/28 (unpublished).

Davies, H.L., Clarke, J.D.A., Stagg, H.M.J., Shafik, S., McGowran, B., Alley, N.F. & Willcox, J.B., 1989 — Maastrichtian and younger sediments from the Great Australian Bight. *Bureau of Mineral Resources, Australia, Report* 288.

Dettmann, M.E., 1981 — The Cretaceous flora. *In* Ecological biogeography of Australia. *W. Junk Publishers, The Hague*, 357—375.

Dettmann, M.E., 1989 — Antarctica: Cretaceous cradle of austral temperate rainforests. *In* Crame, J.A. (editor), Origins and evolution of the Antarctic biota. *Geological Society Special Publication* 47, 89—105.

Dettmann, M.E. & Jarzen, D.M., 1988 — Angiosperm pollen from uppermost Cretaceous strata of southeastern Australia and Antarctic Peninsula. *Association of Australasian Palaeontologists, Memoir* 5, 217—237.

Dettmann, M.E. & Jarzen, M.J., 1990 — The Antarctic/Australian rift valley: Late Cretaceous cradle of northeastern Australian relicts. *Review of Palaeobotany and Palynology*, 65, 131—144.

Dettmann, M.E. & Thomson, M.R.A., 1987 — Cretaceous palynomorphs from the James Ross Island area, Antarctica — a pilot study. *British Antarctic Survey Bulletin*, 77, 13—59.

Dettmann, M.E., Pocknall, D.T., Romero, E.J. & Zamaloa, M. del C., 1990 — *Nothofagidites* Erdtman ex Potonié, 1960: a catalogue of species with notes on the palaeogeographic distribution of *Nothofagus* Bl. (southern beech). *New Zealand Geological Survey, Palaeontological Bulletin* 60.

Dormack, E.W. & Anderson, J.B., 1983 — Marine geology of the George V continental margin: combined results of Deep Freeze 79 and the 1911—1914 Australasian Expedition. *In* Oliver, R.L., James, P.R. & Jago, J.B. (editors), Antarctic earth science. *Australian Academy of Science, Canberra*, 402—406.

Figure 7. Magnification ×790 unless otherwise stated.

A, *Microcachryidites antarcticus*, S6444/1. **B, C,** *Alisocysta reticulata*, high and low focus, ×500, S6430/1. **D, E,** *Fromea* sp., high and low focus, ×500, S6430/1. **F,** *Fromea* sp., S6444/2. Similar to *F. chytra* except for the thicker cyst wall and the fine rugulate ornamentation. **G, H,** *Microdinium ornatum*, high and low focus, S6400/1. **I, J,** *Palaeostomocystis reticulata*. i, Optical section, S6417/1; j, High focus showing reticulate ornamentation, S6444/1. **K,** *Odontochitina porifera*, ×500, S6447/1. **L, M,** *Manumiella conorata*. l, ×500, S6415/2; m, Specimen with less well developed apical and antapical horns, ×500, S6446/1. **N,** *Manumiella druggii*, ×500, S6417/1.

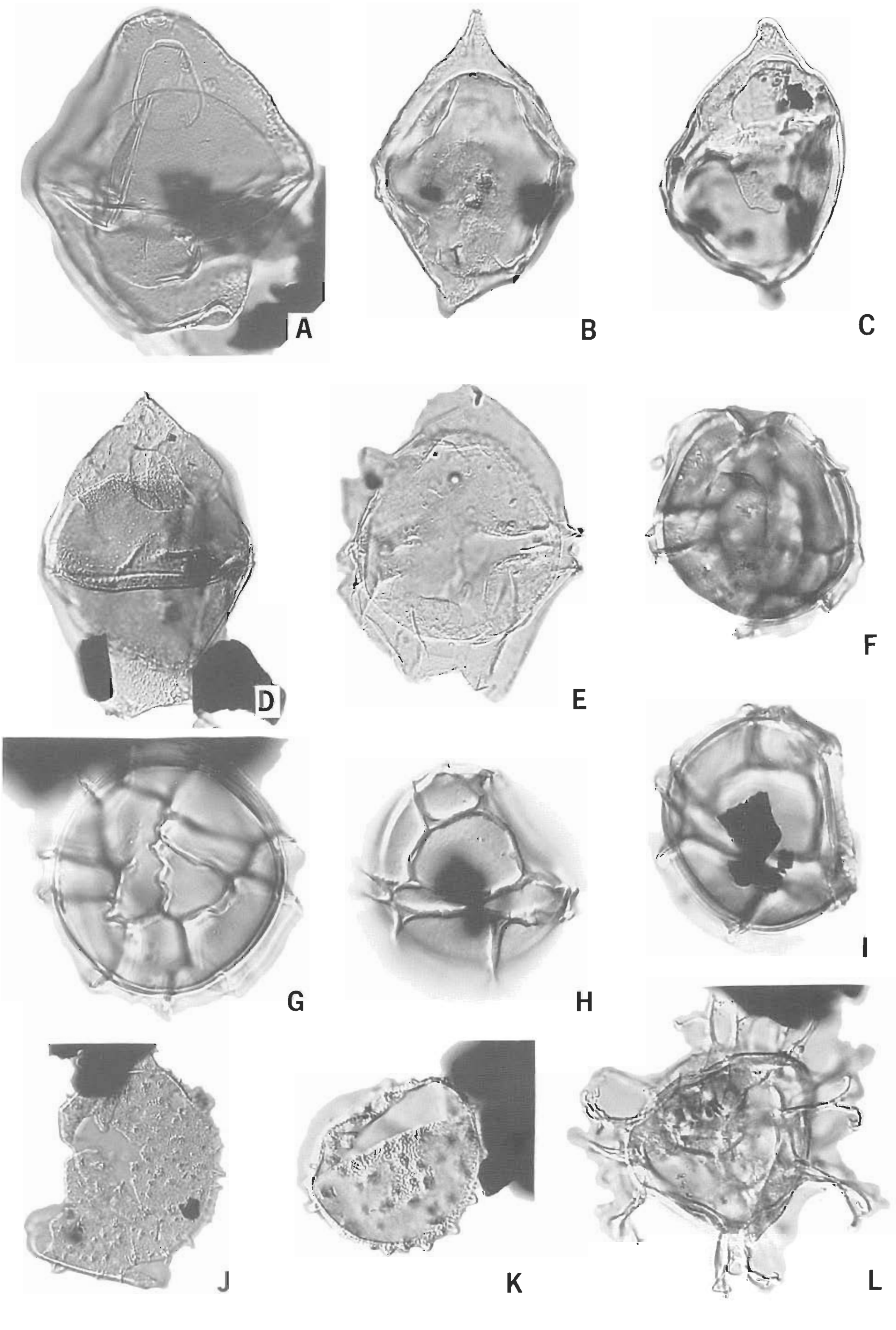
A
B
C
D
E
F
G
H
I
J
K
L

Dormack, E.W., Fairchild, W.W. & Anderson, J.B., 1980 — Lower Cretaceous sediment from the east Antarctic continental shelf. *Nature*, 287, 625—626.

Evans, P.R., 1969 — Upper Carboniferous and Permian palynological stages and their distribution in eastern Australia. *In* Gondwana Stratigraphy. Proceedings of the IUGS Symposium, Buenos Aires 1—15 October, 1967. *UNESCO, Earth Science*, 41—54.

Frakes, L.A., Burger, D., Apthorpe, M., Wiseman, J., Dettmann, M., Alley, N., Flint, R., Gravestock, D., Ludbrook, N., Backhouse, J., Skwarko, S., Scheibnerova, V., McMinn, A., Moore, P.S., Bolton, B.R., Douglas, J.G., Christ, R., Wade, M., Molnar, R.E., McGowran, B., Balme, B.E. & Day, R.A., 1987 — Australian Cretaceous shorelines, stage by stage. *Palaeogeography, Palaeoecology, Palaeoclimatology*, 59, 31—48.

Fraser, A.R. & Tilbury, L.A., 1979 — Structure and stratigraphy of the Ceduna Terrace region, Great Australian Bight. *The APEA Journal*, 19, 53—65.

Gatehouse, C.G. & Cooper, B.J., 1982 — The Late Jurassic Polda Formation, Eyre Peninsula. *Geological Survey of South Australia, Quarterly Geological Notes* 81, 12—16.

Helby, R., Morgan, R. & Partridge, A.D., 1987 — A palynological zonation of the Australian Mesozoic. *Association of Australasian Palaeontologists, Memoir* 4, 1—94.

Jackson, M.J. & van de Graaff, W.J.E., 1981 — Geology of the Officer Basin, Western Australia. *Bureau of Mineral Resources, Australia, Bulletin* 206.

Lowry, D.C., 1970 — Geology of the Eucla Basin. *Western Australia Geological Survey, Bulletin* 122.

McGowran, B., 1991 — Maastrichtian and early Cainozoic, southern Australia: planktonic foraminiferal biostratigraphy. *In* Williams, M.A.J., De Deckker, P. & Kershaw, A.P. (editors), The Cainozoic in Australia: a reappraisal of the evidence. *Geological Society of Australia Special Publication* No. 18, 79—98.

Morgan, R., 1979 — Palynostratigraphy of the Australian Early and Middle Cretaceous. *Geological Survey of New South Wales, Memoir* 18.

Morton, J.G.G., 1990 — Revisions to the stratigraphic nomenclature of the Otway Basin, South Australia. *Geological Survey of South Australia, Quarterly Geological Notes* 116.

Partridge, A.D. & Macphail, M., 1990 — A proposal to establish a 'Stover & Williams' style catalogue of Mesozoic and Cenozoic spore-pollen in the Australian region. *Palynological and Palaeobotanical Association of Australasia Newsletter* 21, 5—7.

Price, P.L., 1983 — A Permian palynostratigraphy for Queensland. *In* Permian geology of Queensland. Symposium on Permian Geology of Queensland, Brisbane 1982, Proceedings. *Geological Society of Australia, Queensland Division*, 155—211.

Quilty, P.G., 1986 — Australia's Antarctic basins — identification and evolution. *The APEA Journal*, 26, 20—46.

Robertson, C.S., Cronk, D.K., Nicholas, E., Mayne, S.J. & Townsend, D.G., 1979 — A review of the petroleum prospects and exploration in the Great Australian Bight region. *Bureau of Mineral Resources, Australia, Record* 1979/20.

Shafik, S., 1990 — The Maastrichtian and early Tertiary record of the Great Australian Bight Basin and its onshore equivalents on the Australian southern margin. *BMR Journal of Australian Geology & Geophysics*, 11, 473—497.

Shafik, S., 1991 — Upper Cretaceous and Tertiary stratigraphy of the Fremantle Canyon, South Perth Basin: a nannofossil assessment. *BMR Journal of Australian Geology & Geophysics*, 12, 65—91.

Stagg, H.M.J., Willcox, J.B., Needham, D.J.L., O'Brien, G.W., Cockshell, C.D., Hill, A.J., Thomas, B. & Hough, L.P., 1990 — Basins of the Great Australian Bight region: geology and petroleum potential. *Bureau of Mineral Resources, Australia, Continental Margins Program, Folio* 5.

Truswell, E.M., 1982 — Palynology of seafloor samples collected by the 1911—1914 Australasian Antarctic Expedition: implications for the geology of coastal East Antarctica. *Geological Society of Australia, Journal* 29, 343—356.

Truswell, E.M., 1983 — Geological implications of recycled palynomorphs in continental shelf sediments around Antarctica. *In* Oliver, R.L., James, P.R. & Jago, J.B. (editors), Antarctic earth science. *Australian Academy of Science, Canberra*, 394—399.

Veevers, J.J., 1984 — Phanerozoic earth history of Australia. *Clarendon Press, Oxford.*

Veevers, J.J., 1986 — Breakup of Australia and Antarctica estimated as mid-Cretaceous (95±5 Ma) from magnetic and seismic data at the continental margin. *Earth and Planetary Science Letters*, 77, 91—99.

Veevers, J.J., 1987 — The conjugate continental margins of Antarctica and Australia. *In* Eittreim, S.L. & Hampton, M.A. (editors), The Antarctic continental margin: geology and geophysics of offshore Wilkes Land. *Circum-Pacific Council for Energy and Mineral Resources Earth Science Series* 5A, 45—73.

Wannesson, J., 1990 — Geology & petroleum potential of the Adelie coast margin, East Antarctica. *In* St. John, B. (editor), Antarctica as an exploration frontier — hydrocarbon potential, geology & hazards. *American Association of Petroleum Geologists, Studies in Geology*, 31, 77—88.

Whyte, R., 1978 — Shell's offshore venture in South Australia. *The APEA Journal*, 18, 44—51.

Willcox, J.B., Stagg, H.M.J. & Davies, H.L., 1988 — 'Rig Seismic' research cruises 10 & 11: geology of the central Great Australian Bight region. *Bureau of Mineral Resources, Australia, Report* 286.

Appendix 1. Palynomorphs referred to in text.

Pollen/spores

Aequitriradites spinulosus (Cookson & Dettmann) Cookson & Dettmann 1961
Alisporites grandis (Cookson) Dettmann 1963
Amosopollis cruciformis Cookson & Balme 1962
Appendicisporites distocarinatus Dettmann & Playford 1968
Araucariacites australis Cookson 1947
Australopollis obscurus (Harris) Krutzsch 1966
Baculatisporites comaumensis (Cookson) Potonié 1956
Baculatisporites disconformis Stover 1973
Balmeisporites glenelgensis Cookson & Dettmann 1958
Beaupreaidites elegansiformis Cookson 1950
Beaupreaidites orbiculatus Dettmann & Jarzen 1988
Beaupreaidites verrucosus Cookson 1950
Biretisporites spectabilis Dettmann 1963
Callialasporites dampierii (Balme) Sukh Dev 1961
Callialasporites segmentatus (Balme) Srivastava 1963
Camarozonosporites amplus (Stanley) Dettmann & Playford 1968
Camarozonosporites bullatus Harris 1965
Ceratosporites equalis Cookson & Dettmann 1968
Cicatricosisporites australiensis (Cookson) Potonié 1956
Cicatricosisporites cuneiformis Pocock 1965
Cicatricosisporites ludbrookiae Dettmann 1963
Cicatricosisporites venestus Deak 1963
Classopollis chateaunovi Reyre 1953
Classopollis simplex (Dánze-Corsin & Laveine) Reiser & Williams 1969
Clavifera triplex (Bolkhovitina) Bolkhovitina 1966
Coronatispora perforata Dettmann 1963
Crybelosporites striatus (Cookson & Dettmann) Dettmann 1963
Cyathidites australis Couper 1953
Cyathidites minor Couper 1953
Cyclosporites hughesii (Cookson & Dettmann) Cookson & Dettmann 1959
Densoisporites velatus Weyland & Kreiger emend. Krasnova 1961
Dictyophyllidites crenatus Dettmann 1963
Dictyophyllidites harrisii Couper 1958
Dictyotosporites complex Cookson & Dettmann 1958
Dictyotosporites speciosus Cookson & Dettmann 1958
Didecitriletes dentatus (Balme & Hennelly) Venkatchala & Kar

Figure 8. Magnification ×790 unless otherwise stated.
A, *Manumiella druggii*, specimen with slightly better developed horns and equatorial bulge, ×500, S6416/1.**B, C,** *Alterbidinium acutulum*. b, Ventral view showing outline of pericyst and well developed antapical horn, S6402/1; c, dorsal view showing intercalary archeopyle, S6402/1. **D,** *Isabelidinium* sp., specimen with strongly granulate periphragm, ×500, S6446/2. **E,** *Senegalinium dilwynense*, specimen with apical horn missing, S6414/1. **F, G,** *Impagidinium dispertitum*. f, Dorsal view showing precingular archeopyle, S6446/1; g, Ventral surface, S6444/2. **H, I,** *Impagidinium* sp., high and low focus, left lateral view, S6414/1. **J,** *Operculodinium flucturum*, ×500, S6430/1. **K,** *Operculodinium* sp., S6422/2. **L,** *Spiniferites ramosus*, ×500, S6413/2.

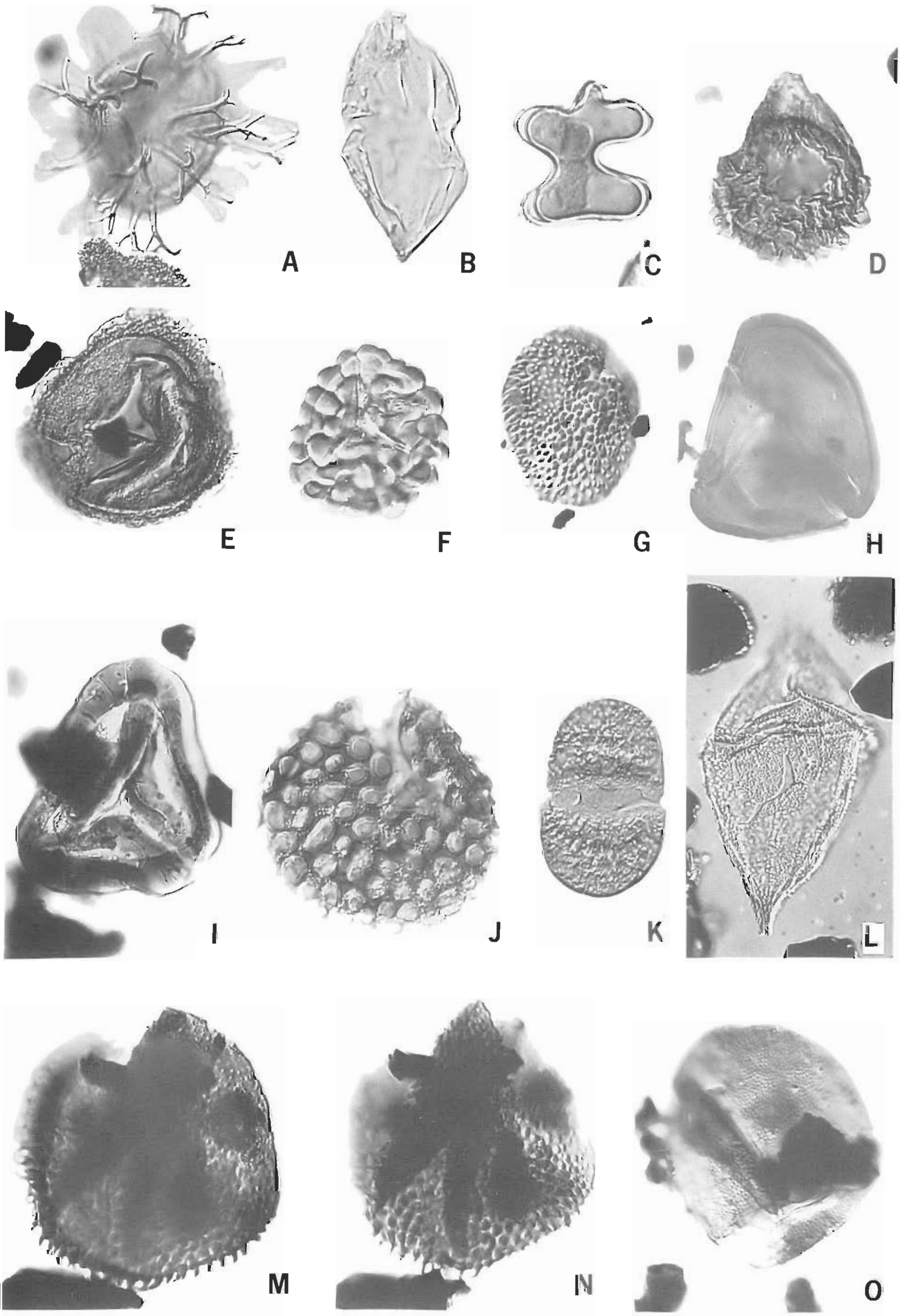
A
B
C
D
E
F
G
H
I
J
K
L
M
N
O

1965
Dilwynites granulatus Harris 1965
Dilwynites tuberculatus Harris 1965
Dulhuntyispora cf. *D. omasi* Price 1983
Foraminisporis asymmetricus (Cookson & Dettmann) Dettmann 1963
Foraminisporis dailyi (Cookson & Dettmann) Dettmann 1963
Forcipites (al. *Tricolpites*) *longus* (Stover & Evans) Dettmann & Jarzen 1988
Forcipites (al. *Tricolpites*) *sabulosus* (Dettmann & Playford) Dettmann & Jarzen 1988
Foveosporites canalis Balme 1957
Foveotriletes parviretus (Balme) Dettmann 1963
Gambierina rudata Stover & Partridge 1973
Gleicheniidites circinidites (Cookson) Dettmann 1963
Gleicheniidites senonicus Ross emend. Skarby 1964
Granulatisporites trisinus Balme & Hennelly 1956
Grapnelispora evansii Stover & Partridge 1984
Ilexpollenites anguloclavatus McIntyre 1968
Ilexpollenites megagemmatus McIntyre 1968
Kraeuselisporites jubatus Dettmann & Playford 1968
Laevigatosporites major (Cookson) Krutzsch 1959
Laevigatosporites ovatus Wilson & Webster 1946
Leptolepidites major Couper 1958
Leptolepidites verrucatus Couper 1953
Lycopodiacidites asperatus Dettmann 1963
Lygistepollenites balmei (Cookson) Stover & Evans 1974
Lygistepollenites florinii (Cookson & Pike) Stover & Evans 1974
Matonisporites cooksonii Dettmann 1963
Microcachryidites antarcticus Cookson 1947
Microfoveolatosporites fromensis (Cookson) Harris 1965
Murospora florida (Balme) Pocock 1961
Neoraistrickia truncatus (Cookson) Potonié 1956
Nothofagidites brachyspinulosus (Cookson) Harris 1965
Nothofagidites endurus Stover & Evans 1973
Nothofagidites flemingii (Couper) Potonié 1960
Nothofagidites senectus Dettmann & Playford 1968
Ornamentifera sentosa Dettmann & Playford 1968
Osmundacidites wellmanii Couper 1953
Peninsulapollis gilli (Cookson) Dettmann & Jarzen 1988
Phidiaesporites fosteri Foster 1979
Phimopollenites pannosus (Dettmann & Playford) Dettmann 1973
Phyllocladidites mawsonii Cookson 1947
Phyllocladidites verrucosus Stover & Evans 1973
Pilosisporites grandis Dettmann 1963
Plicatipollenites densus Srivastava 1970
Podocarpidites ellipticus Cookson 1947
Propylipollis (al. *Proteacidites*) *reticuloscabratus* (Harris) Martin & Harris 1974
Proteacidites amolosexinus Dettmann & Playford 1968
Proteacidites scaboratus Couper 1960
Proteacidites tripartitus Harris 1972
Protohaploxypinus amplus (Balme & Hennelly) 1964
Quadraplanus brossus Stover 1973
Reticulatisporites pudens Balme 1957
Retimonocolpites peroreticulatus (Brenner) Doyle 1975
Retitriletes austroclavatidites (Cookson) Döring & others, 1963
Retitriletes circolumenus Cookson & Dettmann 1958
Retitriletes douglasii Dettmann 1986
Retitriletes facetus (Dettmann) Srivastava 1972
Retitriletes rosewoodensis (de Jersey) McKellar 1974
Retitriletes watherooensis Backhouse 1978
Sestrosporites pseudoalveolatus (Couper) Dettmann 1963
Spinozonocolpites prominatus (McIntyre) Stover & Evans 1973
Stereisporites antiquasporites (Wilson & Webster) Dettmann 1963
Stereisporites viriosus Dettmann & Playford 1968
Stereisporites (*Tripunctisporis*) sp.
Tricolpites reticulatus Cookson ex Couper 1953
Tricolporites apoxyexinus Partridge 1987
Trilobosporites perverulentus (Verbitskaya) Dettmann 1963
Trilobosporites tribotrys Dettmann 1963
Triporoletes reticulatus (Pocock) Playford 1971
Triporopollenites sectilis Stover 1973
Tubulifloridites (al. *Tricolporites*) *lilliei* (Couper) Farabee & Canright 1986
Velosporites triquetrus (Lanz) Dettmann 1963
Vitreisporites pallidus (Reissinger) Nilsson 1958

Microplankton
Alisocysta circumtabulata (Drugg) Stover & Evitt 1978
Alisocysta reticulata Damassa 1979
Alterbidinium acutulum (Wilson) Lentin & Williams 1985
Callaiosphaeridium asymmetricum (Deflandre & Courteville) Davey & Williams 1966
Cassiculosphaeridia magna Davey 1974
Chichaouadinium boydii (Morgan) Bujak & Davies 1983
Diconodinium cristatum Cookson & Eisenack emend. Morgan 1977
Diconodinium davidii Morgan 1975
Diconodinium psilatum Morgan 1977
Dinogymnium nelsonense (Cookson) Evitt 1967
Exochosphaeridium phragmites Davey 1966
Florentinia deanei (Davey & Williams) Davey & Verdier 1973
Fromea chytra (Drugg) Stover & Evitt 1978
Gonyaulacysta cassidata (Eisenack & Cookson) Sarjeant 1966
Heterosphaeridium heteracanthum (Deflandre & Cookson) Eisenack & Kjellström 1971
Hologinella incurvata Cookson & Eisenack 1962
Impagidinium dispertitum (Cookson & Eisenack) Stover & Evitt 1978
Isabelidinium bakeri (Deflandre & Cookson) Lentin & Williams 1977
Isabelidinium belfastense (Cookson & Eisenack) Lentin & Williams 1977
Isabelidinium korojonense (Deflandre & Cookson) Lentin & Williams 1977
Isabelidinium pellucidum (Deflandre & Cookson) Lentin & Williams 1977
Litosphaeridium siphoniphorum (Cookson & Eisenack) Davey & Williams 1966
Manumiella conorata (Stover) Bujak & Davies 1983
Manumiella druggii (Stover) Bujak & Davies 1983
Microdinium ornatum Cookson & Eisenack 1960
Nelsoniella aceras Cookson & Eisenack 1960
Odontochitina porifera Cookson 1956
Operculodinium fluctrum Davey 1969
Palaeohystrichophora infusorioides Deflandre 1935
Palaeostomocystis reticulata Deflandre 1937
Protoellipsodinium densispinum Morgan 1979
Senegalinium dilwynense (Cookson & Eisenack) Stover & Evitt 1978
Spiniferites ramosus (Ehrenberg) Loeblich & Loeblich 1966
Spiniferites wetzeli (Deflandre) Sarjeant 1970
Tanyosphaeridium salpinx Norvick 1975
Xenikoon australis Cookson & Eisenack 1960

Figure 9. Magnification ×790 unless otherwise stated.
A, *Spiniferites* sp., ×500, S6413/2. **B,** Dinogymnium nelsonense, ×500, S6417/2. **C,** *Horologinella* cf. *H. incurvata*, S6414/1. **D,** *Crybelosprites striatus*, S6422/1. **E,** *Densoisporites velatus*, ×500, S6444/1. **F,** *Leptolepidites verrucatus*, S6443/2. **G,** *Foraminisporis asymmetricus*, distal surface, S6446/1. **H,** *Matonisporites cooksonii*, ×500, S6447/1. **I,** *Murospora florida*, 5500, S6443/1. **J,** *Retitriletes circolumenus*, view of distal surface, S6443/1. **K,** *Vitreisporites pallidus*, S6416/1. **L,** *Diconodinium cristatum*, ×500, S6417/1. **M, N,** *Didecitriletes dentatus*, equatorial view, proximal surface towards bottom of photo, 5500, S6422/1. m, View showing reduced ornamentation on the proximal surface; n, View showing strong spinose ornamenation on the distal surface. **o,** *Granulatisporites trisinus*, oblique equatorial view showing finely granulate ornamentation on the proximal surface (towards top of photo), ×500, S6422/1.

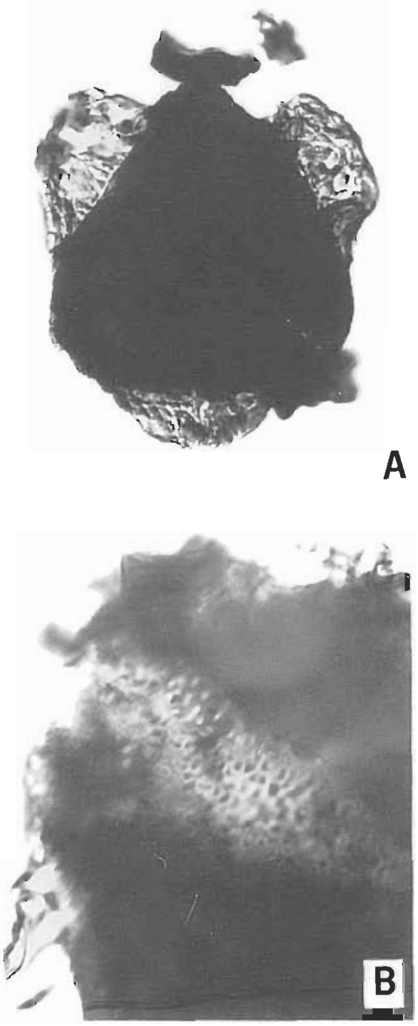

Figure 10. ***Dulhuntyispora* cf. *D. omasi*, specimen very dark and difficult to photograph, S6398/1.**
a, View showing well developed spongeous scutula, 5500; **b,** Reduced reticulate ornamentation in contact areas adjacent to the labra on the proximal surface, 51250.

Appendix 2. Palynological zonation, age, depositional environment and correlation of palynological samples.

Sample number	*Palynological zone*	*Age*	*Unit*	*Depositional environment*
DR01C	—	—	—	—
DR01G	*F. longus/M. druggii*	Maastrichtian/ Early Danian	Potoroo	marine
DR01H	*F. longus/M. druggii*	Maastrichtian/ Early Danian	Potoroo	marine
DR01I	*F. longus*	Maastrichtian/ Early Danian	Potoroo	paralic
DR03A	*F. longus/M. druggii*	Maastrichtian/ Early Danian	Potoroo	marine
DR03C	*X. australis/I korojonense*	?Campanian	?Wigunda	marine
DR03D	—	?Cretaceous	—	marine
DR04	*O. porifera/ Nelsoniella aceras*	Santonian	Potoroo/ Wigunda	marine
DR07A	*F. longus/M. druggii*	Maastrichtian/ Early Danian	Potoroo	marine
DR07E	—	Late Cretaceous/ Early Tertiary	—	paralic
DR07F	*F. longus/M. druggii*	Maastrichtian/ Early Danian	Potoroo	marine
DR07H	*N. senectus/F longus*	Campanian— Maastrichtian	Potoroo/ Wigunda	paralic
DR08C	*Barren*	—	—	—
DR08D	*F. longus/M. druggii*	Maastrichtian/ Early Danian	Potoroo	marine
DR08E	*F. longus/M. druggii*	Maastrichtian/ Early Danian	Potoroo	paralic
DR08F	*F. longus*	Maastrichtian/ Early Danian	Potoroo	paralic
DR09C	*I. korojonense/ M. druggii*	Campanian— Maastrichtian/ Early Danian	Potoroo/ Wigunda	marine
DR09C	*F. longus*	Maastrichtian/ Early Danian	Potoroo	paralic
DR11D	*F. longus*	Maastrichtian/ Early Danian	Potoroo	paralic
DR11E	*F. longus/M. druggii*	Maastrichtian/ Early Danian	Potoroo	marine
DR11F	—	Tertiary	?Pidinga	paralic
DR12D	*F. longus/M. druggii*	Maastrichtian/ Early Danian	Potoroo	marine
DR12E	—	—	—	paralic
DR12F	*F. longus*	Maastrichtian/ Early Danian	Potoroo	paralic
DR12G	*F. longus*	Maastrichtian/ Early Danian	Potoroo	paralic
DR14D	—	—	—	marine
DR14E	—	Cretaceous	—	marine
DR14F	*F. longus*	Maastrichtian. Early Danian	Potoroo	paralic
DR16B	—	Early Cretaceous	Ceduna Formation	marine

Palynofloral zones include
Spore/pollen: *Forcipites* (al. *Tricolpites*) *longus*, *Nothofagidites senectus*
Microplankton: *Manumiella druggii*, *Isabelidinium korojonense*, *Xenikoon australis*, *Nelsoniella aceras*, *Odontochitina porifera*.

Appendix 3. Recycled palynomorphs found in the Late Cretaceous sediments.

Species	*Age*	*Basin*
Upper part of the Potoroo Formation		
Pollen/spores		
Aequitriradites spinulosus	Late Jurassic-Santonian	Duntroon
Alisporites grandis	Triassic-Early Cretaceous	Duntroon
Appendicisporites distocarinatus	Albian-Cenomanian	Duntroon
Balmeisporites glenelgensis	Albian-Santon	Duntroon
Biretisporites spectabilis	Late Jurassic-Aptian	Bight
Callialasporites dampierii	Early Jurassic-Early Cretaceous	Duntroon
C. segmentatus	Early Jurassic-Early Cretaceous	Duntroon
Ceratosporites equalis	Jurassic-Late Cretaceous	Bight, Duntroon
Cicatricosisporites australiensis	Late Jurassic-Early Cretaceous	Bight, Duntroon
C. cuneiformis	Aptian-Cenomanian	Duntroon
C. ludbrookiae	Neocomian-Albian	Bight
C. venestus	?Albian-Cenomanian	Duntroon
Classopollis chateaunovi	Jurassic-Late Cretaceous	Bight
C. simplex	Jurassic-Early Cretaceous	Duntroon
Coronatispora perforata	Late Jurassic-Early Cretaceous	Duntroon
Crybelosporites striatus	Albian-Maastrichtian	Duntroon
Cyclosporites hughesii	Neocomian-Albian	Duntroon
Densoisporites velatus	Late Jurassic-Early Cretaceous	Bight
Dictyophyllidites crenulatus	Late Jurassic-Early Cretaceous	Duntroon

Species	Age	Basin
D. harrisii	Jurassic-Early Cretaceous	Bight
Dictyotosporites complex	Jurassic-Early Cretaceous	Duntroon
D. speciosus	Neocomian-Albian	Duntroon
Dulhuntyispora cf. *D. omasi*	Permian	Duntroon
Foraminisporis asymmetricus	Aptian-Campanian	Duntroon
F. dailyi	Neocomian-Albian	Duntroon
Foveosporites canalis	Late Jurassic-Early Cretaceous	Bight, Duntroon
Foveotriletes parviretus	Late Jurassic-Albian	Bight
Kraeuselisporites jubatus	Albian-Cenomanian	Duntroon
Leptolepidites major	Jurassic-Early Cretaceous	Bight
L. verrucatus	Late Jurassic-Albian	Duntroon
Lycopodiacidites asperatus	Jurassic-Early Cretaceous	Bight, Duntroon
Matonisporites cooksonii	Jurassic-Early Cretaceous	Duntroon
Murospora florida	Jurassic-Albian	Bight
Neoraistrickia truncatus	Jurassic-Early Cretaceous	Bight, Duntroon
Phimopollenites pannosus	Albian-Campanian	Bight, Duntroon
Reticulatisporites pudens	Late Jurassic-Early Cretaceous	Duntroon
Retimonocolpites peroreticulatus	Albian-Cenomanian	Duntroon
Retitriletes circolumenus	Late Jurassic-Early Cretaceous	Duntroon
R. douglasii	Early Cretaceous	Duntroon
R. facetus	Late Jurassic-Albian	Bight, Duntroon
R. rosewoodensis	Late Jurassic-Early Cretaceous	Bight
R. watherooensis	Late Jurassic-Early Cretaceous	Duntroon
Sestrosporites pseudoalveolatus	Late Jurassic-Early Cretaceous	Duntroon
Trilobosporites perverulentus	Neocomian-Albian	Duntroon
T. tribotrys	Albian	Bight
Velosporites triquetrus	Late Jurassic-Albian	Duntroon
Vitreisporites pallidus	Permian-Early Cretaceous	Duntroon
Microplankton		
Chichaouadinium boydii	Aptian-Albian	Duntroon
Diconodinium cristatum	Aptian-Albian	Bight, Duntroon
D. davidii	Aptian	Duntroon
D. psilatum	Albian-Cenomanian	Duntroon
Cassiculosphaeridia magna	Neocomian-Aptian	Bight
Exochosphaeridium phragmites	Early Cretaceous-Late Cretaceous	Duntroon
Gonyaulacysta cassidata	Aptian-?Cenomanian	Duntroon
Lower part of the Potoroo Formation and/or the Wigunda Formation		
Pollen and spores		
Alisporites grandis	Triassic-Early Cretaceous	Duntroon
Biretisporites spectabilis	Late Jurassic-Aptian	Duntroon
Ceratosporites equalis	Jurassic-Early Cretaceous	Duntroon
Cicatricosisporites australiensis	Late Jurassic-Early Cretaceous	Duntroon
Classopollis chateaunovi	Jurassic-Late Cretaceous	Duntroon
Crybelosporites striatus	Albian-Maastrichtian	Duntroon
Dictyophyllidites harrisii	Jurassic-Early Cretaceous	Duntroon
Murospora florida	Jurassic-Albian	Duntroon
Neoraistrickia truncatus	Jurassic-Early Cretaceous	Duntroon
Phidiaesporites fosteri	Permian	Duntroon
Phimopollenites pannosus	Albian-Campanian	Duntroon
Pilosisporites grandis	Albian-Cenomanian	Duntroon
Plicatipollenites densus	Permian	Duntroon
Protohaploxypinus amplus	Permian	Duntroon
Retitriletes nodosus	Late Jurassic-Albian	Duntroon
R. rosewoodensis	Late Jurassic-Early Cretaceous	Duntroon
Triporoletes reticulatus	Neocomian-Cenomanian	Duntroon
Vitreisporites pallidus	Permian-Early Cretaceous	Duntroon

Eocene and Oligocene calcareous nannofossils from the Great Australian Bight: evidence of significant reworking episodes and surface-water temperature changes

Samir Shafik[1]

Eocene and Oligocene assemblages identified from carbonates dredged from the outer margin of the Ceduna Terrace in the Great Australian Bight, southern Australia, document two major Palaeogene reworking episodes with probable counterparts in the western central Pacific Ocean. The first episode (mid Eocene, ~43.5 Ma) coincides with and is related to events affecting deposition on the Australian southern margin, which were initially controlled by a sudden change in seafloor spreading rate between Australia and Antarctica. In this reworking episode, nannofossils of mainly late Cretaceous age (from the Naturaliste Plateau and/or the Eyre Terrace in the Great Australian Bight) were carried eastward and deposited by short-lived bottom currents flowing along the Australian southern margin. In the second episode, nannofossils of mainly Eocene and early Oligocene age were included in mid—upper Oligocene carbonates on the Australian western margin (Carnarvon Terrace and Perth Canyon) and in the Great Australian Bight. There was almost no supply of Eocene or lower Oligocene carbonate debris from onshore areas to the shelf (and deep sea), due to the aridity of the Australian continent during the Oligocene and the lack of diagenetically suitable sediments onshore. Reworked nannofossils in the upper Palaeogene shelf carbonates of western and southern Australia are therefore interpreted as coming from nearby shallow and intermediate oceanic sites during large-scale, late Palaeogene erosion in the southeast Indian Ocean. The late Palaeogene erosive events, although intimately related to the Oligocene cooling, were probably tectonically triggered. Some Oligocene assemblages from the Ceduna Terrace suggest cool surface waters. Others contain low-latitude species and suggest short episodes of warming during the mid to late Oligocene. Warm surface water from northwestern Australia was introduced to southern Australia by an intermittent proto-Leeuwin Current starting in the mid Eocene; the effects of this surface current varied in intensity but generally petered out eastward along the southern margin. The warm-water influences were pronounced during at least two distinct short Oligocene episodes.

Introduction

This study is based on optical microscopic examination of carbonates from a dredge haul (102DR007) and a vibrocore (102VC011) which were recovered on board the *Rig Seismic* during BMR Cruise 102 in the Great Australian Bight, southern Australia (June—July 1991). Dredge haul 102DR007 was collected from the outer margin of the Ceduna Terrace (36° 08.23' S, 134° 53.69' E) at a depth of 4380 m and vibrocore 102VR011 was cut from the continental shelf in the western Great Australian Bight (32° 10.00' S, 128° 01.52' E) at a depth of 22.2 m (Figs 1, 2).

The Maastrichtian—early Tertiary record in the Great Australian Bight, mainly the Ceduna Terrace area, has been discussed by Shafik (1990a). The discussion was based largely on documentation of several calcareous nannofossil assemblages extracted from dredge samples obtained on the *Rig Seismic* during

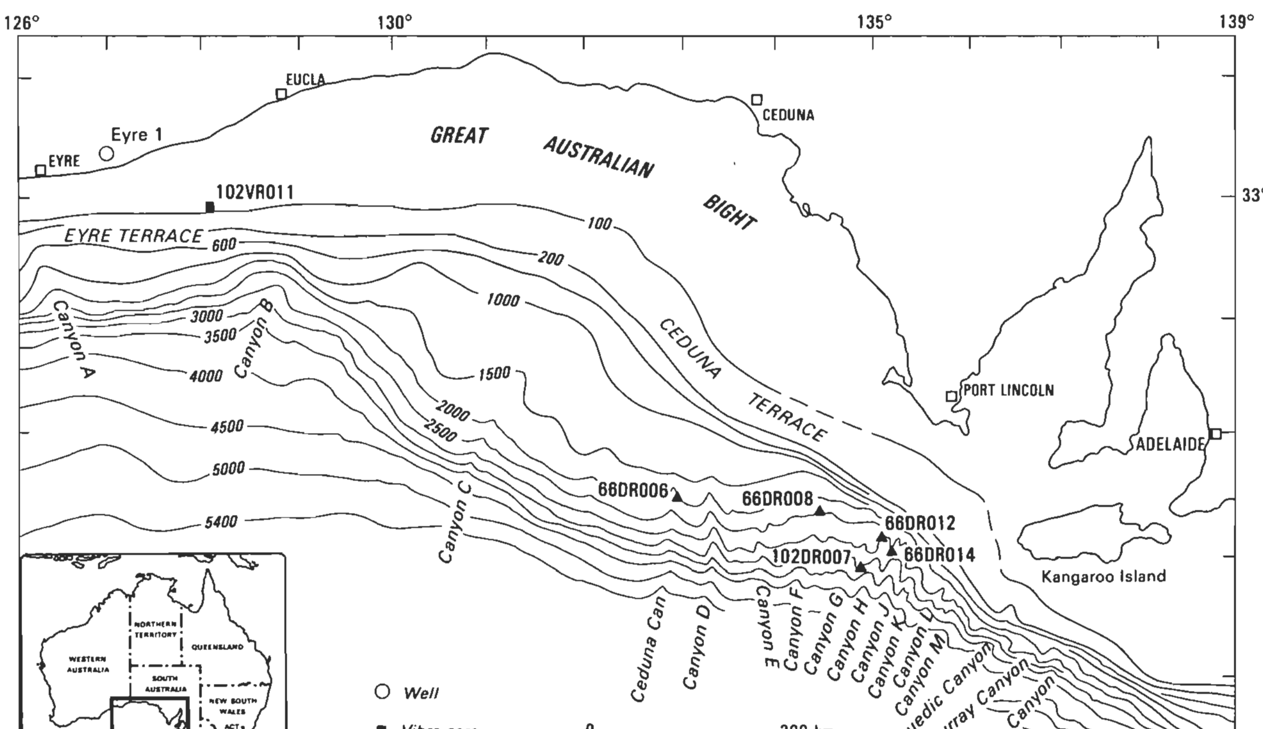

Figure 1. Bathymetric map of the Great Australian Bight showing canyons and location of samples.

[1] Marine Geoscience & Petroleum Geology Program, Bureau of Mineral Resources, Geology & Geophysics, GPO Box 378, Canberra ACT 2601

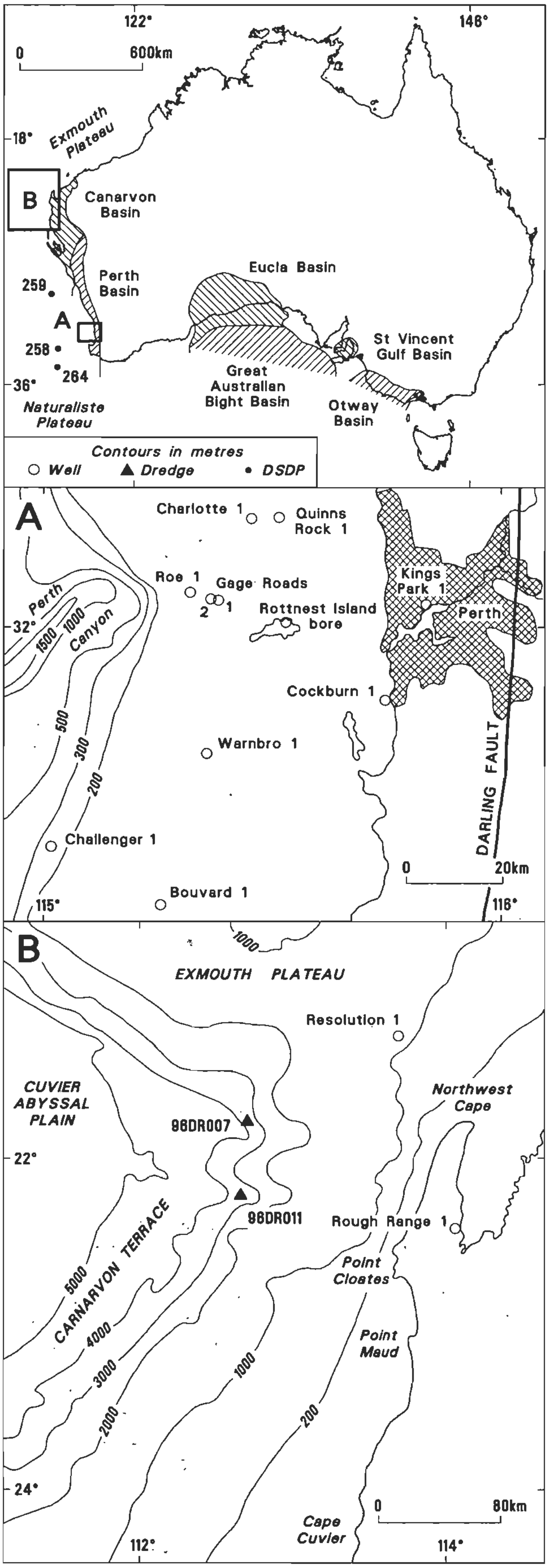

Figure 2. Location maps of the Perth Canyon (A, the offshore Perth Basin), the Carnarvon Terrace (B, the offshore Carnarvon Basin), other Australian basins and the Naturaliste Plateau.

BMR Cruise 66 (Davies & others, 1989). The assemblages pointed to mid—late Oligocene warming, based on the presence of the low-latitude key species *Sphenolithus distentus* and *S. ciperoensis*. Resolution of the question of whether the warming was a short event, a series of short events, or simply encompassed the whole mid to late Oligocene interval, could not be addressed fully because of lack of adequate sampling. By speculative analogy with the Otway Basin in southeastern Australia, the presence of *Sphenolithus ciperoensis* in the Great Australian Bight sequence was attributed to a 'short' warm episode; the other key species, *S. distentus*, has not yet been found in the Otway Basin. The same assemblages indirectly supported the concept of thermal subsidence in the Great Australian Bight as indicated by well data and seismic stratigraphy (e.g. Falvey & Mutter, 1981; Hegarty & others, 1988; Stagg & others, 1990).

It has long been known that nannofossils are prone to reworking because of their small size and their usually great abundance, particularly in pelagic carbonate sediments. Nannofossil assemblages that include displaced species have been used to determine the existence of palaeoceanic currents, and the times at which regional reworking occurred (e.g. Shafik, 1985). Evidence for a short reworking episode during the middle Eocene has already been documented from a specific stratigraphic level in several sections in the Eucla and Otway Basins (Australian southern margin) and in the Perth and Carnarvon Basins (Australian western margin) (Shafik, 1985; 1991). This middle Eocene level evidently had not been dredged hitherto from the Great Australian Bight (see Shafik, 1990a). Evidence for another possibly significant reworking episode, during the mid to late Oligocene, has emerged recently in dredge material from both the Australian southern and western margins: the Great Australian Bight (Shafik, 1990a), Perth Basin (Shafik, 1991) and Carnarvon Basin (Shafik, 1990b).

This study examines the nannofossils from several subsamples taken from the carbonate sediments of dredge haul 102DR007 in order to document evidence of reworking, particularly in the middle Eocene and mid—late Oligocene episodes referred to above, and to elucidate possible changes in surface water temperatures, particularly during the Oligocene.

Assemblages and results

Three Eocene and two Oligocene calcareous nannofossil assemblages were identified.

Middle Eocene assemblage A

Subsample 102DR007-A contained abundant, moderately preserved, and highly diversified nannofossils. The assemblage includes frequent *Blackites spinulus*, rare *Campylosphaera dela* (displaced from older Eocene), rare *Chiasmolithus expansus*, frequent *C. grandis*, rare *C. solitus*, rare *Clausicoccus cribellum*, frequent to common *Coccolithus eopelagicus*, frequent to common *C. formosus*, common to abundant *Cyclicargolithus floridanus*, common to abundant *C. reticulatus* (two distinct sizes: the larger size, probably an oceanic variety, has a relatively smaller central opening; the smaller size, with relatively large central opening, is usually dominant in hemipelagic sediments), rare *Daktylethra punctulata*, rare *Discoaster barbadiensis*, rare *D. binodosus*, rare *D. deflandrei*, rare *D. saipanensis*, rare to frequent *D. tanii nodifer*, frequent *Helicosphaera compacta*, *H. heezenii*, rare *H. lophota*, rare *H. seminulum*, rare *Holodiscolithus macroporus*, frequent *Lanternithus minutus*, rare *Markalius inversus*, frequent to common *Neococcolithes dubius*, frequent *Pontosphaera multipora*, rare *Prediscosphaera cretacea* (reworked from Cretaceous source), rare *Pseudotriquetrorhabdulus inversus* (reworked from older Eocene), frequent *Reticulofenestra hampdenensis*, rare *R. scrippsae*, common *R. umbilicus*, frequent *Sphenolithus moriformis*, rare *S. pseudoradians*, rare *Syracosphaera labrosa*, rare *Transversopontis pulcher*, frequent *T. zigzag*, rare *Vekshinella dorfii* (reworked from Cretaceous source), rare *Watznaueria barbnesae* (reworked from Cretaceous source), *Zygrhablithus bijugatus bijugatus*, and frequent *Z. bijugatus crassus*.

Biostratigraphy and age. The assemblage is assigned to the biostratigraphic datum interval bracketed by the lowest occurrences of *Cyclicargolithus reticulatus* and *Reticulofenestra scissura* (Fig. 3), which correlates with a position high in the planktic foraminiferal P12 Zone (Shafik, 1983, 1990a), at about the middle of NP16 Zone of Martini (1971) or near the base of CP14 Zone of Okada & Bukry (1980). This is based on the presence of *C. reticulatus*, *Chiasmolithus grandis* and other Eocene species (such as *Chiasmolithus solitus*, *Discoaster barbadiensis* and *Neococcolithes dubius*) and the absence of *Reticulofenestra scissura*. The age is middle Eocene, about 43.5 Ma (Shafik, 1990a; see also Truswell & others, 1991).

A similar assemblage (the 66DR14A(5) *Cyclicargolithus reticulatus* Assemblage in Shafik, 1990a), lacking reworked Cretaceous forms, has recently been recorded from the Ceduna Terrace at Canyon J (Fig. 1).

Depositional palaeoenvironment. The assemblage includes *Daktylethra punctulata*, *Lanternithus minutus*, *Pontosphaera multipora*, *Transversopontis pulcher*, *Zygrhablithus bijugatus*, and others which indicate a neritic (shelf) palaeoenvironment (Shafik, 1990a). Displaced nannofossils of mainly late Cretaceous age (such as *Prediscosphaera cretacea*) had been included during the deposition. These were brought to the Ceduna Terrace, presumably mainly from areas to the west, by short-lived bottom currents (Shafik, 1985).

Subsidence of the Ceduna Terrace

On evidence from nearby seismic profiles it is doubtful whether the sediments sampled at a water depth of 4380 m on the outer Ceduna Terrace are *in situ* (H.M.J. Stagg, BMR, personal communication, August 1991). Thus, shelf deposition as indicated by the nannofossils in subsample 102DR007-A does not necessarily mean that the outer margin of the Ceduna Terrace has subsided more than 4000 m since the middle Eocene. A deepening of the sea above the Ceduna Terrace of less than 3000 m since the late Cretaceous, suggested by nannofossil evidence from *in situ* dredge samples from the terrace (see Shafik, 1990a), is more likely; the seismic evidence (Fraser & Tilbury, 1979; Hegarty & others, 1988; Stagg & others, 1990) supports this conclusion.

Older sediments dredged previously from the Ceduna Terrace (Maastrichtian sediments at 66DR014 and Paleocene at 66DR008, from depths around 3000 m; Fig. 1) are nannofossil-free, but palynological evidence suggests deposition in an inner shelf or paralic environment (Alley, 1988; Shafik, 1990a). Middle Eocene (and younger) sediments from the same dredges are nannofossil-rich, and contain indications of deposition on the outer shelf or upper slope (Shafik, 1990a). This increase in the depositional palaeodepth has already been taken as evidence of substantial middle Eocene acceleration of the seafloor subsidence rate in the Great Australian Bight (Shafik, 1990a).

Some important middle Eocene events: a discussion

The assemblage of subsample 102DR007-A is very similar to assemblages known from the Hampton Sandstone and the Wilson Bluff Limestone, at the base of the Tertiary section in the onshore Eucla Basin (see Shafik, 1985). It also resembles an assemblage from the Lacepede Formation in the onshore western Otway Basin (see Shafik, 1983). The similarity between all these assemblages is not limited to the presence of a combination of certain key species (such as *Chiasmolithus solitus*, *Cyclicargolithus reticulatus* and *Neococcolithes dubius*), which shows them to be assignable to the same biostratigraphic datum interval, but also includes the presence of rare reworked upper Cretaceous nannofossils. Evidence of reworking of Cretaceous sediments in the Eocene of the southern margin is limited to the narrow middle Eocene biostratigraphic datum interval bracketed by the lowest occurrences of *Cyclicargolithus reticulatus* and *Reticulofenestra scissura* (age ~43.5 Ma).

The assemblages from the Eucla Basin, referred to above, signify the onset of a major marine transgression (the Wilson Bluff transgression of McGowran & Beecroft, 1986), which reached the western Otway Basin as a marine ingression leaving evidence initially in the form of a single nannofossil-bearing horizon within a barren part of the Lacepede Formation. At about this time, several major events occurred that affected deposition on the Australian southern margin, and probably led to the transgression in the Eucla Basin (Shafik, 1983). The primary event was a major increase in the rate of spreading between Australia and Antarctica (Cande & others, 1981; Cande & Mutter, 1982; Mutter & others, 1985; Veevers & others, 1990) or a resumption of seafloor spreading between Australia and Antarctica, after a long Cretaceous—early Tertiary interval of non-spreading (Middleton, 1991). This indirectly caused several secondary events:

(a) a significant acceleration in the rate of subsidence of the Australian southern margin, which had remained very slow since the mid Cretaceous (Shafik, 1990a);

(b) generation of short-lived, easterly-flowing bottom currents south of Australia (Shafik, 1985); and

(c) initiation of the proto-Leeuwin Current which intermittently brought warm waters from the northeastern Indian Ocean into southern Australia (Shafik, 1990a).

The existence of short-lived, easterly-flowing bottom currents south of Australia during the middle Eocene is suggested by the presence of upper Cretaceous nannofossils among middle Eocene assemblages from several locations on the southern margin (Shafik, 1985), including the assemblage of subsample 102DR007-A (present study). These currents were strong enough to strip upper Cretaceous coccolith-rich sediments off the Naturaliste Plateau and/or the western Great Australian Bight (Eyre Terrace) and to transport the fine fraction (composed mainly of coccoliths) derived from these sediments to the Eucla Basin, eastern part of the Great Australian Bight (Ceduna Terrace area) and the western part of the Otway Basin.

Middle Eocene assemblage B

Subsample 102DR007-B yielded a moderately-preserved assemblage which includes rare *Blackites perlongus*, rare *B. spinulus*, rare *B. tenuis*, extremely rare *Calcidiscus protoannulus*, extremely rare *Campylosphaera dela* (displaced from older Eocene), rare *Chiasmolithus expansus*, rare *C. grandis*, rare *C. solitus*, extremely rare *C. titus*, rare *Clausicoccus cribellum*, frequent to common *Coccolithus eopelagicus*, frequent to common *C. formosus*, common to abundant *Cyclicargolithus floridanus*, common to abundant *C. reticulatus* (two distinct sizes); frequent *Daktylethra punctulata*, rare *Discoaster barbadiensis*, rare *D. saipanensis*, rare to frequent *D. tanii nodifer*, frequent *Helicosphaera compacta*, rare *H. heezenii*, rare *H. seminulum*, frequent to common *Lanternithus minutus*, extremely rare *Markalius astroporus*, frequent to

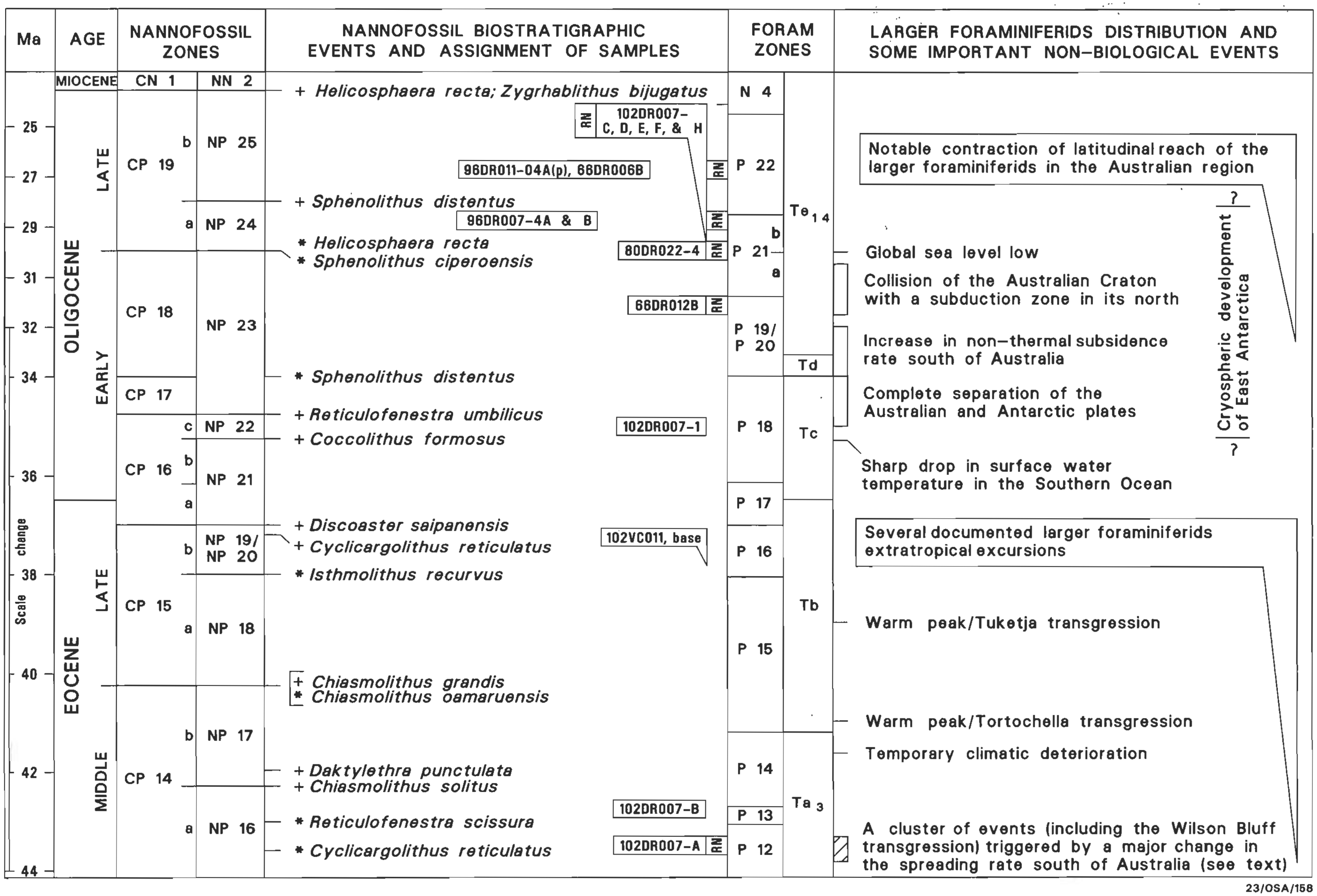

+ *Highest occurrence*   * *Lowest occurrence*   RN *Reworked nannofossils*   ☐ *Limits of uncertainty in dating* common *Neococcolithes dubius*, rare *Pontosphaera multipora*, frequent *Reticulofenestra hampdenensis*, rare *R. scissura*, rare *R. scrippsae*, common *R. umbilicus*, rare *Sphenolithus spiniger*, rare *Transversopontis pulcher*, frequent *T. zigzag*, frequent to common *Zygrhablithus bijugatus bijugatus*, and frequent *Z. bijugatus crassus*.

Biostratigraphy and age. The assemblage is assigned to the biostratigraphic datum interval bracketed by the lowest occurrence of *Reticulofenestra scissura* and the highest occurrence of *Daktylethra punctulata* (Fig. 3) which correlates within the planktic foraminiferal P13 Zone (Shafik, 1983). This assignment is based on the presence of *Chiasmolithus grandis*, *C. solitus*, *Cyclicargolithus reticulatus*, *Daktylethra punctulata* and *R. scissura*. The age of the assemblage is middle Eocene, ~43 Ma (Shafik, 1990a; see also Truswell & others, 1991). In terms of Martini's (1971) or Okada & Bukry's (1980) zonations, the assemblage can be placed within the upper part of NP16 Zone or within CP14a Subzone respectively.

Correlation. The assemblage correlates well with another from the Lacepede Formation of the Otway Basin. The latter represents a marine ingression in the western Otway Basin, following an ingression connected with the onset of the middle Eocene marine transgression over the onshore Eucla Basin (Shafik, 1983, 1985).

The assemblage evidently came from a widespread stratigraphic horizon on the Ceduna Terrace, since similar assemblages were recorded previously from two widely-spaced canyons on the outer Ceduna Terrace (see Shafik, 1990a: the 66DR08B and 66DR14A(6) *Reticulofenestra scissura* Assemblages at Canyons F and J, respectively; Fig. 1); another similar assemblage was identified from subsample 102DR007-G.

Depositional palaeoenvironment. A shelf/neritic depositional environment is indicated by several neritic species such as *Daktylethra punctulata*, *Lanternithus minutus* and *Zygrhablithus bijugatus*.

Wilson Bluff Limestone (late Eocene) assemblage

A poorly-preserved (recrystallised and hence limited) assemblage was identified from a white dolomitic limestone at the base of core 102VC011 (between 70 & 76 cm levels); lithologically the sample is very similar to the Wilson Bluff Limestone. The assemblage includes common *Coccolithus eopelagicus*, rare to frequent *C. formosus*, *Coccolithus* sp. cf. *C. pelagicus*, abundant *Cyclicargolithus floridanus*, frequent *Discoaster saipanensis*, rare (heavily calcified) *D. tanii*, rare (heavily calcified) *Isthmolithus recurvus*, rare *Markalius inversus*, rare *Reticulofenestra scissura*, frequent *R. scrippsae*, frequent *R. umbilicus* and rare to frequent *Zygrhablithus bijugatus crassus*.

Biostratigraphy and age. The assemblage is assigned to the broad biostratigraphic datum interval between the lowest occurrence of *Isthmolithus recurvus* and the highest occurrence of *Discoaster saipanensis*, based on the presence of these two index species. This biostratigraphic interval equates with the combined late Eocene NP19/NP20 Zones of Martini (1971) or the CP15b Subzone of Okada & Bukry (1980). It is difficult to judge whether the absence of the index species *Chiasmolithus oamaruensis* and *Cyclicargolithus reticulatus* from the assemblage is due to diagenetic or ecological factors, and the assemblage could be younger than the extinction datum of *C. reticulatus*.

The assemblage probably belongs to the narrow latest Eocene interval between the highest occurrences of *Cyclicargolithus reticulatus* and *Discoaster saipanensis*, on account of the absence of *C. reticulatus* (Fig. 3). This suggests placement high within the combined NP19/20 Zones or CP15 Zone. The biostratigraphic interval correlates with the planktic foraminiferal late P16 Zone (Shafik, 1981); the age is latest Eocene, ~37.4—37 Ma (as indicated by Berggren & others (1985) for the later part of P16; see also Truswell & others, 1991).

The assemblage at the base of core 102VC011 is younger than the base of the Wilson Bluff Limestone in the onshore Eucla Basin (e.g. in Eyre 1 Well). The middle Eocene assemblage from 102DR007 (discussed above) correlates with the assemblage from the lower part of the Wilson Bluff Limestone in onshore sections (e.g. in Eyre 1 Well).

There is a lack of reworked Cretaceous nannofossils in the middle Eocene assemblage from subsample 102DR007-B, and in the younger Eocene assemblage from subsample 102VC011-base. Reworking of Cretaceous sediments in the Eocene of the southern margin therefore seems to be limited to the narrow middle Eocene biostratigraphic datum interval, bracketed by the lowest occurrences of *Cyclicargolithus reticulatus* and *Reticulofenestra scissura*.

Early Oligocene assemblage

Subsample 102DR007-I yielded a poorly-preserved assemblage, with most species showing signs of recrystallisation or addition of secondary calcite. Species identified include frequent *Coccolithus eopelagicus*, common *Coccolithus* sp. cf. *C. pelagicus*, rare *Corannulus germanicus*, abundant *Cyclicargolithus floridanus* (some specimens mimic the Eocene *C. reticulatus*), rare *Isthmolithus recurvus*, rare to frequent *Reticulofenestra orangensis*, common *R. scissura*, frequent *R. scrippsae*, common *R. umbilicus*, and rare to frequent *Zygrhablithus bijugatus bijugatus*.

Biostratigraphy and age. Species identification has been hampered by poor preservation, and biostratigraphic assignment and age are tentative. The assemblage is assigned to the biostratigraphic datum interval bracketed by the highest occurrences of *Coccolithus formosus* and *Reticulofenestra umbilicus* (Fig. 3), which coincides with NP22 Zone of Martini (1971) and CP16c of Okada & Bukry (1980). The tentative age is early Oligocene, ~35 Ma according to calibrations by Berggren & others (1985) (see also Truswell & others, 1991).

Depositional palaeoenvironment. The overall composition of the assemblage suggests deposition on the shelf in a cool-water regime. This conclusion is based on the presence of *Isthmolithus recurvus* and *Zygrhablithus bijugatus*; poor preservation may have removed the evidence of other species. *Corannulus germanicus* may suggest some warm influence.

Figure 3. Calcareous nannofossil stratigraphic assignment of samples studied from the Ceduna Terrace (*Rig Seismic* Cruises 66 and 102), Perth Canyon (*Rig Seismic* Cruise 80) and the Carnarvon Terrace (*Rig Seismic* Cruise 96) showing climatic and tectonic events in the Australian region.
CP Zones after Okada & Bukry (1980), and NP zones after Martini (1971). Correlation of the CP and NP Zones with the planktic foraminiferal P Zones and the Indo-Pacific larger foraminiferal zones (East Indies Letter Classification) is from Truswell & others (1991 and references therein). Transgressions and pattern of distribution of larger foraminiferids are after McGowran & Beecroft (1986) and McGowran (1986 and references therein) respectively. Timing of the Oligocene tectonic and climatic events is not exact; it is based on various sources using probably different timescales.

Mid to late Oligocene assemblages

Assemblages identified from the carbonates of subsamples 102DR007-C, 102DR007-D, 102DR007-E, 102DR007-F and 102DR007-H are similar. The main elements of these assemblages include *Blackites* spp. (including *B. perlongus*, *B. spinulus* and *B. tenuis*), *Chiasmolithus altus* (either some specimens mimic *C. expansus*, *C. grandis*, *C. oamaruensis* and *C. solitus*, or these species do rarely occur, suggesting displacement from Eocene provenance), *Coccolithus eopelagicus*, *Coccolithus* sp. cf. *C. pelagicus*, *Cyclicargolithus floridanus* (often represented by two sizes), *Discoaster deflandrei*, *D. tanii nodifer*, *Helicosphaera bramlettei*, *H. recta*, *Reticulofenestra orangensis*, *R. scissura*, *R. scrippsae*, *R. umbilicus* (reworked from Eocene or older Oligocene levels), occasional *Sphenolithus moriformis*, *S. predistentus*, *Transversopontis* spp. (probably reworked from Eocene or older Oligocene levels) and *Zygrhablithus bijugatus*.

Both *Helicosphaera bramlettei* and *H. recta* are always very rare. In contrast, *Reticulofenestra umbilicus* and *R. scissura* are common in all assemblages. *Chiasmolithus altus*, usually abundant to common, is rare in subsample 102DR007-H. Very rare specimens of a *Sphenolithus* resembling the key species *S. distentus* were noted in subsample 102DR007-F.

Biostratigraphy and age. The collective assemblage listed above contains species whose stratigraphic ranges do not usually overlap. The key species *Helicosphaera recta* is among the younger species. Its stratigraphic range is known to span the mid to late Oligocene NP24 and NP25 Zones (see Martini, 1971; Perch-Nielsen, 1985) which equate with CP19 Zone of Okada & Bukry (1980); the highest occurrence of *H. recta* has been used widely as a good approximation of the top of the Oligocene. The index species of the NP24 and NP25 Zones, namely *Sphenolithus distentus* and *S. ciperoensis*, were not found in the material examined from dredge haul 102DR007, although they have been recorded previously from other dredges collected from the Ceduna Terrace (see Shafik, 1990a).

The occurrence of *Helicosphaera recta* in the assemblages from dredge haul 102DR007, though rare, suggests that their age is mid to late Oligocene (NP24 and NP25 Zones; Fig. 3), within the bracket 30—23.6 Ma according to data in Berggren & others (1985). The presence of *Helicosphaera bramlettei* supports this age determination.

Depositional palaeoenvironment. The abundance of *Chiasmolithus altus* and the scarcity of discoasters suggest deposition in a cool-water regime. The hemipelagic taxa *Transversopontis* spp. and *Zygrhablithus bijugatus* suggest deposition on the shelf, but their presence could be (partly or wholly) allochthonous, a result of reworking.

Both *Sphenolithus distentus* and *S. ciperoensis* are known to be warm-water species, and their absence agrees with the abundance of the cool-water indicator *Chiasmolithus altus*.

Reworking during the mid to late Oligocene: a widespread phenomenon

The key species *Helicosphaera recta* and *Reticulofenestra umbilicus* do not usually occur together. The highest occurrence of *R. umbilicus* has been widely used to define the top of the lower Oligocene, and the vertical range of *H. recta* is known elsewhere to span the middle and upper Oligocene. Indeed a biostratigraphic gap, represented in continuous stratigraphic sections by NP23 Zone, separates the highest occurrence of *R. umbilicus* and the lowest occurrence of *H. recta* (see Martini, 1971). The co-occurrence of these two species in the carbonates of dredge haul 102DR007 indicates reworking; older sediments (probably Eocene or lower Oligocene and containing *R. umbilicus*) were included during deposition of the mid to late Oligocene *H. recta*. Evidence of similar reworking has been recorded previously in mid and late Oligocene assemblages from the Ceduna Terrace (see Shafik, 1990a), from chalk and limestone collected in dredges 66DR006 and 66DR012 (see Fig. 1).

The assemblage from the fine-grained chalk in dredge 66DR006 (2015—2620 m water depth) shows more obvious reworking than the assemblage from the limestone in dredge 66DR012 (2720—3670 m water depth). The assemblage of 66DR006B is late Oligocene, from the presence of the key species *Sphenolithus ciperoensis*, *Cyclicargolithus abisectus* and *Helicosphaera recta* which, in the absence of *Sphenolithus distentus*, indicate the CP19b Subzone of Okada & Bukry, 1980 or the NP25 Zone of Martini, 1971; both biostratigraphic divisions span the interval 28—23.6 Ma (Berggren & others, 1985). The reworked component includes the diagnostic Eocene species *Discoaster saipanensis* in addition to the Eocene/early Oligocene species *Reticulofenestra hampdenensis* and *R. umbilicus* (Shafik, 1990a).

Evidence of similar reworking in mid or upper Oligocene carbonates has been documented from other basins marginal to Australia: the South Perth Basin (in the Perth Canyon[2]; Shafik, 1991) and the Carnarvon Basin (on the Carnarvon Terrace, Shafik, 1990b) (see Fig. 2). The Perth Canyon assemblage (from 80DR022-4: a white calcilutite with siliceous spicules dredged from 2310—2910 m water depth) is mid Oligocene, as indicated by the presence of the key species *Sphenolithus distentus*, *Sphenolithus* sp. aff. *S. ciperoensis*, *Cyclicargolithus abisectus* and *Helicosphaera recta* (which suggest a biostratigraphic assignment close to the NP23/NP24 boundary, probably at ~28.5 Ma; Fig. 3). The reworked component includes *Chiasmolithus eograndis*, *Coccolithus formosus* and *Reticulofenestra hampdenensis* which collectively suggest an Eocene provenance. The associated foraminiferids are dominated by middle Eocene species (see Apthorpe *in* Marshall & others, 1989).

Two other Oligocene assemblages with reworked Eocene elements, similar to the assemblages detailed above, have been recorded from carbonates dredged from the Carnarvon Terrace at 3070—3700 m water depth (dredges 96DR007 and 96DR011; Fig. 2). The evidence of reworking in the first assemblage from a very soft marl (subsample 96DR011-04A (pipe) collected in a pipe attached to the dredge chain bag) should be regarded with some suspicion because of possible mixing during dredging. However, such mixing is thought unlikely for the soft chalk (subsamples 96DR007-04A & B) which yielded the second assemblage (see Shafik, 1990b). Dominant elements among the first assemblage (in 96DR011-04 (pipe)) suggest a late Oligocene age. These include common to abundant *Helicosphaera euphratis*, *H. obliqua*, *H. recta*, *Sphenolithus ciperoensis*, *Cyclicargolithus abisectus*, *C. floridanus*, *Discoaster deflandrei* and *Coronocyclus nitescens* as well as rare *Chiasmolithus altus* and *Triquetrorhabdulus carinatus*. This association of species suggests a biostratigraphic assignment within the NP25 Zone 28–23.6 Ma (Berggren & others, 1985). Other species in the assemblage include rare *Chiasmolithus grandis*, rare *Clausicoccus cribellum*, rare *Coccolithus eopelagicus*, very rare *C. formosus*, *Discoaster saipanensis*, *Cyclicargolithus reticulatus*, *Helicosphaera compacta*, *H. lophota*, *H. seminulum*, *H. wilcoxonii*, *Lanternithus minutus*, *Pedinocyclus larvalis*, *Pontosphaera multipora*, *Reticulofenestra scissura*, *R. umbilicus*, *Sphenolithus moriformis*, *S. predistentus*, *Syracosphaera labrosa*, *Zygrhablithus bijugatus bijugatus* and *Z. bijugatus crassus* which are mostly reworked from (middle) Eocene sediments. In addition, a few late Cretaceous taxa such as *Ahmuellerella octoradiata, Cribrosphaerella ehrenbergii, Prediscosphaera cretacea* and *Micula staurophora* were encountered. Although the hemipelagic species *Zygrhablithus bijugatus* may be (partly or wholly) autochthonous, the other hemipelagic species *Lanternithus minutus* is displaced, and suggests a shallow to intermediate Eocene/lower Oligocene source.

Age-diagnostic species in the chalk of sample 96DR007-04 pointing to a late Oligocene age are frequent and are somewhat poorly preserved — especially the key sphenoliths. The association of *Chiasmolithus altus, Coronocyclus nitescens, Cyclicargolithus abisectus, Helicosphaera bramlettei, H. euphratis, H. obliqua, H. recta, ?Sphenolithus ciperoensis, S. dissimilis, ?S. distentus* and *Triquetrorhabdulus carinatus*, suggests a probable placement high within the NP24 Zone. This zone spans the 30—28 Ma interval (Berggren & others, 1985). Most other species (which are either restricted to the Eocene or range from Eocene into Oligocene) are relatively less frequent but excellently preserved. These include very rare *Bramletteius serraculoides*, very rare *Chiasmolithus expansus*, very rare *C. oamaruensis, C. solitus, Clausicoccus cribellum, Coccolithus eopelagicus*, very rare *C. formosus, Cyclicargolithus floridanus*, rare *C. reticulatus, Discoaster deflandrei, D. tanii nodifer*, abundant *Helicosphaera compacta*, rare *H. seminulum, H. wilcoxonii*, very rare *Isthmolithus recurvus*, very rare *Lophodolithus nascens*, rare *Markalius inversus, Pedinocyclus larvalis*, very rare *Pontosphaera multipora*, frequent *Reticulofenestra scissura*, abundant *R. scrippsae*, very rare *R. umbilicus*, abundant *Sphenolithus moriformis*, common *S. predistentus*, very rare *S. pseudoradians*, very rare *S. radians, Syracosphaera labrosa* and *Zygrhablithus bijugatus bijugatus*.

It seems from the above that redeposition of the displaced lower Oligocene and Eocene nannofossils on the southern and western margins occurred more than once between 30 Ma and 23.6 Ma. During this interval sea level fluctuated rapidly (Haq & others, 1988), and some drastic changes in the climate and oceanographic circulation took place, probably as consequences of two sets of major tectonic events, amounting to plate readjustment, occurring earlier to the south and north of Australia (see Fig. 3). The first set is closely associated with the mechanical clearing of the Australian and Antarctic plates (at ~35 Ma), and the second with the collision of the Australian craton with a subduction zone to its north (~30 Ma). Dating of these two major events is tenuous; the first is based on a widespread unconformity in seismic sections south of Tasmania (Hinz & others, 1986), and the second on an unconformity in the Papuan Basin which has been interpreted as signifying the start of a foreland basin development in Papua New Guinea (Pigram & others, 1990; Pigram & Symonds, in press). Among the major events associated with the total separation of Australia and Antarctica are an increase in non-thermal subsidence rates south of Australia, observed in several wells in the Great Australian Bight by Stagg & others (1990) at ~32 Ma, and an abrupt cessation of shallow-water deposition on the outer margin of west Tasmania.

Input from the erosion of onshore areas during the mid to late Oligocene carbonate deposition in the Great Australian Bight, and especially in the Perth and Carnarvon Basins, seems to be negligible. The very low supply of Eocene and lower Oligocene carbonate debris from the onshore areas of the western margin (Perth and Carnarvon Basins) to the shelf (and deep sea) was probably due to the aridity of these areas during the Oligocene and the lack of diagenetically-suitable sediments (Loutit & Kennett, 1981); indeed, most of the Australian continent was dry during the Oligocene (BMR Palaeogeographic Group, 1990). Displaced early Oligocene and/or Eocene nannofossils (including hemipelagic species) in these Australian Oligocene carbonates are hence interpreted to have come from nearby (shallow or intermediate) offshore sources.

Oligocene sediments are absent from a number of oceanic sections off southwestern Australia (see Davies, Luyendyk & others, 1974; Hayes, Frakes & others, 1975). Large-scale Oligocene erosion in the ocean has been postulated to account for widespread Palaeogene unconformities in several Deep Sea Drilling Project (DSDP) sections in the southwest Pacific region off southeastern and eastern Australia (Kennett & others, 1972) (the Tasman Sea regional unconformity, Burns, Andrews & others, 1973; see also Kennett & others, 1974; Kennett & von der Borch, 1986), outcrops in New Zealand (the Marshall paraconformity, Carter & Landis, 1972) and oil wells in the offshore Otway Basin and west Tasmania (Hinz & others, 1986). Closer to the Great Australian Bight and the Perth Basin, the stratigraphic section at DSDP site 264 on the Naturaliste Plateau contains a distinct unconformity between nannofossil-rich sediments of middle Eocene and late Miocene age (see Hayes, Frakes & others, 1975; Shafik, 1985), suggesting that the plateau was a site of erosion rather than deposition during the (mid) Oligocene. The entire Palaeogene is missing from the Naturaliste Plateau section at DSDP site 258 where upper Miocene sediments directly overly Santonian (Thierstein, 1974), supporting the erosion scenario.

In contrast to the Naturaliste Plateau and several other oceanic sites in the Australian—southwest Pacific region, the marginal basins of southern and western Australia accumulated marine sediments during the (mid) Oligocene. This is indicated by recently-acquired data, including those discussed above from the Great Australian Bight and the Perth and Carnarvon Basins, and from the previously-known Oligocene in the Otway Basin (e.g. McGowran, 1973) and other basins in southern Australia (e.g. Lindsay, 1969, and Cooper, 1979, for the Oligocene of the St. Vincent Gulf Basin). The nannofossil content of some of these occurrences is not yet known, and may not include reworked Eocene nannofossils. The Oligocene section with the key species *Helicosphaera recta* at DSDP site 282 (west of Tasmania) apparently lacks reworked older Oligocene and/or Eocene nannofossils (distribution chart in Edwards & Perch-Nielsen, 1974), although *Transversopontis obliquipons* in mid-upper Oligocene sediments at this site may have been from a lower Oligocene source; site 282 was probably far removed from the sources of the reworked elements, or not in the path of the agents carrying the displaced nannofossils.

The evidence presented above suggests that nannofossils derived from lower Oligocene and Eocene marine sediments were incorporated into mid-late Oligocene chalks at several locations on the Australian southern and western margins (the Ceduna Terrace, Perth Canyon and the Carnarvon Terrace). Large-scale erosion during the mid to late Oligocene of lower Oligocene and Eocene nannofossil-rich sediments from shallow or intermediate oceanic sections such as the Naturaliste Plateau would put large amounts of nannofossils into suspension. They could then be incorporated into sediments being accumulated in nearby Australian marginal basins (such as the Great Australian Bight and the Perth Basin). If this scenario is true, it would answer *in part* the long-standing question regarding the whereabouts of the sediments lost during formation of the widespread late Palaeogene unconformities in the

[2] Shafik (1991) used the name 'Fremantle Canyon' instead, following Marshall & others (1989) and Quilty & others (in press), but the Hydrographer of the Royal Australian Navy has informed BMR that the name 'Perth Canyon' has precedence.

Australian—southwest Pacific region; another great deal of removed (lower Oligocene and Eocene) sediments, particularly from deeper oceanic sections, would be lost through the corrosive action of the cold bottom water masses that flowed through the Southern Ocean during the late Palaeogene (see Kennett & others, 1972).

Pacific Cainozoic erosive events: analogy with the Australian record

Observations by Thiede (1981) on displaced neritic fossils in Cainozoic sediments in the western central Pacific Ocean have led to the recognition of several erosive events there. Two of these erosive events are of particular interest here. Thiede (1981) indicated that a major erosive episode occurred during the interval 44—42 Ma when vigorous intermediate current regimes were developed. This middle Eocene event is the first major reworking event in the Cainozoic of the central Pacific. Five peaks of erosive events were identified by Thiede (1981) for the remaining part of the Cainozoic, among them an Oligocene event between 32 Ma and 30 Ma. Thiede (1981) argued that the reworked non-coeval fossils in the deep-sea sediments of the central Pacific were provided by mechanical erosion.

The times of the middle Eocene (44—42 Ma) and Oligocene (32—30 Ma) erosive events in the western central Pacific Ocean overlap with those of the middle Eocene (43.5 Ma) and mid to late Oligocene (30—28 Ma) reworking events on the Australian southern and western margins. However, finding a common overriding cause for the events may not prove possible because the hosting sediments in the central Pacific are deep-sea deposits (Thiede, 1981), whereas the hosting sediments on the Australian southern and western margins are shelf deposits. Furthermore, the perceived sea level stands seem to differ. Thiede (1981) argued that neritic fossils were transported episodically from the continental shelves into the adjacent deep-sea in the central Pacific during times of low eustatic sea level stands. The reworking of older nannofossils in the Australian middle Eocene and mid-upper Oligocene sediments occurred at the advent of a major Eocene transgression (the Wilson Bluff transgression) and during a period of mid to late Oligocene rapidly-fluctuating sea level respectively. The reworked nannofossils became available probably as the result of erosion of nearby shallow and intermediate oceanic sections (such as the Naturaliste Plateau) or parts of the Australian margins (such as the western Great Australian Bight, in the case of reworking of Cretaceous nannofossils in the middle Eocene further east along the Australian southern margin).

Correlation of one of the late Palaeogene unconformities in the Australasian region with other widespread unconformities outside the region seems possible. Carter & Landis (1972) alluded to possible correlatives with their Marshall paraconformity in southern South America, east Papua and South Africa.

Discussion. Cainozoic erosive events on the passive continental margins bordering the Atlantic Ocean (U.S. east coast margin, Irish margin and northeast European epicontinental sea: see Miller & others, 1987, and references therein) apparently occurred at times of greatest rate of sea level fall, like the Pacific major erosive events. Miller & others (1987) suggested different causal mechanisms for the early and late Tertiary erosive events which they undiscriminatingly equated with the major offlap ('Type 1') events of Vail & others (1977). Thus they considered that the erosive event during the mid Oligocene was due to glacioeustatic changes (probably coincident with an ice-growth event), and the event which occurred during the late middle Eocene due to tectonoeustatic lowerings caused by global seafloor spreading rate changes. The Australian short mid Eocene erosive event was probably connected with the change in the rate of seafloor spreading occurring at the time south of Australia (Shafik, 1985), but the degree of biostratigraphic resolution of the mid and late Oligocene erosive events of oceanic sections around Australia, and the dating of sea level changes (Haq & others, 1988) are not compatible.

These late Palaeogene erosive events, although apparently intimately related to the Oligocene cooling, were probably tectonically triggered. Thus the strengthening of intermediate currents during the mid to late Oligocene (sufficiently to erode sediments at shallow or intermediate depths such as on the Naturaliste Plateau) was probably directly related to certain oceanographic changes (intensified circulation resulting from steep latitudinal thermal gradients) caused by lowering of surface waters temperature (discussed below). However, the earlier major tectonic events south and north of Australia (the clearance of the Australian and Antarctic plates, and the collision of Australia with a subduction zone in its north) probably set the scene.

It is widely accepted that coastal (aggradation) onlap, observed in seismic profiles, can be of tectonic origin, unrelated to rising sea level (Watts & Thorne, 1984; Christie-Blick & others, 1990). Although the mid and upper Oligocene carbonates, with recycled nannofossils, on the southern and western margins of Australia are probably of tectonoeustatic origin at times of glacioeustatic lowerings, available data are not sufficient to confirm this. Age control on relevant tectonic events, such as the clearance of the Australian and Antarctic plates, is tenuous.

Oligocene surface water temperature changes

Oligocene assemblages identified here suggest a cool-water regime during the early and mid to late Oligocene on the Ceduna Terrace. This supports the climatic scenario in which the opening of the Tasmanian Seaway at shallow depths during the latest Eocene resulted in the flow of cool Indian Ocean waters south of Australia (Kennett & others, 1975), cooling the surface waters of the incipient Southern Ocean, and thus marking the onset of sequential Oligocene climatic deterioration (Corliss & others, 1984; Fig. 3). This culminated in the establishment and strengthening of the circum-Antarctic Current during the mid to late Oligocene (Kennett, 1977; 1978; Kennett & von der Borch, 1986). Evidence for an early Oligocene significant drop in surface water temperature in the Southern Ocean (see Wei, 1991 and references therein) is compelling, and the presence of an early Oligocene ice-sheet over East Antarctica (Shipboard Scientific Party, Leg 119, 1988) has been confirmed (Shipboard Scientific Party and Shore-based Contributors, 1989).

Oligocene cryospheric development of East Antarctica (Kennett & Barker, 1990) was particularly strong at times during the early, middle and late Oligocene when ice growth took place (see, e.g., Miller & others, 1987). The Oligocene cryospheric evolution was driven by progressive increase of latitudinal thermal gradients (from the late Eocene through the late Oligocene: Murphy & Kennett, 1986) and the strengthening of the circum-Antarctic Current later in the Oligocene. The best palaeontological evidence of cool conditions south of Australia during the mid to late Oligocene is the distribution of the tropical larger foraminiferids. A lack of mid to late Oligocene larger foraminiferids from the southern Australian record has already been noted (McGowran, 1986). This is particularly significant when considered with the several documented late middle—late Eocene occurrences of these neritic faunas in the

Southern Hemisphere, including southern Australia (see McGowran, 1986 and references therein; Fig. 3).

Two previously-recorded Oligocene assemblages from the Ceduna Terrace (*in* Shafik, 1990a) indicate surface water warming during the mid and late Oligocene. One assemblage from 66DR012B contains *Helicosphaera obliqua* and the low-latitude species *Sphenolithus distentus* which suggest a mid Oligocene age (within CP18 Zone or NP23 Zone, 34—30 Ma; Berggren & others, 1985), and another assemblage from 66DR006B includes *Helicosphaera recta* and the low-latitude species *Sphenolithus ciperoensis* which indicate a late Oligocene age (within NP25 Zone which spans the bracket 28—23.6 Ma; Berggren & others, 1985). Evidence of late Oligocene warming, namely the presence of *S. ciperoensis*, has already been documented in the Otway Basin and off west Tasmania (Shafik, 1987). Thus surface water temperatures fluctuated during the mid and late Oligocene along the Australian southern margin, particularly in the Great Australian Bight.

As the Ceduna Terrace assemblages containing the low-latitude species *S. distentus* and *S. ciperoensis* came from a location that was at about latitude 56°S at 26 Ma during the late Oligocene, according to the Australian apparent polar wander path (Idnurm, 1985), the surface waters would be expected to be relatively cool. Other indications for cool surface waters during the mid to late Oligocene interval south of Australia are discussed above (see also Fig. 3). Ocean warming at that time was probably due to external factors. Shafik (1990a) suggested that the key factor was a warm and intermittent proto-Leeuwin Current, thought to have started in the middle Eocene, that brought low-latitude species such as *Sphenolithus distentus* or *S. ciperoensis* from the northeastern Indian Ocean into southern Australia during the mid to late Oligocene. The distribution of low-latitude species in mid-upper Oligocene sediments of the Great Australian Bight and the Otway Basin suggests that the effects of the proto-Leeuwin Current varied along the southern margin. During a short late Oligocene episode, indicated by the presence of S. *ciperoensis* in both the Great Australian Bight and the Otway Basin, current effects were more widespread along the southern margin than during a short earlier Oligocene episode (indicated by the presence of *S. distentus* in the Great Australian Bight and its apparent absence from the Otway Basin to the east).

Discussion. The stratigraphic range of *Sphenolithus distentus* in the Ceduna Terrace Oligocene, or of *S. ciperoensis* in the Ceduna Terrace and the Otway Basin sequences, does not necessarily equate with the stratigraphic ranges of these species in low-latitude sections such as those used in the development of the zonations of Martini (1971) or Bukry (1973; 1975 which are the basis for Okada & Bukry's 1980 scheme). The temporal ranges of the species in the southern Australian sequences probably represent only parts of their ranges in the low-latitude sections. The local stratigraphic and geographic ranges of species depended on the duration and overall intensity of the intermittent proto-Leeuwin Current during the Oligocene.

The scenario of the proto-Leeuwin Current bringing *Sphenolithus distentus* and *S. ciperoensis* to southern Australia would mean that the lowest appearance level of either of these species in the southern Australian record is most likely to be isochronous.

Hiatuses and climatic changes

Theories relating oceanic hiatuses and climatic changes (McGowran, 1986) assume that increased erosion by bottom currents occurs during cool periods when oceanographic temperature gradients steepen and circulation intensifies; deep-sea hiatuses resulting from erosive action of bottom currents occur during cool periods in spite of possible increase in the carbonate and silica production due to upwelling. The theories also assume that increased dissolution (nondeposition) and lowered supply of pelagic material occur during warm periods when oceanographic gradients flatten and circulation slackens. As discussed above, the mid to late Oligocene interval was cool to cold (Fig. 3), and most of the oceanic Palaeogene unconformities in the Australian region are thought to have resulted from erosion by bottom and intermediate currents.

The theory suggests that at times of cooler, drier climate and lower sea level, hiatuses due to deep-sea erosion should correlate with hiatuses on the continental margins (McGowran, 1986). Marine Oligocene is either very poorly represented or totally absent from both offshore (at several DSDP sites, off southwestern, southern and eastern Australia) and onshore sections in adjacent marginal basins (e.g. in the Eucla Basin; see Hocking, 1990). This fits the theory well. However, what little there is of marine Oligocene in the Carnarvon, Perth, Great Australian Bight and Otway Basins does not fit the theory. Although their occurrence is restricted, Oligocene sediments in these basins roughly equate with stratigraphic gaps in the oceanic sections around Australia. (The case of the Oligocene in the offshore of southeastern Australia is more complicated: at the shallow DSDP site 281 on the South Tasman Rise, the Oligocene is missing, whereas at the much deeper DSDP site 282 west of Tasmania, most of the Oligocene section is preserved; see Kennett, Houtz & others, 1974.)

The complex Oligocene pattern of sediment removal and deposition around and on the Australian southern and western margins is matched by a history of changing gateways around Australia during a period of rapidly fluctuating sea level. Changes in the gateways and barriers complicate the theory relating hiatuses in the deep sea and on the continental margins during cool periods (McGowran, 1986). During the Oligocene, a high-latitude deep gateway south of Tasmania was opened connecting the Indian/Southern Ocean with the Pacific, and a lower-latitude (pre-mid Oligocene) seaway north of Australia was closed. Thus the total separation of the Australian and Antarctic plates (at about 35 Ma; Hinz & others, 1986) cleared the way for deep waters south of Tasmania, and the collision of Australia with a subduction zone in its north (at ~30 Ma; Pigram & others, 1990; Pigram & Symonds, in press) eventually closed a seaway north of Australia connecting the Indian and Pacific Oceans.

Summary

The middle Eocene assemblages recorded from the outer Ceduna Terrace include indicators of deposition on the shelf. Evidence from nearby seismic profiles suggests that the sediments containing these assemblages may not be *in situ* at a water depth of 4380 m on the outer Ceduna Terrace. The concept of thermal subsidence of the Ceduna Terrace (e.g. Hegarty & others, 1988) therefore cannot be fully tested here. A deepening of the sea above the Ceduna Terrace of less than 3000 m since the late Cretaceous has been suggested (based on data in Shafik, 1990a), and this agrees with the seismic evidence (Fraser & Tilbury, 1979; Stagg & others, 1990).

One of the recorded middle Eocene assemblages (102DR007-A), with rare reworked Cretaceous nannofossils, correlates well with others which were recorded previously from the base of the Wilson Bluff Limestone (and the Hampton Sandstone) at the base of the Tertiary section in the onshore Eucla Basin, and from the Lacepede Formation in the western Otway Basin in southeastern Australia. The assemblages from the Eucla and

Otway Basins also contain rare reworked Cretaceous nannofossils. These assemblages are assigned to the narrow biostratigraphic datum interval bracketed by the lowest occurrences of *Cyclicargolithus reticulatus* and *Reticulofenestra scissura*, which suggests an age of ~43.5 Ma. At about this time, an acceleration in the rate of spreading in the incipient Southern Ocean or a resumption of seafloor spreading between Australia and Antarctica led to and/or was associated with a major transgression in the Eucla Basin (the Wilson Bluff transgression), a significant acceleration in the rate of subsidence of the Australian southern margin, generation of short-lived, easterly-flowing, erosive bottom currents south of Australia, and initiation of an intermittent surface current, the proto-Leeuwin Current.

No reworked Cretaceous species were found in the other (younger) Eocene assemblages recorded from the Ceduna Terrace, which emphasises the brevity of the middle Eocene reworking episode.

Age determination for the assemblages containing the long-ranging Oligocene species could not be narrowed, because of the absence of the key mid and late Oligocene species *Sphenolithus distentus* and *S. ciperoensis*. The scarcity of *H. recta* and the abundant occurrence of older species (such as *Reticulofenestra umbilicus*) in the assemblages added to the difficulty of precise age determination.

A contrasting stratigraphic situation is indicated by the presence of mid and upper Oligocene marine carbonates in the marginal basins of southern and western Australia and their absence from several DSDP sites adjacent to Australia in the southeastern Indian Ocean and southwest Pacific Ocean, and from oil wells in offshore southern Australia. The upper Palaeogene carbonate sediments on the Ceduna Terrace (Shafik, 1990a; present study) and in other marginal areas as widely spaced as the Perth Canyon (Shafik, 1991) and Carnarvon Terrace (Shafik, 1990b) contain evidence of reworking of mainly Eocene and lower Oligocene nannofossil-rich sediments. During the late Palaeogene sea level fluctuated rapidly (Haq & others, 1988), and some drastic changes in the climate and oceanographic circulation took place probably as consequences of plate readjustment south and north of Australia. Cool conditions prevailed during the Oligocene. Oceanographic temperature gradients steepened and circulation intensified (Murphy & Kennett, 1986), increasing the erosive power of bottom (and intermediate) currents (McGowran, 1986). Large-scale late Palaeogene erosion (of probably Eocene and lower Oligocene marine sediments) on the Naturaliste Plateau and other oceanic sections in the Indian and southwest Pacific regions by intermediate currents put large amounts of nannofossils into suspension. Deposition of mid and late Oligocene marine carbonates on the Ceduna Terrace, at the Perth Canyon site and on the Carnarvon Terrace evidently incorporated these suspended nannofossils.

If the displaced Eocene and early Oligocene nannofossils in the Australian mid and upper Oligocene carbonates are the product of the large-scale mid to late Oligocene erosion of nearby shallow or intermediate oceanic sections, as suggested here, this partly explains the whereabouts of lost upper Palaeogene sediments from several oceanic sections.

The middle Eocene and mid-late Oligocene reworking events on the Australian southern and western margins occurred about the same time as others in the western central Pacific Ocean.

Surface waters were cool for most of the Oligocene in the Great Australian Bight. The proto-Leeuwin Current, thought to have existed since the middle Eocene (Shafik, 1990a), intermittently brought warmer surface waters containing low-latitude species into the high latitudes of the Great Australian Bight during the mid to late Oligocene. The effects of the current in the Great Australian Bight during the Oligocene are shown by two distinct short episodes; these effects varied in intensity but generally petered out along the southern margin in an easterly direction.

Acknowledgements

I thank my colleagues in the BMR's Marine Geoscience and Petroleum Geology Program, especially H.M.J. Stagg, C.J. Pigram, N.F. Exon and J.B. Willcox, for their fruitful discussions and constructive criticism of an earlier draft of the manuscript. I also thank Dr Brian McGowran (Adelaide University) and Mr A.R. Edwards (Stratigraphic Solutions, New Zealand), who refereed the manuscript, for their perceptive comments.

Calcareous nannofossil species referred to in this paper

Cainozoic species

Blackites perlongus (Deflandre) Shafik, 1981
Blackites spinulus (Levin) Roth, 1970
Blackites tenuis (Bramlette & Sullivan) Sherwood, 1974
Bramletteius serraculoides Gartner, 1969
Calcidiscus protoannulus (Gartner) Loeblich & Tappan, 1978
Campylosphaera dela (Bramlette & Sullivan) Hay & Mohler, 1967
Chiasmolithus altus Bukry & Percival, 1971
Chiasmolithus eograndis Perch-Nielsen, 1971
Chiasmolithus expansus (Bramlette & Sullivan) Gartner, 1970
Chiasmolithus grandis (Bramlette & Riedel) Radomski, 1968
Chiasmolithus oamaruensis (Deflandre) Hay, Mohler & Wade, 1966
Chiasmolithus solitus (Bramlette & Sullivan) Locker, 1968
Chiasmolithus titus Gartner, 1970
Clausicoccus cribellum (Bramlette & Sullivan) Prins, 1979
Coccolithus eopelagicus (Bramlette & Riedel) Bramlette & Sullivan, 1961
Coccolithus formosus (Kamptner) Wise, 1973
Coccolithus pelagicus (Wallich) Schiller, 1930
Corannulus germanicus Stradner, 1962
Coronocyclus nitescens (Kamptner) Bramlette & Wilcoxon, 1967
Cyclicargolithus abisectus (Müller) Wise, 1973
Cyclicargolithus floridanus (Roth & Hay) Bukry, 1971
Cyclicargolithus reticulatus (Gartner & Smith) Bukry, 1971
Daktylethra punctulata Gartner *in* Gartner & Bukry, 1969
Discoaster barbadiensis Tan Sin Hok, 1929
Discoaster binodosus Martini, 1958
Discoaster deflandrei Bramlette & Riedel, 1954
Discoaster saipanensis Bramlette & Riedel, 1954
Discoaster tanii Bramlette & Riedel, 1954
Discoaster tanii nodifer Bramlette & Riedel, 1954
Helicosphaera bramlettei Müller, 1970
Helicosphaera compacta Bramlette & Wilcoxon, 1967
Helicosphaera euphratis Haq, 1966
Helicosphaera heezenii Bukry, 1971
Helicosphaera lophota Bramlette & Sullivan, 1961
Helicosphaera obliqua Bramlette & Wilcoxon, 1967
Helicosphaera recta Haq, 1966
Helicosphaera seminulum Bramlette & Sullivan, 1961
Helicosphaera wilcoxonii Gartner, 1971
Holodiscolithus macroporus (Deflandre) Roth, 1970
Isthmolithus recurvus Deflandre *in* Deflandre & Fert, 1954
Lanternithus minutus Stradner, 1962
Lophodolithus nascens Bramlette & Sullivan, 1961
Markalius astroporus (Stradner) Mohler & Hay *in* Hay & others, 1967
Markalius inversus (Deflandre) Bramlette & Martini, 1964
Neococcolithes dubius (Deflandre) Black, 1967
Pedinocyclus larvalis (Bukry & Bramlette) Loeblich & Tappan, 1973
Pontosphaera multipora (Kamptner) Roth, 1970

Pseudotriquetrorhabdulus inversus (Bramlette & Bukry) Wise *in* Wise & Constans 1976
Reticulofenestra hampdenensis Edwards, 1973
Reticulofenestra orangensis (Bukry) Shafik, 1990
Reticulofenestra scissura Hay, Mohler & Wade, 1966
Reticulofenestra scrippsae (Bukry & Percival) Shafik, 1981
Reticulofenestra umbilicus (Levin) Martini & Ritzkowski, 1968
Sphenolithus ciperoensis Bramlette & Wilcoxon, 1967
Sphenolithus dissimilis Bukry & Percival, 1971
Sphenolithus distentus (Martini) Bramlette & Wilcoxon, 1967
Sphenolithus moriformis (Brönnimann & Stradner) Bramlette & Wilcoxon, 1967
Sphenolithus predistentus Bramlette & Wilcoxon, 1967
Sphenolithus pseudoradians Bramlette & Wilcoxon, 1967
Sphenolithus radians Deflandre *in* Grassé, 1952
Sphenolithus spiniger Bukry, 1971
Syracosphaera labrosa Bukry & Bramlette, 1969
Transversopontis obliquipons (Deflandre) Hay, Mohler & Wade, 1966
Transversopontis pulcher (Deflandre) Perch-Nielsen, 1967
Transversopontis zigzag Roth & Hay *in* Hay & others, 1967
Triquetrorhabdulus carinatus Martini, 1965
Zygrhablithus bijugatus bijugatus (Deflandre) Deflandre, 1959
Zygrhablithus bijugatus crassus Locker, 1967

Cretaceous species

Ahmuellerella octoradiata (Görka) Reinhardt, 1967
Cribrosphaerella ehrenbergii (Arkhangelsky) Deflandre *in* Piveteau, 1952
Micula staurophora (Gardet) Stradner, 1963
Predicosphaera cretacea (Arkhangelsky) Gartner, 1968
Vekshinella dorfii (Bukry) Shafik, 1990
Watznaueria barnesae (Black) Perch-Nielsen, 1968

References

Alley, N.F., 1988 — Preliminary palynological results. *Bureau of Mineral Resources, Australia, Record* 1988/16, Appendix 4, 1—2.

Berggren, W.A., Kent, D.V. & Flynn, J.J., 1985 — Jurassic to Paleogene: Part 2 Paleogene geochronology and chronostratigraphy. *In* Snelling, N.J. (editor), The chronology of the geological record. *The Geological Society, Memoir* 10, 141—195.

BMR Palaeogeographic Group, 1990 — Australia: evolution of a continent. *Bureau of Mineral Resources, Australia.*

Bukry, D., 1973 — Low-latitude coccolith biostratigraphic zonation. *In* Edgar, N.T., Saunders, J.B. & others, Initial Reports of the Deep Sea Drilling Project, 15. *U.S. Government Printing Office, Washington* 685—703.

Bukry, D., 1975 — Coccolith and silicoflagellate stratigraphy, Northwestern Pacific Ocean, Deep Sea Drilling Project Leg 32. *In* Larson, R.L., Moberly, R. & others, Initial Reports of the Deep Sea Drilling Project, 32. *U.S. Government Printing Office, Washington* 677—701.

Burns, R.E., Andrews, J.E. & others, 1973 — Initial Reports of the Deep Sea Drilling Project, 21. *U.S. Government Printing Office, Washington.*

Cande, S.C. & Mutter, J.C., 1982 — A revised identification of the oldest seafloor spreading anomaly between Australia and Antarctica. *Earth and Planetary Science Letters*, 58, 151—161.

Cande, S.C., Mutter, J.C. & Weissel, J.F., 1981 — A revised model for the break-up of Australia and Antarctica. *Eos*, 62, 384.

Carter, R.M. & Landis, C.A., 1972 — Correlative Oligocene unconformities in southern Australasia. *Nature (Physical Sciences)*, 237(70), 12—13.

Christie-Blick, N., Mountain, G.S. & Miller, K.G., 1990 — Seismic stratigraphic record of sea-level change. *Studies in Geophysics, Sea-level Changes, National Research Council*, 116—140.

Cooper, B.J., 1979 — Eocene to Miocene stratigraphy of the Willunga Embayment. *Department of Mines and Energy, Geological Survey of South Australia, Report of Investigations* 50.

Corliss, B.H., Aubry, M.-P., Berggren, W.A., Fenner, J.M., Keigwin, L.D. & Keller, G., 1984 — The Eocene/Oligocene event in the deep sea. *Science*, 226, 806—810.

Davies, H.L., Clarke, J.D.A., Stagg, H.M.J., Shafik, S., McGowran, B., Alley, N.F. & Willcox, J.B., 1989 — Maastrichtian and younger sediments from the Great Australian Bight. *Bureau of Mineral Resources, Australia, Report* 288.

Davies, T.A., Luyendyk, B.P. & others, 1974 — Initial Reports of the Deep sea Drilling Project, 26. *U.S. Government Printing Office, Washington.*

Edwards, A.R. & Perch-Nielsen, K., 1974 — Calcareous nannofossils from the southern Southwest Pacific, Deep Sea Drilling Project, Leg 29. *In* Kennett, J.P., Houtz, R.E. & others, Initial Reports of the Deep Sea Drilling Project, 29. *U.S. Government Printing Office, Washington*, 469—539.

Falvey, D.A. & Mutter, J.C., 1981 — Regional plate tectonics and the evolution of Australia's passive margins. *BMR Journal of Australian Geology & Geophysics*, 6, 1—29.

Fraser, A.R. & Tilbury, L.A., 1979 — Structure and stratigraphy of the Ceduna Terrace region, Great Australian Bight. *The APEA Journal*, 19, 53—65.

Haq, B.U., Hardenbol, J. & Vail, P.R., 1988 — Mesozoic and Cenozoic chronostratigraphy and cycles of sea-level change. Sea-level changes — an integrated approach. *Society of Economic Paleontologists and Mineralogists, Special Publication* No. 42, 71—108.

Hayes, D.E., Frakes, L.A., Barrett, P.J., Burns, D.A., Chen, P.-H., Ford, A.B., Kaneps, A.G., Kemp, E.M., McCollum, D.W., Piper, D.J.W., Wall, R.E. & Webb, P.N., 1975 — Initial Reports of the Deep Sea Drilling Project, 28. *U.S. Government Printing Office, Washington.*

Hegarty, K.A., Weissel, J.K. & Mutter, J.C., 1988 — Subsidence history of Australia's southern margin: constraints on basin models. *American Association of Petroleum Geologists, Bulletin* 72, 615—633.

Hinz, K., Willcox, J.B., Whiticar, M., Kudrass, H.-R., Exon, N.F. & Feary, D.A., 1986 — The west Tasmanian margin: an underrated petroleum province? *In* Glenie, R.C. (editor), *Second South-Eastern Australia Oil Exploration Symposium, Petroleum Exploration Society of Australia Symposium, Melbourne, 1985*, 395—410.

Hocking, R.M., 1990 — Eucla Basin. *In* Geology and mineral resources of Western Australia. *Western Australia Geological Survey Memoir*, 3, 548—561.

Idnurm, M., 1985 — Late Mesozoic and Cenozoic palaeomagnetism of Australia 1: A redetermined apparent polar wander path. *Geophysical Journal of Royal Astronomical Society*, 83, 399—418.

Kennett, J.P., 1977 — Cenozoic evolution of the Antarctic glaciation, the circum-Antarctic Ocean, and their impact on global paleoceanography. *Journal of Geophysical Research*, 82(27), 3843—3860.

Kennett, J.P., 1978 — The development of planktonic biogeography in the Southern Ocean during the Cenozoic. *Marine Micropaleontology*, 3, 301—345.

Kennett, J.P. & Barker, P.F., 1990 — Latest Cretaceous to Cenozoic climate and oceanographic developments in the Weddell Sea, Antarctica: an ocean-drilling perspective. *In* Barker, P.F., Kennett, J.P. & others, Proceedings of the Ocean Drilling Program, Scientific Results, 113. *College Station, TX (Ocean Drilling Program)*, 937—960.

Kennett, J.P., Burns, R.E., Andrews, J.E., Churkin, M., Davies, T.A., Dumitirica, P., Edwards, A.R., Galehouse, J.S., Packham, G.H. & van der Lingen, G.J., 1972 — Australian—Antarctic continental drift, palaeocirculation changes and Oligocene deep-sea erosion. *Nature (Physical Science)*, 239 (91), 51—55.

Kennett, J.P., Houtz, R.E. & others, 1974 — Initial Reports of the Deep Sea Drilling Project, 29, *U.S. Government Printing Office, Washington.*

Kennett, J.P., Houtz, R.E., Andrews, J.E., Edwards, A.R., Gostin, V.A., Hajos, M., Hampton, M.A., Jenkins, D.G., Margolis, S.V., Ovenshine, A.T. & Perch-Nielsen, K., 1974 — Cenozoic paleoceanography in the southwest Pacific Ocean, Antarctic glaciation and development of the circum-Antarctic current. *In* Kennett, J.P., Houtz, R.E. & others, Initial Reports of the Deep Sea Drilling Project, 29. *U.S. Government Printing Office, Washington*, 1155—1169.

Kennett, J.P. & von der Borch, C.C., 1986 — Southwest Pacific Cenozoic paleoceanography. *In* Kennett, J.P., von der Borch, C.C. & others, Initial Reports of the Deep Sea Drilling Project, 90. *U.S. Government Printing Office, Washington*, 1493—1517.

Lindsay, J.M., 1969 — Cainozoic foraminifera and stratigraphy of the Adelaide Plains Sub—basin, South Australia. *Geological Survey of South Australia, Bulletin* 42.

Loutit, T.S. & Kennett, J.P., 1981 — Australian Cenozoic sedimentary cycles, global sea level changes and the deep sea sedimentary record. Oceanologica Acta, 1981, *Actes 26ᵉ Congrès Géologique International, Colloque Géologie des marges continentales, Paris, 7—17 July 1980*, 45—63.

Marshall, J.F., Ramsay, D.C., Lavering, I., Swift, M.G., Shafik, S., Graham, T.G., West, B.G., Boreham, C.J., Summons, R.E., Apthorpe, M. & Evans, P.R., 1989 — Hydrocarbon prospectivity of the offshore South Perth Basin. *Bureau of Mineral Resources, Australia, Record* 1989/23.

Martini, E., 1971 — Standard Tertiary and Quaternary calcareous nannoplankton zonation. *In* Farinacci, A. (editor), *Proceedings of the II Planktonic Conference, Roma 1970, Edizioni Tecnoscienza, Roma*, 2, 739—785.

McGowran, B., 1973 — Observation bore No. 2, Gambier Embayment of the Otway Basin: Tertiary micropalaeontology and stratigraphy. *Mineral Resources Review, South Australia*, 135, 43—55.

McGowran, B., 1986 — Cainozoic oceanic and climatic events: the Indo-Pacific foraminiferal biostratigraphic record. *Palaeogeography, Palaeoclimatology, Palaeoecology*, 55, 247—265.

McGowran, B. & Beecroft, A., 1986 — Neritic, southern extratropical foraminifera and the terminal Eocene event. *Palaeogeography, Palaeoclimatology, Palaeoecology*, 55, 23—34.

Middleton, M.F., 1991 — Tectonic history of the southern continental margin of Western Australia. *Geological Survey of Western Australia, Record* 1990/8.

Miller, K.G., Fairbanks, R.G. & Mountain, G.S., 1987 — Tertiary oxygen isotope synthesis, sea level history, and continental margin erosion. *Paleoceanography*, 2, 1—19.

Murphy, M.G. & Kennett, J.P., 1986 — Development of latitudinal thermal gradients during the Oligocene: oxygen-isotope evidence from the southwest Pacific. *In* Kennett, J.P., von der Borch, C.C. & others, Initial Reports of the Deep Sea Drilling Project, 90. *U.S. Government Printing Office, Washington*, 1347—1360.

Mutter, J.C., Hegarty, K.A., Cande, S.C. & Weissel, J.K., 1985 — Breakup between Australia and Antarctica: a brief review in the light of new data. *Tectonophysics*, 114, 255—279.

Okada, H. & Bukry, D., 1980 — Supplementary modification and introduction of code numbers to the low-latitude coccolith biostratigraphic zonation (Bukry, 1973; 1975). *Marine Micropaleontology*, 5, 321—325.

Perch-Nielsen, K., 1985 — Cenozoic calcareous nannofossils. *In* Bolli, H.M., Saunders, J.B. & Perch-Nielsen, K. (editors), Plankton stratigraphy, Cambridge earth science series. *Cambridge University Press, Cambridge*, 427—554.

Pigram, C.J., Davies, P.J., Feary, D.A., Symonds, P.A. & Chaproniere, G.C.H., 1990 — Controls on Tertiary carbonate platform evolution in the Papuan Basin: new play concepts. *In* Carman, G.J. & Carman, Z. (editors), Petroleum exploration in Papua New Guinea. *Proceedings of the first PNG Petroleum Convention, Port Moresby, 12–14 February 1990*, 185–195.

Pigram, C.J. & Symonds, P.A., in press — A review of the timing of the major tectonic events in the New Guinea orogen. *Journal of Southeast Asian Earth Sciences*.

Quilty, P.G., Lowry, D.C., Moore, A.M.G. & Thomas, B.M., in press — The Fremantle Canyon, Western Australia — a description and geological history. *Marine Geology*.

Shafik, S., 1981 — Nannofossil biostratigraphy of the *Hantkenina* (foraminiferid) interval in the upper Eocene of southeastern Australia. *BMR Journal of Australian Geology & Geophysics*, 6, 108—116.

Shafik, S., 1983 — Calcareous nannofossil biostratigraphy: an assessment of foraminiferal and sedimentation events in the Eocene of the Otway Basin, southeastern Australia. *BMR Journal of Australian Geology & Geophysics*, 8, 1—17.

Shafik, S., 1985 — Cretaceous coccoliths in the middle Eocene of the western and southern margins of Australia. *BMR Journal of Australian Geology & Geophysics*, 9, 353—359.

Shafik, S., 1987 — Tertiary nannofossils from offshore Otway Basin and off West Tasmania. *Bureau of Mineral Resources, Australia, Record* 1987/11, 67—96.

Shafik, S., 1990a — The Maastrichtian and early Tertiary record of the Great Australian Bight Basin and its onshore equivalents on the Australian southern margin: a nannofossil study. *BMR Journal of Australian Geology & Geophysics*, 11, 437—497.

Shafik, S., 1990b — Calcareous nannofossil age determination of dredge subsamples, BMR Cruise 96. *Bureau of Mineral Resources, Australia, Record* 1990/85, 56—82.

Shafik, S., 1991 — Upper Cretaceous and Tertiary stratigraphy of the Fremantle Canyon, South Perth Basin: a nannofossil assessment. *BMR Journal of Australian Geology & Geophysics*, 12, 65—91.

Shipboard Scientific Party and Shore-based Contributors, 1989 — Principal results and summary. *In* Schlich, R., Wise, S.W. & others, Proceedings of the Ocean Drilling Program, Initial Reports, 120, *College Station, TX (Ocean Drilling Program)*, 73—85.

Shipboard Scientific Party, Leg 119, 1988 — Early glaciation of Antarctica. *Nature*, 333, 303—304.

Stagg, H.M.J., Cockshell, C.D., Willcox, J.B., Hill, A.J., Needham, D.J.L., Thomas, B., O'Brien, G.W. & Hough, L.P., 1990 — Basins of the Great Australian Bight region: geology and petroleum potential. *Bureau of Mineral Resources, Continental Margins Program Folio* 5.

Thiede, J., 1981 — Late Mesozoic and Cenozoic sedimentation along oceanic island margins: analog to continental margins. Oceanologica Acta, 1981, *Actes 26ᵉ Congrès Géologique International, Colloque Géologie des marges continentales, Paris, 7—17 July 1980*, 65—70.

Thierstein, H.R., 1974 — Calcareous nannoplankton — Leg 26, Deep Sea Drilling Project. *In* Davies, T.A., Luyendyk, B.P.& others, Initial Reports of the Deep Sea Drilling Project, 26. *U.S. Government Printing Office, Washington*, 619—667.

Truswell, E.M., Chaproniere, G.C.H. & Shafik, S. (compilers), 1991 — Australian Phanerozoic timescales: 10. Cainozoic biostratigraphic chart and explanatory notes. *Bureau of Mineral Resources, Australia, Record* 1989/40.

Vail, P.R., Mitchum, R., Todd, R.G., Widmier, J.M., Thompson, S., Sangree, J.B., Bubb, J.N. & Hatelid, W.G., 1977 — Seismic stratigraphy and global changes of sea level. *American Association of Petroleum Geologists, Memoir*, 26, 49—205.

Veevers, J.J., Stagg, H.M.J., Willcox, J.B. & Davies, H.L., 1990 — Pattern of slow seafloor spreading (<4 mm/year) from breakup (96 Ma) to A20 (44.5 Ma) off the southern margin of Australia. *BMR Journal of Australian Geology & Geophysics*, 11, 499—507.

Watts, A.B. & Thorne, J., 1984 — Tectonics, global changes in sea level and their relationship to stratigraphical sequences at the U.S. Atlantic continental margin. *Marine and Petroleum Geology*, 1, 319—339.

Wei, W., 1991 — Evidence for an earliest Oligocene abrupt cooling in the source waters of the Southern Ocean. *Geology*, 19, 780—783.

BMR Journal of Australian Geology & Geophysics, 13, 143-185

Late Carboniferous and Early Permian palynostratigraphy of the Joe Joe Group, southern Galilee Basin, Queensland, and implications for Gondwanan stratigraphy

M.J. Jones[1] & E.M. Truswell[2]

Five new Carboniferous to Permian palynological Oppel-zones have been identified through detailed analyses of core samples taken from the Joe Joe Group sediments of the Galilee Basin. In ascending stratigraphic order, and in relation to their host formations, the Oppel-zones are: the *Verrucosisporites basiliscutis* Oppel-zone (A), spanning the Lake Galilee Sandstone and the basal Jericho Formation; the *Brevitriletes leptoacaina* Oppel-zone (B), in the mid-Jericho Formation; the *Diatomozonotriletes birkheadensis* Oppel-zone (C), in the upper Jericho Formation; the *Asperispora reticulatispinosus* Oppel-zone (D), encompassing much of the Jochmus Formation and the uppermost part of Jericho Formation (including the Oakleigh Siltstone Member); and the *Microbaculispora tentula* Oppel-zone (E), in the upper part of the Jochmus Formation. The three oldest Oppel-zones are grouped to form the Carboniferous (Namurian A—upper Westphalian D) *Spelaeotriletes queenslandensis* Superzone, which correlates with the *Spelaeotriletes ybertii* Assemblage of earlier workers. The overlying *Asperispora reticulatispinosus* Oppel-zone (D) (upper Westphalian D—Upper Autunian, or early Asselian) mostly correlates with the *Potonieisporites* Assemblage. The uppermost *Microbaculispora tentula* Oppel-zone (E), late Autunian (late Carboniferous) to early Tastubian (Early Permian), correlates with the Upper Stage 2. Application of the Oppel-zones has clarified relationships between outcrop sections of the earlier defined Joe Joe Formation of the Galilee Basin and lithological units subsequently identified in the subsurface. Stratigraphic interpretation of the Oppel-zones with their lithostratigraphic equivalents suggests that late Palaeozoic glaciation began in the Westphalian D and continued until the late Asselian/earliest Tastubian, when climatic warming resulted in sea level rise associated with continental glacial melting. The palynological record shows the impact of this glacial episode, which caused significant global compositional changes in palynofloras in the Late Carboniferous/Early Permian. These changes may allow correlations between Gondwana and Laurasia. Eleven new species of miospore are described.

Introduction

The age relationships and biostratigraphy of immediately pre-glacial and glacial Late Carboniferous/Early Permian sediments are probably the least understood of any part of the Late Palaeozoic sequence in Australia. The sediments, deposited in

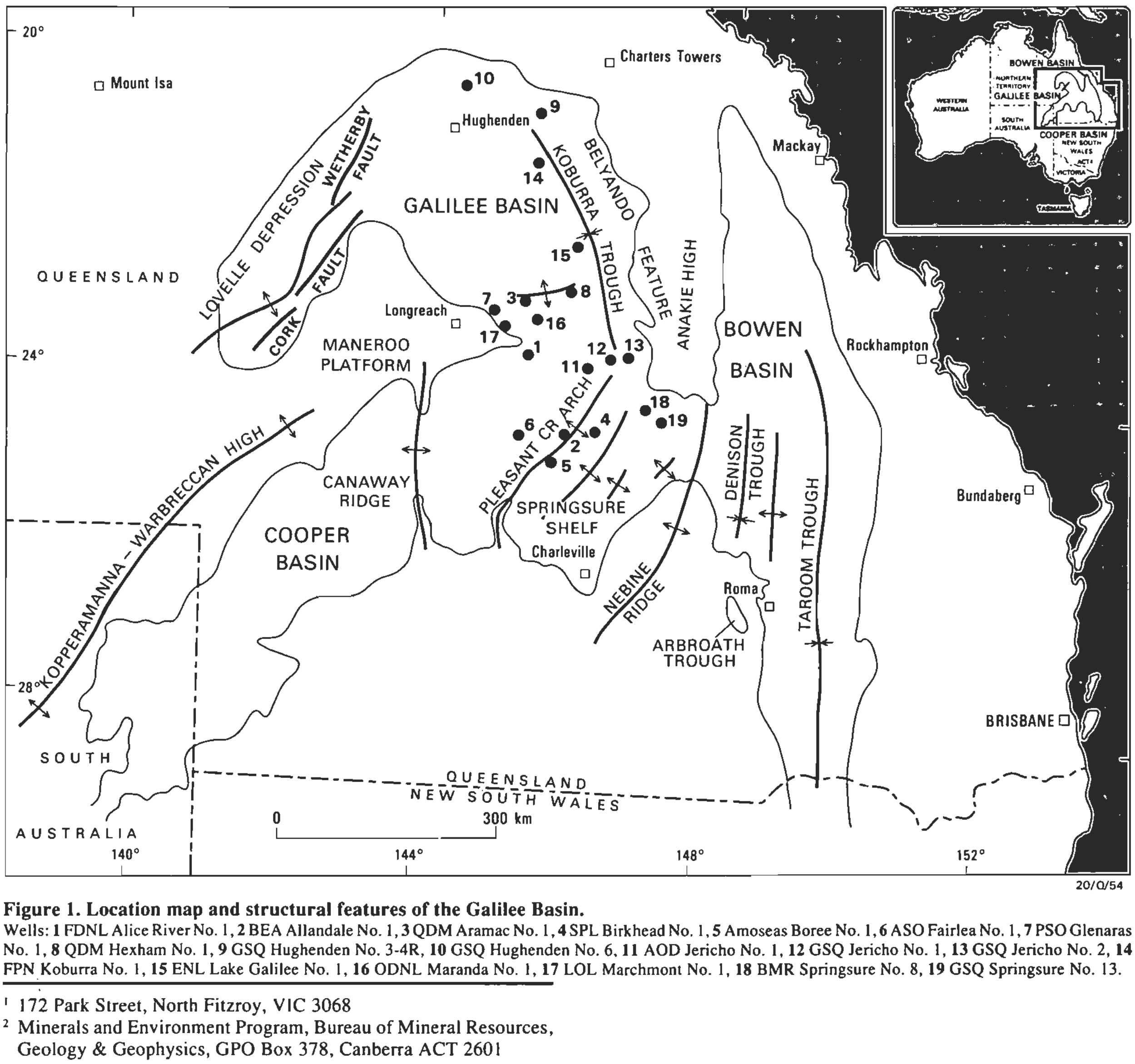

Figure 1. Location map and structural features of the Galilee Basin.
Wells: **1** FDNL Alice River No. 1, **2** BEA Allandale No. 1, **3** QDM Aramac No. 1, **4** SPL Birkhead No. 1, **5** Amoseas Boree No. 1, **6** ASO Fairlea No. 1, **7** PSO Glenaras No. 1, **8** QDM Hexham No. 1, **9** GSQ Hughenden No. 3-4R, **10** GSQ Hughenden No. 6, **11** AOD Jericho No. 1, **12** GSQ Jericho No. 1, **13** GSQ Jericho No. 2, **14** FPN Koburra No. 1, **15** ENL Lake Galilee No. 1, **16** ODNL Maranda No. 1, **17** LOL Marchmont No. 1, **18** BMR Springsure No. 8, **19** GSQ Springsure No. 13.

[1] 172 Park Street, North Fitzroy, VIC 3068
[2] Minerals and Environment Program, Bureau of Mineral Resources, Geology & Geophysics, GPO Box 378, Canberra ACT 2601

only a few basins immediately before the clear establishment of the *Glossopteris* flora, are difficult to date because of the lack of associated marine faunas, a history of confusion over the identity of megafloral remains, and uncertainties about the extent of erosion and loss of section associated with glacial processes. In Western Australia significant pre-glacial Late Carboniferous sedimentary sequences occur only in the Bonaparte and Canning Basins; in eastern Australia such sediments are preserved sporadically in the New England and Yarrol Orogens, and within the Galilee Basin.

This paper documents the palynofloras from the Late Carboniferous Joe Joe Group of the Galilee Basin. The zoning of the Galilee Basin sequence involved detailed systematic taxonomic examination of palynomorphs, principally recovered from cores in the stratigraphic boreholes GSQ Jericho 1, GSQ Jericho 2 and GSQ Springsure 13. Eleven new species were identified and are formally described, and some established taxa are revised. Relationships between some previously described palynostratigraphic units have been reinterpreted.

Galilee Basin

The Galilee Basin is a 250 000 km² intracratonic basin of early Late Carboniferous to Middle Triassic age in central Queensland (Figs 1, 2); it mostly underlies the younger cover of the Great Artesian Basin. Only the Galilee Basin's northeastern margin is exposed, where it abuts the Anakie High. The Nebine Ridge, a meridional subsurface continuation of the Anakie High, divides the Galilee from the Bowen Basin, and underlies an area of sediment thinning known as the Springsure Shelf (Evans, 1980). The Galilee Basin is divided in two by its constriction around the Maneroo Platform. The northern section of the basin contains two major depocentres — the Lovelle Depression and Koburra Trough (Vine & others, 1964; Benstead, 1973; Allen, 1974; Evans, 1980; Jackson & others, 1981). Deposition began in the Koburra Trough where sediments overlap, with minor disconformity, the Devonian to Early Carboniferous Drummond Basin (Mollan & others, 1969; Olgers, 1972; Evans, 1980; Fenton & Jackson, 1989). Sedimentation continued and expanded from this depocentre until the Early Permian when a major tectonic event took place, corresponding with the initiation of sedimentation in the Bowen and other Australian late Palaeozoic intracratonic basins (i.e. the Cooper, Arckaringa and Pedirka Basins). The Galilee Basin may have developed from a Late Carboniferous to Middle Triassic north—northwesterly trending dextral shear couple (Evans & Roberts, 1978; Evans, 1980).

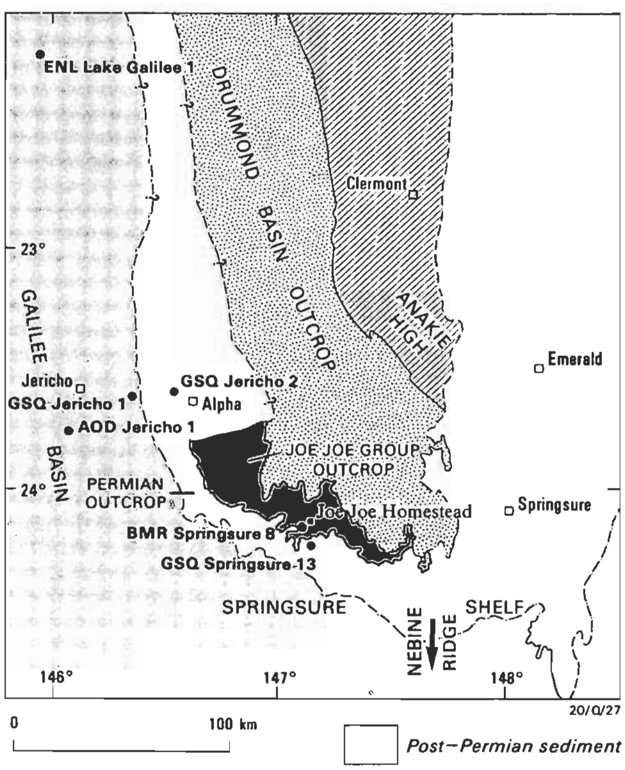

Figure 2. Southern Galilee Basin showing outcrop geology and location of wells examined in detail (from Gray, 1976).

Subsurface nomenclature for the Late Carboniferous to Early Permian strata of the Galilee Basin used here has been adopted from Gray & Swarbrick (1975) (Fig. 3), who subdivided the Joe Joe Formation — as previously applied to surface outcrops within the Tambo and Jericho 1:250 000 Sheet-area — into the Jochmus Formation, Jericho Formation and Lake Galilee Sandstone of the subsurface, thereby elevating the former Joe Joe Formation to group status.

The Koburra Trough contains the stratigraphically oldest unit, the fluvially derived Lake Galilee Sandstone (Gray & Swarbrick, 1975) which is conformably overlain by the Late Carboniferous to Early Permian sediments of the Jericho Formation, the Jochmus Formation, and the Aramac Coal Measures (Fig. 3). These younger sediments extend beyond the Koburra Trough and appear to have been deposited under glacially influenced fluvio-lacustrine conditions (Gray & Swarbrick, 1975).

Proposed palynozonation of the Galilee Basin sequence

Moderately diverse, although often sparse, well preserved palynological assemblages were found in core samples from GSQ Springsure 13, GSQ Jericho 2, and GSQ Jericho 1 (Fig. 4, Table 1). Thirty-nine palynomorph species were recognised. A few forms, which are extremely rare or with very generalised morphologies, remain undescribed. Diversity in the assemblages is lower than in the Early Carboniferous palynofloras of the underlying Drummond Basin; Playford (1978) described 68 species from the Ducabrook Formation of that basin.

Two of the species in this study, *Quadrisporites horridus* Hennelly ex. Potonié & Lele 1961 and *Maculatasporites minimus* Segroves 1967, are probably algal. The remainder are spores and pollen. Most of these (28 species) are trilete spores; smooth-walled forms referable to *Calamospora* and *Punctatisporites* often account for 80% of a single assemblage. Verrucate spores are common; five species are listed. Apiculate spores, both cavate and acavate, are another major morphological element. Pollen is dominated by monosaccate taxa, including the radially symmetrical *Plicatipollenites* and *Cannanoropollis*. Bilaterally symmetrical forms include *Potonieisporites*, *Caheniasaccites* and, less frequently, taeniate disaccate pollen assignable to *Protohaploxypinus*.

In terms of broad botanical affinities two species, belonging to the genera *Calamospora* and *Retusotriletes*, are possibly allied with the articulates, or Sphenopsida; 21 species (including smooth, apiculate and verrucate trilete spores) may be allied with the ferns; another 8 species may be lycopods (including the cavate trilete spores, but see Foster & others 1985); and a further eight taxa of monosaccate and disaccate pollen may be of gymnospermous origin.

The ranges of the identified species were plotted against sample depths. Five local palynological Oppel-zones (outlined below), each named after a prominent component species, were

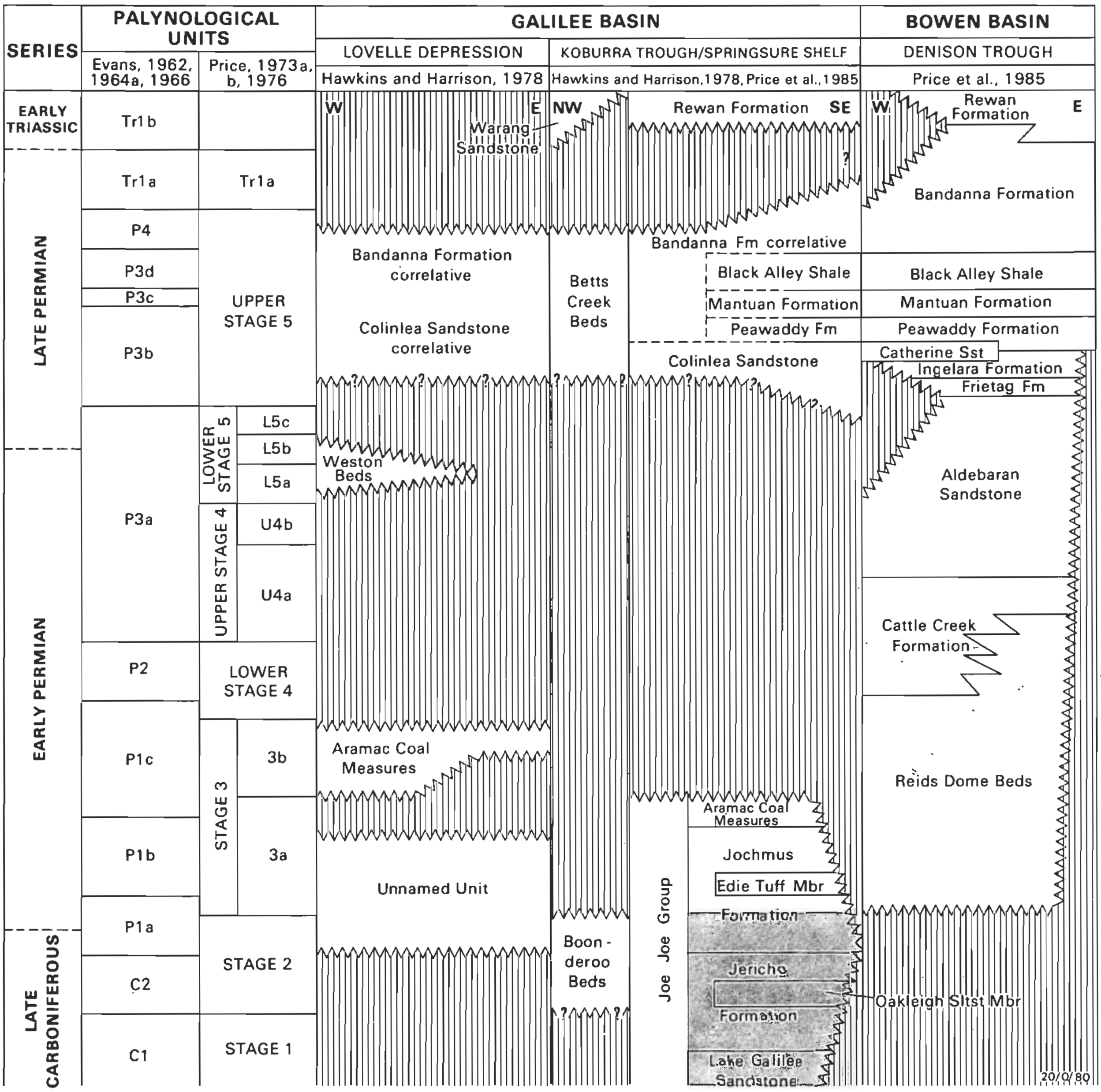

Figure 3. Lithostratigraphic nomenclature for the Galilee Basin and associated units from the Bowen Basin, showing interval investigated in this paper (shaded section of Joe Joe Group).

delineated. Samples or sections do not necessarily contain all diagnostic species for a specified zone (Fig. 5).

Spelaeotriletes queenslandensis Superzone

This Superzone is indicated by the incoming of *S. queenslandensis* sp. nov., and is subdivided into three zones (A—C):

1.1 *Verrucosisporites basiliscutis* Oppel-zone (A)

Assemblage characteristics This assemblage is identified by association of the radially symmetrical monosaccate pollen *Cannanoropollis janakii* Potonié & Sah 1960 and *Potonieisporites novicus* Bharadwaj 1954 with trilete spores including *Verrucosisporites basiliscutis* sp. nov., *Cyclogranisporites firmus* sp. nov., *'Apiculiretusispora' arcuatus* sp. nov. and *Spelaeotriletes queenslandensis* sp. nov.

Reference section GSQ Jericho 2, 1169—1052 m

Reference slide MFP 6860/4 (1169 m), GSQ Jericho 2

Lithostratigraphic association Lake Galilee Sandstone and lowermost Jericho Formation

Age Early Namurian

Equivalent palynostratigraphic units Lower Stage 1 (Norvick, 1974; Price, 1976), lower *Spelaeotriletes ybertii* Assemblage (Powis, 1979)

Identified in sections GSQ Jericho 2, 1169—1052 m

1.2 *Brevitriletes leptoacaina* Oppel-zone (B)

Assemblage characteristics This zone is identified by the introduction of *Brevitriletes leptoacaina* sp. nov. and the presence of *Dibolisporites disfacies* sp. nov., *Potonieisporites elongatus* comb. nov. and nom. nov., and *Caheniasaccites elephas* sp. nov. The species *Reticulatisporites bifrons* sp. nov.,

Table 1. Abundances of miospore taxa from GSQ Jericho 2, GSQ Springsure 13, GSQ Jericho 1 and BMR Springsure 8.
Percentages are based upon a minimum count of 200 miospores per sampled horizon, rounded off to the nearest half per cent. Taxa encountered in levels below 0.5% are indicated by a black dot. Oppel-zones shown are: *Verrucosisporites basiliscutis* Oppel-zone A; *Brevitriletes leptoacaina* Oppel-zone B; *Diatomozonotriletes birkheadensis* Oppel-zone C; *Asperispora reticulatispinosus* Oppel-zone D; *Microbaculispora tentula* Oppel-zone E.

Well	Biozone	Depth (m)	*Calamospora* sp. cf. *C. microrugosa*	*Punctatisporites gretensis*	*P. lucidulus*	*Retusotriletes nigritellus*	*Psomospora detecta*	*Verrucosisporites basiliscutus*	*V. nitidus*	*V. aspratilis*	*V. quasigobbettii*	*V.* sp	*Brevitriletes leptoacaina*	*Apiculiretusispora arcuatus*	*Dibolisporites disfacies*	*Anapiculatisporites concinnus*	*Ahrensisporites cristatus*	*Diatomozonotriletes birkheadensis*	*Rugospora ? australiensis*	*Spelaeotriletes queenslandensis*	*Auroraspora solisortus*	*Densoisporites* sp.	*Cristatisporites* sp.	*C.* sp. cf. *C. kuttungensis*	*Asperispora reticulatispinosus*	*Potonieisporites novicus*	*P. elongatus*	*Plicatipollenites densus*	*P. gondwanensis*	*Cannanoropollis janakii*	*Striomonosaccites* sp.	*Caheniasaccites elephas*	*Protohaploxypinus* sp. cf. *P. goraiensis*	*Cyclogranisporites firmus*	*Reticulatisporites bifrons*	*Rattiganispora apiculata*	*Apiculatisporis pseudoheles*	*Horriditriletes ramosus*	*Microbaculispora tentula*	*Quadrisporites horridus*	*Maculatasporites minimus*		*Others*
BMR Springsure 8	D	18	21.5	25	9.5	●		1			●	0.5	1	0.5	0.5	0.5					1			5	4.5	5		4.5	1	7.5			0.5	1.5									9.5
BMR Springsure 8	D	28	29.5	24	7			10	1	0.5	1	4	1	0.5		1	●		1	6		1.5	0.5	0.5	●	1		0.5		1			1	●									7
BMR Springsure 8	D	32	18	23	13		●	6	4.5	5.5	3	1	2	1	0.5	1			1.5	2	●	0.5		1		0.5	2	1		2	1	●		3.5	●								6.5
GSQ Jericho 1	E	391	15	19.5	41							1							1.5									1.5		20.5													0
GSQ Jericho 1	E	429	38	18	14.5	3	0.5		0.5		0.5		2		●				0.5			0.5			●		●	0.5		1			0.5			0.5	4.5	10.5	0.5		0.5		3
GSQ Jericho 1	D	435	23	15	28	6			●				1						1	1		●				1		●		●			●			2	8				●		12
GSQ Jericho 1	D	480	26	11	19	1		1	2				6															1									3	21					6
GSQ Jericho 1	D	528	54	11	9								1						3.5	4					●	1.5	●	1		11.5		●	2										1
GSQ Jericho 1	D	531	33	22	19.5	●													4	0.5		1			0.5	●				17.5													1.5
GSQ Jericho 1	D	760	19.5	31	30								11						0.5					0.5	2			2		1.5			1										1
GSQ Springsure 13	D	64	24	32	16.5	●							2.5		1.5				3			1.5		3.5	0.5	1		2.5		4		2											4
GSQ Springsure 13	D	169	13	17	9		●	11	4	1				1					7	3		1					●			●				23	1								9
GSQ Springsure 13	D	210	17	27	24				1		1		6	2		7			6				3	0.5				3					0.5										2
GSQ Springsure 13	D	262	27.5	19	15				0.5				0.5	9								3		11		0.5		0.5		0.5	0.5	5			0.5								7
GSQ Springsure 13	D	289	30	18.5	16.5		●	2.5					2.5	●	●	●		●	4	6	●	3	0.5	2				2		2	1	1		5	1					●			0.5
GSQ Springsure 13	D	341	72	10	5			5		0.5	●	0.5							3.5	0.5	●		●				0.5			0.5			0.5	0.5									0.5
GSQ Springsure 13	D	343	38	7.5	13		●	11.5			0.5	●	1	●	0.5	●		●	5	4		●	●		●	●		●		●		●		12	1	●							5.5
GSQ Springsure 13	C	438	26	32	18		1	1.5	1.5			0.5	2		1				2.5			0.5		0.5				1		1				2	1								8
GSQ Springsure 13	C	488	40	20	17			0.5	0.5		0.5	0.5	5.5		4.5	0.5			4.5			0.5	0.5	0.5						1.5				3									0
GSQ Springsure 13	C	536	50	10.5	15.5				0.5		0.5	0.5	3		4	0.5			2.5	2.5			1.5	3		0.5	●	1.5				●		2									1
GSQ Springsure 13	B	571	24	31	19			5			●		2		1				2	4						●																	11
GSQ Springsure 13	B	622	33	18.5	16			2.5	1		3	2	1		1	2.5			5.5	2.5		1								0.5													10
GSQ Springsure 13	B	624	12	28	16			3	0.5		6	0.5	3.5		1	3			2.5	2.5								0.5		1													20
GSQ Springsure 13	B	670	26.5	23.5	21			5	1.5	1	1.5	1	2.5		2.5	1			3		0.5	2					●	0.5		1													5
GSQ Springsure 13	B	687	35	16	27.5			7.5	1.5	0.5	1.5	0.5	1.5	0.5	1				0.5	1		●						1															4
GSQ Springsure 13	B	722	35	19	19		●	6	1	2	4		5	2					1	1		1				0.5		●		0.5		●		0.5	●								1
GSQ Springsure 13	B	772	34	14.5	19			3.5		1.5	2		3		3				13	2	0.5	0.5								0.5													3
GSQ Jericho 2	D	79	41.5	12.5	9								13.5						0.5											1.5					1.5	●	20						0
GSQ Jericho 2	D	129	21.5	32	25.5	●	2						9.5						1.5	●	●					●		●		0.5					0.5		6.5			0.5			0
GSQ Jericho 2	D	207	24	5	55														3																								13
GSQ Jericho 2	D	223	10	14	6	6				1	1		5							1			3		4	1				45.5													1
GSQ Jericho 2	D	226	11.5	26.5	18.5	●													19.5	0.5					0.5					21.5			●										1
GSQ Jericho 2	D	324	25	28	16			1.5	3	●		1.5	4.5		●	●		●	6.5				●		8	●		●		2.5				1.5	●								1
GSQ Jericho 2	D	328	13.5	12.5	22.5			1.5	0.5		1		2						0.5							16.5	2	3.5		15.5			0.5	0.5	0.5								6
GSQ Jericho 2	D	424	18	22.5	26			1	0.5		0.5		1		2				0.5			0.5	0.5			1	0.5	1		20			1	2.5									0.5
GSQ Jericho 2	D	426	40	3	31.5			3	●	1	0.5	●		●	2	●			6	●					●	0.5	●	0.5	●	10			●										0
GSQ Jericho 2	D	519	17	45	16			1.5							1.5	3		1	0.5					2		1	1	3	1.5														5
GSQ Jericho 2	D	603	23.5	15	9								2	6.5		6			1				5	5.5		6	0.5	3							●	●							17
GSQ Jericho 2	D	652	77	6	3			1	1	1									1	1					●	1		1		3													4
GSQ Jericho 2	C	654	25	19	34.5			4	2.5	2	1		0.5			1				0.5			0.5	0.5		1				0.5		1		3	0.5								3
GSQ Jericho 2	C	655	46.5	25	15.5			0.5		0.5					3				1	3.5		0.5								3.5		0.5											0
GSQ Jericho 2	C	705	24	9.5	7		1	4.5	2.5	3	4	3.5	2.5	4					3.5	18.5		●				1	0.5	0.5		2	1		●	●		●							7
GSQ Jericho 2	C	746	7	28	22				1	0.5			2	2.5					15.5	16	0.5			1.5						1					0.5								1.5
GSQ Jericho 2	C	795	19	24	15			4	2	1			2	2	1				7	4			3	4		1	1			5	1		●			●							2
GSQ Jericho 2	C	900	24	14	20			2	0.5	1	1.5		1	0.5	1.5	1		1	5.5	2.5	●	2	7.5	●		1.5	0.5		0.5	1		1.5		4	0.5								4.5
GSQ Jericho 2	B	951	24	38	23			1	3		2								1											3				1									4
GSQ Jericho 2	B	989	18	27.5	30			5	3.5	0.5	1	0.5							4		1.5					1.5	0.5			1	2			1	0.5								2
GSQ Jericho 2	B	1018	28	15	14.5			1	0.5	2	0.5		0.5	2		●	●		2	0.5	2	●				12.5	2	1.5		1	4	2.5											7.5
GSQ Jericho 2	A	1052	24	53	6			3	2	3	1	1														1				1													5
GSQ Jericho 2	A	1123	20	20	41			4	1		1			1					6	1		1				1																	3
GSQ Jericho 2	A	1169	23	48	9			6.5		5		1				0.5										2		1		1				●									2.5

20/Q/34

Ahrensisporites cristatus Playford & Powis 1979 and *Striomonosaccites*? first appear in this zone in GSQ Jericho 2.

Reference section GSQ Springsure 13, 772—571 m

Reference slide MFP 6907A/2 (669.74 m), GSQ Springsure 13

Lithostratigraphic association Mid-Jericho Formation

Age Namurian—?early Westphalian

Equivalent palynostratigraphic units Upper Stage 1 (Norvick, 1974; Price, 1976), mid *Spelaeotriletes ybertii* Assemblage (Powis, 1984)

Identified in sections GSQ Springsure 13, 772—571 m; GSQ Jericho 2, 1018—951 m

1.3 *Diatomozonotriletes birkheadensis* Oppel-zone (C)

Assemblage characteristics This assemblage is marked by the introduction of *Cristatisporites* sp. cf. *C. kuttungensis* (Playford & Helby) comb. nov. and *Cristatisporites pseudozonatus* Lele & Makada 1972. The species *Protohaploxypinus* sp. cf. *P. goraiensis* (Potonié & Lele) Hart 1964 and *Diatomozonotriletes birkheadensis* (Powis, 1984) first appear in this zone in GSQ Jericho 2.

Reference section GSQ Jericho 2, 900—654 m

Reference slide MFP 6853/3 (898.12 m), GSQ Jericho 2

Lithostratigraphic association Upper Jericho Formation

Age ?Late Namurian to Westphalian D

Equivalent palynostratigraphic units Uppermost Stage 1/ lowermost Stage 2 (Norvick, 1974; Price, 1976), upper *S. ybertii* Assemblage (Powis, 1979), *D. birkheadensis* Assemblage (Powis, 1984)

Identified in sections GSQ Jericho 2, 900—654 m; GSQ Springsure 13, 536—438 m

Asperispora reticulatispinosus Oppel-zone (D)

Assemblage characteristics This zone is marked by the cavate spore *Asperispora reticulatispinosus* sp. nov. and a sudden marked increase in numbers of the monosaccate *Cannanoropollis janakii* Potonié & Sah 1960 (Tables 1, 3, 4). *Apiculatisporis pseudoheles* sp. nov., *Horriditriletes ramosus* (Balme & Hennelly) Bharadwaj & Salujha 1964 (noted in GSQ Jericho 1) and *Retusotriletes nigritellus* (Luber) Foster 1979 appear towards the top of this Oppel-zone. *Diatomozonotriletes birkheadensis* extends upwards into this zone.

Reference section GSQ Jericho 2, 652—79 m

Reference slide MFP 6816A/2 (222.65 m), GSQ Jericho 2

Lithostratigraphic association Upper Jericho Formation (Oakleigh Siltstone Member) and lower Jochmus Formation

Age Westphalian D to Late Autunian (early Asselian)

Equivalent palynostratigraphic units Lower Stage 2 (Price, 1976; Norvick, 1974), Unit I (Balme *in* Kemp & others, 1977), *Potonieisporites novicus* Assemblage (Powis, 1979), Stage 1 (Powis, 1984)

Identified in sections GSQ Jericho 1 (760—435 m); GSQ Jericho 2 (652—79 m); GSQ Springsure 13 (343—64 m). Elements of this assemblage were also found in BMR Springsure 8 and AOD Jericho 1, suggesting that they also contain *A. reticulatispinosus* Oppel-zone (D) palynofloras.

Microbaculispora tentula Oppel-zone (E)

Assemblage characteristics This assemblage was primarily identified by the introduction of *Microbaculispora tentula* Tiwari 1965 and absence of many species typical of the older Oppel-zones.

Reference section GSQ Jericho 1, 429—391 m

Reference slide MFP 6757/3 (428.80 m), GSQ Jericho 1

Lithostratigraphic association Upper Jochmus Formation

Age Late Autunian (early Asselian) to early Tastubian

Equivalent palynostratigraphic units Upper Stage 2 (Norvick, 1974; Price, 1976), Unit I/Unit II (Balme *in* Kemp & others, 1977), *Horriditriletes ramosus* Assemblage (Powis, 1979), Stage 2 (Powis, 1984).

Identified in sections GSQ Jericho 1, 429—391 m

Elements of the older *Grandispora maculosa* microflora of Playford & Helby (1968) occur sporadically in these assemblages. These include *Punctatisporites lucidulus* Playford & Helby 1968, *Verrucosisporites quasigobbettii* sp. nov., *V. aspratilis* Playford & Helby 1968, *Cristatisporites* sp. cf. *C. kuttungensis*, *Psomospora detecta* Playford & Helby 1968, *Rugospora australiensis* (Playford & Helby) comb. nov., and *Rattiganispora apiculata* Playford & Helby 1968. The colour of the specimens and their preservation is similar to that of other species from the same assemblages, so we consider the species to be long-ranging within the Carboniferous and not recycled from older deposits.

Palynomorph counts (Tables 3, 4) show that spore and pollen diversity increase through Oppel-zones C and D. Laevigate trilete spores (*Calamospora, Punctatisporites* and *Retusotriletes*) dominate the sequence. Cavate/zonate spores (*Asperispora, Cristatisporites*) reach a maximum in Oppel-zone C and diminish thereafter; apiculate spores (*Brevitriletes, 'Apiculiretusispora', Dibolisporites, Anapiculatisporites*) increase to a maximum in Oppel-zone D. Verrucate spores, by contrast, diminish progressively from a maximum abundance in Oppel-zone A, although their numbers are fairly constant throughout the *Spelaeotriletes queenslandensis* Superzone. Monosaccate pollen increases significantly in abundance in Oppel-zones D and E. Disaccate pollen first appears in Oppel-zone C and becomes slightly more abundant, although it is still sporadic in Oppel-zones D and E.

Apart from the long-ranging *Calamospora* sp. cf. *C. microrugosa* (Ibrahim) Schopf, Wilson & Bentall 1944 (*sensu* Segroves 1970), few species which Playford (1978) described from the Ducabrook Formation of the underlying Drummond Basin were seen in this survey. Rare and possibly reworked spores found in GSQ Springsure 13 included *Reticulatisporites vitiosus* Playford 1978, *Knoxisporites erratus* Playford 1978, *Granulatisporites frustulentus* Balme & Hassell emend. Playford 1971, *Retispora lepidophyta* (Kedo) Playford 1976 and *Emphanisporites* sp.

Evans (1966) assigned C1 ages to assemblages recovered from cores 7 and 9 taken from AOD Jericho 1, just below the Oakleigh Siltstone Member of the Jericho Formation. These samples were re-examined by us (Table 2). Core 7 yielded a

Table 2. Miospores recovered from AOD Jericho 1.
Core 7 contained a probable *A. reticulatispinosus* Oppel-zone D Assemblage: Core 9 a probable *D. birkheadensis/A. reticulatispinosus* (Oppel-zone C/ Oppel-zone D) Assemblage.

B.M.R. Preparation No.	*MFP 3587*	*MFP 3583*
Core No.	*9*	*7*
Depth (m)	*116.3*	*101.5*
Calamospora sp. cf. *C. microrugosa*		+
Punctatisporites gretensis		+
P. lucidulus	+	+
Verrucosisporites basiliscutis	+	+
V. nitidus	+	+
V. aspratilis		+
V. quasigobbettii	+	
Verrucosisporites sp.		+
Brevitriletes leptoacaina	+	?
'Apiculiretusispora' arcuatus		+
Anapiculatisporites concinnus	+	
Spelaeotriletes queenslandensis	+	+
Auroraspora solisortus	+	
Densoisporites sp.	+	+
Cristatisporites sp.	+	
C. sp. cf. *C. kuttungensis*	+	+
Asperispora reticulatispinosus	?	+
Potonieisporites novicus	+	+
P. elongatus		+
Plicatipollenites densus		+
Cyclogranisporites firmus	+	+
Reticulatisporites bifrons	+	
Convolutispora sp.	+	
Laevigatosporites sp.		+

probable Oppel-zone D or A. *reticulatispinosus* Assemblage; Core 9 contained a poorly preserved Oppel-zone C—Oppel-zone D (or a *D. birkheadensis* —*A. reticulatispinosus* Assemblage).

Existing Australian Permo—Carboniferous palynostratigraphies

Earlier palynological biostratigraphies relating to non-marine Late Carboniferous and Early Permian sediments in Australia are shown in Figure 6. The time relationships of these historical palynozonations are based upon our re-assessments of the available data.

Evans (1964, 1966) developed a biostratigraphy for eastern Australian sediments based upon the incoming of form taxa (Fig. 3), which defined discrete intervals subsequently termed 'stages' (Evans 1967, 1969). More recently, Price (1983) formalised these stages and re-named them as interval-zones. In Western Australia, Balme (*in* Kemp & others, 1977, and Balme, 1980) developed a series of zones or 'units', which are broadly defined Oppel-zones. These two systems support most subsequent palynological zonations of the Late Carboniferous—Permian of Australia.

In an attempt to clarify the sequence of palynomorph assemblages in both the Early and Late Carboniferous, Playford & Helby (*in* Kemp & others, 1977) introduced a series of informal palynofloras based on assemblages arising from earlier work of Helby (1969b). The *Anabaculites ybertii* (now *Spelaeotriletes ybertii*) Assemblage was placed in the Namurian with a speculative upper limit in the Westphalian, and the *Potonieisporites* Assemblage, occurring in sediments with a pronounced glacial imprint, was tentatively assigned to the Stephanian.

Relationships between the units and stages of Balme and Evans are more complex than indicated in Kemp & others (1977, 203, fig. 12). For example, the *Potonieisporites* Assemblage, correlated with Evans' stage 1 and Balme's unit I may be equated with unit I which was partially defined by the abundance of monosaccate pollen (Helby, 1969b). However, Evans (1966, 1969), Price (1976, 1983) and Norvick (1974) identified the base of their Stage 1 by the incoming of monosaccate pollen, which thus equates to the base of Helby's *Spelaeotriletes* Assemblage.

Similarly, Stage 2 of Kemp & others (1977) was recognised by the consistent appearance of taeniate disaccate of pollen. As this pollen occurs rarely and sporadically throughout the stage 2 of Evans, Norvick and Price, we consider their Stage 2 to be older, at least at its base, than the Stage 2 of Kemp & others (1977). Taeniate disaccate pollen appears to have been recognised lower within stratigraphic sequence in the Galilee Basin than elsewhere in Australia. Its persistence throughout Balme's unit II suggests that the assemblage can be equated in part with Stage 2 of Kemp & others (1977) (see Balme, 1980, 47, text-fig. 4). Balme's Unit II is principally identified by an abundance of *Microbaculispora tentula* and so must commence at a level equivalent to high in Norvick's Upper Stage 2 — which was defined by the incoming of *M. tentula*.

Powis (1979) designated four assemblage-zones, based upon modifications of Balme's units, from pre-glacial, glacial and post-glacial deposits of the Grant Group in the Canning Basin, and a further zone, the *Diatomozonotriletes birkheadensis* Assemblage-zone (Powis, 1983), from the Galilee Basin underlying the *Potonieisporites novicus* Assemblage-zone. He later described the Galilee Basin species *D. birkheadensis*, modified and renamed his earlier zones, and attempted to define a continent-wide Late Carboniferous palynozonation (Powis, 1984). He proposed that the *D. birkheadensis* Assemblage was either a lateral facies equivalent of the *S. ybertii* assemblage, or derived from a younger parent flora. The *S. ybertii* Assemblage gives way up section to a *D. birkheadensis* Assemblage in both the Canning and Bonaparte Basins, but appears to be absent from eastern Australia.

Foster (*in* Foster & Waterhouse, 1988) described a palynoflora from the Grant Group of the Canning Basin, which he termed the *Granulatisporites confluens* Oppel-zone after its nominate taxon. He observed that the zone lay conformably above the *D. birkheadensis* Assemblage in the Bonaparte Basin but was uncertain of the relationship of the *G. confluens* Oppel-zone to Stage 1, and proposed that Stage 1 was either facies controlled, or a product of a unique vegetational habitat, thereby implying that this Stage is of limited stratigraphic utility.

Previous palynozonation of the Joe Joe Group and associated plant macrofossils

As the Joe Joe Group of the Galilee Basin contains no marine sediments, correlation of these strata have relied predominantly upon palynology. The early P and C palynological subdivisions of the Australian Permo—Carboniferous developed by Evans (1964a), later to become the five stage palynozonal scheme, were based on studies in this basin (Fig. 3). Norvick (1974) reviewed the palynological studies of 42 petroleum exploration wells from the Galilee Basin and observed that the Joe Joe Formation of Vine (1976) spanned Stages 1 and 2.

Little (1976) and McKellar (*in* Swarbrick & Wallin, 1976) found that the Jericho Formation generally contained Stage 1 to Stage 2 palynofloras, the Jochmus Formation Stage 2 to Stage 2—3 palynofloras, and noted an aberrant Stage 3 palynoflora from the Jericho Formation in GSQ Jericho 1 (Little, 1976). We re-examined the assemblages from GSQ Jericho 1 and did not find any evidence for Little's Stage 3 assignment. McKellar (*in* Swarbrick & Wallin, 1976) found Stage 2 palynofloras in the upper part of the Jericho Formation, and Stage 2—3 palynofloras within the Jochmus Formation. Thus, the Lake Galilee Sandstone and basal Jericho Formation have been considered to

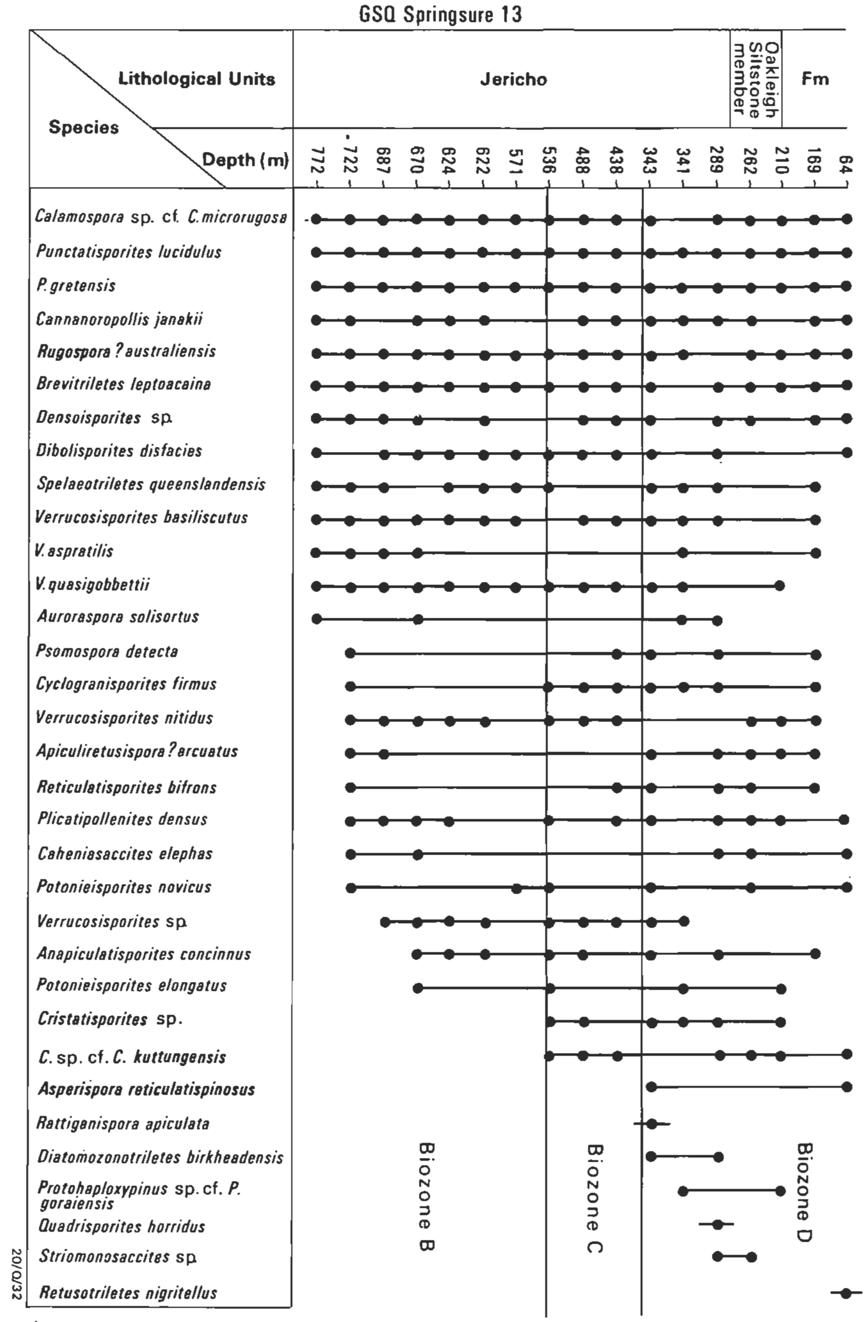

Figure 4. Appearance of taxa in (a) GSQ Springsure 13, (b) GSQ Jericho 2, (c) GSQ Jericho 1, and (d) BMR Springsure 8. Lithostratigraphy for each well is shown beside the sample depths, and Oppel-zones are shown on the right.

contain a Stage 1 palynoflora, with Stage 2 palynofloras straddling the Jericho and Jochmus Formations and Stage 3 palynofloras in the upper Jochmus Formation.

We applied the stages of Evans (1967) to assemblages recovered from the three stratigraphic holes studied here in detail. Stage 1 encompasses the Lake Galilee Sandstone and basal Jericho Formation (i.e. Oppel-zones A, B and basal C); Stage 2 commences within the Jericho Formation, below the Oakleigh Siltstone Member, and continues through the Jochmus Formation (i.e. encompassing Oppel-zones D and E and part C).

The Oppel-zones we delineated correspond reasonably well with the interval defined by the *Spelaeotriletes* and *Potonieisporites* Assemblages of Helby (*in* Kemp & others, 1977) and the modified Stage 2 of Powis (1984). Spore counts (Tables 3, 4) help to tie our assemblages to the previously defined biostratigraphic units. A sharp increase in abundance of monosaccate pollen (Table 4) beginning in Oppel-zone D (mainly *Cannanoropollis janakii* or *'Parasaccites'*) and a corresponding decrease in the percentage of the population constituted by other spore types strongly suggest the *Potonieisporites* Assemblage. Oppel-zone D, however, is also marked by an increase in the diversity of non-monosaccate species which is atypical of the *Potonieisporites* Assemblage. *Asperispora reticulatispinosus*, an indicative form for our Oppel-zone D, is included in Helby's unpublished working plates as a component of his *Potonieisporites* Assemblage. We therefore consider that Oppel-zone D may be equated with the *Potonieisporites* Assemblage and that the increased diversity of non-monosaccate species may reflect the parent vegetation.

Oppel-zone E is primarily delineated by the introduction of *M.*

Table 3. Relative abundance of taxa for each Oppel-zone, based on averaged percentage data from Table 1.

Species	*Oppel-zone* *A* %	*Oppel-zone* *B* %	*Oppel-zone* *C* %	*Oppel-zone* *D* %	*Oppel-zone* *E* %
Calamospora sp. cf. *C. microrugosa*	22.1	27.3	29.2	29.4	26.6
Punctatisporites gretensis	39.9	23.4	20.3	18.6	18.8
P. lucidulus	18.5	20.8	18.4	18.6	27.8
Retusotriletes nigritellus				0.6	1.5
Psomospora detecta		*	0.2	0.08	0.3
Verrucosisporites basiliscutis	4.4	4.0	1.9	1.7	
V. nitidus	2.3	1.3	1.2	0.6	0.3
V. aspratilis	2.6	0.8	0.9	0.2	
V. quasigobbettii	0.7	2.2	0.8	0.2	0.3
Verrucosisporites sp.	0.7	0.5	0.6	0.08	0.5
Brevitriletes leptoacaina		1.9	2.1	2.9	1.0
Apicutiretusispora? arcuatus	0.3	0.5	1.0	0.8	
Dibolisporites disfacies		1.0	1.7	0.3	*
Anapiculatisporites concinnus	0.2	0.7	0.3	0.7	
Ahrensisporites cristatus		*			
Diatomozonotriletes birkheadensis		0.1	0.04		
Rugospora australiensis	2.0	3.5	4.7	3.3	1.0
Spelaeotriletes queenslandensis	0.3	1.4	5.3	0.9	
Auroraspora solisortus		0.5	0.06	*	
Densoisporites sp.	0.3	0.5	0.4	0.4	0.3
Cristatisporites? sp.			1.5	0.5	
C. sp. cf. *C. kuttungensis*			1.1	1.1	
Asperispora reticulatispinosus				0.7	*
Potonieisporites novicus	1.3	1.5	0.6	1.3	
P. elongatus		0.3	0.2	0.2	*
Plicatipollenites densus	0.3	0.4	0.3	1.0	1.0
P. gondwanensis			0.06	0.06	
Cannanoropollis janakii	0.7	0.9	1.7	6.6	10.8
Striomonosaccites sp.			0.2	0.06	
Caheniasaccites elephas		*	0.3	0.3	
Protohaploxypinus sp. cf. *P. goraiensis*			*	0.2	0.3
Cyclogranisporites firmus	*	0.3	1.6	1.9	
Reticulatisporites bifrons		0.1	0.3	0.3	
Rattiganispora apiculata				0.08	0.3
Apiculatisporis psuedoheles				1.6	2.3
Horriditriletes ramosus				0.9	5.3
Microbaculispora tentula					0.3
Quadrisporites horridus			*	0.02	
Maculatasporites minimus					0.3
Others	3.5	6.8	3.0	4.1	1.5

* Insignificant amount

Table 4. Main biozone characters, showing relative diversity of taxa per biozone (Section I) and relative abundance of the major palynomorphic groups throughout the Oppel-zones (Section II).

		Biozone *A*	*Biozone* *B*	*Biozone* *C*	*Biozone* *D*	*Biozone* *E*
Section I Relative spore & pollen diversity per Oppel-zone	Total spore disaccate pollen diversity (Number of taxa identified)	14	20	24	29	19
	Monosaccate pollen diversity (number of taxa identified)	3	4	7	7	3
Section II Percentages of major morpho-logical groups per Oppel-zone	Laevigate spores	80.5	71.5	67.9	67.2	74.7
	Cavate/zonate spores	2.6	5.9	13.1	6.9	1.3
	Apiculate spores	0.5	4.1	5.2	6.4	3.6
	Verrucate spores	10.7	9.1	7.0	4.7	1.1
	Monosaccate pollen	2.3	3.1	3.4	9.5	11.8
	Disaccate pollen	—	—	*	0.2	0.3
	Others	3.5	6.9	3.4	5.4	7.7

tentula, and may thus be reasonably equated with Powis's modified Stage 2 and Upper Stage 2 of Norvick (1974, 1981).

Oppel-zones A to C have much in common with the Canning Basin *Spelaeotriletes ybertii* Assemblage (Powis, 1979), which remains poorly documented. Forms in common are *Brevitriletes leptoacaina*, *Punctatisporites gretensis* Balme & Hennelly 1956, *Verrucosisporites nitidus* (Naumova) Playford 1964, *V. aspratilis*, *Psomospora detecta*, *Ahrensisporites cristatus*, *Anapiculatisporites concinnus* Playford 1962, '*Apiculiretusospora*' *arcuatus*, *Verrucosisporites quasigobbettii* and *Auroraspora solisortus* Hoffmeister, Staplin & Malloy 1955. *Spelaeotriletes ybertii* (Marques-Toigo) Playford & Powis 1979 is not present in the Queensland material but a similar form, *S. queenslandensis*, was identified and described by us. The nominate taxon of the Western Australian Assemblage, *S. ybertii*, extends into the *Potonieisporites* Assemblage, and similarly *S. queenslandensis* extends up into Oppel-zone D.

The *Grandispora maculosa* and *S. ybertii* Assemblages from samples taken from Pelican Island No. 1 of the Petrel sub-

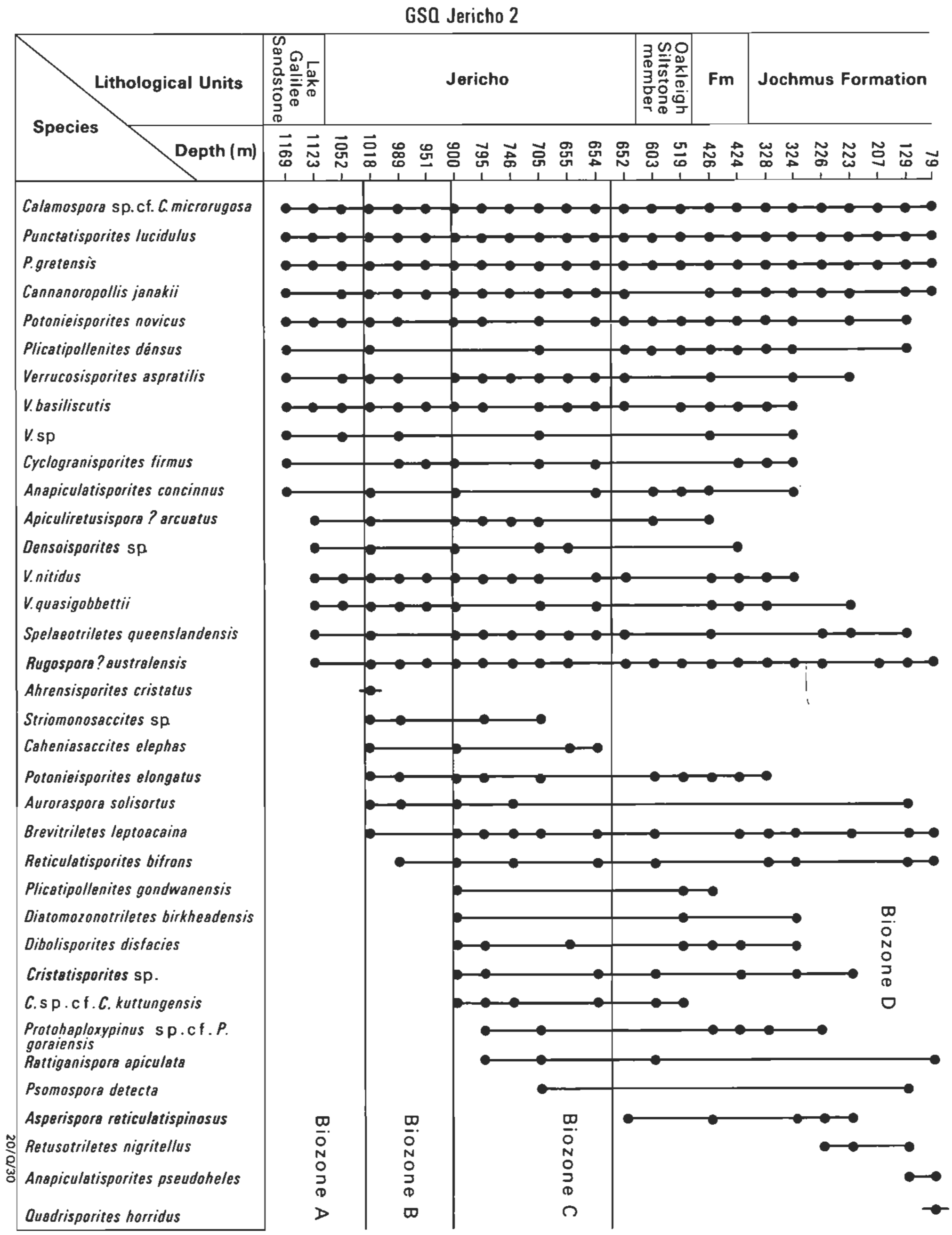

Figure 4b.

Basin, Bonaparte Basin (lent by R. Helby) were examined to provide a stratigraphic and geographic framework for the Galilee Basin zones. Examination of the *S. ybertii* Assemblage indicated that many forms from our *S. queenslandensis* Assemblage were present, including *'Apiculiretusispora' arcuatus*, *Cristatisporites* sp. cf. C. *kuttungensis*, *Densoisporites* sp., *Reticulatisporites bifrons*, *Rugospora australiensis*, *Verrucosisporites nitidus*, *V. aspratilis*, *V. quasigobbettii*, *V. basiliscutis*, *Cyclogranisporites firmus*, *Auroraspora* sp., and the previously undescribed spore *Spelaeotriletes queenslandensis*. In the Bonaparte Basin the species *S. queenslandensis* ranges down into the *G. maculosa* Assemblage, where it was associated with *S. ybertii*. The presence of the previously unrecognised *S. queenslandensis* within thel *S. ybertii* Assemblage in the Bonaparte Basin, the overall floristic similarity of the *Spelaeotriletes* Assemblages, and their similar stratigraphic ranges, all suggest that these two assemblages are similar and contemporaneous (Fig. 6).

The informal *Diatomozonotriletes birkheadensis* Assemblage which Powis (1983) identified in the Galilee Basin probably equates with our *Spelaeotriletes queenslandensis* Superzone, given that it was said to range from the Lake Galilee Sandstone to the Jericho Formation, underlies the *Potonieisporites* Assemblage, and lacks *Spelaeotriletes ybertii*. From our studies, *Diatomozonotriletes birkheadensis* ranges down only into our Oppel-zone C.

Sparsely recorded megafloras from the Joe Joe Group have been collected from a broad stratigraphic interval and may be associated with these palynofloras (Fig. 7). Specimens collected north and west of Joe Joe Homestead (White, 1969) belong to the *Botrychiopsis* flora, (Retallack, 1980), traditionally associated with a *Potonieisporites* or Stage 1 palynoflora (Gould, 1975; Kemp & others, 1977). The association is sufficiently constant for Retallack (1980) to suggest that *Potonieisporites* is the pollen of *Botrychiopsis* which might

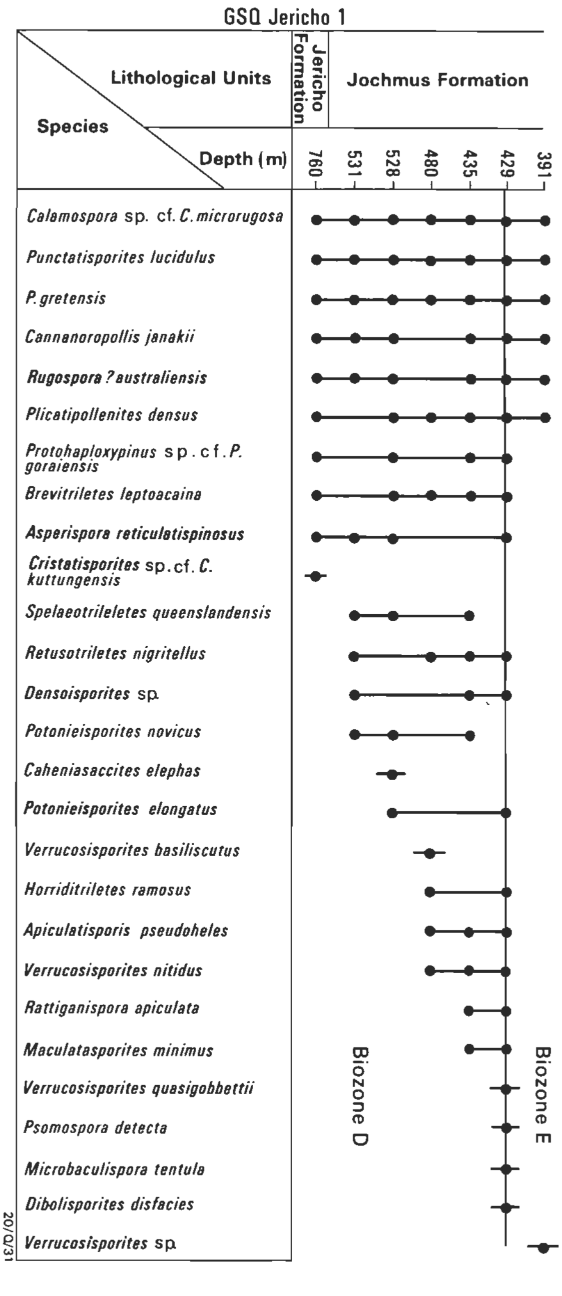

Figure 4c.

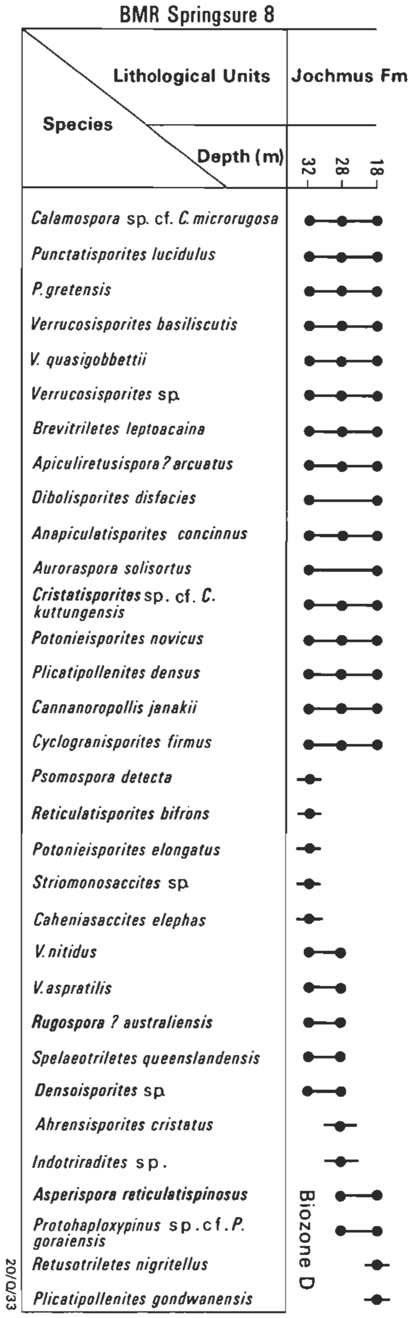

Figure 4d.

have formed a sparse, low growing tundra replacing an older, more diverse *Sphenopteridium* flora as climatic conditions became colder and drier.

The report (Morris, 1985) of a *Sphenopteridium* or 'enriched *Nothorhacopteris*' flora in the Joe Joe Group suggests that macrofossil floras older than the *Botrychiopsis* flora are present. We are unaware of the localities for such records. The *Sphenopteridium* Flora referred to has been associated with the *Spelaeotriletes ybertii* palynoflora (Kemp & others, 1977; Playford, 1985) which pre-dates the *Potonieisporites* Assemblage. The present study suggests that the pre-*Potonieisporites* Assemblage sequences in the Joe Joe Group are confined to the deepest parts of the basin and do not crop out around its margins.

Younger *Glossopteris* macrofloras occur in the Joe Joe Group (White, 1964) in the Boonderoo Beds of Galah Gorge, in beds which are considered lithological equivalents of the Jochmus Formation (Gray, 1977). McKellar (1977) recovered Lower Stage 2 assemblages from subsurface sections near the locality, on the extreme northern margin of the Galilee Basin. Norvick (1981) believed the *Glossopteris* bearing interval correlated with his Upper Stage 2.

Australian correlations and global chronostratigraphy

The palynofloral zones discussed above may be tied to an international timescale through correlative invertebrate assemblages, radiometrically datable intercalated volcanics, and by directly correlating species to forms found in the Northern Hemisphere. Carboniferous plant macrofossils and palynomorphs have been found in association with marine macrofossils in the Hunter/Myall districts of the Tamworth

Shelf, the Petrel Sub-Basin of the Bonaparte Basin, and the Canning Basin (Fig. 7).

The Australian Late Carboniferous palynozones contain few species recognised as being in common with North American or European taxa. Some species of the early Carboniferous *Anapiculatisporites largus* Assemblage can be correlated with British palynofloras (Playford, 1978). The apparent endemism of the later Carboniferous palynofloras may reflect increased isolation of the Gondwanan parent floras from Laurasia, although further systematic work may show species in common with Laurasian species and, indeed, many taxa from our Oppel-zones are comparable with species from the Late Carboniferous of Laurasia.

Although specific correlations with Euro-American palynostratigraphic zones are not yet possible, three events can be used as time datums and thus correlation tie points: the introduction of monosaccate pollen, the peak development in both abundance and diversity of monosaccate pollen, and the introduction, and increase in abundance of, striatitid (taeniate) disaccate pollen.

Introduction of monosaccate pollen. In Australia monosaccate pollen first appears in the *Spelaeotriletes ybertii* Assemblage which, according to associated invertebrate fossils, is close to, if not at the base of, the Namurian (Fig. 7). Monosaccate pollen also seems to appear synchronously in the Namurian A in Laurasia (Sullivan & Mishell, 1971; Clayton & others, 1977; Coquel & others, 1979).

The synchronous global introduction of monosaccate pollen therefore makes a good datum. It probably reflects the rise of hardy cordaitalean plants, which rapidly took advantage of dry upland niches previously used only marginally by sphenopsid and pteridosperm floras.

Peak development of monosaccate pollen. The *Potonieisporites* Assemblage encompasses an extensive interval at the same stratigraphic level in several Australian basins. Balme (1980) observed that palynofloras with abundant *Potonieisporites* and radial monosaccates are typical of the Stephanian, and especially the late Stephanian, of western Europe. He noted reports of an increased relative abundance of monosaccate pollen near the base of the Kasimovian/Gzhelian in the Soviet Union, correlative with the Stephanian. Clayton & others (1977) reported that *Potonieisporites* spp. first appear in the Westphalian C of the Netherlands, and that *P. novicus* and *P. bharadwaj* are characteristic species of the western European Stephanian and Autunian. Peppers (1979) indicated that *Florinites* spp. increase in abundance in the *Cadiospora magna—Mooreisporites inusitatus* (MI) Assemblage-zone of the Spoon Formation in Illinois, which correlates to approximately the Westphalian C/D boundary. Balme (1980) further remarked upon the increase in abundance of monosaccate pollen in North America, which he placed at the Desmoinesian/Missourian boundary, correlative with the Westphalian/Stephanian boundary. Thus in Laurasian sequences, monosaccate morphotypes have increased in abundance at approximately the Westphalian/Stephanian boundary, and remained abundant throughout the Stephanian to Autunian.

Balme (1980) further suggested that the change from cryptogam-dominated palynofloras to assemblages abundant in *Potonieisporites* and *Cordaitina* coincided with the cessation of coal-swamp development in Laurasia, indicating a global climatic change corresponding with cooling in Gondwana. This event apparently began within the Westphalian D. The consequential lowering of global precipitation allowed hardy plants which tolerated dry conditions, such as the proto-coniferous cordaitales that produced monosaccate pollen, to dominate the vegetation communities.

Striatitid (taeniate) disaccate pollen. Balme suggested that the introduction of taeniate disaccate pollen, associated with an increase in diversity of cryptogam spores, was globally synchronous and induced by rapid global climatic amelioration following the glaciation of Gondwana.

The introduction of consistently recognisable taeniate disaccate pollen within Stage 2 *sensu* Kemp & others (1977) and Unit II of Balme (1980) may be equated with the western European *Disaccites striatiti* (DS) Zone of Clayton & others (1977) and Zone VIII of Coquel & others (1976), which are dated as late Autunian or early Asselian. Interestingly, Clayton & others (1977) observed that *Disaccites striatiti* pollen extended sporadically down into the Westphalian C, and Ravn (1986) reported taeniate disaccate pollen from the Morrowan, or Westphalian A equivalent, of Iowa. The sporadic incoming of taeniate disaccate pollen in North America and western Europe therefore mirrors its advent in coeval Australian strata.

The increase in abundance of disaccate pollen, in association with an increase in diversity of cryptogam spores, probably reflects global warming and increasing precipitation following the cessation of continental glaciation in Gondwana. This is certainly reflected in the rapid eustatic sea-level rise recorded in strata contemporaneous with these assemblages.

Comparison with other Gondwanan assemblages

In India, the oldest Late Palaeozoic deposits are represented by the Talchir Formation, which rests mainly on Precambrian basement. Palynological studies of this glacially-associated unit were partly reviewed by Truswell (1980), who noted the two- and threefold palynological subdivisions effected in the Talchir by Lele (1975) and Tiwari (1975). A more comprehensive overview (Chandra & Lele, 1979) provided lists of spore and pollen species present in 'Early' and 'Late Talchir' palynofloral assemblages from a number of different basins. From these, it appears that the Talchir correlates primarily with Stage 2 (*sensu* Kemp & others, 1977), with a possible downward extension into an interval coeval with the *Potonieisporites* Assemblage of Australia.

The Indian suites are dominated by monosaccate pollen types to a much greater degree than are assemblages in the Galilee Basin; abundances of 95% are common (see Lele & Karim, 1971; Lele & Shukla, 1980). The relatively high diversity of taeniate striate taxa, even in 'Early Talchir' assemblages, and the presence of the monosulcate *Ginkgocycadophytus* spp., and of species of *Horriditriletes*, indicate that most Talchir assemblages relate most closely to an interval high in Stage 2, equivalent to Norvick's Upper Stage 2 or younger. Cavate zonate taxa such as those assigned in this study to *Asperispora reticulatispinosus* and *Cristatisporites pseudozonatus* are present in both the Australian and Indian assemblages.

In southern Africa, the oldest relevant Late Palaeozoic sediments are the diamictites and varved shales of the Dwyka Formation of the Karoo Basin. From the comprehensive palynological study of Anderson (1977) and the detailed comparison of the African and Australian palynological sequences by Truswell (1980), it appears that the Dwyka assemblages correlate with Australian Upper Stage 2 assemblages, as those are defined by the first appearance of *Microbaculispora tentula*. The abundance (up to 40%) of *M. tentula* in the Dwyka is reminiscent of Units II and III of Balme's (*in* Kemp & others, 1977) Western Australian sequence.

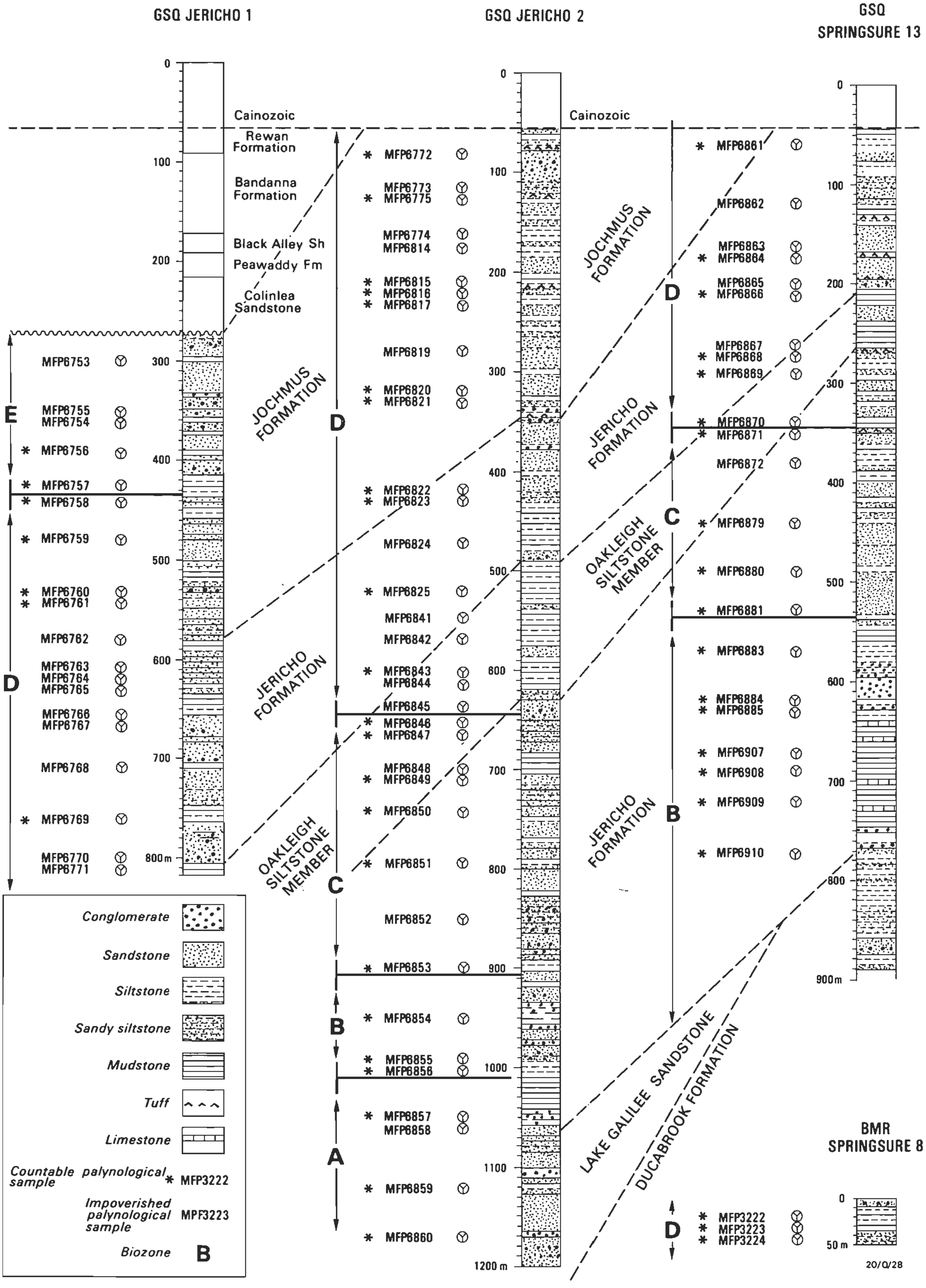
GSQ JERICHO 1
GSQ JERICHO 2
GSQ SPRINGSURE 13
Cainozoic
Rewan Formation
Bandanna Formation
Black Alley Sh
Peawaddy Fm
Colinlea Sandstone
JOCHMUS FORMATION
JERICHO FORMATION
OAKLEIGH SILTSTONE MEMBER
LAKE GALILEE SANDSTONE
DUCABROOK FORMATION
A
B
C
D
E
MFP6753
MFP6755
MFP6754
MFP6756
MFP6757
MFP6758
MFP6759
MFP6760
MFP6761
MFP6762
MFP6763
MFP6764
MFP6765
MFP6766
MFP6767
MFP6768
MFP6769
MFP6770
MFP6771
MFP6772
MFP6773
MFP6775
MFP6774
MFP6814
MFP6815
MFP6816
MFP6817
MFP6819
MFP6820
MFP6821
MFP6822
MFP6823
MFP6824
MFP6825
MFP6841
MFP6842
MFP6843
MFP6844
MFP6845
MFP6846
MFP6847
MFP6848
MFP6849
MFP6850
MFP6851
MFP6852
MFP6853
MFP6854
MFP6855
MFP6856
MFP6857
MFP6858
MFP6859
MFP6860
MFP6861
MFP6862
MFP6863
MFP6864
MFP6865
MFP6866
MFP6867
MFP6868
MFP6869
MFP6870
MFP6871
MFP6872
MFP6879
MFP6880
MFP6881
MFP6883
MFP6884
MFP6885
MFP6907
MFP6908
MFP6909
MFP6910
BMR SPRINGSURE 8
MFP3222
MFP3223
MFP3224
0
100
200
300
400
500
600
700
800 m
900 m
1000
1100
1200 m
50 m
Conglomerate
Sandstone
Siltstone
Sandy siltstone
Mudstone
Tuff
Limestone
Countable palynological sample
* MFP3222
Impoverished palynological sample
MPF3223
Biozone
B
20/Q/28

In Antarctica, sparse palynomorph suites from glacially-associated sedimentary units in the Darwin, Ohio and Wisconsin Ranges, assigned by Kyle (1977) to the *Parasaccites* Zone, are probably also correlatives of Stage 2, or Upper Stage 2 in the sense of Norvick (1974, 1981) (Fig. 6). There are no records from Antarctica of pre-glacial Carboniferous palynofloras.

From the northern Gondwana margins in Oman, palynofloras apparently similar to Australian assemblages were reported from diamictites and associated claystones by Braakman & others (1982) and by Besems & Schuurman (1987). Monosaccate pollen, abundant *Cristatisporites* spp., and rare taeniate disaccate pollen (Braakman & others, 1982) suggest correlation with the Australian *Potonieisporites* Assemblage. The palynofloras identified by Besems & Schuurman (1987) contained *Microbaculispora tentula* and *Horriditriletes ramosus* amongst other forms typical of Upper Stage 2, or the *Microbaculispora tentula* Assemblage of Powis (1979). The palynofloras of Besems & Schuurman (1987) also contained some miospores typical of the older *Spelaeotriletes* Assemblages, such as *Dibolisporites disfacies, 'Apiculiretusispora' arcuatus* and *Ahrensisporites cristatus* which may indicate that these Omanian assemblages are older than the *M. tentula* Assemblage.

The best intercontinental correlations of the *Spelaeotriletes* and *Potonieisporites* palynofloras are in South America. Azcuy's (1979) five stage palynozonational scheme for the Paganzo and Parana Basins was later expanded in the basal three divisions, and the lowest, the *Ancistrospora* Palynozone or Palynozone I, was equated with the *Spelaeotriletes* Assemblage of Australia (Azcuy & Jelin, 1980). Genera common to the two palynofloras are *Spelaeotriletes, Cristatisporites, Anapiculatisporites, 'Apiculiretusispora', Retusotriletes, Punctatisporites, Verrucosisporites, Convolutispora* and *Raistrickia*, as well as radially symmetrical monosaccate pollen. Azcuy & Jelin (1980) tentatively suggested that this South American palynozone is as old as the Namurian, but may have extended into the Westphalian.

The Australian *Potonieisporites* Assemblage palynoflora may be represented in South America by Azcuy's Palynozone II, the *Potonieisporites* Palynozone of Azcuy & Jelin. This palynoflora, as with the Australian equivalent, shows an increase in abundance of radially symmetrical monosaccate pollen from Palynozone I. Species typical of the *Ancistrospora* palynozone extended into this higher zone. Azcuy & Jelin dated this palynozone as Stephanian because it occurs above the Namurian to Westphalian *Ancistrospora* Palynozone and below the Palynozone III, which was tentatively dated as Early Sakmarian. These ages broadly correspond with those assigned to the Australian *Spelaeotriletes* and *Potonieisporites* palynofloral Assemblages.

Conclusions

We have determined the following ages for the major Australian Carboniferous to Early Permian palynozones:

Anapiculatisporites largus Assemblage (*sensu* Kemp & others, 1977) — Asbian to earliest Namurian in the Bonaparte, Canning and Drummond Basins (on palynofloral comparisons with Britain, Foraminiferida in AOD Bonaparte No. 1, and microfossil associations in the Canning Basin). Possibly extends down to the Tournaisian/Visean boundary (Kemp & others, 1977).

Grandispora maculosa Assemblage (*sensu* Kemp & others, 1977) — Holkerian/Asbian to earliest Namurian in the Tamworth Shelf (associated with *G. tenuirugosus* brachiopod zone and occurs below *Levipustula levis* brachiopod zone), Visean to earliest Namurian in the Bonaparte Basin (foraminifera in AAP Kulshill No. 1).

Spelaeotriletes ybertii Assemblage (*sensu* Kemp & others, 1977; Powis, 1979) — Namurian A to uppermost Westphalian D (on basis of global introduction of monosaccate pollen and increase in relative abundance of monosaccate pollen). Introduced in the earliest Namurian in the Bonaparte Basin (associated microfossils in AAP Kulshill No. 1), Namurian in the Tamworth Shelf (associated with *Levipustula levis* brachiopod zone). Equivalent to our *S. queenslandensis* Superzone.

Potonieisporites Assemblage (sensu Kemp & others, 1977, Powis, 1979) — Uppermost Westphalian D to Upper Autunian, or early Asselian (based upon increase in global abundance of monosaccate pollen and increase in abundance of striatitid, disaccate pollen associated with the overlying *M. tentula* Assemblage). Correlates with our Oppel-zone D.

Microbaculispora tentula Assemblage (*sensu* Powis, 1979) — Upper Autunian, or mid-Asselian (based upon global increase in abundance of taeniate disaccate pollen). Upper Asselian to Tastubian in the Canning Basin (associated macrofauna), ?Stephanian to Asselian in the Cranky Corner Basin (associated macrofauna). Correlates with our Oppel-zone E.

Stage 3a (sensu Price, 1976; Kemp & others, 1977). Equivalent to Stage 3a/b of Powis 1984) — late Tastubian to early Sterlitamakian in the Perth Basin (based upon associated ammonoids); Sterlitamakian for Unit III assemblages (Stage 3a/ basal Stage 3b) in the Canning Basin (based on associated ammonoids).

Powis (1984) was ambivalent about the stratigraphic relationships between his *Diatomozonotriletes birkheadensis* Assemblage and the *S. ybertii* Assemblage. Powis (pers. comm. to MJJ, 1983) indicated that in the Galilee Basin his *D. birkheadensis* Assemblage ranged into the Lake Galilee Sandstone, which suggests that this Assemblage equates with our *S. queenslandensis* Superzone. We found the nominate species of the *D. birkheadensis* Assemblage, however, to range down only to our Oppel-zone C within the Jericho Formation; we therefore have restricted usage of the *D. birkheadensis* Oppel-zone accordingly, distinguishing it from the broader concept of Powis' *D. birkheadensis* Assemblage.

The excellent preservation and the relatively diverse composition of assemblages from the Galilee Basin deserve comment, especially in view of the glacial nature of at least part of the Joe Joe Group sediments. Mollan & others (1969) identified terrestrial moraine in the outcrop Joe Joe Formation on the Springsure Shelf, and fluvio-glacial or glacial lake depositional environments have been suggested for Jochmus Formation sediments in the subsurface (Gray & Swarbrick, 1975; Hawkins, 1978). On the basis of *Botrychiopsis* macrofossils found in outcrop, sequences on the Springsure Shelf should be equivalent to *Potonieisporites* Assemblage or Oppel-zone D palynofloras, and the section in BMR Springsure 8, drilled near the type section of the original Joe Joe Formation, yielded an *Asperispora reticulatispinosus* Oppel-zone (D) Assemblage. Surface exposures in the area are probably not as old as the *S. queenslandensis* Superzone. The diversity and abundance of miospores in the Superzone suggest that the parent flora may have been marginally influenced by glaciation.

Figure 5. Correlations of lithostratigraphic and palynological zones for GSQ Springsure 13, GSQ Jericho 2, GSQ Jericho 1 and BMR Springsure 8.
Horizons providing pollen counts for this study are shown by an asterisk. Line of section AA—AA' indicated on Figure 2 (horizontal not to scale).

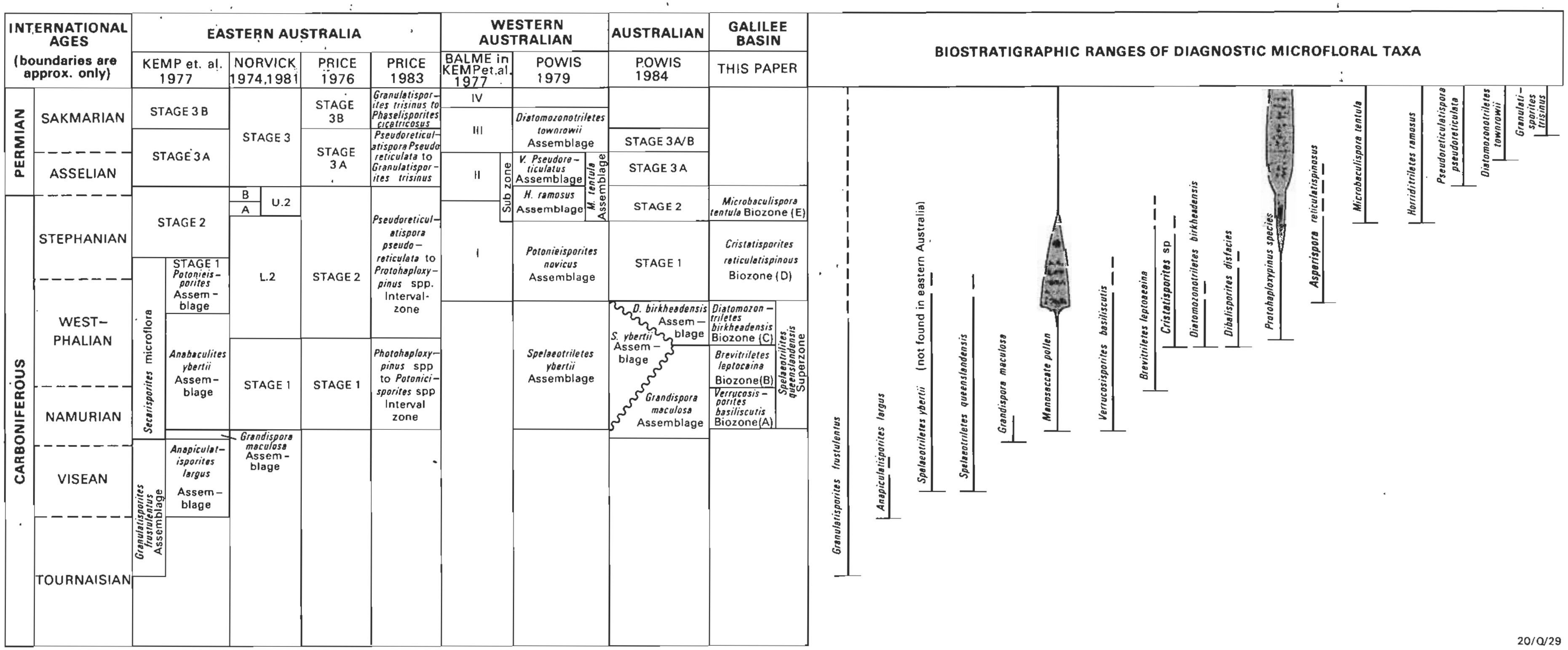

Figure 6. Palynozonational schemes for the Australian Carboniferous-Permian.
Ranges and relative abundances of important taxa are shown.

This is the correct Figure 6 for Jones & Truswell,
BMR Journal of Australian Geology & Geophysics,
Volume 13, 143–185.

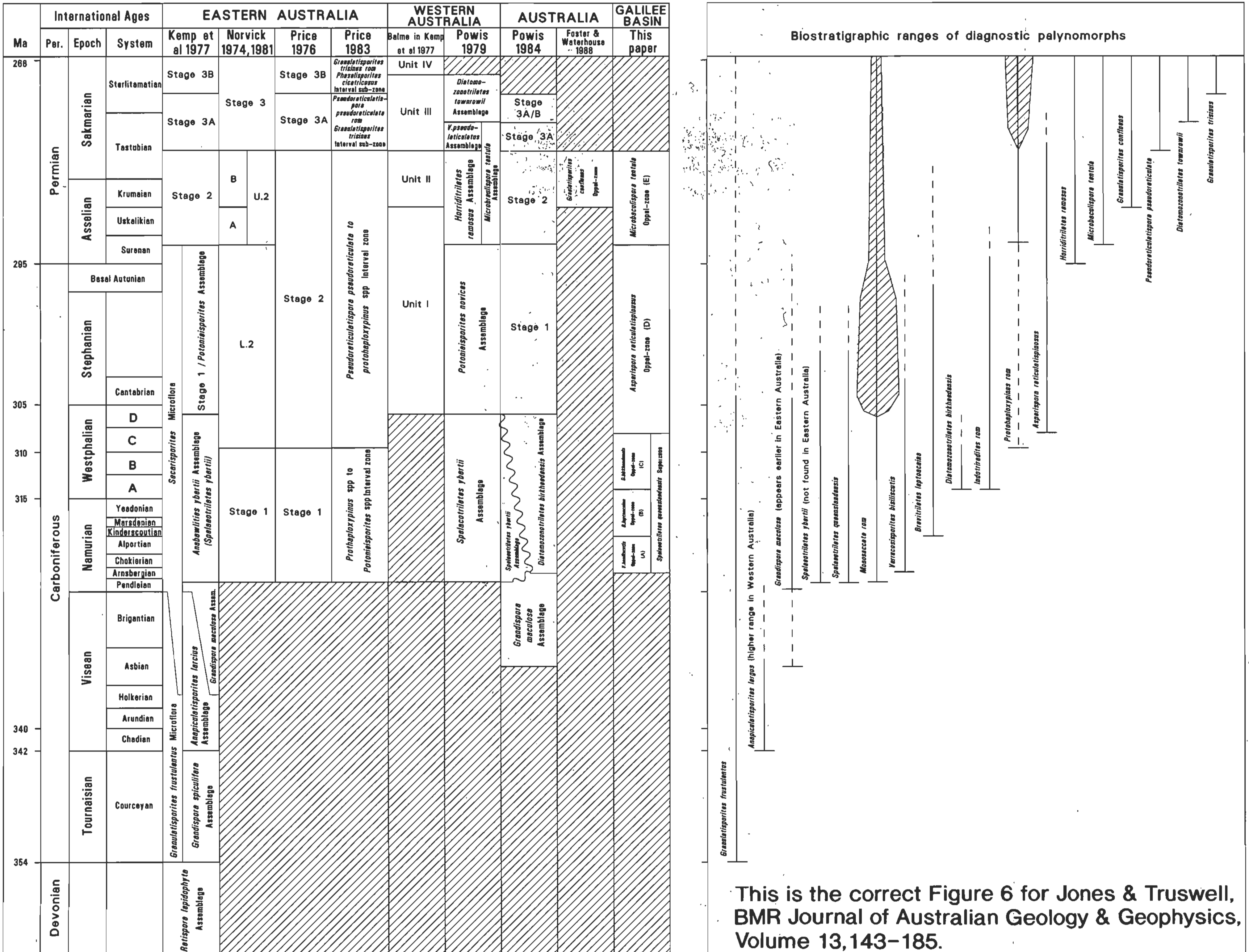

This is the correct Figure 6 for Jones & Truswell, BMR Journal of Australian Geology & Geophysics, Volume 13,143–185.

The *Potonieisporites* Assemblage of the Galilee Basin has a more diverse range of species than elsewhere in Australia. This may imply that the glacial effect often associated with this palynoflora (i.e. Kemp & others 1977) was not pronounced in this region. *Potonieisporites* Assemblages have been recovered from basins with diagenetic histories as subdued as the Galilee Basin; the diversity is therefore unlikely to be due to a gentle diagenetic history. Crowell & Frakes (1971a,b) and Herbert (1980) suggested that glaciation in the Late Carboniferous was confined to alpine or valley glaciation. Dickins (1985) in a review of data bearing on Carboniferous glaciation in Australia, also suggested restriction to elevated regions. Veevers & Powell (1987) proposed that the major phase of glaciation actually predated the bulk of the glacigenic sediments, and is marked by a predominantly Namurian widespread depositional lacuna. However, we believe that there is now sufficient evidence for considerable deposition of sediments in the Namurian within Australia. The most probable cause of the high palynomorph diversity noted in Oppel-zone D or the *Potonieisporites* Assemblage of the Galilee Basin is the remoteness of the parent flora from alpine glaciation.

Our age determinations of the Australian Carboniferous to Early Permian palynological biozones have enabled us to refine most of the timing of the late Palaeozoic glaciation and eustatic sea level change (Fig. 7).

Cooling of Australia began in the late Westphalian D, and was marked by the introduction of the *Potonieisporites* Assemblage and the development of the impoverished *Botrychiopsis* Flora. It coincided with the demise of the Laurasian coal-swamps, as a result of a decrease in global precipitation levels (Balme, 1980). Sedimentation continued during the Westphalian and Stephanian within the Galilee and Canning Basins, and in parts of the Tamworth Shelf, which suggests that the glaciation was limited to alpine regions. In the early Asselian, which may have been the time of major ice sheet development in southern Australia, the tectonic regime in Australia changed (Murray & others, 1987) and several extensional intracratonic basins developed, trapping mixed glacial and fluvial/lacustrine derived sediments. In the late Asselian/early Tastubian the climate ameliorated and glaciation receded.

The climatic warming was accompanied by a global floristic change marked by the advent of the *Gangamopteris* parent flora, the incoming of cheilocardidoid spores, and a global increase in the relative abundance of striatitid (taeniate) disaccate pollen. High energy fluviatile systems became increasingly common in many basins, as shown by the seismically defined extensive and deep erosional channelling within the Grant Group, Canning Basin. A rapid post-glacial eustatic sea-level rise during the time of the upper *M. tentula* Assemblage caused extensive marine sediment deposition. The transgression penetrated inland as far as the Arckaringa Basin (Harris & McGowran, 1973; Gilby, 1983; Jones, 1987) and the infra-Murray Basins (O'Brien, 1986). Evidence for this transgression is also found in Tasmania (Calver & others, 1984), the Cranky Corner Basin (Herbert, 1980; Briggs, 1985), the Canning Basin (Foster & Waterhouse, 1988), and the Keyling Formation of the Bonaparte Basin (Laws & Brown, 1976). The marine transgression and continued glacial melting caused sub-normally saline marine conditions in some restricted basins, resulting in algal blooms. The algal blooms are preserved as the *Tasmanites* horizon in Tasmania, and the *'Leiosphaeridia'* sp. horizon in the Arckaringa Basin (Truswell, 1978; Calver & others, 1984; Jones, 1987). Shortly after this transgressive event the land-locked intracratonic basins filled with deltaic sediments and were finally capped with continental coal-swamp facies. Termination of the glaciation was relatively abrupt, although evidence for iceberg rafting persisted until the late Early Permian, which may indicate ice-cap development somewhere to the south of Australia (Herbert, 1980).

Acknowledgements

For many enlightening discussions, special thanks are due to Dr P.J. Jones, Mr P.L. Price, Dr R.J. Helby and Dr C.B. Foster who commented on earlier versions of the manuscript and offered invaluable criticisms, and to Prof. B.E. Balme and Dr G. Playford for discussions and critical review of the final manuscript. Dr R.J. Helby lent samples from Pelican Island No. 1 in the Petrel sub-Basin. Other comments were received from Prof. K.S.W. Campbell, Dr J.M. Dickins, Dr G.W. Powis, G. Wood and R. Taylor. We would like to thank J.S. Preston of the A.N.U. Scanning Electron Microscope Facility, and L. Kracuik and A. Wilson of the BMR for their technical support. C.S.R. Oil and Gas Division and SANTOS Ltd allowed the use of personnel and equipment at various stages of development of this study.

Systematics

Most of the core material for the study was provided by the Geological Survey of Queensland. The stratigraphic boreholes GSQ Jericho 1, GSQ Jericho 2 and GSQ Springsure 13 (Figs 2 and 5) were sampled by E.M. Truswell in 1975, when systematic work commenced. In 1983 M.J. Jones undertook a preliminary study as part of a B.Sc.(Hons) project in the Geology Department, Australian National University, Canberra, followed by further study at the BMR in 1984. The data from the Geological Survey of Queensland's stratigraphic boreholes have been augmented by examination of three cuttings samples from BMR Springsure 8, close to the type section of the former Joe Joe Formation, and from two core samples from AOD Jericho 1 (see Fig. 2). The study is mainly based on examination of 76 core samples from GSQ Jericho 1, GSQ Jericho 2 and GSQ Springsure 13, 48 of which yielded quantitative miospore data (see Fig. 5), after processing by standard preparation techniques.

Quantitative data are based on counts of an average of 200 miospores per sample and expressed as a percentage in Table 1. All slides, mounted in glycerine jelly, are registered with MFP numbers and stored at the BMR, Canberra. Types and figured specimens, with designations from the Commonwealth Palaeontological Collection (CPC), and type assemblage slides are housed in the type collection in the BMR. Spore and pollen co-ordinates refer to Leitz Orthoplan binocular microscope No. 895191 at the BMR.

Scanning electron micrographs were taken at the BMR and at the Forestry Department, Australian National University. Slides were prepared for the SEM by placing drops of water containing palynomorphs onto a slide which was then allowed to dry before being gold coated and scanned.

Terminology has been adapted from Dettmann (1963), Kremp (1965), Grebe (1971), and Foster (1979). Unless otherwise stated, equatorial diameters given do not include sculptural elements which project from the equator and are given as a minimum, arithmetic mean (in parentheses) and maximum values.

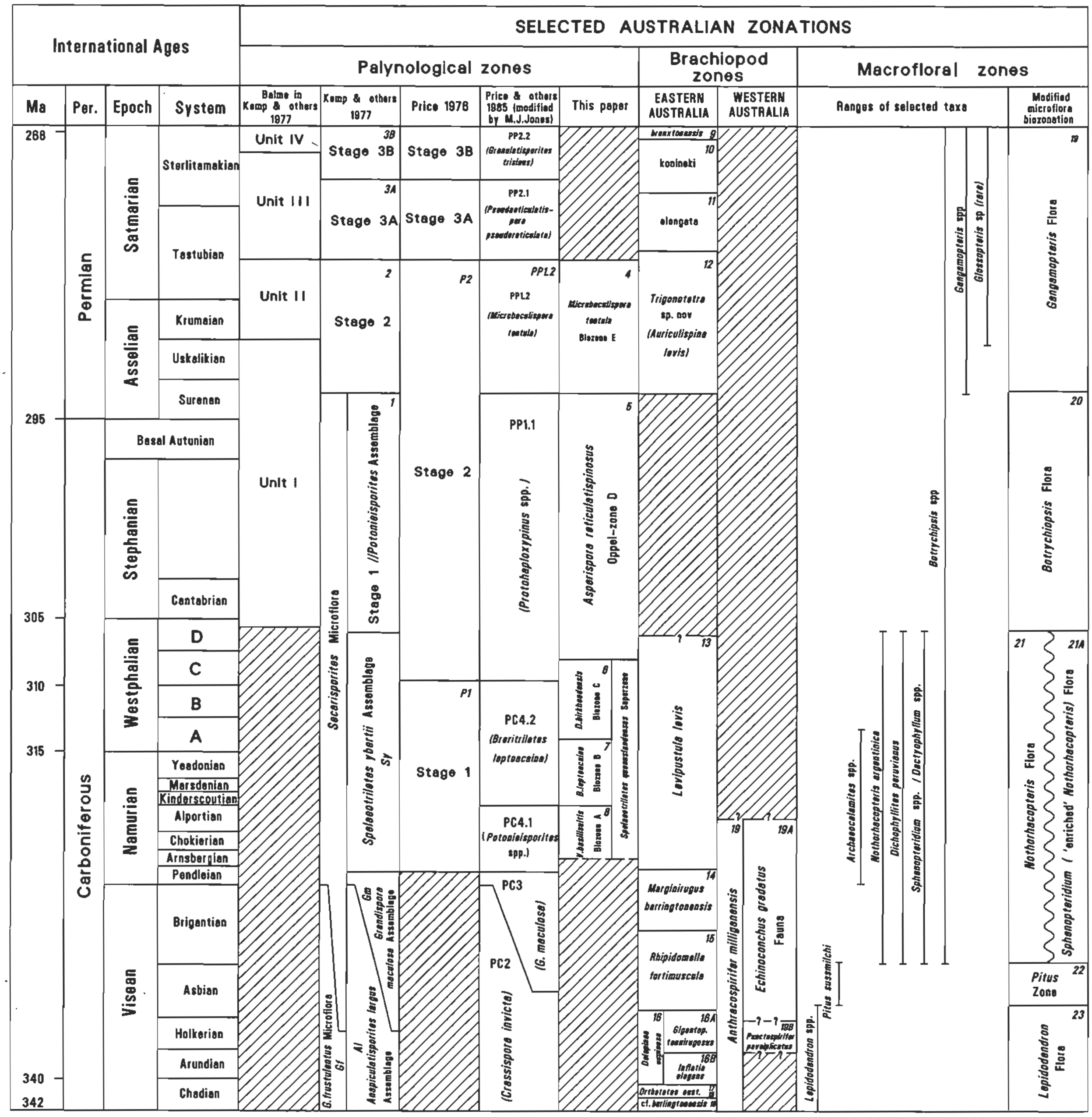

Supplementary fossil notations

Gc *Granulatisporites confluens* Oppel–zone (Foster & Waterhouse, 1988)

Db *Diatomozonotriletes birkheadensis* Assemblage (Powis, 1984)

F3 Tasmanian Faunizone 3 (Clarke & Banks, 1973)

F2 Tasmanian Faunizone 2 (Clarke & Banks, 1973; Calver and others, 1984)

F1 Tasmanian Faunizone 1 (Clarke & Banks, 1973; Calver and others, 1984)

Figure 7. Correlations of selected Late Carboniferous/Early Permian Australian sedimentary basins.
Eustatic sea level drops from the Early Carboniferous to the Westphalian D when glaciation commences. Eustatic sea level rise in the late Asselian coincides with glacial melting and a change in the continental structural regime to sinistral-shear. Glaciation indicated on the chart is on a gross scale only, no attempt has been made to identify interglacial events. A maximum in eustatic sea level rise is reached in the early Tastubian, resulting in extensive marine deposition throughout Australia and the development of algal bloom horizons in marine, sub-saline, confined basins. Sea level decline occurs within the late Tastubian/ early Sterlikamakian, as indicated in the Canning and Cranky Corner Basins. Fluvial-deltaic infilling of intra-cratonic basins and coal-swamp development follow the extensive Tastubian sea level rise. Radiometric ties: Harland & others (1982). Note the older dates on the Paterson Volcanics by Roberts & others, 1991. **Eastern Australian brachiopod zones:** Carboniferous, after Roberts & others, (1976); Permian, Runnegar & McClung (1975). **Western Australian brachiopod zones:** after Roberts (1971). **Macrofloral biozones** after Retallack (1980), Morris (1985). **Lovelle Depression:** Hawkins & Harrison (1978), Hawkins (1978). **Koburra Trough/Springsure Shelf/Drummond Basin:** Gray & Swarbrick (1975), Gray (1976), Playford (1978), Fenton & Jackson (1988). **Cooper Basin:** Price & others (1985), Thornton (1979). **Arckaringa Basin:** Townsend & Ludbrook (1975), Jones (1987). **Pedirka Basin:** Thornton (1979), Wopfner (1981). **Tamworth Shelf:** Evernden & Richards (1962), Rattigan (1967), Helby (1969a, 1969b), McClung (1975), Runnegar & McClung (1975), Kemp & others (1977), Roberts & Engel (1980), Briggs (1985), Engel (1985), Morris (1985), Roberts (1985). **Bonaparte Basin:** Duchemin & Creevey (1966), Mamet & Belford (1968), Playford (1971), Roberts (1971), Kemp & others (1977), Gunn (1988), Lee & Gunn (1988), Mory (1988), Mory & Beere (1988). **Canning Basin:** Jones & others (1973), Dickins & others (1978), Powis (1984), Lehmann (1986), Foster & Waterhouse (1988). **Perth Basin:** McWhae & others (1958), Glenister & others (1973), Playford & others (1975), Kemp & others (1977), Archbold (1982), Foster & others (1985).

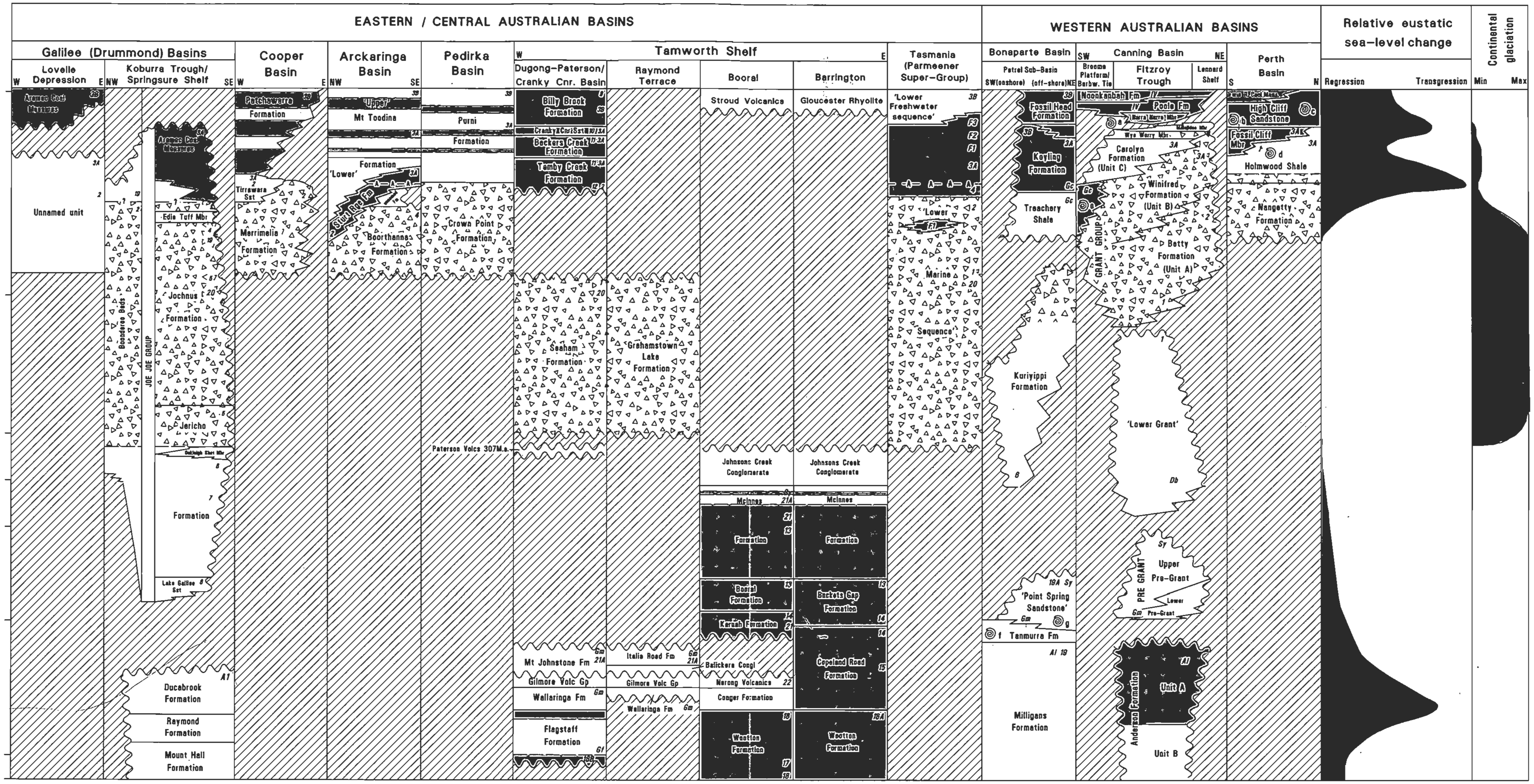

a — Sterlitmakian ammonoids (Glenister & Furnish, 1961)

b — Tastubian ammonoids (Glenister & Furnish, 1961)

c — Late Tastubian/ Sterlitamakian ammonoids (Glenister and others, 1973)

d — Sakmarian ammonoids (Glenister & Furnish, 1961)

e — Mid/Late Asselian macrofauna (Foster & Waterhouse, 1988); reviewed as Asselian/Early Tastubian (Archbold & Dickins, 1991)

f — Early Namurian, Mamet's foraminiferal Zone 17, Core 2 AOD Bonaparte No.1 (Mamet & Belford, 1968)

g — Visean ostracodes, AAP Kulshill No.1 (Duchemin & Creevey, 1966)

Coal deposits

Glacial deposits

Marine sediment deposits

-A- -A- *Marginal marine algal horizons (Sub-normal salinities)*

Sporae

Anteturma **Proximegerminates** Potonié 1970

Turma **Triletes** Reinsch emend. Dettmann 1963

Suprasubturma **Acavatitriletes** Dettmann 1963

Subturma **Azonotriletes** Luber emend. Dettmann 1963

Infraturma **Laevigati** Bennie & Kidston emend. Potonié 1956

Genus ***Calamospora*** Schopf, Wilson & Bentall 1944

Type species, by original designation: *Calamospora hartungiana* Schopf (*in* Schopf & others,1944); U.S.A., Illinois; Late Carboniferous.

Calamospora sp. cf. ***C. microrugosa*** (Ibrahim) Schopf & others, 1944 (*sensu*) Segroves 1970 (not illustrated)

See Segroves (1970, p. 48) for a suggested synonymy of *Calamospora* sp. cf. *C. microrugosa.*

Dimensions (26 specimens). Equatorial diameter 49 (82) 99 μ m.

Remarks. *Calamospora* sp. cf. *C. microrugosa* varies slightly from *C. microrugosa* in its greater range of size and the folding which tends to obscure the trilete mark.

Previous records. Namurian to Westphalian of Europe (Schopf & others, 1944; Smith & Butterworth, 1967); Visean to Late Carboniferous of Canada (Barss, 1967); Early Permian of Brazil (Pons, 1976); Late Devonian to Late Permian in Australia (Balme & Hassell, 1962; Segroves, 1970; Foster, 1975; Playford, 1977).

Range. Oppel-zone A to Oppel-zone E.

Genus ***Punctatisporites*** Ibrahim emend. Potonié & Kremp 1954

Type species, by original designation: *Punctatisporites punctatus* (Ibrahim) Ibrahim 1933; Ruhr area, West Germany; Late Carboniferous.

Punctatisporites lucidulus Playford & Helby 1968 (not illustrated)

1968 *Punctatisporites lucidulus* Playford & Helby, p. 107; pl. 9, figs 1, 2

Dimensions (20 specimens). 43 (58) 73 μ m.

Remarks. *Punctatisporites lucidulus* is distinguished from *P. gretensis* Balme & Hennelly 1956 by its smaller size, generally longer laesurae and thinner exine.

Previous records. Late Carboniferous, Hunter Valley, New South Wales (Playford & Helby, 1968); Canning Basin, Western Australia (Powis, 1979).

Range. Oppel-zone A to Oppel-zone E.

Punctatisporites gretensis Balme & Hennelly 1956 Fig. 8 0

1956 *Punctatisporites gretensis* Balme & Hennelly, pp. 245—246; pl. 2, figs 11—13

For suggested synonymies refer to Piérart (1974, p. 182) and Foster (1975, p. 127).

Dimensions (25 specimens). Equatorial diameter 49 (86) 131 μ m.

Remarks. *Punctatisporites gretensis* may be separated from a similar western European form, *P. obesus* (Loose) Potonié & Kremp 1955, by its smaller size and the lack of darkened exine commonly found along the laesurae of *P. gretensis.*

The exinal structure of *P. gretensis* ranges from homogeneous to highly endoreticulate to endopunctate. The morphologic variation suggests that these features are preservational.

Previous records. This spore is found throughout the Late Carboniferous to Permian of Australia (e.g. Balme & Hennelly, 1956; Balme, 1964; Segroves, 1970; Foster, 1975; Rigby & Hekel, 1977; Powis, 1979), Africa (Bose & Kar, 1966; Bose & Maheshwari, 1968; Jardiné, 1974; Anderson, 1977), South America (Cousminer, 1965; Pant & Srivastava, 1965; Archangelsky & Gamerro, 1979) and India (Potonié & Lele, 1961; Bharadwaj, 1962; Sinha, 1972).

Range. Oppel-zone A to Oppel-zone E.

Infraturma **Retusotrileti** Streel 1964

Genus ***Retusotriletes*** Naumova emend. Streel 1964

Type species, by subsequent designation (Potonié, 1958, p. 13): *Retusotriletes simplex* Naumova 1953; Kuluga Province, U.S.S.R.; Middle Devonian.

Retusotriletes nigritellus (Luber) Foster 1979 Fig. 8 D

1941 *Azonotriletes nigritellus* Luber *in* Luber & Waltz, p. 53; pl. 12, fig. 180
1979 *Retusotriletes nigritellus* (Luber) Foster, p. 30; pl. II, figs 7, 16

For additional synonymies see Foster (1979, p. 30).

Dimensions (10 specimens). Equatorial diameter 22 (30) 36 μ m.

Previous records. See Foster (1979).

Range. Oppel-zone D to Oppel-zone E.

Infraturma **Apiculati** Bennie & Kidston emend. Potonié 1956

Subinfraturma **Verrucati** Dybová & Jachowicz 1957

Genus ***Verrucosisporites*** Ibrahim emend. Smith & Butterworth 1967

Type species, by original designation: *Verrucosisporites verrucosus* (Ibrahim) Ibrahim 1933, Ruhr area, West Germany, Late Carboniferous.

Verrucosisporites aspratilis Playford & Helby 1968 Fig. 8 A, B

1968 *Verrucosisporites aspratilis* Playford & Helby, p. 108; pl. 9, figs 3—5

Dimensions (15 specimens). Equatorial diameter 34 (53) 64 μ m.

Remarks. The relatively wide spacing and the occasionally elongate basal outline of some of the verrucae distinguish *Verrucosisporites aspratilis* from other species of *Verrucosisporites.* Specimens described originally from the Italia Road Formation have a slightly thinner exine than the GSQ Jericho 2 forms. *V. aspratilis* differs from

V. nitidus (Naumova) Playford 1964, and *V. basiliscutis* Jones & Truswell n. sp. (*q.v.*) in not having its sculptural elements set close enough to produce a negative reticulum; and from *V. donarii* Potonié & Kremp 1955 by its larger size and broader spacing of the sculptural elements. The specimen included by Price (1983, pl. 2, figs 8—10) has a distinct negative reticulum, and is thus not referable to *V. aspratilis*; it is probably closer to *V. basiliscutus*.

Previous records. Hunter Valley, New South Wales, Australia; Late Carboniferous (Playford & Helby, 1968).

Range. Oppel-zone A to Oppel-zone D.

Verrucosisporites nitidus (Naumova) Playford 1964
Fig. 8 I

1953 *Lophotriletes grumosus Naumova*, p. 57; pl. 7, figs 14, 15

1964 *Verrucosisporites nitidus* Playford, pp. 13—14; pl. III, figs 3—6

For additional synonymy see Playford, 1971, p. 15.

Dimensions (12 specimens). Equatorial diameter 34 (58) 70 μ m.

Remarks. *Verrucosisporites nitidus* differs from *V. gobbettii* Playford 1962 in having smaller verrucae which tend to be more closely packed, and from *V. quasigobbettii* Jones & Truswell n. sp. (*q.v.*) in lacking pila. The form of *V. nitidus* encountered was slightly larger than noted by previous authors (Naumova, 1953; Ischenko, 1956; Playford, 1964), but this difference may be due to either geothermally induced shrinkage or infraspecific size variation.

Previous records. *V. nitidus* is a typically Late Devonian to Early Carboniferous form recorded from Europe (Ibrahim, 1933), Canada (Playford, 1964; Barss, 1967) and Australia (Playford, 1971, 1978). Its presence has also been noted from the Late Carboniferous of the Canning Basin (Powis, 1979).

Range. Oppel-zone A to Oppel-zone E.

Verrucosisporites basiliscutis sp. nov.
Fig. 8 C, E—H, J—L

?1983 *Verrucosisporites aspratilis* auct non. Playford & Helby; Price, p. 169, pl. 2, figs 8—10

Description. Spores radial, trilete, amb circular to subcircular, specimens often with off-polar compression, laesurae indistinct to perceptible, straight, simple, length 1/3 of spore radius. Exine densely sculptured by verrucae, semi-circular in section with occasionally flattened apices, ~0.5 μ m high; circular, sub-circular to irregularly rectangular and polygonal in plan, 2—3 μ m broad, ~0.5 μ m apart giving a fine negative reticulum. Rare small grana may occur between verrucae. Exine 1—3 μ m thick, often with concentric semi-lunar compressional folds.

Dimensions (20 specimens). Equatorial diameter 41 (55) 76 μ m.

Type material. Holotype MFP 6845/8; 94.4, 39.8; CPC25792; Fig. 8 J, K.

Type locality. Jericho Formation, Galilee Basin, Late Carboniferous, GSQ Jericho 2, 652.05 m.

Derivation of name. Latin *basiliscus* lizard, *cutis* skin.

Holotype. Latero-proximal aspect. Amb circular to sub-circular, slightly undulose because of the verrucate ornamentation; equatorial diameter 56 μ m; trilete mark faintly visible, simple, 1/3 to 1/2 spore radius. Exine ~1 μ m thick, ornamented by discrete verrucae ~0.5 μ m high, semi-circular to slightly bevelled in section, 2—3 μ m broad with circular to polygonal outlines, ~0.5 μ m apart. Exine with a few compressional curvilinear folds.

Remarks. *Verrucosisporites basiliscutis* is very similar to the Westphalian *V. verrucosus* (Ibrahim) Ibrahim 1933 in the form of the sculpture and poorly defined trilete mark. Krutzsch (1959) redescribed the holotype of *V. verrucosus* and noted that its ornamentation coalesced into elongate welts and had irregular, rectangular, basal sections; these features differentiate it from *V. basiliscutus*. The latter also differs by having shorter laesurae and tends to be within the smaller size range of *V. verrucosus*. *V. basiliscutis* differs from *V. nitidus* (Naumova) Playford 1964 in its much smaller verrucae, and from *V. aspratilis* Playford & Helby 1968 by its closer packed verrucae. The species which Evans (1964b) termed *Rugulatisporites* sp. 22 from the early Permian of eastern Australia is very similar to *V. basiliscutis*; *Rugulatisporites* sp. 22 has a thinner exine, more apparent trilete mark and lacks the compressional folds of *V. basiliscutis* (see Price 1983; p. 169, pl. 2, 8—10). Recently, Backhouse (1988) described *V. andersonii* from the Early Permian of Western Australia which, from the description and associated photomicrographs, is probably conspecific with *Rugulatisporites* sp. 22.

Range. Oppel-zone A to Oppel-zone E.

Verrucosisporites quasigobbettii sp. nov.
Fig. 8 N, P, Q

1968 *Verrucosisporites* sp. cf. *V. gobbettii* Playford & Helby, pp. 108—109, pl. 9, figs 6, 7

Description. Spores radial, trilete, amb subcircular, disrupted by verrucate projections. Laesurae distinct, ~3 μ m broad, simple, extending to 4/5 of spore radius. Exine 2—4 μ m thick, ornamented on both proximal and distal faces by prominent smooth rounded verrucae and occasional pila, 2—6 μ m high, 3—10 μ m basal diameter (basal outline variable). Variable spacing of sculptural elements ~2—6 μ m apart. Exine between projecting elements laevigate.

Dimensions (31 specimens). Equatorial diameter 49 (66) 79 μ m.

Type material. Holotype MFP 6849/5; 109.1, 38.2; CPC25798; Fig. 8 P.

Type locality. Jericho Formation, Galilee Basin, GSQ Jericho 2, 706 m.

Derivation of name. Latin prefix *quasi* almost, proposing that this species is similar to but not identical with V. *gobbettii* Playford (1962).

Holotype. Proximal aspect, circular amb, diameter 60 μ m, amb irregularly undulating, 16 verrucae visible at equator. Laesurae simple, distinct, to 4/5 of spore radius, terminations slightly deflected because of rupturing. Sculptured with verrucae and pila (3 μ m high, 4—5 μ m basal diameter, 2—6 μ m apart). Exine 3 μ m thick.

Remarks. *Verrucosisporites quasigobbettii* differs from *V. gobbettii* Playford, described originally from the Early Carboniferous of Spitsbergen (Playford, 1962), by its thicker exine, mixed sculpture of both verrucae and pila which do not coalesce, and the height of the sculptural elements which reach 6 μ m.

Previous records. *V. quasigobbettii* was first described as *Verrucosisporites* sp. cf. *V. gobbettii* and was identified in the *Grandispora maculosa* Assemblage from the Hunter Valley, New South Wales (Playford & Helby, 1968).

Range. Oppel-zone A to Oppel-zone E.

Verrucosisporites sp.
Fig. 8 M, R

Description. Trilete radial spores, amb circular to sub-circular, margin undulating with verrucae in profile. Trilete mark distinct, laesurae straight, simple, extending to 4/5 of spore radius. Exine ornamented by discrete verrucae, circular to oval or polygonal in basal outline (3—6 μ m broad), semi-circular in profile (1—2 μ m high); exine between sculptural elements occasionally ornamented by micro-vermiculae. Exine 2—4 μ m thick.

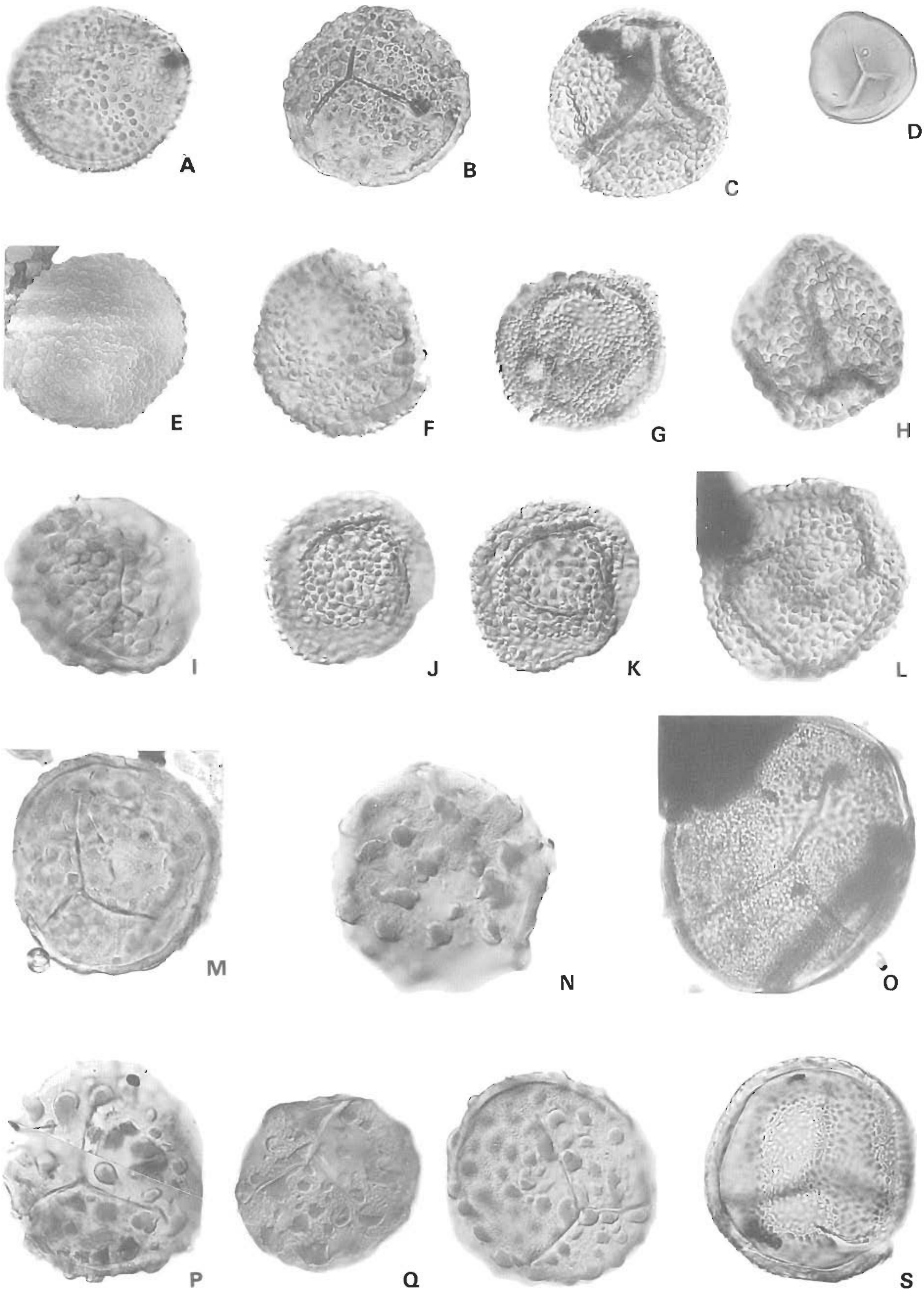
A
B
C
D
E
F
G
H
I
J
K
L
M
N
O
P
Q
S

Dimensions (32 specimens). Equatorial diameter 52 (72) 106 μ m.

Remarks. This form cannot be adequately assigned to any known species. *V. nitidus* Playford has more closely spaced verrucae producing a negative reticulum. *V. quasigobbettii* is distinguished from this form by the presence of pila and the greater height of the verrucae. There does, however, appear to be a morphological gradation between *V. quasigobbettii* and these forms. The micro-vermiculae found on the exine of this form may be a preservational feature. The species is distinguished from other forms of *Verrucosisporites* by its well spaced, dome-like verrucae.

Range. Oppel-zone A to Oppel-zone E.

Subinfraturma **Granulati** Dybová & Jachowicz 1957

Genus *Cyclogranisporites* Potonié & Kremp 1954

Type species, by original designation: *Cyclogranisporites leopoldii* Potonié & Kremp 1954; Germany, Late Carboniferous.

Cyclogranisporites firmus sp. nov.
Figs 8 S; 9 K, L, O—V

Description. Spores radial, trilete, amb circular to sub-circular, occasionally preserved in off-polar compression. Laesurae typically simple, sometimes with slight labra, <1 μ m wide and high. Commissures often gaping at pole; tapering to margin. Laesurae extending at least 3/4 of spore radius, and often to equator. Exine bearing low grana and irregular, often anastomosing verrucae which are ~0.2 μ m high, 0.5—2 μ m broad at base, 0.5 μ m apart. Elements delineate a fine negative reticulum. Exine 3—4 μ m thick, homogeneous in appearance. Compressed spores often split along end of the laesurae.

Dimensions (40 specimens). Equatorial diameter 48 (57) 71 μ m.

Type material. Holotype MFP 6871/8; 109.5, 30.9; CPC25812; Fig. 9 Q, R.

Type locality. Jericho Formation, Galilee Basin, Late Carboniferous, GSQ Springsure 13, 343.4 m.

Derivation of name. Latin, *firmus* strong, powerful, referring to the sturdy appearance of the grains.

Holotype. Proximo-lateral aspect. Amb circular with slightly undulose margin because of sculpturing; equatorial diameter 66 μ m. Trilete mark distinct with prominent laesurae 31 μ m long, tapering towards equator, and bordered by faint labra. Exine 3.5—4 μ m thick, comprehensively ornamented by small uniform grana 1—2 μ m broad, 0.5 μ m apart, close set resulting in a negative reticulum.

Remarks. This species shows intraspecific variation from finely to coarsely ornamented types. The holotype is toward the finer end of the sculptural spectrum; an example of the coarser sculpture is shown on Fig. 8 S.

C. firmus is separable from most other species of *Cyclogranisporites* by its thicker exine. *C. flexuosus* Playford 1962 from the Early Carboniferous of Spitsbergen has a similar thick exine, but is distinguished by its thick labra. *C. pisticus* Playford 1978, from the Early Carboniferous Drummond Basin, is smaller and thinner-walled.

Range. Oppel-zone A to Oppel-zone D.

Subinfraturma **Nodati** Dybová & Jachowicz 1957

Genus *Apiculiretusispora* Streel emend. Streel 1967

Type species, by original designation: *Apiculiretusispora brandtii* Streel 1964; Goe, Belgium, Middle Devonian.

'Apiculiretusispora' arcuatus sp. nov.
Fig. 9 F—J, M, N

Description. Trilete, cavate(?), radial spores, amb circular to subcircular. Laesurae distinct, straight or slightly sinuous, length 2/3 to 4/5 of spore radius, labra 0.5 μ m broad. Contact areas distinct and laevigate, delineated by raised curvaturae. Distal face sculptured with evenly distributed discrete coni, or spinae, basal diameter and height 0.5—1 μ m. Exoexine 1—3 μ m thick. Sculpture extends on to proximal face to limit of curvaturae. Intexine discernible, smooth, <1 μ m thick, occasional specimens may show slight separation from exoexine equatorially and distally.

Dimensions (16 specimens). Equatorial diameter 41 (46) 67 μ m.

Type material. Holotype MFP 6869/5, 108.0, 45.9; CPC25806; Fig. 9 H—I.

Type locality. Jericho Formation, Galilee Basin, Late Carboniferous; GSQ Springsure 13, 289.46 m.

Derivation of name. Latin *arcuatus* curved, bow shaped, describing the form of the curvaturae.

Holotype. Proximal aspect. Amb circular, diameter 41 μ m. Distinct laesurae, slightly sinuous, length 2/3—3/4 of spore radius, 0.5—2 μ m, including labra <1 μ m broad. Contact area deeply depressed, laevigate, delineated by prominent curvaturae. Exoexine 1—1.5 μ m thick at equator, intexine <1 μ m thick, laevigate. Discernible separation of exinal layers of 1 μ m. Distal exoexine densely covered with spinae and occasional coni, up to 1.2 μ m high and usually <0.5 μ m in basal diameter.

Remarks. *'Apiculiretusispora' arcuatus* differs from *Apiculiretusispora* sp. A of Foster (1975), from the Permian of the Bowen Basin, in being larger with simple unsculptured laesurae. It differs from *Apiculiretusispora* sp. A of Playford (1971), from the Early Carboniferous of the Bonaparte Basin, in having finer, more closely spaced sculpture and longer laesurae. Assignment of *'A.' arcuatus* to *Apiculiretusispora* is provisional, as the species sometimes shows a slight separation of exinal layers, a feature not reported in Streel's (1964) description of the type species. There is some resemblance of *'A.' arcuatus* to miospores assigned to *Geminospora* Balme 1962, but these have more pronounced curvaturae and less prominent separation of exinal layers.

Range. Oppel-zone A to Oppel-zone D.

Genus *Anapiculatisporites* Potonié & Kremp 1954

Type species, by original designation: *Anapiculatisporites isselburgensis* Potonié & Kremp, 1954; Ruhr area, Germany, Middle Carboniferous.

Remarks. The emendation of *Anapiculatisporites* proposed by Smith & Butterworth (1967) is not accepted here: as Playford (1971) has

Figure 8. Spore species from Galilee Basin assemblages.
Magnification X~650 . **A, B,** *Verrucosisporites aspratilis* Playford & Helby 1968. A, CPC25785, distal view, MFP 6820/6; 94.3, 43.7; B, CPC25786, proximal view, MFP 3224/2; 98.0, 44.8. **D,** *Retusotriletes nigritellus* (Luber) Foster 1979, CPC25788, proximal aspect, MFP 6861A/3; 109.1, 42.0. **C, E—H, J—L,** *Verrucosisporites basiliscutis* sp. nov. C, CPC25788, distal view, MFP 3585/1; 98.2, 29.6. E, Scanning electron micrograph, proximal surface, MFP 6820. F, CPC25789, lateral compression, MFP 6856/3; 97.3, 31.2. G, CPC25790, lateral compression, MFP 6845/3; 108.5, 31.1. H, CPC25791, proximal view, MFP 3224/1. J, K, CPC25792, holotype, lateral compression, MFP 6845/8; 94.4, 39.8. L, CPC25793, proximo-lateral compression, MFP 6845/6; 103.8, 33.5. I, *Verrucosisporites nitidus* (Naumova) Playford 1964. CPC25794, proximal view, MFP6823/4; 103.8, 28.5. **M, R,** *Verrucosisporites* sp. M, CPC25795, proximal aspect, MFP 6820/7; 112.2, 48.9. R, CPC25796, proximal aspect, MFP 6849/7; 94.3, 40.0. **N, P, Q,** *Verrucosisporites quasigobbettii* sp. nov. N, CPC25797, distal aspect, MFP 6856/7; 111.5, 48.1. P, holotype, CPC25798, proximal aspect, composite photograph, MFP 6849/5; 109.1, 38.2. Q, CPC25799, proximal aspect, MFP 3224/2; 98.0, 40.4. **O,** *Punctatisporites gretensis* Balme & Hennelly 1956, CPC25800; proximal view of specimen in which corrosion has emphasised infrapunctae, MFP 6849/2; 114.5, 7.7. **S,** *Cyclogranisporites firmus* sp. nov., CPC25801; distal aspect. MFP 6871/7; 93.1, 31.3.

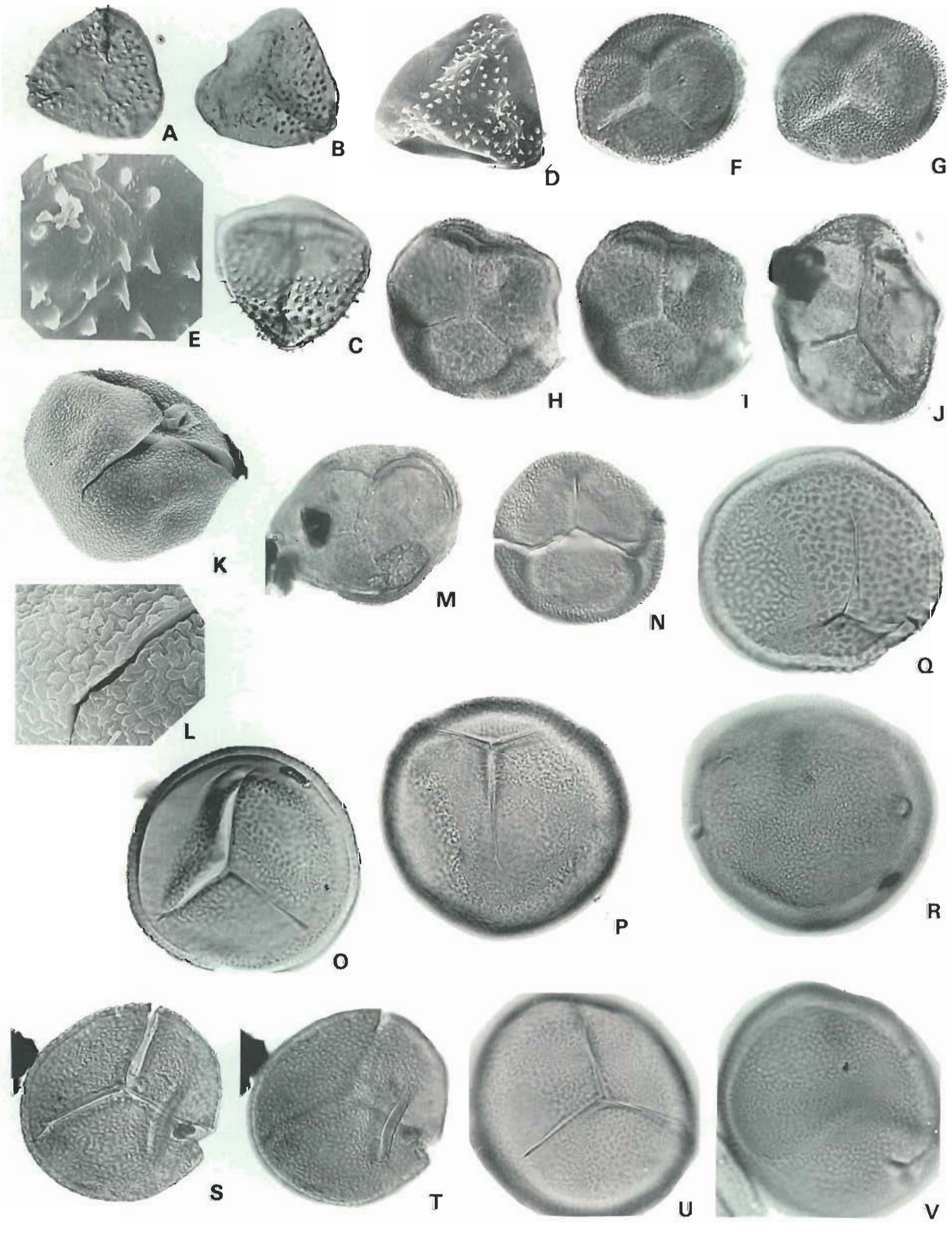
A
B
D
F
G
E
C
H
I
J
K
M
N
Q
L
O
P
R
S
T
U
V

pointed out, the restriction proposed by these authors is not in accord with the morphology of the type species.

Anapiculatisporites concinnus Playford 1962
Fig. 9 A—E

1962 *Anapiculatisporites concinnus* Playford, pp. 587—588; pl. 80, figs 9—12

1975 *Anapiculatisporites argentinensis* Azcuy, p. 42; pl. 13, figs 76—80

Dimensions (18 specimens). Equatorial diameter 22 (36) 38 μ m.

Remarks. Scanning electron microscopy (Fig. 9 C, D) shows the coni of the distal face to be regular, and comparable in spacing and dimensions with those of *Anapiculatisporites concinnus*. Scattered micrograna are apparent between the coni. *A. minor* (Butterworth & Williams) emend. Smith & Butterworth 1967 appears very similar to *A. concinnus* Playford, but differs in having shorter laesurae, distal spinae, and a consistently smaller equatorial diameter. *A. amplus* Playford & Powis 1979, from the Late Carboniferous of the Canning Basin, is much larger and sturdier. *A. argentinensis* Azcuy 1975 from the Namurian/Westphalian of Argentina is conspecific with *A. concinnus* Playford.

Previous records. Previously published records from Australia are confined to Powis' (1984) somewhat generalised record from the Bonaparte and Galilee Basins. Other records are from the Early Carboniferous of Spitsbergen (Playford, 1962), the Visean of Britain (Smith & Butterworth, 1967), and the Namurian/Westphalian of Argentina (Azcuy, 1975).

Range: Oppel-zone A to Oppel-zone D.

Genus *Apiculatisporis* Potonié & Kremp, 1956

Type species, by original designation: *Apiculatisporis aculeatus* (Ibrahim) Potonié 1956, Ruhr area, Germany, Late Carboniferous.

Apiculatisporis pseudoheles sp. nov.
Fig. 13 C—I

Description. Spores radial, trilete, amb circular to sub-circular. Laesurae straight, distinct, extending to equator, labra to 2 μ m wide and 1 μ m high, segmented in appearance, narrowing slightly towards equator. Proximal surface sculptured with scattered low verrucae ~1 μ m broad. Distal surface sculptured with coni tapering sharply or surmounted by slender spinulae. Spinulae often broken off coni, giving distal surface a verrucate appearance. Coni mainly discrete, with small verrucae developed between, but often close set to produce a negative reticulum. Coni bases circular to sub-circular in surface view 1—2 μ m broad, 0.5—1 μ m high, to 0.5 μ m apart. Exine 1—1.5 μ m thick.

Dimensions (15 specimens). Equatorial diameter 16 (25) 38 μ m.

Type material. Holotype MFP 6757/5, 93.6, 40.8; CPC25852; Fig. 13 C, D

Type locality. Jochmus Formation, Galilee Basin, Late Carboniferous/Early Permian, GSQ Jericho 1, 432.5 m.

Derivation of name. Greek *pseudo* false, *hel* wart.

Holotype. Proximal view. Amb circular with irregular margin from projecting spinae; equatorial diameter 38 μ m. Trilete mark distinct, laesurae straight to slightly sinuous, extending to margin, one laesura bifurcates to form curvatura imperfecta, labra 3 μ m wide tapering to 2 μ m near equator, segmented in appearance. Distal surface sculptured by biform elements with broad (~1.5 μ m) sub-circular to circular conate bases to 0.5 μ m apart tapering sharply to apiculate elements; occasionally fused giving a rugulate appearance. Apiculate elements projecting from margin are up to 1 μ m high. Proximal surface sculptured by sparse, low relief, isolated verrucae. Exine 1.5 μ m thick.

Remarks. The essentially spinose ornamentation of these specimens occurs on the distal and equatorial surfaces. The low proximal verrucae are best seen under SEM or phase contrast microscopy. *A. pseudoheles* may be separated from most forms of *Apiculatisporis* by its thick, close set, conate element bases. *Apiculiretusispora tuberculata* Azcuy 1975, from the late Carboniferous of Argentina, appears similar to *Apiculatisporis pseudoheles* but has smaller discrete spinae and more pronounced curvaturae imperfectae. *Anaplanisporites* sp. A (Azcuy, 1975), also from the late Carboniferous of Argentina, is similar to the examined specimens in that the spine bases may be sufficiently close to produce a negative reticulum, but this form tends to have coarser sculptural elements.

Range: Oppel-zone D to Oppel-zone E.

Genus *Brevitriletes* Bharadwaj & Srivastava 1969

Type species, by original designation: *Brevitriletes communis* Bharadwaj & Srivastava, 1969; India, Early Permian.

Brevitriletes leptoacaina sp. nov.
Fig. 13 M—Z, AA, BB

Description. Trilete radial miospores, mostly with circular, rarely rounded-triangular, amb. Laesurae distinct, straight, simple, extending to equator; curvaturae imperfectae developed variably. Exine 1.5—2 μ m thick, except at proximal pole where a darker area is sometimes visible and may indicate exinal thickening. Exine of proximal face laevigate; distal face comprehensively sculptured with apiculae. Elements evenly spaced, 2—3 μ m apart; increasing in length from equator to distal pole, 1.5—2 μ m high at distal pole and ~0.3—0.9 μ m in basal diameter. SEM indicates processes are set on very small conical bases, with diameters only slightly greater than of the processes themselves. Spinae straight-sided. Distal ends of processes show small bifurcating tips, or are bluntly broken; distal bifurcations may be discerned under an oil immersion objective. Exine between processes appears punctate when viewed with SEM.

Dimensions (50 specimens from GSQ Springsure 13 at 289.46 m). Equatorial diameter 31 (39) 49 μ m.

Type material. Holotype MFP 6869/4; 102.3, 32.8, CPC25859; Fig. 13 0, P.

Type locality. Jericho Formation, Late Carboniferous, GSQ Springsure 13, 289.46 m.

Derivation of name. Greek *leptos* thin, slender, *akaina* thorn, spine.

Holotype. Specimen in proximo-distal compression. Laesurae distinct, extending to equator, simple, straight, with weakly developed curvaturae. Exine at equator 1.8 μ m thick. Projections on distal face 1.5—2 μ m high, 0.8—0.9 μ m in basal diameter decreasing in stature towards equator where they form low verrucae. Grapnel-shaped tips are discernible on some distal apiculae. Equatorial diameter 43 μ m.

Figure 9. Spore species from Galilee Basin assemblages.
Magnification X~650 unless otherwise stated **A—E,** *Anapiculatisporites concinnus* Playford 1962. A, CPC25802, proximal view, MFP 6843/2; 102.0. 37.5. B, CPC25803, distal focus, MFP 6820/3; 111.8, 41.7. C, D, scanning electron micrographs, specimen from MFP 6869, distal view, C, 5800, D, 52400. E, CPC25804, lateral compression, MFP 6869/5; 108.0, 45.9. **F—J, M, N,** '*Apiculiretusispora*' *arcuatus* sp. nov. F, G, CPC25805, proximal and distal foci, MFP 6849/6; 98.0, 33.5. H, I, CPC25806, holotype, distal and proximal foci, MFP 6869/5; 108.0, 45.9. J, CPC25807, proximal focus, MFP 3685/6; 112.4, 42.5. M, CPC25808, proximal focus, MFP 3585/2; 101.7, 32.8. N, CPC25809, proximal focus, MFP 6849/6: 103.4, 40.8. **K, L, O—V,** *Cyclogranisporites firmus* sp. nov. K, L, scanning electron micrographs, specimen from MFP 6871, proximal view, K, 5750, L, 52100. O, CPC25810, proximal focus, MFP 6871/7; 93.1, 32.3. P, CPC25811, proximal focus, MFP 6871/8; 98.8, 35.8. Q, R, holotype, CPC25812, proximal and distal foci, MFP 6871/8; 109.5, 30.9. S, T, CPC25813, proximal and distal foci, MFP 3224/2; 109.6, 47.5. U, V, CPC25814, proximal and distal foci, MFP 6871/9; 98.1, 35.6.

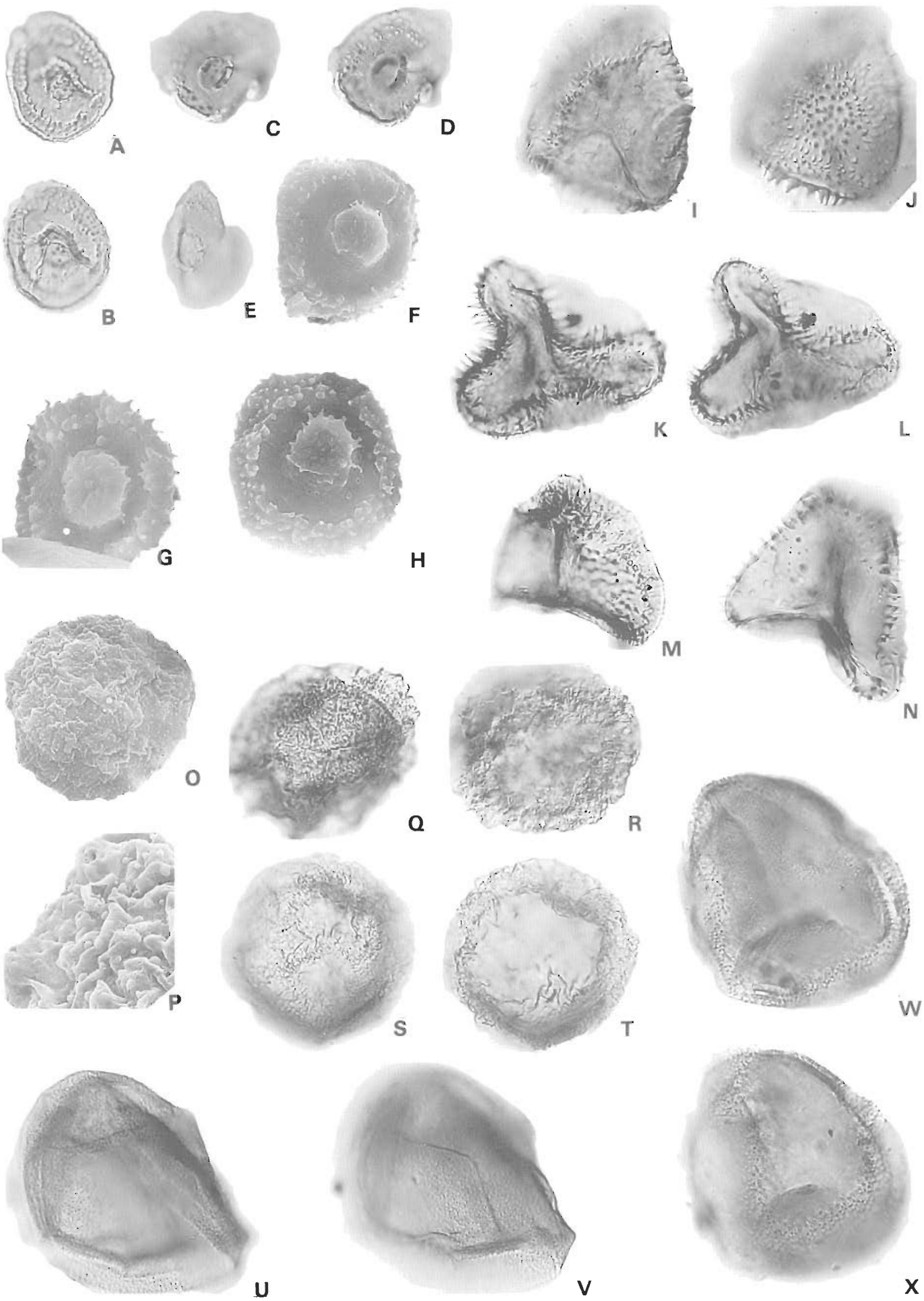
A
B
C
D
E
F
G
H
I
J
K
L
M
N
O
P
Q
R
S
T
U
V
W
X

Remarks. The species is closely comparable to *Brevitriletes levis* (Balme & Hennelly) Bharadwaj & Srivastava 1969, originally described from the Early Permian Collie Coalfield, Western Australia. We examined two paratype specimens of *B. levis* (Balme & Hennelly, 1956, pl. 2, figs 20, 21) and ten additional specimens from that type slide, and concluded that the specimens from the Joe Joe Group are quite distinct; to include them within *B. levis* would extend the morphological concept of that species and restrict the potential stratigraphic value of the available records. In *B. levis*, the distal processes arise from conical bases which are much more pronounced than in *B. leptoacaina*; the bases in *B. levis* are up to 2 μ m in diameter, give the appearance of a negative reticulum at some focal levels, and give the equatorial profile of the spore a distinctly serrated aspect. In all specimens of *B. levis*, the distance between processes was 0.8—1 μ m. Specimens recorded as *B. levis* by Foster (1979, pl. 5, fig. 13) and Rigby & Hekel (1977, pl. 3, fig. 4) from younger Permian sequences in Queensland, conform to the paratype material and are distinct from *B. leptoacaina*.

Range. Oppel-zone B to Oppel-zone E.

Genus *Dibolisporites* Richardson 1965 emend. Playford 1976

Type species. *Dibolisporites echinaceus* (Eisenack) Richardson 1965; Germany, Middle Devonian.

Remarks. Specimens described here clearly fall within *Dibolisporites* as emended by Playford (1976, p. 14). They display compound biform projections which are absent from the proximal face. Playford noted that the Carboniferous records he provided showed that the genus clearly extended beyond the Siegenian—Frasnian limits for it indicated by Richardson (1969); the record described here demonstrates that it extends into yet younger Carboniferous strata.

Dibolisporites disfacies sp. nov.
Fig. 11 A—M

?1984 *Brevitriletes* sp. A. Powis, pl. l, fig. 2a,b (no description)
1987 *Dibolisporites* sp. Besems & Schuurman 1987, pl. 1, fig. 6

Description. Trilete radial miospores, amb circular to oval. Laesurae rarely discernible, as proximal face is frequently missing; where visible, extending ~3/4 of distance to equatorial margin and enclosed within low, membranous, undulating labra. Proximal face (when present) laevigate, hyaline or ruptured and folded back towards the equator of the spore. Distal and equatorial regions bear a distinctive sculpture of compound, biform processes. Each element consists of a verrucate base, 1.5—2 μ m in diameter, nearly circular in plan, and 1—1.5 μ m high; base surmounted by a blunt spine 0.5—0.8 μ m long. Sculptural elements discrete, never anastomosing or fused, and separated by areas of smooth exine 0.5—1 μ m wide.

Dimensions (54 specimens from GSQ Springsure 13, 289.46 m). Equatorial diameter, including processes, 41 (51) 72 μ m.

Type material. Holotype MFP 6869/3; 102.3, 43.5; CPC25826; Fig. 11A,B.

Type locality. Jericho Formation, Late Carboniferous, GSQ Springsure 13, 289.46 m.

Derivation of name. Latin dis without, *facies* face.

Holotype. This specimen was selected as holotype because the proximal pole is intact, apart from a radial split which affects both poles of the spore. Laesurae length more than 3/4 of the spore radius with slightly folded membranous labra. Proximal face laevigate. Maximum diameter 49 μ m. Distal face with compound, biform sculpture elements; process bases 1.6—2 μ m in diameter, 1.1—1.3 μ m high, surmounted by blunt spines 0.6—0.8 μ m long.

Remarks. The morphology of this species is fairly uniform, but there is a variant in which the processes are finer than average; in these the basal section of the biform element is elongated, and the surmounting spine much longer in relation to the total length of the projection (Fig. 11 G, H, K—M). Specimens gradational between the morphology shown by the holotype and the finely ornamented form were observed, so the long-spined variant is for the present grouped within *D. disfacies*. *Brevitriletes* sp. A of Powis (1984), from the Canning Basin, appears similar to *D. disfacies*, although sculptural details are obscure. The projections in *D. disfacies* are similar to those of *D. microspicatus* Playford 1978, from the Early Carboniferous Ducabrook Formation of Queensland, but that species has a thicker exine and the proximal face is not so readily removed.

Previous records. Although not formally described, miospores referable to *Dibolisporites disfacies* have been illustrated from the *Diatomozonotriletes birkheadensis* Assemblage of the Canning Basin (Powis, 1984), and the late Carboniferous of Oman (Besems & Schuurman, 1987).

Range. Oppel-zone B to Oppel-zone E.

Subinfraturma **Baculati** Dybová & Jachowicz 1957

Genus *Horriditriletes* Bharadwaj & Salujha 1964

For suggested synonymy see Foster (1979, p. 38).

Type species, by original designation: *Horriditriletes curvibaculosus* Bharadwaj & Salujha, 1964; India, Permian, Raniganj Stage.

Horriditriletes ramosus (Balme & Hennelly) Bharadwaj & Salujha 1964
Fig. 13 J—L

For suggested synonymy see Foster (1979, p. 39).

Dimensions (25 specimens). Equatorial diameter 22 (29) 35 μ m.

Previous records. See Foster (1979).

Range. Oppel-zone D to Oppel-zone E.

Genus *Microbaculispora* Bharadwaj 1962

Type species, by original designation: *Microbaculispora gondwanensis* Bharadwaj 1962; India, Permian, Raniganj Stage.

Microbaculispora tentula Tiwari 1965
Fig. 13 A, B

1965 *Microbaculispora tentula* Tiwari, pp. 175—176; pl. 2, figs 35—36
1968 *Microbaculispora minutus* Venkatachala & Kar, p. 65; pl.1, figs 28—32
1975 *Microbaculispora tentula* Tiwari; Foster, pars. p. 133, pl. 2, figs 9—10
1979 *Microbaculispora tentula* Tiwari; Foster, p. 42, pl. 7, figs 8, 13—15

Figure 10. Spore species from Galilee Basin assemblages.
Magnification X~650 unless otherwise stated. **A—H,** *Rattiganispora apiculata* Playford & Helby 1968. A, B, CPC25815, median and distal views, MFP 6871/6; 106.4, 29.0. C, D, CPC25816, distal foci on boss and circumpolar apiculate zone, MFP 6871/6; 100.7, 31.1. E, CPC25817, lateral compression, MFP 6871/6; 92.7, 45.6. F—H, scanning electron micrographs, distal surface, sample MFP 6871. F, H, 51000; G, 51200. **I—N,** *Diatomozonotriletes birkheadensis* Powis 1984. I, J, CPC25818, median and distal foci, MFP 6820/7; 104.3, 37.7. K, L, CPC25819, median foci on distorted specimen, MFP 6871/2; 96.0, 29.0. M, CPC25820, median focus, MFP 6869/3; 107.3, 31.2. N, CPC25821, proximal and equatorial focus, MFP 6871/4; 107.0, 33.5. **O—T,** *Rugospora australiensis* Playford & Helby comb. nov. 1968. O, P, scanning electron micrographs, O, 5650, P, 51200, MFP 6849. Q, R, CPC25822, proximal and median foci, MFP 6869/2; 93.3, 37.2. S, T, CPC25823, distal and median foci, MFP 6849/9; 92.8, 37.9. **U, V,** *Spelaeotriletes* sp. cf. *S. queenslandensis* sp. nov. Morphotype with thin exine and proximal ornament. CPC25824, distal and proximal foci, MFP 6760/A/2; 102.7, 36.3. **W, X,** *Spelaeotriletes queenslandensis* sp. nov. CPC25825, proximal and distal foci, MFP 6849/5; 105.1, 31.1.

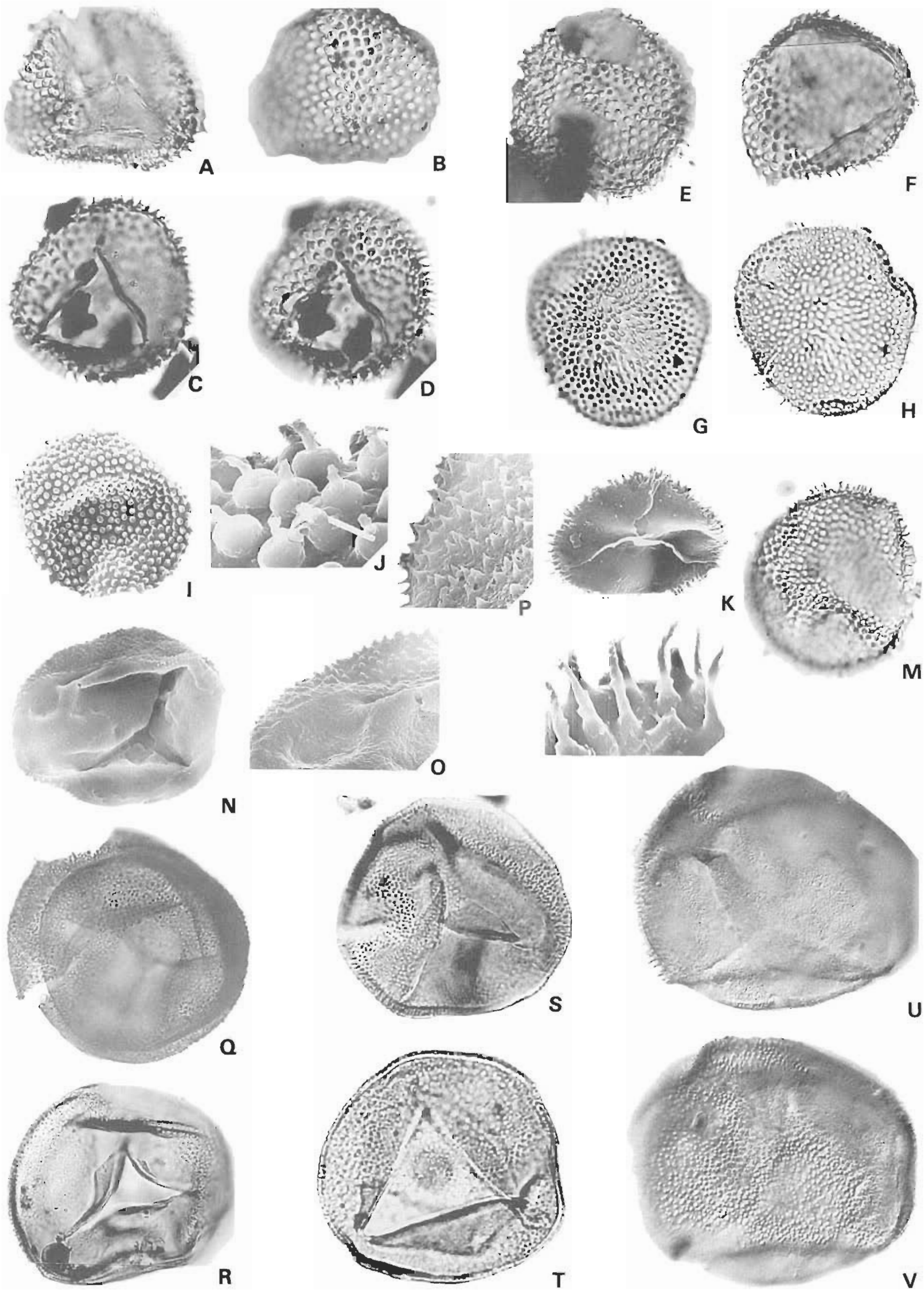

Dimensions (25 specimens). Equatorial diameter 22 (29) 35μ m.

Previous records. Common in the Early Permian of Gondwana (Foster, 1979).

Range. Oppel-zone E.

Infraturma **Murornati** Potonié & Kremp 1954

Genus ***Reticulatisporites*** Ibrahim emend. Potonié & Kremp 1954

Type species, by original designation: *Reticulatisporites reticulatus* (Ibrahim) Ibrahim 1933; Ruhr area, Germany, Late Carboniferous.

Remarks. This genus is used in the sense of Playford (1978).

Reticulatisporites bifrons sp. nov. Fig. 12 U—W, Zl, Z2

1984 *Reticulatisporites* sp. A Powis; pl. l, fig. 8 (no description)

Description. Trilete spores, amb sub-circular, oval, occasionally rounded-triangular, outline distorted by projecting muri. Laesurae straight, simple, 2/3 spore radius in length. Both proximal and distal faces ornamented with a coarse reticulum, the muri of which appear to be formed by folding of the exine. Each murus appears double in optical section, with two parallel bands separated by a narrow gap which represents the centre of the upfolded exine. On the proximal face the muri form a contorted zone adjacent to the laesurae, in which muri are thrown into a series of tight folds. Distally the muri form an irregular reticulum with irregular, polygonal, lumina 10—22 μ m broad. Muri 3—4 μ m wide, upfolded to a height of 3—4 μ m, and rounded in profile. Exine surface smooth, exine 1—1.5 μ m thick.

Dimensions (6 specimens). Equatorial diameter 48 (61) 74 μ m.

Type material. Holotype MFP 3224/3; 95.2, 31.3; CPC25847; Fig. 12 U, V.

Type locality. Jericho Formation, Late Carboniferous, BMR Springsure 8, cuttings from 110—120 ft.

Derivation of name. Latin *bifrons* with two faces, referring to the different sculpture on proximal and distal faces.

Holotype. Specimen oriented with proximal face uppermost. Amb rounded triangular, modified by 6 rounded projections where muri in profile impinge on the equator. Laesurae straight, simple, 2/3 spore radius in length. Reticulum consists of folded 'muri'; distally these define irregularly polygonal lumina, 10—20 μ m in diameter. Proximally the muri form a dense zone adjacent to the laesurae in which they are contorted, obervermiculate; this zone extends for about 1/3 radius of each contact area. Muri 3—5 μ m wide, 3—4 μ m high, rounded in profile. Equatorial diameter 65 μ m.

Remarks. The nature of the muri in *R. bifrons*, which appear to have been formed not by differential thickening of the exine but by arching and folding, renders this species distinct from all others attributed to *Reticulatisporites*. The contorted zone on the proximal face is another distinctive feature. The species is probably the same as that designated *Reticulatisporites* sp. 43 (or *Dictyototriletes* sp. 43) in Evans (1966) and Norvick (1974, 1981), and reported from Evans' Unit C2-Pla (equivalent to Oppel-zones D and E). The species was figured by Powis (1984) from his Late Carboniferous *Diatomozonotriletes birkheadensis* Assemblage of the Canning Basin. Foster & Waterhouse (1988) noted this miospore in the Early Permian *Granulatisporites confluens* Oppel-zone from the Grant Group, Canning Basin.

Range. Oppel-zone B to Oppel-zone D.

Genus ***Rattiganispora*** Playford & Helby 1968

1968 *Rattiganispora* Playford & Helby, p. 111
1983 *Diademaspora* Playford, pp. 272—273
1986 *Rattiganispora* Playford, pp. 85—86

Type species, by original designation: *Rattiganispora apiculata* Playford & Helby, 1968; New South Wales, Australia, Early Carboniferous.

Discussion. Playford (1983) erected the genus *Diademaspora* for acingulate, apiculate and annulate spores with a distinct circumpolar depression. He separated forms assigned to the genus *Rattiganispora* from *Diademaspora* on the basis of these types possessing a circumpolar murus. Playford (1986) later re-examined better preserved specimens of *Rattiganispora apiculata* from topotype material, and suggested that closer similarities existed between that species and *Diademaspora acuminata* Playford 1983, the type species of *Diademaspora*, than had been evident when *Diademaspora* was instituted. Hence it was suggested that *Diademaspora* was a junior synonym of *Rattiganispora*. Independently, and based on examination of topotype material of *Rattiganispora apiculata* (provided by G. Playford), we came to the same conclusion. In this material we noted the presence of a smooth circumpolar zone which corresponds to the circumpolar depression described for *Diademaspora*, providing evidence for clear morphological similarity between the two genera.

Rattiganispora apiculata Playford & Helby 1968 Fig.10 A—H

1968 *Rattiganispora apiculata* Playford & Helby, pp. 111—112, pl. 11, figs 1—3

Dimensions (15 specimens). Equatorial diameter 25 (29) 32 μ m. Distal boss diameter 8 (10) 12 μ m.

Remarks. Examination of the Galilee Basin specimens, and those from the type locality of *R. apiculata*, clearly show a distal boss surrounded by a depressed laevigate annular depression. The boss bears apiculate elements which are more pronounced, or better preserved, on the margins than on the surface. The Galilee Basin forms have shorter apiculate elements (0.5—1 μ m high) and tend to fall within the smaller size range of the Italia Road specimens. These differences are slight and do not warrant specific segregation.

Previous records. Carboniferous, Italia Road Formation, Hunter Valley, New South Wales (Playford & Helby, 1968).

Range. Oppel-zone C to Oppel-zone E.

Figure 11. Spore species from Galilee Basin assemblages.
Magnification X~650 unless otherwise stated. **A—M,** *Dibolisporites disfacies* sp. nov. A, B, Holotype, CPC25826, proximal and distal foci, MFP 66869/3; 102.3, 43.5. C, CPC25827, distal focus, MFP 6823/5; 106.4, 31.2. D, CPC25828, median and distal focus, MFP 6869/6; 97.8, 43.0. E, F, CPC25829, proximal and distal foci, MFP 3585/4; 92.7, 37.7. G, H, CPC25830, gracile morphotype, distal and median foci, MFP 6869/4; 100.7, 37.3. I, J, scanning electron micrograph, distal focus, MFP 6869, I, 5650, J, 51500. K, L, scanning electron micrograph, gracile morphotype, proximal focus, MFP 6869, L, 52500. M, gracile morphotype, CPC25831, distal focus, MFP 6869/3; 98.5, 28.7. **N—V,** *Spelaeotriletes queenslandensis* sp. nov. N—P, scanning electron micrographs, proximal focus, MFP 6849. O, P, 51200. Q, CPC25832, specimen in which exoexine is thinner than average, and more clearly separated from intexine, MFP 6761/A4; 101.8, 48.9. R, CPC25833, distal focus, MFP 6869/2; 99.0, 43.5. S, CPC25834, proximal focus, MFP 6869/4; 93.5, 37.2. T, CPC25835, median focus, MFP 104.3, 30.3. U, V, holotype CPC25836, proximal and distal foci, MFP 6849/5; 100.0, 33.0.

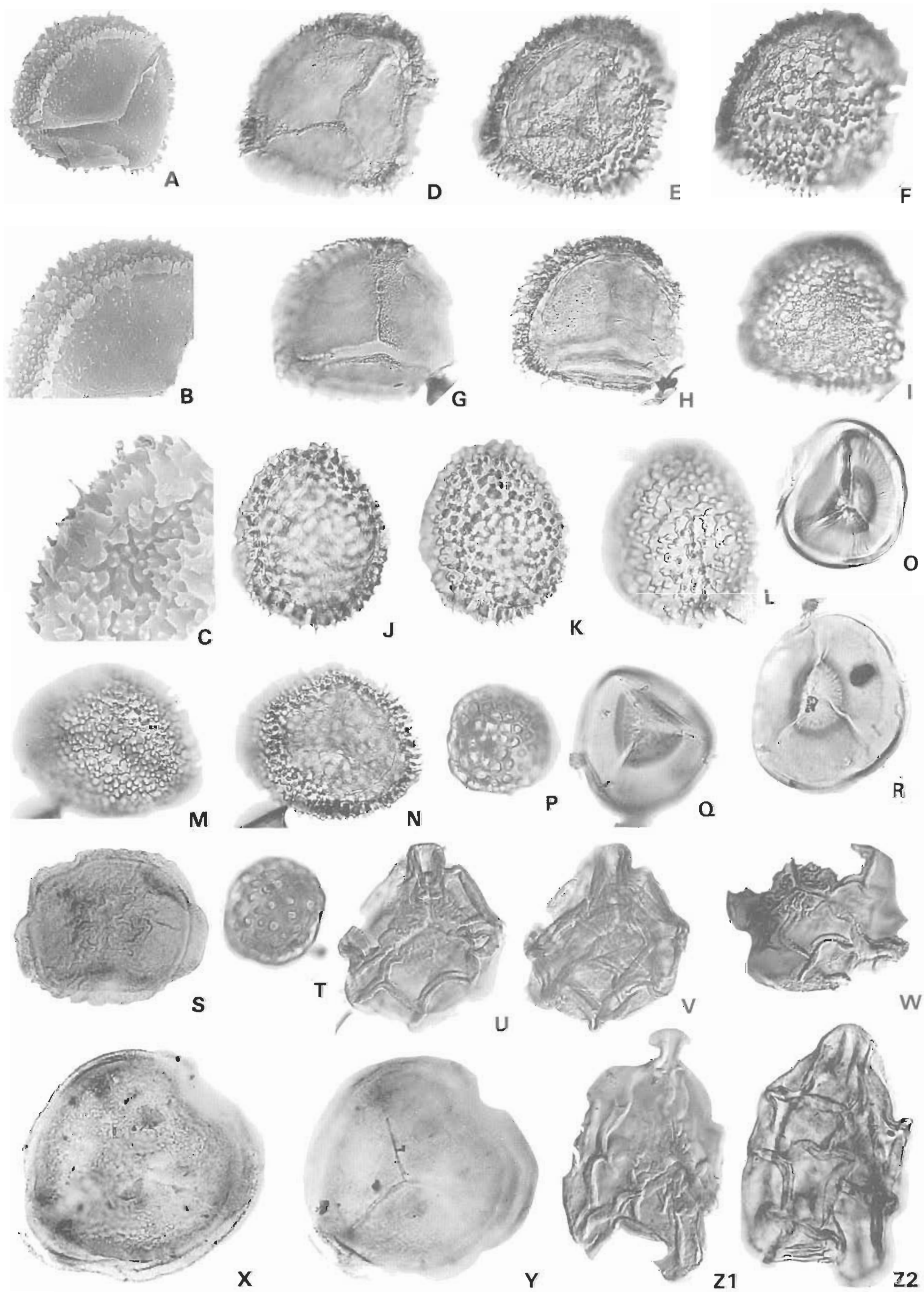
A
D
E
F
B
G
H
I
C
J
K
L
O
M
N
P
Q
R
S
T
U
V
W
X
Y
Z1
Z2

Subturma **Zonotriletes** Waltz emend Potonié and Kremp 1954

Infraturma **Auriculati** Schopf emend. Dettmann 1963

Genus ***Ahrensisporites*** Potonié & Kremp 1954

Type species, by original designation: *Ahrensisporites guerickei* (Horst) Potonié & Kremp 1954, West Germany, Ruhr area, Late Carboniferous.

Ahrensisporites cristatus Playford & Powis 1979
Fig. 13 CC, DD

1979 *Ahrensisporites cristatus* Playford & Powis, pp. 382—385; fig. 2; pl. III, figs 1—7

Dimensions (3 specimens). Equatorial diameter 82—108 μ m.

Remarks. In all the samples studied only three specimens were found. No other species comparable to this form is described in the literature.

Previous records. Playford & Powis (1979) described this species from the Late Carboniferous Grant Formation of the Canning Basin and assigned it to the *Spelaeotriletes ybertii* Assemblage. Braakman & others (1982) and Besems & Schuurman (1987) have reported this species from glacigene sediments in Oman.

Range. Oppel-zone B.

Infraturma **Tricrassati** Dettmann 1963

Genus ***Diatomozonotriletes*** Naumova ex Playford 1963

Type species, by subsequent designation: *Diatomozonotriletes saetosus* (Hacquebard & Barss) & Playford 1961; Northwest Territories, Canada, Early Carboniferous.

Diatomozonotriletes birkheadensis Powis 1984
Fig. 10 I—N

1984 *Diatomozonotriletes birkheadensis* Powis; Appendix 1, pp. 436, 438; pl. 1, figs 4—6

Dimensions (14 specimens). Equatorial diameter 40 (54) 71 μ m.

Remarks. Specimens observed in the present study conform well to the description given by Powis. There is considerable morphological variation among specimens. On some, the proximal face bears occasional spinae. There is some variation in the basal thickness, density, and spacing of processes in the corona; some specimens (e.g. Fig. 10 I, J) have bulbous bases, others are more gently tapering. All are treated as falling within *D. birkheadensis*, although Powis (1984) did not describe the morphological limits of the species. The species described by Anderson (1977) as *Microbaculispora spinosa* shows some resemblance to *D. birkheadensis*, but is more gracile and much smaller.

Previous records. Late Carboniferous *Diatomozonotriletes birkheadensis* Assemblage of the Galilee Basin, Bonaparte and Canning Basins (Powis, 1984), and from the Early Permian *Granulatisporites confluens* Oppel-zone of the Grant Group, Canning Basin (Foster & Waterhouse, 1988).

Range. Oppel-zone C to Oppel-zone D.

Subturma **Zonolaminatitriletes** Smith & Butterworth 1967

Infraturma **Cingulicavati** Smith & Butterworth 1967

Genus ***Cristatisporites*** (Potonié & Kremp 1954) emend. Butterworth, Jansonius, Smith & Staplin 1964

1972 *Jayantisporites* Lele & Makada, pp. 46—48, text-figs 3—4

Type species, by original designation: *Cristatisporites indignabundus* (Loose) Potonié & Kremp emend. Staplin & Jansonius 1964, Rhur, West Germany, Late Carboniferous, Westphalian B.

Discussion. The genus *Cristatisporites* was emended by Staplin & Jansonius (1964) to include cavate zonate miospores distinguished by an irregular amb due to scattered processes on, or incision of, the zona, and by having prominent distal sculpture often composed of warts which in part may bear setose tips. The exoexine may be minutely foveolate or vacuolate. Lele & Makada (1972) initiated the genus *Jayantisporites* on the basis that the zona was composed of fused elements which occasionally did not unite to form a complete zona. However the fusion of these elements does result in a recognisable ring, which is clear from their camera lucida sketches (Lele & Makada 1972, p. 48, text-fig. 4), and which is distinct from the distal ornamentation, thus constituting a zona. In many forms of *Cristatisporites* the zona is deeply incised, and not clearly marked, e.g. *C. indignabundus* (Staplin & Jansonius, 1964, p. 109) and apparently not entire. We consider that these cavate miospores which have a strongly dentate, and discernable, ring of sculptural differentiation are in fact zonate and should be retained within the genus *Cristatisporites*.

Kraeuselisporites Leschik has been applied to a number of Australian taxa of similar morphology, but *Kraeuselisporites* is acavate (Scheuring, 1974). Some Australian taxa should therefore be reallocated to the genus *Cristatisporites*. Foster (1979) placed some Australian cavate, zonate miospores, including *K. enormis* Segroves 1970, into the Indian genus *Indotriradites* (Tiwari) emend. Foster 1979. However, as Foster (1979) points out in his emendation of the genus, *Indotriradites* has a distinct zona and a continuous or notched amb. *K. enormis* has a ragged amb caused by its pronouncedly cristate zona, with incisions often almost reaching the central body. As *K. enormis* has a cristate zona and distal apiculae, it is best accommodated within *Cristatisporites*, i.e. *Cristatisporites enormis* (Segroves) Foster 1979 comb. nov. Basionym: *Indotriradites enormis* (Segroves) Foster 1979, p.56, pl. 16, fig. 4.

Cristatisporites **sp. cf.** ***C. kuttungensis*** (Playford & Helby) comb. nov.
Fig. 14 A—F

cf. 1968 *Kraeuselisporites kuttungensis* Playford & Helby, p. 112, pl. 11, figs 6, 7

Description. Miospores trilete, cavate, with rounded triangular amb and distinct zona. Laesurae extend almost to the equator in spore radii; sinuous, bordered by elevated labra 1—3 μ m wide. Zona 1/4—1/3 spore radius in width; margin usually dentate, rarely entire. Zona usually bears spinose or conate processes similar to those on the distal face; such processes may be incorporated into the zona itself, giving rise to the dentate margin. Inner margin of zona may be interrupted by foveolae up to 2 μ m in diameter, apparently an expression on the zona of the sometimes vacuolate nature of distal process bases. Proximal

Figure 12. Spore species from Galilee Basin assemblages.
Magnification X~650 unless otherwise stated. **A—N,** *Asperispora reticulatispinosus* sp. nov. A—C, scanning electron micrographs, A, B, proximal focus, MFP 6871, B, 51000. C, distal focus on specimen from MFP 6871, 52000. D—F, holotype, CPC25837, proximal median and distal foci, MFP 6871/7; 98.8, 41.4. G—I, CPC25838, proximal, median and distal foci, MFP 6871/7; 101.0, 29.8. J—L, CPC25839, median and distal foci, MFP 6871/8; 104.4, 32.3. M, N, CPC25840, distal and proximal foci, MFP 6871/7; 102.2, 44.5. **P, T,** *Maculatasporites minimus* Segroves 1967. P, CPC25841, MFP 6757/4; 95.2, 31.8. T, CPC25842, MFP 6758/3; 92.8, 34.3. **O, Q, R,** *Psomospora detecta* Playford & Helby 1968, O, CPC25843, proximal focus, MFP 6871/7; 102.5, 49.6. Q, CPC25844, proximal focus, MFP 3585/3; 100.1, 43.0. R, CPC25845, proximal focus, MFP 6871/6; 93.2, 48.4. **S,** *Auroraspora* sp. CPC25846, distal focus, MFP 6869/6A; 99.7, 55.8. **U, V, W, Z1, Z2,** *Reticulatisporites bifrons* sp. nov. U, V, holotype, CPC25847, proximal and distal foci, MFP 3224/3; 95.2, 31.3. W, CPC25848, proximal focus, MFP 6869/4; 109.3, 37.2. Z1, Z2, CPC25849, proximal and distal foci, MFP 6909/A3; 108.4, 43.2. **X, Y,** *Densoisporites* sp., CPC25850, distal and proximal foci, MFP 6869/6A; 99.7, 55.8.

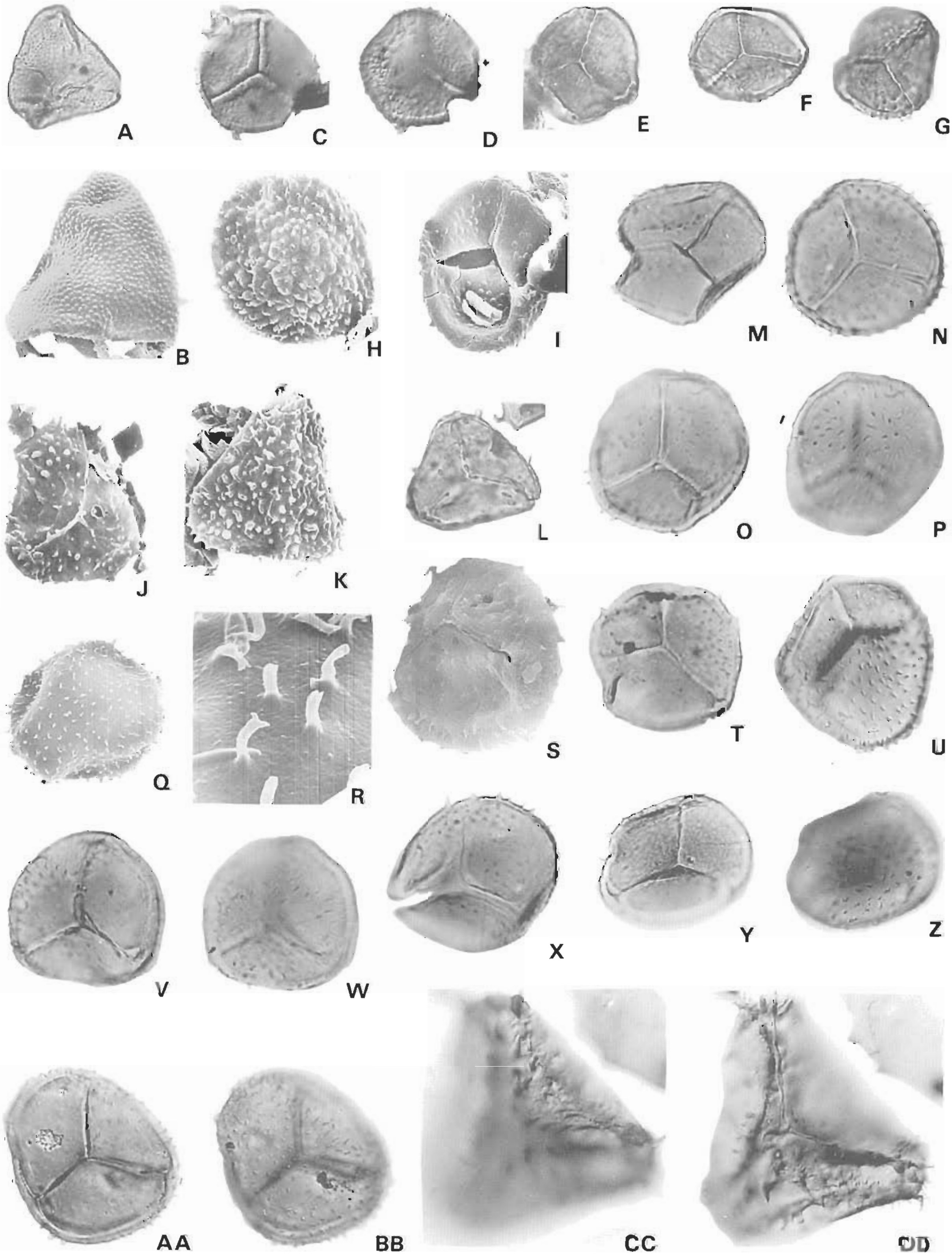
A
C
D
E
F
G
B
H
I
M
N
J
K
L
O
P
Q
R
S
T
U
V
W
X
Y
Z
AA
BB
CC
DD

face laevigate or punctate. Distal bears variable cover of prominent coni or spinae of diverse form but mostly sturdy coni 2—4 μ m high and 1—3 μ m in basal diameter, with bases frequently vacuolate. Processes usually discrete at bases. Exine between bases scabrate or punctate.

Dimensions (15 specimens). Equatorial diameter 57 (60) 79 μ m. Intexine diameter 29 (37) 53 μ m.

Remarks. From our observations, cavate, zonate, strongly ornamented taxa such as this are highly variable, as seen in such features as the shape and thickness of the zona, the size, shape, and degree of separation of the distal processes, and the separation of the exine layers. In some of these features these spores may overlap with specimens assigned here to *C. pseudozonatus*; but we have tried to maintain C sp. cf. *C kuttungensis* for specimens in which the zona forms a distinct band around the spore equator, rather than being deeply dissected as it is in *C. pseudozonatus*, and in which the distal processes are usually separate, not united at their bases.

The species described here appears to have a thicker, firmer zona than *C. kuttungensis* Playford & Helby 1968 from the Early Carboniferous of the northern Sydney Basin but in other features, such as the nature of the distal processes, it resembles that species. The Laurasian species *Cristatisporites indignabundus* (Loose) Staplin & Jansonius 1964 bears some resemblance to *C.* sp. cf. *C. kuttungensis* but lacks the large vacuoles within the zona and has indistinct laesurae. *C.* sp. cf. *C. kuttungensis* resembles the species *Cristatisporites enormis* (Segroves) Foster 1979 emend. from the Late Permian of the Perth Basin, but the latter species lacks a vacuolate zona and has thinner distal processes.

Range. Oppel-zone C to Oppel-zone D.

Cristatisporites pseudozonatus Lele & Makada 1972 comb. nov. Fig. 14 G—L

1972 *Jayantisporites pseudozonatus* Lele & Makada 1972, p. 49, pl. 1, figs 6—13, text-figs 5, 6, 6A
1983 *Cristatisporites* sp. 890 Price, p. 170, pl. 6, figs 10—12
1984 *Cristatisporites* sp. A of Powis, pl. 1, fig. 12
1988 *Jayantisporites pseudozonatus* Foster & Waterhouse, p. 140, figs 4g, j—l

Description. Trilete cavate miospores with rounded triangular amb. Pseudozonate, with strongly dentate margin. Laesurae distinct, extending to inner margins of zona, sinuous, with labra 1-2 μ m wide. Intexine usually discernible, smooth, folded; degree of separation of exine layers highly variable. Proximal face smooth or punctate. Distal face sculptured with prominent processes, either coni or spinae, 2—9 μ m in height, 1—4 μ m in basal diameter. Spinae more common, highly variable in shape, often acutely pointed, sometimes bearing a fine spine superimposed on the process tip. Shaft of process straight or swelling and contracting throughout its length; rare elements bifurcate. Bases of processes frequently united in a meandering chain of spines, which may interconnect at distal pole forming a loose reticulum. Zona occasionally partly absent, usually deeply dissected, and formed apparently by the welding together and expansion of processes similar to those on the distal face; occasionally pitted by erosion at its base, giving vacuolate appearance.

Dimensions (20 specimens). Equatorial diameter 55 (67) 77 μ m; intexine diameter 30 (36) 41 μ m.

Remarks. Lele & Makada (1972) described the size of *Cristatisporites pseudozonatus* as 70—90 μ m. The taxa described here are slightly smaller, but the variation in size may be due either to geothermally induced shrinkage, or intraspecific size variation. We feel that the sculpturing characteristics of this species are sufficiently distinctive to allow specific assignment, regardless of the small discrepancy in size.

This species might intergrade with *C.* sp cf *C. kuttungensis*. We have separated it on the basis of its usually deeply dissected zona, and on the tendency of the distal processes to be basally united.

C. indolatus Playford & Satterthwait 1988, from the Namurian of the Bonaparte Basin, is similar to *C. pseudozonatus* in its distal sculpturing of projecting elements which fuse together to form anastomosing cristae. The distal ornamentation of *C. indolatus*, however, is predominantly composed of bacula and coni rather than spinae or mammillate elements.

Previous records. Early Permian of India (Lele & Makada, 1972); Australia, Galilee Basin (Price, 1983), Canning Basin *D. birkheadensis* Assemblage (Powis, 1984) and *G. confluens* Oppel-zone Foster & Waterhouse (1988).

Range. Oppel-zone C to Oppel-zone D.

Genus *Asperispora* Staplin & Jansonius 1964

Type species, by original designation: *Asperispora naumovae* Staplin & Jansonius 1964; MacKenzie District, Northwest Territories, Canada; Givetian, Devonian.

Asperispora reticulatispinosus sp. nov. Fig. 12 A—N

Description. Spores radial, trilete, cavate, with an equatorial zona or zona formed of fused processes. Amb sub-circular to rounded triangular with a dentate margin. Laesurae distinct, extending to spore margins, straight or slightly sinuous. Labra 1-2 μ m high, development variable. Intexine usually discernible, smooth, folded, usually occupying about 4/5 of the spore cavity. Exoexine ornamented distally by a reticulum of closely packed verrucae which form muri 1—1.5 μ m wide, separating sinuous lumina 2—6 μ m wide. Small spinae or coni 1—2.5 μ m high distributed irregularly along surface of verrucae. Zona formed by aggregation, elongation and lateral fusion of elements of the distal reticulum. Scanning electron microscopy demonstrates that gaps may occur between swollen processes in the zona, and that structure is thickest on inner margins. Zona uniformly narrow, 4—7 μ m wide, thinning to form small dentate projections. Proximal face mostly smooth; may bear scattered small spinae.

Dimensions (25 specimens). Equatorial diameter 30 (37) 45 μ m.

Type material. Holotype MFP 6871/7; 98.8, 41.4; CPC25837; Fig. 12 D—F.

Type locality. Jericho Formation, Galilee Basin, Late Carboniferous, GSQ Springsure 13, 345 m.

Derivation of name. Latin *reticulatus* netlike, netted, *spinosus* thorny, in reference to the spinose reticulum of the distal surface.

Figure 13. Spore species from Galilee Basin assemblages.
Magnification X~650 unless otherwise stated. **A, B,** *Microbaculispora tentula* Tiwari 1965 A, CPC25851, proximal focus, MFP 6757/4; 95.7, 28.5. B, scanning electron micrograph, distal surface, MFP 6757, 51500. **C—I,** *Apiculatisporis pseudoheles* sp. nov. C, D, CPC25852, holotype, proximal and distal foci, MFP 6757/5; 93.6, 40.8. E, CPC25853, proximal focus, MFP 6757/5; 110.2, 34.9; F, CPC25854, proximal focus, MFP 6757/4; 93.7, 34.9. G, CPC25855, proximal focus, MFP 6757/4; 101.8, 39.2. H, I, scanning electron micrographs, MFP 6757, H, distal focus, 51000; I, proximal view, 51000. **J—L,** *Horriditriletes ramosus* (Balme & Hennelly) Bharadwaj & Salujha 1964. J, K, scanning electron micrographs, Sample MFP 6757, proximal and distal foci, 51000. L, CPC25856, proximal focus, MFP 6757/5; 97.2, 46.7. **M—BB,** *Brevitriletes leptoacaina* sp. nov. M, CPC25857, proximal focus, MFP 6869/5. 102.6, 36.1. N, CPC25858, proximal focus, MFP 6869/2; 102.5, 30.2. O, P, holotype, CPC25859, proximal and distal foci, MFP 6869/4; 102.3, 32.8. Q, R, S, scanning electron micrographs, Q, distal focus, MFP 6869, 5700. R, same specimen, 53000. S, proximal focus, MFP 6757, 5900. T, CPC25860, proximal focus, MFP 6869/4; 105.3, 32.8. U, CPC25861, distal focus, MFP 6869/6; 112.1, 51.0. V, W, CPC25862, proximal and distal foci, MFP 6869/5; 107.8, 32.3. X, CPC25863, MFP 6869/5; 110.6, 37.5. Y, Z, CPC25864, proximal and distal foci, MFP 6869/3; 104.5, 48.6. AA, BB, CPC25865, MFP 3585/4; 107.7, 39.7. **CC, DD,** *Ahrensisporites cristatus* Playford & Powis 1979, CPC25866, equatorial and proximal foci, MFP 6856/8; 106.4, 37.8.

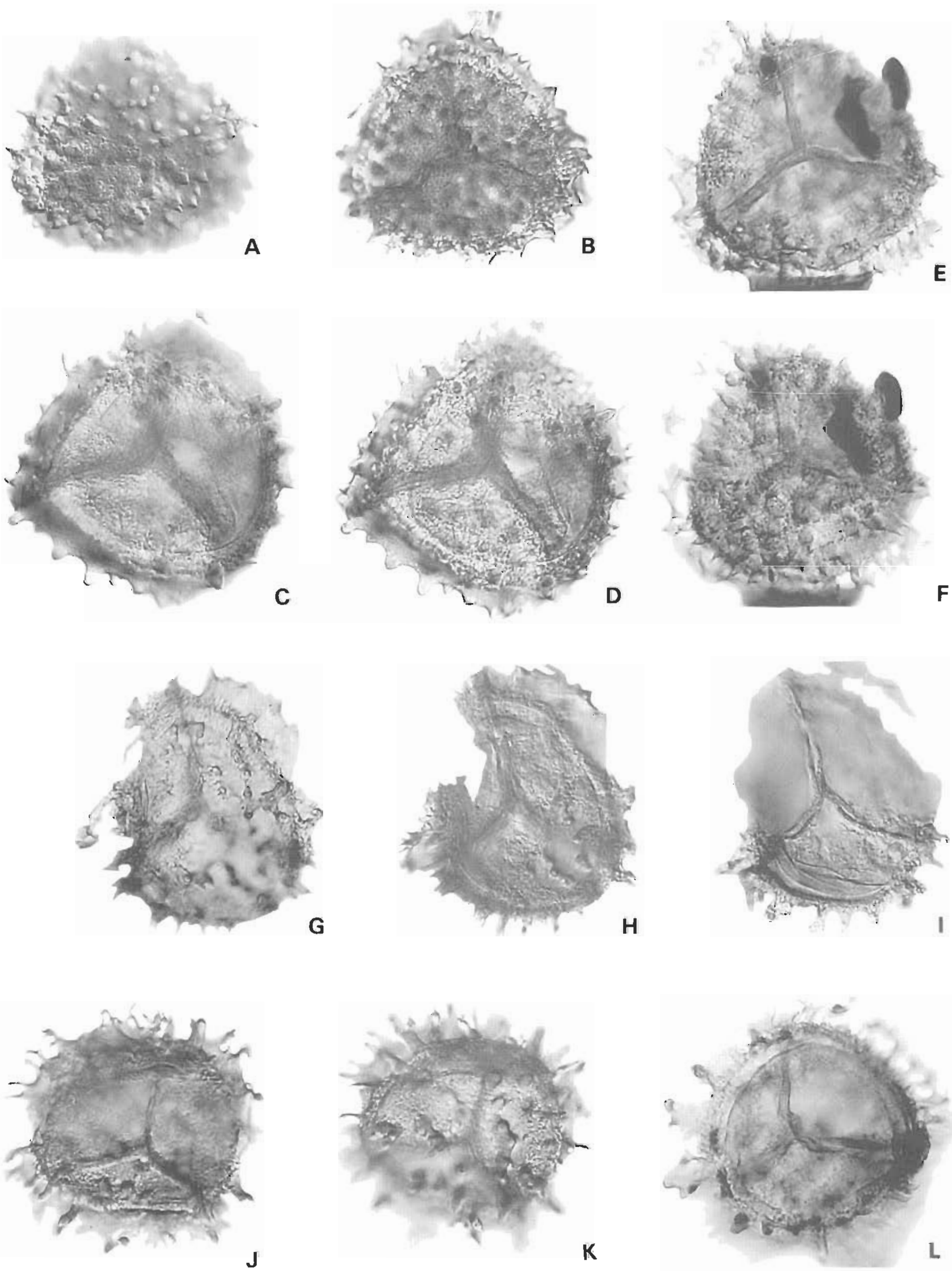

A
B
E
C
D
F
G
H
I
J
K
L

Holotype. Specimen compressed proximo-distally, trilete, amb rounded triangular, margin dentate. Equatorial diameter 45 μ m, trilete mark distinct, laesurae with labra 2 μ m wide, extending onto zona. Proximal surface sculptured with sparse spinae. Exoexine 2 μ m thick, sculptured distally with a mammillate reticulum, with muri 1—1.5 μ m wide, separating lumina 2—6 μ m wide. Spinae 1—2 μ m high at intervals along muri. Zona 4—6 μ m wide, grading equatorially into dentate structures 1—2.5 μ m high. Intexine laevigate, slightly folded, outline conformable to amb.

Remarks. The well developed distal mammillate reticulum and its modification to form a distinctly thin equatorial zona characterise this species. Staplin & Jansonius 1964 instituted the genus *Asperispora* to include cavate miospores with a narrow zona and distal setose apiculae or verrucae which may coalesce; *A. reticulatispinosus* falls within this generic definition. The closest species hitherto described is *C. pseudozonatus* Lele & Makada 1972 emend., from the Talchir Formation of Jayanti Coalfield, Bihar, India, which resembles *A. reticulatispinosus* in the distal reticulum of cristate ridges. In the Indian genus, however, the miospores are much larger; have a less persistently developed and broader zona; more variable apiculate sculpturing consisting of mixed baculae, coni and spina; and a less well developed, if at all, distal reticulum with broader muri. Ravn (1986) described a similar form from the Westphalian B-C Kilbourne Formation and Laddsdale Coal of the Floris Formation, Iowa, which he tentatively called *Lycospora* sp. 1. This taxon also has a distal reticulum which fuses around the equator to form a zona. However, Ravn (1986) suggested that *Lycospora* sp. 1. was not cavate, which makes it distinct from the taxon we have described.

Range. Oppel-zone D to Oppel-zone E.

Genus *Densoisporites* Weyland & Krieger, emend. Bharadwaj & Kumar 1972

Type species, by original designation: *Densoisporites velatus* Weyland & Krieger 1953; Aachen, Germany, Upper Cretaceous (Senonian).

Densoisporites sp.

Fig. 12 X, Y

Description. Radial spores, trilete, cavate, with a rounded triangular amb. Trilete mark distinct, laesurae straight to slightly sinuous, extending 3/4 of spore radius; labra ~1 μ m wide, prominent only at the proximal pole. Exoexine 0.5—1 μ m thick. Intexine thin, laevigate or finely granulate. Exine layers show narrow (1—2 μ m) separation equatorially. Exoexine has a narrow cingulum, 2—3 μ m wide, of finely interwoven structural elements. Distal surface densely ornamented with fine spinae or grana (individual elements <1 μ m high).

Dimensions (18 specimens). Equatorial diameter 51 (66) 77 μ m; intexine diameter 37 (46) 64 μ m.

Remarks. To the authors' knowledge, this is the first record of the genus from the Australian Late Carboniferous. The form is separable from the similar *Densoisporites solidus* Segroves 1970 by its consistently larger size, thinner exine and narrower cingulum. Insufficient well-preserved specimens were found to delineate it as a new species.

Range. Oppel-zone A to Oppel-zone E.

Suprasubturma **Pseudosaccitriletes** Richardson 1965

Infraturma **Monopseudosacciti** Smith & Butterworth 1967

Genus *Spelaeotriletes* Neves & Owens 1966

Type species, by original designation: *Spelaeotriletes triangulus* Neves & Owens 1966; England, Late Carboniferous.

Remarks. For a discussion of this genus see Playford & Powis (1979).

Spelaeotriletes queenslandensis sp. nov.

Fig. 10 W, X; Fig. 11 N—V

Description. Spores radial, trilete, cavate. Amb irregular, sub-circular to oval, occasionally sub-rectangular. Laesurae long, distinct to obscure, usually extending to periphery, often with labra 1—2 μ m wide, <1 μ m high. Intexine ~1.5 μ m thick, indistinct to perceptible, laevigate, outline usually conformable to margin, degree of separation from exoexine variable, attached to proximal exoexine. Exoexine 1—2 μ m thick, proximally laevigate to micropunctate except for equatorial—radial encroachment of apiculate sculptural elements. Distally sculptured by predominantly discrete (occasionally fused at base) evenly spaced spinae, 1—2 μ m high, with circular bases ~0.5 μ m broad, 0.5—3 μ m apart. Contact areas lack ornamentation. Exoexine often with compressional folds.

Dimensions (29 specimens). Equatorial diameter 54 (76) 90 μ m.

Type material Holotype MFP 6849/5; 33.0, 100.0; CPC25836; Fig. 11 U,V.

Type locality. Galilee Basin, Jericho Formation, Late Carboniferous, GSQ Jericho 2, 705 m.

Derivation of name. From Queensland, where the species was first identified.

Holotype. Distal aspect. Amb sub-circular, equatorial diameter 77 μ m, trilete mark indistinct, laesurae with irregular labra, ~2 μ m wide, unequal, extending to equator. Intexine distinct, dark, laevigate ~1.5 μ m thick, outline generally conformable to margin. Exoexine (2 μ m thick) distally sculptured with predominantly discrete spinae which may occasionally be fused at their bases, 1—1.5 μ m tall, with circular basal outlines 0.5 μ m broad, 0.5—2.5 μ m apart. Proximal surface laevigate. Ratio of exoexine to intexine 1:1.4.

Remarks. *Spelaeotriletes queenslandensis* differs from *S. ybertii* (Marques-Toigo) Playford & Powis 1979 by being smaller and having smaller, distinct, and constantly spinose sculptural elements rather than bacula and coni. The Brazilian species *Spelaeotriletes dulcis* (Bharadwaj, Kar & Navale) Playford & Powis 1979 differs in having grana and coni as sculptural elements. *S. vibrissus* Playford & Satterthwait 1988, from the Namurian of the Bonaparte Basin, is much larger than *S. queenslandensis* and is differentiated by being densely sculptured with bacula, coni, grana and verrucae.

Two rare morphotypes close to but not strictly conformable with *S. queenslandensis* were observed. In one (Fig. 11 Q), the exoexine is thinner than average, and more distinctly separated from the intexine than in most specimens of *S. queenslandensis*. This form, which occurs high within Oppel-zone D, is provisionally included within the species. The other form (Fig. 10 U, V) has a thinner exoexine, and bears grana on its proximal face. It is for the present considered as *Spelaeotriletes* sp. cf. *S. queenslandensis*.

Range. Oppel-zone A to Oppel-zone D.

Genus *Rugospora* (Neves & Owens 1966) emend. Turnau 1978

Type species, by original description: *Rugospora corporata* Neves & Owens, 1966 Pennines, England, Namurian.

Rugospora australiensis Playford & Helby 1968 comb. nov.

Fig. 10 O—T

1968 *Wilsonites australiensis* Playford & Helby, pp. 114—115, pl. 11,

Figure 14. Spore species from Galilee Basin assemblages.
Magnification X~650. **A—F,** *Cristatisporites* sp. cf. *C. kuttungensis* (Playford & Helby) comb. nov. A, B, CPC25867, distal and median foci, MFP 6881/9; 109.0, 42.1. C, D, CPC25868, median and distal focus, MFP 6869/4; 111.0, 39.8. E, F, CPC25869, proximal and distal foci, MFP 3585/4; 97.4, 29.3. **G—L,** *Cristatisporites pseudozonatus* Lele & Makada 1972 G—I, CPC25870, distal, median and proximal foci, MFP 6816/A1; 93.2, 31.0. J, K, CPC25871, proximal and distal foci, MFP 6869/2; 102.8, 41.3. L, CPC25872, proximal focus, MFP 6869/2; 104.0, 40.5.

figs 15—19
1984 '*Wilsonites*' *australiensis* Playford & Helby; Powis, pl. 1, fig. 10 (no description)

Dimensions (21 specimens). Equatorial diameter 45 (60) 79 μ m.

Remarks. The specimens recovered in this study from the Galilee Basin appear identical with *Wilsonites australiensis* Playford & Helby 1968, described from the Italia Road Formation in New South Wales. Scanning electron microscopy (Fig. 10 O—Q) shows the exoexine to be intensely folded, with scattered grana on the folded surface. The granulations are clearly discernible with a light microscope, and were noted by Playford & Helby (1968).

Assignment of this Australian species to *Wilsonites* is inappropriate, as that genus was instituted for morphotypes which clearly have an endoreticulum (see Kosanke, 1950, 1959). In their original description of *W. australiensis*, Playford & Helby (1968) described the specimens from the Italia Road Formation as 'intrareticulate'; our examination of specimens from the type sample suggests that the appearance of an infrareticulum results from dense folding of the thin exoexine. Similar miospores with a perine layer have been included within the genus *Perotrilites* (Erdtmann 1947 ex Couper 1953), but Evans (1970) re-examined the type species *P. granulatus* Couper 1953 and emended the generic definition to include zonate forms. Evans (1970) also emended the definition of *Diaphanospora* Balme & Hassell 1962 to include forms with both proximal and equatorial areas of thicker zones of spongy exoexine. Clearly the forms ascribed to *W. australiensis* do not fall within these generic definitions. The description of *Velamisporites* given by Bharadwaj & Venkatachala (1962) suggests that this genus is morphologically closer to the Australian taxon, but it is described as having a distinct trilete mark and thick layer of exine. Our specimens lack these characteristics. The genus *Rugospora* was erected by Neves & Owens (1966) to include camerate miospores with an indistinct intexinal body, and thin exoexine which is folded and sculptured with small verrucae. Turnau (1978) emended this diagnosis so that species with laevigate exoexine are included. The taxa we have described fall within the original and emended diagnoses of *Rugospora*.

Previous records. Hunter Valley, New South Wales, Italia Road Formation, Late Carboniferous (Playford & Helby, 1968), Canning Basin, *D. birkheadensis* Assemblage (Powis, 1984).

Range. Oppel-zone A to Oppel-zone E.

Genus *Auroraspora* Hoffmeister, Staplin & Malloy 1955

Type species, by original designation: *Auroraspora solisortus* Hoffmeister, Staplin & Malloy 1955; Kentucky, U.S.A., Early Carboniferous (Mississippian).

Discussion. Distinction between the genera *Auroraspora*, *Diaphanospora* Balme & Hassell 1962, and *Hymenospora* Neves 1961 is not clear. Balme & Hassell (1962) distinguished *Auroraspora* from *Diaphanospora* on the grounds that the outer layer of the exine in the former was less randomly crumpled than in the latter; Neves (1961) characterised *Hymenospora* as having the two exine layers in contact along the compressional furrows of the exoexine. The foregoing distinctions are difficult to apply in practice. In all definitions the external exoexine is described as either punctate or smooth.

Specimens identified in this study are assigned to *Auroraspora*, but with reservations arising from the poorly defined limits of related genera. Specimens referred to *Auroraspora* sp. in particular are assigned provisionally; the exoexine in that species is clearly granulate.

Auroraspora solisortus Hoffmeister, Staplin & Malloy, 1955
(not illustrated)

1955 *Auroraspora solisortus* Hoffmeister, Staplin & Malloy, p. 381, pl. 37, fig. 3

Dimensions (8 specimens). Equatorial diameter 68 (74) 71 μ m; intexine diameter 22 (33) 47 μ m.

Previous records. Late Mississippian of U.S.A. (Hoffmeister, Staplin & Malloy, 1955; Felix & Burbridge, 1967); Late Carboniferous of Canada (Barss, 1967); Visean of England (Sullivan, 1964); Early Carboniferous of the Bonaparte Gulf Basin, Australia (Playford, 1971).

Range. Oppel-zone B to Oppel-zone D.

Auroraspora sp.
Fig. 12 S

Remarks. This category includes rare specimens in which the laesurae are distinct, 2/3 spore radius in length, sinuous and with narrow labra. The exoexine is densely crumpled and is sculptured with grana which are 1—1.5 μ m apart. The presence of grana casts some doubt on the validity of assignment to *Auroraspora*.

Dimensions (3 specimens). Equatorial diameter 49—52 μ m; intexine diameter 42—48 μ m.

Occurrence. GSQ Springsure 13, 289.46 m, Biozone B.

Turma **Hilates** Dettmann, 1963

Genus *Psomospora* Playford & Helby 1968

Type species, by original designation: *Psomospora detecta* Playford & Helby 1968; Italia Road Formation, New South Wales, Late Carboniferous.

Psomospora detecta Playford & Helby 1968
Fig. 12 O, Q, R

1968 *Psomospora detecta* Playford & Helby, pp. 113—114; pl. II, figs 8—14, text-figs 3a—d

Dimensions (33 specimens). Equatorial diameter 26 (40) 52 μ m. Diameter of proximal hilate region 14 (19) 23 μ m.

Remarks. The Galilee Basin specimens recorded here show a differential staining (?exine thickening) at the margin of the proximal hilum. Fine radial plications are common on the proximal face, either confined to the hilate area or extending on to the contact faces beyond it. Both of these features are apparent, although not pronounced, in the material originally described from the Hunter Valley by Playford & Helby (1968).

Previous records. Late Carboniferous of the Hunter Valley, New South Wales (Playford & Helby, 1968); Argentina (Azcuy, 1975); Canning Basin, Western Australia (Powis, 1979).

Range. Oppel-zone B to Oppel-zone E.

Pollenites

Anteturma **Variegerminantes** Potonié 1970

Turma **Saccites** Erdtman 1947

Subturma **Monosaccites** Chitaley emend. Potonié & Kremp 1954

Infraturma **Vesiculomonoradites** Pant 1954

Genus *Potonieisporites* Bhardwaj 1954

Type species, by original designation: *Potonieisporites novicus* Bhardwaj 1954; Saar Basin, West Germany, Late Carboniferous.

Potonieisporites novicus Bhardwaj 1954
Fig. 15 N

1954 *Potonieisporites novicus* Bhardwaj, p. 521; text-fig. 10
1955 *Potonieisporites novicus* Bhardwaj, pl. 2, figs 13, 14 (no description)

1970 *Potonieisporites novicus* Bhardwaj *in* Balme, p. 358, pl. 9, figs 1, 2
1977 *Potonieisporites* sp. Kemp & others, fig. 9 Z (no description)

Dimensions (20 specimens). Total breadth 124 (160) 180 μ m. Corpus breadth 47 (76) 93 μ m. Corpus length 56 (67) 78 μ m. Saccus offlap 37 (56) 76 μ m.

Remarks. Balme (1970) discussed the difficulty of separating the published species of *Potonieisporites*, which is exacerbated by inadequate illustration of the type species, *P. novicus*. Potonié & Lele (1961) reported difficulty in separating *P. novicus* from *P. neglectus* Potonié & Lele 1961, and concluded that only the rounded polygonal corpus in *P. neglectus* differentiated it from *P. novicus*. The Galilee Basin species are provisionally assigned to *P. novicus*; they vary, especially in corpus shape and the position of intexinal folds. There is usually a circumpolar fold about the periphery of the corpus, but other folds parallel to the corpus length are less consistently present. Many specimens are poorly preserved; they often lack a corpus, which appears to weather out of the saccus.

Previous records. Early to Late Permian of Australia (Kemp & others, 1977); Africa (e.g. Jardiné, 1974); India and Pakistan (e.g. Maheshwari, 1967, Balme, 1970); Brazil (Pons, 1976); Late Carboniferous of Australia (Powis, 1979) and Western Europe (Bharadwaj, 1964).

Range. Oppel-zone A to Oppel-zone D.

Potonieisporites elongatus comb. nov. & nom. nov.
Fig. 15 O

1964 *Vestigisporites densus* Singh, p. 256, pl. 46, figs 2, 3
1964b *Vestigisporites* sp. Evans p. 19, pl. 9, fig. 61

Remarks. *Potonieisporites* Bhardwaj 1954 appears to be more appropriate for the species assigned by Singh (1964) to *Vestigisporites* Balme & Hennelly 1955. In *Vestigisporites*, as typified by its type species, *V. rudis* Balme & Hennelly 1955 (see also the diagnosis by Jansonius & Hills, 1976), the construction is essentially disaccate, with sacci sometimes linked in the equatorial, lateral areas, adjacent to the corpus, by a narrow ribbon of exoexine. *Potonieisporites*, by contrast, encompasses forms which are clearly monosaccate, although bilaterally symmetrical.

Transfer of Singh's species *V. densus* to *Potonieisporites* creates a nomenclatural problem in that *Potonieisporites densus* Singh 1964 becomes a junior homonym of *Potonieisporites densus* Maheshwari 1967. A new name is therefore required.

Derivation of name. Latin *elongatus* prolonged, referring to the transversely elongate form of the saccus.

Description. Monosaccate pollen, monolete, amb transversely oval to sub-rectangular, bilaterally symmetrical. Distinct monolete or occasionally dilete tetrad scar on proximal surface. Corpus sub-circular to circular, dark, intexine thick (3—4 μ m), smooth or punctate. Saccus transversely elongate, attached proximo-equatorially, detached distally; saccus densely endoreticulate with brochi radially arranged (4—11 μ m long), intexinal folds commonly developed at base of saccus roots.

Dimensions (15 specimens). Total breadth 106 (134) 168 μ m. Corpus breadth 46 (60) 77 μ m. Corpus length 39 (48) 63 μ m. Saccus offlap 46 (48) 71 μ m.

Comparisons. *P. elongatus* is differentiated from other species in the genus by its small, dark, circular corpus and transversely elongate saccus. The illustrations of *P. elongatus* (as *V. densus*) given by Singh (1964) from the Chia Zairi Formation of Iraq lack definition, especially in regard to the corpus, so it is not possible to discern whether the intexinal folding frequently visible in the Australian taxon is present.

The Australian monosaccate form shows many similar features to forms assigned to *Striomonosaccites*, such as size range, bilateral symmetry, the form of the saccus, with a slight lateral constriction, and a small dark, circular corpus with intexinal folds developed at the saccus roots. This similarity suggests a morphological gradation from *Striomonosaccites* to *P. elongatus*, but we continue to use the presence of taeniae (Hart, 1965) for generic segregation.

Previous records. Iraq, Late Permian (Singh, 1964); Australia, Finke area, Northern Territory, Early Permian (Evans, 1964b); Canning Basin, Western Australia, Late Carboniferous to Early Permian (Powis, 1979).

Range. Oppel-zone B to Oppel-zone E.

Infraturma **Triletesacciti** Leschik 1955

Genus ***Cannanoropollis*** Potonié & Sah 1960

Type species, by original designation: *Cannanoropollis janakii* Potonié & Sah, 1960; Cannanore Beach, India, Tertiary.

Cannanoropollis janakii Potonié & Sah 1960
Fig. 15 M

For synonymy see Foster, 1979.

Dimensions (20 specimens). Total diameter 104 (136) 150 μ m. Corpus diameter 68 (97) 113 μ m. Maximum width of saccus 18 (27) 50 μ m.

Remarks. In features such as the length of laesurae, the saccus overlap, and lack of any infold, the Galilee specimens conform well with the definition of *C. janakii*.

Previous records. Widespread throughout Gondwana. *C. janakii* has been noted in Australia from the Permian of the Blair Athol and Baralaba Coal Measures of Queensland (Foster, 1979) and from the Fossil Cliff Formation of the Perth Basin (Foster & others, 1985). Powis (1979) noted this taxon from the Late Carboniferous of the Canning Basin. Indian occurrences were listed by Foster (1979). In South Africa similar specimens were included (in part) by Anderson (1977) in *Vestigisporites gondwanensis* (Balme & Hennelly).

Range. Oppel-zone A to Oppel-zone E.

Genus ***Plicatipollenites*** Lele 1964

Type species. (Potonié & Sah) Foster 1975; Talchir Formation, India, Early Permian.

Discussion. Balme (1970, p. 355) discussed the validity of this genus, deciding to use *Plicatipollenites* for radially symmetrical, trilete, monosaccate forms with a prominent intexinal infold system.

Foster (1979, pp. 68—69) supported the utilisation of this genus from Transmission Electron Microscope (TEM) studies of monosaccate pollen. The studies showed that all specimens sectioned which possessed an intexinal infold system also had a correspondingly thick intexine.

Plicatipollenites densus Srivastava 1970
Fig. 15 H, J

1970 *Plicatipollenites densus* Srivastava, pp. 159—169; pl. 1, figs 7, 8
For more extensive synonymy see Foster (1979, p. 68).

Dimensions (15 specimens). Total diameter 57 (83) 92 μ m. Corpus diameter 30 (54) 71 μ m. Maximum width of saccus 18 (22) 36 μ m.

Remarks. *Plicatipollenites densus* Srivastava 1970 may be distinguished from *P. gondwanensis* (Balme & Hennelly) Lele 1964 by its

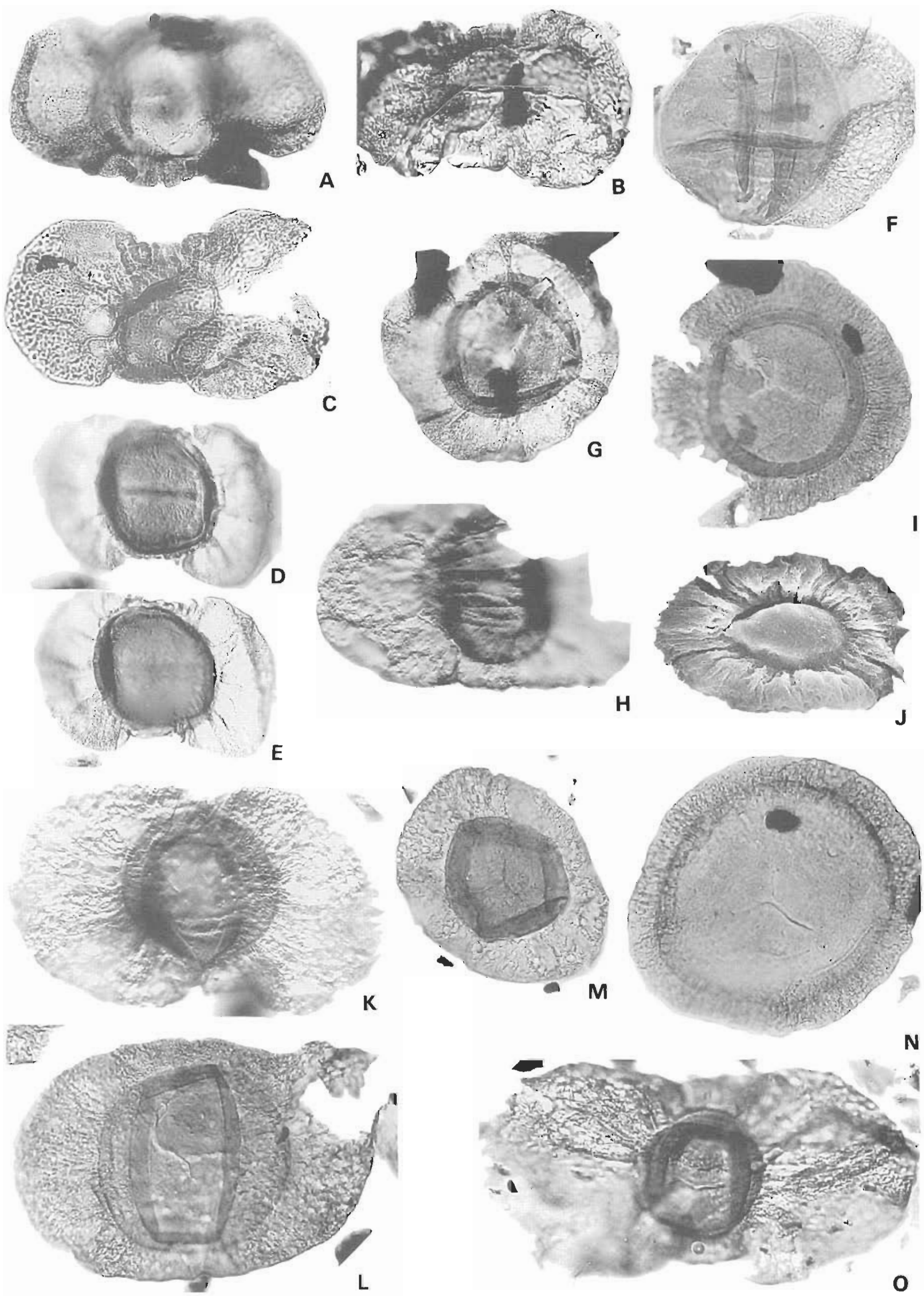
A
B
F
C
G
I
D
H
J
E
K
M
N
L
O

single annular intexinal fold, and from *P. malabarensis* (Potonié & Sah) Foster 1975 by its consistently smaller size, and greater width of saccus relative to overall diameter. Scanning electron microscopy (Fig. 15 J) shows that the annular infold has a surface expression, and strongly constricts the saccus at its inner margin. Externally, the saccus is strongly radially pleated.

Previous records. Recorded from Early Permian sediments in Africa and India. In Australia, Foster (1979) reported *P. densus* from the Permian Blair Athol Coal Measures and Powis (1979) reported it from the Late Carboniferous Grant Group.

Range. Oppel-zone A to Oppel-zone E.

Plicatipollenites gondwanensis (Balme & Hennelly) Lele 1964
Fig. 15 G, L

1956 *Nuskoisporites gondwanensis* Balme & Hennelly, p. 253; pl. 7, figs 66—67
1964 *Plicatipollenites gondwanensis* (Balme & Hennelly) Lele, pp. 154—156; pl. 2, fig. 11; text-figs 4 1—c, 12b
1969 *Parasaccites gondwanensis* (Balme & Hennelly) Segroves, pp. 183—184; pl. 2, fig. B
non 1977 *Vestigisporites gondwanensis* (Balme & Hennelly) Anderson, p. 99, pl. 107—112

For additional synonymy see Lele (1964, pp. 155—156).

Dimensions (4 specimens). Total diameter 97 (186) 199 μ m. Corpus diameter 64 (102) 36 μ m. Maximum width of saccus 20 (37) 53 μ m.

Remarks. The distinctive polygonal infold system of *Plicatipollenites gondwanensis* differentiates it from other forms in this genus. Powis (pers. comm., 1984) suggested that the polygonal form of the annulate fold around the corpus does not constitute a criterion for specific segregation, as this may be a chance compressional artifact. Foster (pers. comm., 1984), suggested that the polygonal infolding results from compression of a highly convex distal face, reflecting a specific feature, and justifying the specific segregation.

In one specimen (Fig. 15 G) the infold system is transitional between the neat circular infold of *P. densus* and the polygonal folds of *P. gondwanensis*. We have included the form in *P. gondwanensis*, although this may extend the species beyonds its original concept.

Previous records. Permian of all Gondwanan continents (see Foster, 1979).

Range. Oppel-zone C to Oppel-zone D.

Infraturma **Caheniasacciti** Bose & Kar 1966

Genus ***Caheniasaccites*** Bose & Kar 1966

Type species, by original designation: *Caheniasaccites flavatus* Bose & Kar 1966; Zaire, Africa; Early Permian.

Caheniasaccites elephas sp. nov.
Fig. 15 A—C

Description. Monosaccate pollen, 'pseudo-diploxylonoid', amb frequently dumbbell shaped. Corpus distinct to perceptible, outline circular to sub-circular, cappa and cappula equal-sized, square to subrectangular in form, approximately 2/3 of corpus diameter, micropunctate or finely endoreticulate. Compressional intexine folds usually developed at saccus roots parallel to corpus length. Intexine ~1 μ m thick. Saccus expanded into two lobes connected laterally by contracted exoexine, lobes 8—10 μ m broad with fluted margins, up to 8 indentations of lateral saccus present. Lateral 'flutes' of sacci with dense endostructure, brochi of internal reticulum showing radial alignment, to 4.0 μ m broad. Sacci lobes occasionally distally inclined, often with an angular margin, saccus breadth greater than corpus. Monolete scar discernible to imperceptible, often associated with a fold parallel to the corpus breadth. Thinned, subrectangular region on distal face of corpus between sacci roots may represent a tenuitas.

Dimensions (18 specimens). Total breadth 110 (144) 167 μ m. Corpus breadth 47 (58) 78 μ m. Corpus length 47 (62) 86 μ m. Saccus offlap 34 (53) 84 μ m.

Type specimen. Holotype MFP 6869/2; 109.7, 33.9; CPC25873; Fig. 15 A.

Type locality. Galilee Basin, Jericho Formation, Late Carboniferous; GSQ Springsure 13, 289.46 m.

Derivation of name. Latin *elephas* elephant, referring to the resemblance of these grains to a frontal view of an elephant's head.

Holotype. Distal aspect. Pollen grain disaccate with undulating margin, especially adjacent to corpus; total breadth 112 μ m, corpus breadth 53 μ m, corpus length 50 μ m, sacci length 50 and 54 μ m, sacci offlap 36 μ m. Corpus distinct, endoreticulate, cappula thinned, except adjacent to the monolete mark, intexinal folds developed at sacci roots, parallel to corpus length. Distal face of corpus thinned, may represent a subrectangular tenuitas. Sacci endoreticulate, brochi to 4 μ m broad. Sacci form angular lobes with diameter roughly equal to corpus breadth, connected equatorially to form fluted margin adjacent to the corpus, with 6—8 lobes 7—10 μ m broad; endoreticulum within lobes very dense, with some radial alignment. Monolete scar gaping, about 1/2 corpus breadth.

Remarks. The 'pseudodiploxylonoid' form and the fluted folding of the saccus to form a frill in the equatorial region are characteristic of *Caheniasaccites*, as shown in the type species, *C. flavatus* Bose & Kar 1966. The presence of a monolete mark (not mentioned in the description of *C. flavatus*) suggests proximal germination; a distal tenuitas, in the form of a rectangular thinning of the distal face, suggests germination may also have occurred at that site. Foster (1983) noted several Carboniferous to Triassic protodisaccate and disaccate genera from Euro-american with two possible germinal areas. He also remarked that the protomonosaccate *Barakarites rotatus* Bharadwaj & Salujha 1964, from the Gondwanan Permian, has similar di-germinal features. The present record of *C. elephas* from the Late Carboniferous of Australia is, to the authors' knowledge, the oldest noted occurrence of possibly di-germinal pollen from Gondwana.

Caheniasaccites flavatus Bose & Kar 1966, (p. 85) differs from *C. elephas* by having an oval corpus and oval to elliptical amb. *C. elongatus* Bose & Kar 1966 (p. 86) is generally smaller, has a distinctly rectangular cappa, and an un-frilled lateral saccus. *C. ovatus* Bose & Kar 1966 (p. 87) has an oval to sub-rectangular amb, is slightly smaller and lacks the distinctively broad saccus lobes of *C. elephas*. *C. indicus* Srivastava 1970 (p. 162) was differentiated from *C. ovatus* by being larger, having weakly developed undulations in the zone of saccus attachment, and a diffused zone of saccus attachment. Photomicrographs (Srivastava, 1970, plate 2, figs 16, 17) of *C. indicus* are indistinguishable from those of the holotype and isotype of *C. ovatus*, suggesting that *C. indicus* is a junior synonym of *C. ovatus*. *C. elephas* is distinguishable from other forms of this genus by its distinctive 'elephant-head' form. The specimen referred by Foster & others

Figure 15. Pollen species from Galilee Basin assemblages.
Magnification X~650. **A—C,** *Caheniasaccites elephas* sp. nov. CPC25873, holotype, proximal focus, MFP 6869/2; 109.7, 33.9. B, CPC25874, composite photograph, MFP 6881/6; 100.2, 42.9. C, CPC25875, MFP 6856/6; 94.3, 44.5. **D, E,** *Caheniasaccites* sp., CPC25876, proximal and median foci, MFP 6760/A2; 107.3, 45.0. **F,** *Protohaploxypinus* sp. cf. *P. goraiensis* (Potonié & Lele) Hart 1964 CPC25877, specimen with one saccus missing, MFP 6871/7; 92.5, 35.7. **G, L,** *Plicatipollenites gondwanensis* (Balme & Hennelly) Lele 1964. G, CPC25878, morphotype with an infold system transitional between *P. gondwanensis* and *P. densus*, MFP 99.3, 38.0. L, CPC25879, MFP 6820/6; 108.6, 29.9. **H, J,** *Plicatipollenites densus* Srivastava 1970. H, CPC25880, MFP 6871/7; 105.2, 45.7. J, scanning electron micrograph showing surface expression of infold system, MFP 6820. **I, K,** *Striomonosaccites* sp. I, CPC25881, proximal focus, MFP 6856/9; 109.2, 32.5. K, CPC25882, median focus, MFP6849/5; 106.0, 30.7. **M,** *Cannanoropollis janakii* Potonié & Sah 1960, CPC25883, MFP 6871/9; 95.5, 34.5. **N,** *Potonieisporites novicus* Bharadwaj 1964, CPC25884, MFP 6871/7; 106.1, 31.4. **O,** *Potonieisporites elongatus* comb. nov., nom. nov., CPC25885, MFP 6849/3; 104.3, 35.0.

(1985) to *Caheniasaccites*, from the Fossil Cliff Formation, Western Australia, has thinner sacci and a more elongate form than *C. elephas*.

Range. Oppel-zone B to Oppel-zone D.

Caheniasaccites sp.
Fig. 15 D, E

Dimensions (1 specimen). Total breadth 101 μ m. Corpus breadth 52 μ m. Saccus length 72 μ m. Corpus length 54 μ m. Saccus offlap 28 μ m.

Remarks. The single specimen here assigned to *Caheniasaccites* appears distinct from *C. elephas*. It is exceptionally well preserved, but the differences between it and *C. elephas* do not appear to be solely a result of preservation. This specimen has a dense corpus, with a cappa in which the exoexine surface is thrown into closely spaced verrucae. The monolete scar is distinct, somewhat depressed, and surrounded by a smooth area of ?exoexine. The distal face bears a thinned, approximately rectangular tenuitas. The exoexine of the sacci is thinner than that in *C. elephas*, and the brochi of the saccus endoreticulum is more dense.

The smooth area surrounding the monolete scar suggests an exoexinal operculum detachment. With the presence of a distal tenuitas, or rectangular area of exoexinal thinning, it suggests that this pollen was di-germinal.

Occurrence. GSQ Jericho 1, 529.76 m, Jochmus Formation, Biozone D.

Infraturma **Striasacciti** Bharadwaj 1962

Genus ***Striomonosaccites*** Bharadwaj 1962

Type species, by original designation: *Striomonosaccites ovatus* Bharadwaj 1962; India, Late Permian.

'Striomonosaccites' sp.
Fig. 15 I, K

Description. Monosaccate pollen grains, bilaterally symmetrical, taeniate, monolete. Amb sub-rectangular to oval to dumbbell shaped, margin slightly undulating from folding of saccus. Corpus distinct, dark, outline circular to subcircular; two compressional folds to 9 μ m broad developed at saccus roots; oval to subrectangular cappa and cappula both approximately same size; intexine 1—2 μ m thick, generally laevigate, occasionally endovermiculate to endopunctate. Two to 12 transverse taeniae on proximal surface, 2—9 μ m broad, taeniae edges often indented, clefts ~1 μ m wide, convoluted to straight, continuous to discontinuous across cappa, often forming wedges extending to infolded bands. In some specimens there is a suggestion of a monolete mark. Saccus may be either laterally pinched-in giving a dumbbell shaped amb, or slightly pinched-in giving only a slight lateral fluting of saccus (~5.0 μ m broad) resulting in a subrectangular to oval amb. Saccus equatorially attached, occasionally distally expanded to giving a 'pseudo-diploxylonoid' appearance, densely endoreticulate with radially orientated brochi. In forms with more pronounced lateral saccus pinching, the saccus lobes are distally inclined.

Dimensions (7 specimens). Total breadth 109 (148) 186 μ m. Corpus breadth 50 (64) 84 μ m. Corpus length 50 (60) 89 μ m. Saccus offlap 50 (57) 74 μ m.

Remarks. *Striatolebachiites* Varyukhina & Zauer 1971 (*in* Varyukhina, 1971), has a much larger, more constantly taeniate, and thicker walled corpus than these forms. Jansonius & Hills (1976) concluded that the genus is invalid because its type species has not been described. *Wapellites* Ravn 1979 (p. 51) from the Pennsylvanian of Iowa tends to have a more laterally constricted saccus and an alete corpus lacking taeniae. *Caheniasaccites* Bose & Kar 1966 (p. 95) is very similar to some of these forms, but lacks taeniae. *Vestigisporites* (Balme & Hennelly) Hart 1963 and *Potonieisporites* Bhardwaj 1954 are also similar to some of these forms but again lack taeniae. The Permian *Striomonosaccites* Bharadwaj 1962 includes 'monosaccate pollen grains of subcircular to circular overall shape' (Bharadwaj, 1962, p. 87). This excludes bilaterally symmetrical grains such as these but, as few specimens were found, erection of a new genus to accommodate them is not justifed. Until there is sufficient material for revision, they are retained in *Striomonosaccites*.

Range. Oppel-zone B to Oppel-zone C.

Subturma **Disaccites** Cookson 1947

Infraturma **Striatiti** Pant 1954

Genus ***Protohaploxypinus*** Samoilovich emend. Morbey 1975

Type species, by original designation: *Protohaploxypinus latissimus* (Luber) Samoilovitch 1953; Western Cis-Urals, USSR, Permian.

Discussion. Foster (1979) succinctly outlined the emendations of *Protohaploxypinus* proposed by Hart (1964) and Morbey (1975) and we accept Morbey's emendation. Foster (1979) has provided a comprehensive synonymy for the genus.

Protohaploxypinus sp. cf. ***P. goraiensis*** (Potonié & Lele) Hart 1964
Fig. 15 F

Discussion. Specimens haploxylonoid or slightly diploxylonoid. Corpus is distinct, slightly oval in a longitudinal sense, proximal face bearing 10 to 15 taeniae 2—8 μ m wide, narrower taeniae frequently wedge out across corpus. A fine endoreticulum is present in the taeniae, discernible mainly in broken sections. Folding of the corpus, in a direction parallel to the saccus roots, is a common feature. Sacci semicircular in outline, distally inclined, may be linked by a narrow band of exoexine at lateral margins of corpus. Endoreticulum of sacci consists of brochi 2—4 μ m in diameter.

Dimensions (6 specimens). Total breadth 109 (150) 180 μ m. Corpus breadth 50 (82) 88 μ m. Corpus length 93 (103) 112 μ m. Saccus offlap 27 (45) 68 μ m.

Remarks. The Galilee Basin species differs from *P. goraiensis*, described originally by Potonié & Lele (1961) from probably coeval strata in the Talchir Stage of India, in having a much more distinct corpus and generally narrower taeniae. The sacci are narrower than those in *P. amplus* (Balme & Hennelly) Hart 1964.

Previous records. Similar specimens, referred to *P. goraiensis*, have been reported from the Permian of India and West Pakistan (Bharadwaj & Salujha, 1964; Balme 1970), Africa (Kar & Bose, 1967), Antarctica (Balme & Playford, 1967), and from the Crown Point Formation, Finke Area, Northern Territory (Evans, 1964b), and the Carboniferous—Permian of the Canning Basin (Powis, 1979).

Range. Oppel-zone C to Oppel-zone E.

Algae

Turma **Aletes** Ibrahim 1933

Subturma **Azonaletes** Luber emend. Potonié & Kremp 1954

Infraturma **Reticulonapiti** Erdtman ex. Vimal 1952

Genus ***Maculatasporites*** Tiwari 1964

Type species, by original designation: *Maculatasporites indicus* Tiwari, 1964; India, Early Permian.

Maculatasporites minimus Segroves 1967
Fig. 12 P, T

1967 *Maculatasporites minimus* Segroves p. 298, 300; pl. 3, figs 11—14

Dimensions (2 specimens): Equatorial diameter 26 (28) 30 µ m.

Previous records. This acritarch, probably a non-marine algal cyst (Tappan,1980), was found only within Biozone E. It has been identified from the Early Permian of Western Australia in the Perth, Collie, and Canning Basins (Segroves, 1967; Glikson, 1972; Powis, 1979) and from Africa and Madagascar (Bose & Maheshwari, 1968; Rakotoarivelo, 1970; Anderson, 1977). It is widespread throughout the Permian Cooper Basin and Denison Trough.

Range. Oppel-zone E.

Incertae sedis

Genus *Quadrisporites* Hennelly ex Potonié & Lele 1961

Type species, by subsequent designation (Potonié & Lele, 1961, p. 25): *Quadrisporites horridus* Hennelly ex. Potonié & Lele 1961; New South Wales, Permian.

Quadrisporites horridus Hennelly ex. Potonié & Lele 1961
(not illustrated)

Dimensions (1 specimen). Tetrad diameter 56 µ m; mean equatorial diameter of members 25 µ m.

Previous records. Permian of Australia, Africa, India and South America (see Foster, 1979).

Range. Oppel-zone C to Oppel-zone D.

References

Allen, R.J., 1974 — Hydrocarbon significance of Upper Palaeozoic sediments associated with the Koburra Trough, Galilee Basin. *The APEA Journal*, 14, 59—65.

Anderson, J.M., 1977 — The biostratigraphy of the Permian and Triassic. Part 3. A review of Gondwana Permian palynology with particular reference to the northern Karoo Basin, South Africa. *Memoirs of the Botanical Survey of South Africa*, 41.

Archangelsky, S. & Gamerro, J.C., 1979 — Palinologia del Paleozoico Superior en el Subsuelo de la Cuenca Chacoparanense, República Argentina. I. Estudio sistemático de los palinomorfos de tres perforaciones de la Provincia de Cordoba. *Revista Española de Micropaleontologia*, XI(3), 417—478.

Archbold, N.W., 1982 — Correlation of the Early Permian faunas of Gondwana; implications for the Gondwanan Carboniferous—Permian Boundary. *Journal of the Geological Society of Australia* 29(3), 267—275.

Archbold, N.W. & Dickins, J.M., 1991 — Australian Phanerozoic timescales - 6 Permian. A standard for the Permian System in Australia. *Bureau of Mineral Resources, Geology and Geophysics, Australia, Record* 1989/36.

Azcuy, C.L., 1975 — Miosporas del Namuriano y Westfalano de la comarca Malanzán - Loma Larga, Provincia de la Rioja, Argentina II. Descripciones sistematicás y significado estratigráfico de las microfloras. *Ameghiniana*, 12(2), 113—163.

Azcuy, C.L., 1979 — A review of the early Gondwana palynology of Argentina and South America. *IV International Palynological Conference, Lucknow (1976-77), Proceedings*, 2, 175—185.

Azcuy, C.L. & Jelin, R., 1980 — Los palynozonas del limite Carbónico-Pérmico en la Cuenca Paganzo. *Actas II Congres Argentino de Paleontologia y Biostratigrafia y I Congreso Latinoamericano de Paleontologia. Buenos Aires 1978, IV*, 51—67.

Backhouse, J., 1988 — Permian trilete spores from the Collie Basin, Western Australia. *In* Jell, P.A. & Playford, G. (editors), Palynological and palaeobotanical studies in honour of Basil E. Balme. *Association of Australasian Palaeontologists, Memoir* 5, 41—52.

Balme, B.E., 1964 — The palynological record of Australian pre-Tertiary floras. *In* Cranwell, L.M. (editor), Ancient Pacific floras. *University of Hawaii Press*, 49—80.

Balme, B.E., 1970 — Palynology of Permian and Triassic strata in the Salt Range and Surghar Range, West Pakistan. *In* Kummel, B. & Teichert, C. (editors), Stratigraphic boundary problems: Permian and Triassic of West Pakistan. *University of Kansas Press, U.S.A.*, 306—453.

Balme, B.E., 1980 — Palynology and the Carboniferous—Permian boundary in Australia and other Gondwana continents. *Palynology*, 4, 43—56.

Balme, B.E. & Hassell, C.W., 1962 — Upper Devonian spores from the Canning Basin, Western Australia. *Micropalaeontology*, 8, 1—28.

Balme, B.E. & Hennelly, J.P.F., 1956 — Trilete sporomorphs from Australian Permian sediments. Australian Journal of *Botany*, 4, 240—260.

Balme, B.E. & Playford, G., 1967 — Late Permian plant microfossils from the Prince Charles Mountains, Antarctica. *Revue de Micropalaéontologie*, 10, 179—192.

Barss, M.S., 1967 — Illustrations of Canadian fossils. Carboniferous and Permian spores of Canada. *Geological Survey of Canada, Paper*, 67(11), 1—94.

Benstead, W.L., 1973 — Galilee Basin. *Geological Survey of Queensland, Record* 1973/20 (unpublished).

Besems, R.E. & Schuurman, W.M.L., 1987 — Palynostratigraphy of the Late Paleozoic glacial deposits of the Arabian Peninsula with special reference to Oman. *Palynology*, 11, 37—53.

Bharadwaj, D.C., 1962 — The miospore genera in the coals of Raniganj Stage (Upper Permian), India. *Palaeobotanist*, 9(1, 2), 68—106.

Bharadwaj, D.C., 1964 — *Potonieisporites* Bharad., ihre morphologie, systematic und stratigraphie. *Fortschritte in der Geologie von Rheinland und Westfalen*, 12, 45—54.

Bharadwaj, D.C. & Salujha, S.R., 1964 — Sporological study of Seam VIII in Raniganj Coalfield Bihar (India). Part I — Description of Sporae Dispersae. *Palaeobotanist*, 12(2), 181—215.

Bharadwaj, D.C. & Srivastava, S.C., 1969 — Some new miospores from Barakar Stage, Lower Gondwana, India. *Palaeobotanist*, 17(2), 220—229.

Bharadwaj, D.C. & Venkatachala, B.S., 1962 — Spore assemblage out of a Lower Carboniferous shale from Spitzbergen. *Palaeobotanist*, 10, 18—47.

Bhardwaj, D.C., 1954 — Einige neue Sporengattungen des Saarkarbons. *Neues Jahrbuch für Geologie und Paläontologie*, Monatshefte, Stuttgart, 512—525.

Bhardwaj, D.C., 1955 — The spore genera from the Upper Carboniferous coals of the Saar and their value in stratigraphical studies. *Palaeobotanist*, 4, 119—149.

Bose, M.N. & Kar, R.K., 1966 — Palaeozoic sporae dispersae from Congo I — Kindu-Kalimu and Walikale regions. *Musée Royal de l'Afrique, Tervuren Belgique, Serie IN8°, Sciences Géologiques*, 53, 1—168.

Bose, M.N. & Maheshwari, H.K., 1968 — Palaeozoic sporae dispersae from Congo 7 — Coal measures near Lake Tanganyika, south of Albertville. *Musée Royal de l'Afrique, Tervuren Belgique, Serie IN8°, Sciences Géologiques*, 60, 1—116.

Braakman, J.H., Levell, B.K., Martin, J.H., Potter, T.L. & Van Vliet, A., 1982 — Late Palaeozoic Gondwana glaciation in Oman. *Nature*, 299 (5878), 48—50.

Briggs, D., 1985 — Age of the Late Palaeozoic glaciations of central eastern New South Wales. *Advances in the study of the Sydney Basin. Proceedings of the nineteenth symposium. Department of Geology, University of Newcastle*, 98—101.

Calver, C. R., Clarke, M. J. & Truswell, E. M. 1984 — The stratigraphy of a Late Palaeozoic borehole section at Douglas River, eastern Tasmania: a synthesis of marine invertebrate and palynological data. *Papers and Proceedings of the Royal Society of Tasmania*, 118, 137—161.

Chandra, A. & Lele, K.M., 1979 — Talchir microfloras from South Rewa Gondwana Basin, India and their biostratigraphical significance. *Proceedings, Fourth International Palynological Conference. Birbal Sahni Institute of Palaeobotany, Lucknow*, 11, 117—151.

Clayton, G., Coquel, R., Doubinger, J., Gueinn, K.J., Loboziak, S., Owens, B. & Streel, M., 1977 — Carboniferous miospores of western Europe: illustration and zonation. Report of Commission Internationale de Microflore du Paléozoïque working group on the Carboniferous stratigraphical palynology. *Mededelingen Rijks Geologische Dienst*, 29.

Coquel, R., Doubinger, J., & Loboziak, S. 1976 — Les microspores — guides du Westphalien à l'Autunien d' Europe occidentale. *Revue de Micropaléontologie*, 18(4), 200—212.

Coquel, R., Stanislas, L., Owens, B. & Tereriuk,V. K., 1979 — Comparaison entre la distribution des principales microspores — guide du Namurien et du Westphalien en Europe occidentale et dans le bassin du Donetz (URSS). Neuvième Congrès International de Stratigraphie et de Géologie du Carbonifère. Washington and Champaign-Urbana May 17-26, 1979. *Compte Rendu*, 2, 443—446.

Cousminer, H.L., 1965 — Permian spores from Apillapampa Bolivia. *Journal of Paleontology*, 36(6), 1097—1111.

Crowell, J.C. & Frakes, L.A., 1971a — Late Palaeozoic glaciation of Australia. *Journal of the Geological Society of Australia*, 17(2), 115—155.

Crowell, J.C. & Frakes, L.A., 1971b — Late Paleozoic glaciation, Part IV, Australia. *Geological Society of America, Bulletin*, 82(9), 2515—2540.

Dettmann, M.E., 1963 — Upper Mesozoic microfloras from south-eastern Australia. *Proceedings of the Royal Society of Victoria*, 77, 1—148.

Dickins, J.M., 1985 — Late Palaeozoic glaciation. *BMR Journal of Australian Geology & Geophysics*, 9(2), 163—169.

Dickins, J.M., Townsend, R.R. & Crowe, R.W.A., 1978 — A Permian cold water marine fauna in the Grant Formation of the Canning Basin, Western Australia. *Journal of the Palaeontological Society of India*, 20, 275—278.

Duchemin, E.A. & Creevey, K., 1966 — Well completion report, Aquitaine Kulshill No. 1. *Report to Australian Aquitaine Petroleum Pty. Ltd. (unpublished)*.

Engel, B.A., 1985 — Australia: Myall Region. *In* Diaz, C.M. (editor), The Carboniferous of the World. II Australia, Indian subcontinent, South Africa, South America, and North Africa *I.U.G.S.*, 20, 33—38.

Evans, P.R., 1964a — A correlation of some deep wells in the north-eastern Eromanga Basin, central Queensland. *Bureau of Mineral Resources, Australia, Record* 1964/197.

Evans, P.R., 1964b — Lower Permian microfloras from the Crown Point Fm., Finke area, N.T. *Bureau of Mineral Resources, Australia, Record* 1964/197.

Evans, P.R., 1966 — Palynological studies in the Longreach, Jericho, Galilee, Tambo, Eddystone and Taroom 1:250,000 Sheet areas, Queensland. *Bureau of Mineral Resources, Australia, Record* 1966/61.

Evans, P.R., 1967 — Upper Carboniferous and Permian palynological stages and their distribution in eastern Australia. *Bureau of Mineral Resources, Australia, Record* 1967/99.

Evans, P.R., 1969 — Upper Carboniferous and Permian palynological stages and their distribution in Eastern Australia. *In* Gondwana Stratigraphy, *IUGS 1st Gondwana Symposium, Buenos Aires, 1967. UNESCO*, 41—53.

Evans, P.R., 1970 — Revision of the miospore genera *Perotrilites* Erdtm. ex Couper 1953 and *Diaphanospora* Balme and Hassell 1962. *Bureau of Mineral Resources, Australia, Bulletin* 116, 65—74.

Evans, P.R., 1980 — Geology of the Galilee Basin. *In* Henderson, R.A. & Stephenson, P.J. (editors), Geology and geophysics of north-eastern Australia. *Geological Society of Australia, Queensland Division*, 299—305.

Evans, P.R. & Roberts, J., 1978 — Evolution of central eastern Australia during the Late Palaeozoic and Early Mesozoic. Third Australian Geological Convention, Program abstracts. *Geological Society of Australia, Queensland Division*, 43.

Evernden, J.K. & Richards, J.R., 1962 — Potassium—Argon ages in eastern Australia. *Journal of the Geological Society of Australia*, 9(1), 1—49.

Felix, C.J. & Burbridge, P.P., 1967 — Palynology of the Springer Formation of Southern Oklahoma, U.S.A. *Palaeontology*, 10(3), 349—425.

Fenton, M. W. & Jackson, K. S., 1989 — The Drummond Basin: low-cost exploration in a high-risk area. *The APEA Journal*, 29 (1), 220—234.

Foster, C.B., 1975 — Permian plant microfossils from the Blair Athol Coal Measures, central Queensland, Australia. *Palaeontographica* Abt. B, 154, 121—74.

Foster, C.B., 1979 — Permian plant microfossils of the Blair Athol Coal Measures, Baralaba Coal Measures, and basal Rewan Formation of Queensland. *Geological Survey of Queensland Publication* 372, *Palaeontological Paper* 45.

Foster, C.B., 1983 — *Jugasporites* Leschik 1956, a Late Palaeozoic operculate pollen genus. *Association of Australasian Palaeontologists, Memoir* 1, 327—38.

Foster, C.B. & Waterhouse, J.B., 1988 — The *Granulatisporites confluens* Oppel-zone and the Early Permian marine faunas from the Grant Formation on the Barbwire Terrace, Canning Basin, Western Australia. *Australian Journal of Earth Sciences*, 35, 135—157.

Foster, C.B., Palmieri, V. & Fleming, P.J.G., 1985 — Plant microfossils, Foraminiferida and Ostracoda, from the Fossil Cliff Formation (Early Permian, Sakmarian), Perth Basin, Western Australia. *South Australian Department of Mines and Energy, Special Publication* 5, 61—105.

Gilby, A. R., 1983 — Early Permian palynology, stratigraphy and environments of the Stuart Range and Mount Toondina Formations, Arckaringa Basin. *B.Sc. (Hons) thesis, University of Adelaide* (unpublished).

Glenister, B.F. & Furnish, W.M., 1961 — The Permian ammonoids of Australia. *Journal of Paleontology*, 35, 673—736.

Glenister, B.F., Windle, D.L. & Furnish, W. M. 1973 — Australian Metalegoceratidae (Lower Permian ammonoids). *Journal of Paleontology*, 47, 1031—1043.

Glickson, M., 1972 — Permian palynology of the Collie Basin, Western Australia. *Ph.D. thesis, University of Western Australia* (unpublished).

Gould, R.E., 1975 — The succession of Australian pre-Tertiary megafossil floras. *Botanical Review*, 41(4), 453—483.

Gray, A.R.G., 1976 — Stratigraphic relationships of Late Palaeozoic sediments between Springsure and Jericho. *Queensland Government Mining Journal*, 77, 147—164.

Gray, A.R.G., 1977 — Stratigraphic drilling in the Hughenden 1:250,000 sheet area, 1974—75. *Queensland Government Mining Journal*, 78, 382—392.

Gray, A.R.G. & Swarbrick, C.F.S., 1975 — Nomenclature of Late Palaeozoic strata in the northeastern Galilee Basin. *Queensland Government Mining Journal*, 76, 344—352.

Grebe, H., 1971 — Microfossils organiques du Paléozoique, les spores 4. Terminologie morphographique recommandée et method description des spores. *Commission Internationale de Microflore du Paléozoïque*, 11—34.

Gunn, P. J., 1988 — Bonaparte Basin: Evolution and structural framework. *In* Purcell, P.G. & Purcell, R. R. (editors), The North West Shelf Australia. *Proceedings North West Shelf Symposium Perth, W.A. 1988*, 275—285.

Harland, W.B., Cox, A.V., Llewellyn, P.G., Pickton, C.A.G., Smith, A.G. & Walters, R., 1982 — A geologic time scale. *Cambridge University Press, Cambridge*, 1—131.

Harris, W. K. & McGowran, B., 1973 — S.A.D.M. Cootanoorina No. 1 well. *In* Allchurch, P.D., Wopfner, H., Harris, W.K. & McGowran, B. *Geological Survey of South Australia, Report of Investigations*, 40, 1—80

Hart, G.F., 1964 — A review of the classification and distribution of the Permian miospore: disaccate Striatiti. Congrès International de Stratigraphie et de Géologie du Carbonifère (5th), Paris, 1963, *Compte Rendu*, 1171—1199.

Hart, G.F., 1965 — The systematics and distribution of Permian miospores. *Witwatersrand University Press, Johannesburg*.

Hawkins, P.J., 1978 — Galilee Basin — review of petroleum prospects. *Queensland Government Mining Journal*, 79, 96—112.

Hawkins, P.J. & Harrison, P.L., 1978 — Stratigraphic and seismic investigations in the Lovelle Depression, western Galilee Basin. *Queensland Government Mining Journal*, 79, 623—650.

Helby, R.J., 1969a — The Carboniferous—Permian boundary in eastern Australia: an interpretation on the basis of palynological information. *Geological Society of Australia, Special Publication* 2, 69—72.

Helby, R.J., 1969b — Preliminary palynological study of Kuttung sediments in central eastern New South Wales. *Geological Survey of New South Wales. Record*, 11, 4—14.

Herbert, C., 1980 — Evidence for glaciation in the Sydney Basin and Tamworth Synclinorial Zone. *In* Herbert, C. & Helby, R. (editors), A guide to the Sydney Basin. *New South Wales Geological Survey, Bulletin*, 26, 274—293.

Hoffmeister, W.S., Staplin, F.L. & Malloy, R.E. 1955 — Mississipian plant spores from the Hardinsburg Formation of Illinois and Kentucky *Journal of Paleontology*, 29, 372—399.

Ibrahim, A.C., 1933 — Sporenformen des Ägirhorizons des Rhur-Reviers. *Konrad Triltsch, Würzburg*.

Ishchenko, A.M., 1956 — Spory i pyltsa nizhnekamennovyolnykh osadkov zapadnogo prodolzheniya Donbassa i ikh znachenie dyla stratigraphiï. *Akademiya Nauk Ukrainskoi SSR, Institut Geologicheskikh Nauk, Trudy, Seriya Stratigrafiï i Paleontologiï, Kiev*, 11.

Jackson, K.S., Horvath, Z. & Hawkins, P.J., 1981 — An assessment of the petroleum prospects for the Galilee Basin, Queensland. *The APEA Journal*, 21(1), 172—186.

Jansonius, J. & Hills, L.V. 1976 — Genera file of fossil spores. *Department of Geology, University of Calgary, Canada — Special publication*.

Jardiné, S., 1974 — Microflores des formations du Gabon attribuées au Karoo. *Review of Palaeobotany and Palynology*, 17, 75—112.

Jones, M. J., 1987 — Review of palynology, Arckaringa Basin (Newmont NB/SR 12, Birribiana No.1 and Hanns Knob No.1). *Palynological laboratory report, Delhi Petroleum Pty Ltd* (unpublished).

Jones, P.J., Campbell, K.S.W. & Roberts, J., 1973 — Correlation chart for the Carboniferous System of Australia. *Bureau of Mineral Resources, Australia, Bulletin* 156A.

Kar, R.K. & Bose, M.N., 1967 — Palaeozoic sporae dispersae from Congo 3 — Assise des schistes noirs de la Lukuga. *Musée Royal de l'Afrique, Tervuren Belgique, Serie IN8° ,Sciences Géologiques* , 54, 1—59.

Kemp, E.M., Balme, B.E., Helby, R.J., Kyle, R.A., Playford, G. & Price, P.L., 1977 — Carboniferous and Permian palynostratigraphy in Australia and Antarctica: a review. *BMR Journal of Australian Geology & Geophysics*, 2, 177—208.

Kosanke, R.M., 1950 — Pennsylvanian spores of Illinois and their use in correlation. *Bulletin Illinois Geological Survey*, 74, 1—128.

Kosanke, R.M., 1959 — Nomenclatural notes: *Wilsonites*, new name for *Wilsonia* Kosanke, 1950. *Journal of Paleontology*, 33(4), 700.

Kremp, G.O.W., 1965 — Morphologic encyclopedia of palynology. *University of Arizona Press, Tucson*.

Krutzsch, W., 1959 — Mikropaläontologische (sporenpaläontologische) Untersuchungen in der Braunkohle des Geiseltales. *Geologie 8, Beiheft* 21-22, 1—425.

Kyle, R.A., 1977 — Palynostratigraphy of the Victoria Group of South Victoria Land, Antarctica. *New Zealand Journal of Geology and Geophysics*, 10, 1081—1102.

Laws, R. A. & Brown, R. S., 1976 — Bonaparte Gulf Basin - south eastern part. *In* Leslie, R.B., Evans, H.J. & Knight, C.L. (editors), Economic geology of Australia and Papua New Guinea 3. Petroleum. *The Australasian Institute of Mining and Metallurgy*, 200—212.

Lee, R.J. & Gunn, P.J., 1988 — Bonaparte Basin *In* Petroleum in Australia; the first century. *Australian Petroleum Exploration Association Ltd, Special Publication*, 252—269.

Lehmann, P. R., 1986 — The geology and hydrocarbon potential of the EP 104 permit, northwest Canning Basin, Western Australia. *The APEA Journal*, 26(1), 261—284.

Lele, K.M., 1964 — Studies in the Talchir Flora of India: 2 Resolution of the spore genus *Nuskoisporites* Pot. and Kl. *Palaeobotanist*, 12(2), 147—168.

Lele, K.M., 1975 — Studies in the Talchir flora of India — 10. Early and Late Talchir microfloras from the West Bokaro Coalfield, Bihar. *Palaeobotanist*, 22, 219—235.

Lele, K.M. & Karim, R., 1971 — Studies in the Talchir flora of India — 6. Palynology of the Talchir Boulder Bed in Jayanti coalfield, Bihar. *Palaeobotanist*, 19, 52—69,.

Lele, K.M. & Makada, R., 1972 — Studies in the Talchir Flora of India — 7. Palynology of the Talchir Formation in the Jayanti Coalfield, Bihar. *Geophytology*, 2, 41—73.

Lele, K.M. & Shukla, M.M., 1980 — Studies in the Talchir flora of India — 12. Palynology of the Talchir Formation of Hutar Coalfield, Bihar. *Geophytology*, 10, 231—238.

Little, S.V., 1976 — Palynology of some core samples from the Galilee Basin, Central Queensland. *Queensland Government Mining Journal*, 77(897), 277—282.

Luber, A.A. & Waltz, I.E., 1941 — Atlas microspori i pyl'tsy paleozoya SSSR. *Vsesoyuznyi Nauchno-Issledovatelskiï Geologicheskiï Institut, Trudy, Moscow*, 139.

Maheshwari, H.K., 1967 — Studies in the *Glossopteris* flora of India 29. Miospore assemblage from the Lower Gondwana exposures along Bansloi River in Rajmahal Hills, Bihar. *Palaeobotanist*, 15(3), 258—280.

Mamet, B.L.& Belford, D.J., 1968 — Carboniferous foraminifera, Bonaparte Gulf Basin, northwestern Australia. *Micropaleontology*, 14, 339—347.

McClung, G., 1975 — Late Palaeozoic glacial faunas of Australia: distribution and age. *In* Campbell, K.S.W. (editor), Gondwana geology. *Papers presented at the Third Gondwana Symposium, Canberra. Australian National University Press*, 381—390.

McKellar, J.L., 1977 — Palynostratigraphy of core samples from the Hughenden 1:250,000 Sheet area, northern Galilee and Eromanga Basins. *Queensland Government Mining Journal*, 78(910), 393—399.

McWhae, J.R.H., Playford, P.E., Linder, A.W., Glenister, B.F. & Balme, B.E., 1958 — The stratigraphy of Western Australia. *Journal of the Geological Society of Australia*, 4(2).

Mollan, R.G., Dickins, J.M., Exon, N.F. & Kirkegaard, A.G., 1969 — Geology of the Springsure 1:250,000 Sheet area. *Bureau of Mineral Resources, Geology and Geophysics, Australia, Report* 123.

Morbey, S.J., 1975 — The palynostratigraphy of the Rhaetian Stage, Upper Triassic in the Kendelbachgraben, Austria. *Palaeontographica* Abt. B, 152, 1—75.

Morris, L.N., 1985 — Australia: The floral succesion in eastern Australia. *In* Diaz, C.M. (editor), The Carboniferous of the World II. Australia, Indian subcontinent, South Africa, South America, and North Africa *I.U.G.S.*, 20, 118—123.

Mory, A.J. 1988 — Regional geology of the Offshore Bonaparte Basin. *In* Purcell, P.G. & Purcell, R. R. (editors), The North West Shelf Australia. *Proceedings North West Shelf Symposium Perth, W.A. 1988*, 287—309.

Mory, A.J. & Beere, G.M., 1988 — Geology of the onshore Bonaparte and Ord Basins in Western Australia. *Geological Survey of Western Australia, Bulletin*, 134.

Murray, C.G., Fergusson, P.G., Whitaker, W.G. & Korsch, R.J., 1987 — Plate tectonic model for the Carboniferous evolution of the New England Fold Belt. *Australian Journal of Earth Sciences*, 34, 213—236.

Murray, C.G & Kirkegard, A.G., 1978 — The Thomson Orogen of the Tasman Orogenic Zone. *Tectonophysics*, 48, 299—325.

Naumova, S.N. 1953 — Sporo-pyltsevye kompleksy verkhnego devona Russkoi platformy i ikh znachenie dyla stratigrafiï. *Akademiya Nauk SSSR, Institut Geologicheskikh Nauk, Trudy 143, Seryia Geologicheskaya*, 60.

Neves, R., 1961 — Namurian plant spores from the Southern Pennines, England. *Palaeontology*, 4, 247—279.

Neves, R. & Owens, B., 1966 — Some Namurian camerate miospores from the English Pennines. *Pollen et Spores*, 8, 337—360.

Norvick, M. 1974 — Permian and Late Carboniferous palynostratigraphy of the Galilee Basin, Queensland. *Bureau of Mineral Resources, Australia, Record* 1974/141.

Norvick, M., 1981 — Permian and Late Carboniferous palynostratigraphy of the Galilee Basin, Queensland. *Bureau of Mineral Resources, Australia, Report* 219, (BMR Microform MF114).

O'Brien, P. E., 1986 — Stratigraphy and sedimentation of the Late Palaeozoic glaciomarine sediments beneath the Murray Basin, and their palaeogeographic and palaeoclimatic significance. *BMR Journal of Australian Geology & Geophysics*, 10, 53—63.

Olgers, F., 1972 — Geology of the Drummond Basin, Queensland. *Bureau of Mineral Resources, Geology and Geophysics, Australia, Bulletin* 132.

Pant, D.D. & Srivastava, G.K., 1965 — Some Lower Gondwana miospores from Brazil. *Micropaleontology*, 11(4), 468—478.

Pemberton, R.L., 1965 — Lake Galilee No. 1, Well Completion Report. *Exoil No Liability, report*. (unpublished).

Peppers, R.A., 1979 — Comparison of miospore assemblages in the Pennsylvanian System of the Illinois Basin with those in the Upper Carboniferous of Western Europe. Neuvième Congrès International de Stratigraphie et de Géologie du Carbonifère. Washington and Champaign-Urbana May 17—26,1979. *Compte Rendu*, 2, 483—502.

Piérart, P., 1974 — Étude morphologique et biométrique de deux espèces de spore du Gondwana (*Punctatisporites gretensis* and

Krauselisporites brazilensis). *In* Palynology of proterophyte and palaeophyte. *Proceedings of the Third International Palynological Conference, Moscow*, 181—191.

Playford, G., 1962 — Lower Carboniferous microfloras of Spitsbergen Part.1. *Palaeontology*, 5(3), 550—618.

Playford, G., 1964 — Miospores from the Mississippian Horton Group, Eastern Canada. *Geological Survey of Canada, Bulletin*, 107.

Playford, G., 1971 — Lower Carboniferous spores from the Bonaparte Gulf Basin, Western Australia and Northern Territory. *Bureau of Mineral Resources, Australia, Bulletin* 115.

Playford, G., 1976 — Plant microfossils from the Upper Devonian and Lower Carboniferous of the Canning Basin, Western Australia. *Palaeontographica* Abt. B, 158, 1—71.

Playford, G., 1977 — A lower Carboniferous palynoflora from the Drummond Basin, east-central Queensland. *Proceedings of the Royal Society of Queensland*, 88, 75—81.

Playford, G., 1978 — Lower Carboniferous spores from the Ducabrook Formation, Drummond Basin, Queensland. *Palaeontographica* Abt. B, 167B, 105—160.

Playford, G., 1983 — Two new genera of trilete *Sporae Dispersae* from the Lower Carboniferous of Queensland. *Pollen et Spores*, 25(2), 265—278.

Playford, G., 1985 — Australia: Spores and Pollen. *In* Diaz, C.M. (editor), The Carboniferous of the World. II Australia, Indian subcontinent, South Africa, South America, and North Africa. *I.U.G.S.*, 20, 123—126.

Playford, G., 1986 — Morphological and preservational variation of *Rattiganispora* Playford and Helby 1968, from the Australian Carboniferous. *Pollen et Spores*, 28(1), 83—96.

Playford, G. & Helby, R.J., 1968 — Spores from a Carboniferous section in the Hunter Valley, New South Wales. *Journal of the Geological Society of Australia*. 15, 103—119.

Playford, G. & Powis, G.D., 1979 — Taxonomy and distribution of some trilete spores in Carboniferous strata of the Canning Basin, W.A. *Pollen et Spores*, 21, 371—394.

Playford, G. & Satterthwait, D.F., 1988 — Lower Carboniferous (Visean) spores of the Bonaparte Gulf Basin, Northwestern Australia: part three. *Palaeontographica* Abt. B, 208, 1—26.

Playford, P.E., Cope, R.N., Cockbain, A.E., Low, G.H. & Lowry, D.C., 1975 — Phanerozoic: Perth Basin. *In* The geology of Western Australia. *Geological Survey of Western Australia, Memoir*, 2, 227—259.

Pons, M.E., 1976 — Estudo palinológico do Sub-Grupo Itararé na "Coluna White", Permiano inferior, Santa Catarina, Brasil. Parte I. *Ameghiniana*, 13(2), 109—125.

Potonié, R., 1958 — Synopsis der Gattungen der Sporae dispersae. II Teil: Sporites (Nachtrage) Saccites, Aletes, Praecolpates, Polyplicates, Monocolpates. *Beiheft zum Geologische Jahrbuch*, 31, 1—114.

Potonié, R. & Lele, K.M., 1961 — Studies in the Talchir flora of India-1. Sporae dispersae from the Talchir Beds of South Rewan Gondwana Basin. *Palaeobotanist*, 8, 22-37.

Potonié, R. & Sah, S.C.D., 1960 — Sporae dispersae of the lignites from Cannanore Beach, on the Malabar Coast of India. *Palaeobotanist* , 7, 121—135.

Powis, G.D., 1979 — Palynology of the Late Palaeozoic glacial sequence, Canning Basin, W.A. *Ph.D. thesis, University of Western Australia* (unpublished).

Powis, G.D., 1983 — The palynostratigraphy of the Permo-Carboniferous of the Galilee Basin, Queensland. *In* Permian geology of Queensland. *Geological Society of Australia, Queensland Division*, 213.

Powis, G.D., 1984 — Palynostratigraphy of the Late Carboniferous Sequence, Canning Basin, W.A. *In* Purcell, P.G. (editor), The Canning Basin W.A. *Proceedings G.S.A./P.E.S.A. Canning Basin Symposium Perth, 1984*, 429—438.

Price, P.L., 1976 — Permian palynology of the Bowen Basin. *In* Jensen, A.R., Exon, N.F., Anderson, J.C.& Koppe, W.H., A guide to the geology of the Bowen and Surat Basins in Queensland. *Excursion Guide 3C, 25th International Geological Congress*, .

Price, P.L., 1983 — A Permian palynostratigraphy for Queensland. *In* Permian geology of Queensland. *Geological Society of Australia, Queensland Division*, 155—212.

Price, P.L., Filatoff, J., Williams, A.J., Pickering, S.A. & Wood, G.R., 1985 — Late Palaeozoic and Mesozoic palynostratigraphical units. *CSR Oil and Gas Division, Palynological Facility, Report, 274/25* (unpublished).

Rakotoarivelo, H.J., 1970 — Palynostratigraphie comparée du bassin houiller Gondwanien de la Sakoa-Sakamena, Madagascar. *D.Sc. thesis, University of Paris* (unpublished).

Rattigan, J. H., 1967 — Cyclic sedimentation in the Carboniferous continental Kuttung facies, New South Wales, Australia. *Journal of the Proceedings of the Royal Society of New South Wales*, 100, 119—128.

Ravn, R.L., 1979 — An introduction to the stratigraphic palynology of the Cherokee Group (Pennsylvanian) coals of Iowa. *Iowa Geological Survey, Technical Paper* 6.

Ravn, R.L., 1986 — Palynostratigraphy of the lower and middle Pennsylvanian coals of Iowa. *Iowa Geological Survey, Technical Paper*, 7.

Retallack, G., 1980 — Late Carboniferous to Middle Triassic megafossil floras from the Sydney Basin. *In* Herbert, C. & Helby, R. (editors), A guide to the Sydney Basin. *New South Wales Geological Survey, Bulletin*, 26, 384—430.

Richardson, J.B., 1969 — Devonian spores. *In* Tschudy, R.H. & Scott, R.A. (editors), Aspects of palynology. *Wiley - Interscience*, 193—222.

Rigby, J.F. & Hekel, H., 1977 — Palynology of the Permian sequence in the Springsure Anticline, central Queensland. *Geological Survey of Queensland, Publication* 363.

Roberts, J., 1971 — Devonian and Carboniferous brachiopods from the Bonaparte Gulf Basin, northwestern Australia. *Bureau of Mineral Resources, Australia, Bulletin* 122.

Roberts, J., 1985 — Australia, Introduction, Tasman Mobile Belt: Hunter Region. *In* Diaz, C.M. (editor), The Carboniferous of the World. II Australia, Indian subcontinent, South Africa, South America, and North Africa *I.U.G.S.*, 20, 9—15 and 23—33.

Roberts, J. & Engel, B.A., 1980 — Carboniferous palaeogeography of the Yarrol and New England Orogens, Eastern Australia. *Journal of the Geological Society of Australia*, 27, 167—186.

Roberts, J., Claoue-Long, J. & Jones, P.J., 1991 — SHRIMP zircon dating and Australian Carboniferous time. *12ème Congrès International de Stratigraphie et de Géologie du Carbonifère, Compte Rendu, Buenos Aires 1991*.

Roberts, J., Hunt, J.W. & Thompson, D.M., 1976 — Late Carboniferous marine invertebrate zones of eastern Australia. *Alcheringa*, 1, 197—225.

Runnegar, B. & McClung, G., 1975 — A Permian time scale for Gondwanaland. *In* Campbell, K.S.W. (editor), Gondwana geology. *Papers presented at the Third Gondwana Symposium, Canberra. Australian National University Press, Canberra*, 425—441.

Scheuring, B.W., 1974 — *Kraeuselisporites* Leschik and *Thomsonisporites* Leschik — a revision of the type material of two disputed genera. *Review of Palaeobotany and Palynology*, 17, 187—203.

Schopf, J.M., Wilson, L.R. & Bentall, R., 1944 — An annotated synopsis of Paleozoic fossil spores and the definition of generic groups. *Illinois Geological Survey, Report of investigations*, 91, 1—66.

Segroves, K.L., 1967 — Cutinised microfossils of probable non-vascular origin from the Permian of Western Australia. *Micropaleontology*, 13, 289—305.

Segroves, K.L., 1970 — Permian spores and pollen grains from the Perth Basin, Western Australia. *Grana*, 10(1), 43—73.

Singh, H.P., 1964 — A miospore assemblage from the Permian of Iraq. *Palaeontology*, 7(2), 240—265.

Sinha, V., 1972 — Sporae dispersae from Jhingaralah Seam, Singrauli Coalfield (M.P.) India. *Palaeobotanist*, 19(2), 175—201.

Smith, A.H.V. & Butterworth, M.A., 1967 — Miospores in the coal seams of the Carboniferous of Great Britain. *Special papers in palaeontology, Palaeontological Association, London* 1.

Srivastava, S.C., 1970 — Microfossil investigations in some coals of Talchir coalfields (Orissa) India. *Palaeobotanist*, 18(2), 154—166.

Staplin, F.L. & Jansonius J., 1964 — Elucidation of some Palaeozoic Densospores. *Palaeontographica* Abt. B, 114, 95—117.

Streel, M., 1964 — Une association de spores du Givetian inférieur de la Vesdre, a Goe. *Annales de la Société geologique de Belgique*, 87, B1-B30.

Sullivan, H.J., 1964 — Miospores from the Lower Limestone Shales (Tournaisian) of the forest of Dean Basin, Gloucestershire. *Congrès International de Stratigraphie et de Géologie du Carbonifère (5th), Paris, 1963, Compte Rendu*, 3, 1249—1259.

Sullivan, H.J. & Mishell, D. R., 1971 — The Mississipian—Pennsylvanian boundary and its correlation with Europe. Congrès International de Stratigraphie et de Géologie du Carbonifère (6th), Sheffield, 1967, *Compte Rendu*, 5, 1533—1540.

Swarbrick, C.F.J. & Wallin, C.I., 1976 — Well completion report — QDM Aramac 1 and Hexham 1. *Geological Survey of Queensland, Report*, 92, 62 pp.

Tappan, H., 1980 — The paleobiology of plant protists. *W.H. Freeman and Company, San Francisco.*

Thornton, R.C.N., 1979 — Regional stratigraphic analysis of the Gidgealpa Group, Southern Cooper Basin, Australia. *Geological Survey of South Australia, Bulletin*, 49.

Tiwari, R.S., 1964 — New miospore genera in the coals of Barakar stage, (Lower Gondwana) of India. *Palaeobotanist*, 12, 250—259.

Tiwari, R.S., 1965 — Miospore assemblage in some coals of Barakar Stage (Lower Gondwana) of India. *Palaeobotanist*, 13(2), 168—214.

Tiwari, R.S., 1975 — Palynological composition of the basal Gondwana in India. *Bulletin de la Société Belge de Geologie*, 84, 11—17.

Townsend, I.J. & Ludbrook, N.H., 1975 — Revision of Permian and Devonian nomenclature of four formations in and below the Arckaringa Basin. *Geological Survey of South Australia, Quarterly Geological Notes*, 53, 1—7.

Truswell, E.M., 1978 — Palynology of the Permo-Carboniferous in Tasmania: an interim report. *Bulletin of the Geological Survey of Tasmania*, 56, 1—39.

Truswell, E.M., 1980 — Permo-Carboniferous palynology of Gondwanaland: progress and problems in the decade to 1980. *BMR Journal of Australian Geology & Geophysics*, 5, 95—111.

Turnau, E., 1978 — Spore zonation of the uppermost Devonian and Lower Carboniferous deposits of western Pomerania. *Mededelingen Rijks Geologiische Dienst*, 30-1, 1—35.

Varyukhina, L.M., 1971 — Spory i pyl'tsa krasnotsvetnykh i uglenosnykh otlozheniy permi i triasa severo — vostoka evropeyskoy chasti S.S.S.R. *Akademiya Nauk S.S.S.R., Komissiya po Filial, Institut Geologii, Leningrad.*

Veevers, J.J. & Powell, C.McA., 1987 — Late Palaeozoic glacial episodes in Gondwanaland reflected in transgressive—regressive depositional sequences in Euramerica. *Geological Society of America, Bulletin* 98, 475—487.

Venkatachala, B.S. & Kar, R.K., 1968 — Palynology of the Karanpura sedimentary Basin, Bihar, India — 1. Barakar Stage at Badam. *Palaeobotanist*, 16(1), 56—90.

Vine, R.R., 1976 — Galilee Basin. *In* Leslie, R.B., Evans, H.J. & Knight, C.L. (editors), Economic geology of Australia and Papua New Guinea. *Australian Institute of Mining and Metallurgy, Melbourne*, 316—322.

Vine, R.R., Casey, D.J. & Johnson, N.E.A., 1964 — Progress report, 1963, on the geology of part of the northeastern Eromanga Basin. *Bureau of Mineral Resources, Australia, Explanatory Notes SF/ Hughenden 55/9.*

White, M.E., 1964 — 1963 plant fossil collections from the Hugheden area, Great Artesian Basin. *Bureau of Mineral Resources, Geology and Geophysics, Australia, Record* 1964/64.

White, M.E., 1969 — Appendix 3: Plant Fossils from the Springsure Sheet area. *In* Mollan, R.G., Dickens, J.M. & Exon, N.F., Geology of the Springsure 1:250,000 Sheet area, Queensland. *Bureau of Mineral Resources, Australia, Report* 123, 97—107.

Wopfner, H., 1981 — Development of Permian infracratonic basins in Australia. *In* Cresswell, M.M. & Vella, P. (editors), Gondwana Five. *Balkema, Rotterdam*, 185–190.

BMR Journal of Australian Geology & Geophysics, 13, 187–188

NOTE: More on earthquake fatalities in Australia

K. F. McCue[1] & A. McArdle[2]

An average of about 10 000 deaths a year have been recorded this century as a result of earthquakes worldwide. Most of these resulted from the collapse of human-made structures. Secondary effects of earthquakes (landslides and tsunamis) have made a lesser but significant contribution to the total.

McCue & others (1990) asserted that no earthquake-related deaths had occurred in Australia before the Newcastle earthquake, but Doyle (1991) recalled the mention (Everingham, 1968) of an earlier event which resulted in the death of a miner. Everingham noted that in the event at Kalgoorlie of 28 August 1917 (given incorrectly by Curlewis as 29 August 1917 in the *West Australian* of 25 January 1940):

> An earth movement occurred towards midnight resulting in a fall of rock in the Great Boulder (mine). One man (Jack Flanagan) was killed and several injured. The fall of rock occurred at the 2250 ft level where ten men were working in a stope when a peculiar rumbling noise was heard. There were slight earth tremors followed by a loud report and a large mass of rock fell from the roof of the stope. The stope immediately below was also affected and altogether it is estimated that about 1000 tons of rock fell and heavy timber was smashed like matchwood.

Curlewis stated that the Kalgoorlie 'tremor' was felt as far as Albany but, according to Everingham, an earthquake felt near Albany by the Breaksea lighthouse keeper was two months earlier, on 10 June 1917, and at a different time of day, between 6 and 7.30 pm. The 'tremor' at Kalgoorlie was felt only locally and caused damage in the mine, and was therefore almost certainly a rockburst rather than a tectonic earthquake.

Recent evidence has come to light that shows that, even if the Great Boulder mine casualty was attributed to an earthquake (which we dispute), the unfortunate miner was not the *first* Australian earthquake casualty. The evidence concerns interpretation of cause of death following an earthquake.

The State Coroner of New South Wales, enquiring into the deaths at Newcastle, concluded that a thirteenth victim lost his life as a result of the earthquake when he suffered a fatal heart attack. The coroner's finding has a bearing on an earlier earthquake we have investigated as part of an ongoing study into the historical seismicity of Australia. The Warooka earthquake, named after the Yorke Peninsula town which suffered most damage on the night of Friday 19 September 1902, is the second largest earthquake in South Australia since European habitation (McCue, 1975; Everingham & others, 1982). The Adelaide newspaper The Advertiser of 23 September 1902 reported from Warooka that

> At a few minutes past 8 o'clock the inhabitants were startled by a strange rumbling noise, and immediately afterwards experienced a most violent shock, closely succeeded by another one of equal violence. Women and children rushed screaming into the street, cows bellowed, horses stampeded as if mad . . . The buildings shook violently, pictures and ornaments being hurled to the floor, and it seemed as though the whole township would be destroyed . . . It is indeed a wonder that no lives were lost. Had the shock come a few hours later, when all were in bed, several fatalities would undoubtedly have had to be recorded. As it was a number of miraculous escapes were experienced.

The paper also carried two stories from Adelaide:

> **A death after the shock**
> The earthquake which caused such general alarm on Friday evening had a most serious effect upon many people. Men and women susceptible to nervous attacks suffered, and are still suffering, greatly as a result of the earth tremors. A death, which was accelerated by Saturday[3] evening's shock, occurred during the evening. Mrs Walker, who resided at Eastwood, and who for some time past had been under the care of Dr. Sweetapple for heart troubles, received such a shock, when the house began to rattle that she expired almost immediately. Several women are reported to be in a semi-unconscious state, the slightest noise having a most distressing effect upon their nerves. Other people are suffering to a greater or lesser extent, and it will be some time before many recover from the excited state into which they have been thrown.
>
> **Another death**
> On Monday morning Mr. S. J. Heinrich, of High-street Kensington, reported to the Marryatville police that Mr. Charles Masters, a retired farmer aged 70 years, who resided with him, had died suddenly that morning. For his age he was a strong, healthy man, but the earthquake shock which occurred on Friday night seriously upset him for the time being. He appeared to recover from the shock, but on Sunday evening complained of being unwell and retired to bed. When visited at 6 a.m. on Monday he seemed in good health, but an hour later he was heard to be groaning and he died before medical aid arrived.

We may therefore conclude that the 1902 earthquake claimed two lives and that Mrs Walker and Mr Masters are the earliest known casualties of Australian earthquakes. Whether Aborigines suffered a similar fate will probably never be known, but the risk from rockfalls was not negligible, as the following extract from the Maitland Mercury of 30 June 1868 shows:

> **The late earthquake** — The effects of the recent convulsion have been hitherto noticed only in connection with the damage done to buildings, but we are told that in Cabbage-tree Gully (a depression among the range of mountains bordering the Paterson) the earth-wave has left marks of its progress of an entirely different character: there huge rocks have been split and rent, and stones which for years have been embedded in the soil are upheaved and overturned.

Doyle's (1991) brief discussion on rockbursts is interesting, but rockbursts cannot be considered the same as natural earthquakes in the context of fatalities and risk. Mining is a dangerous occupation and the risks engendered by mining are presumably accepted by miners and their employers. Earthquakes do not have the same causal link with human activity. Their risk could be avoided to some extent if people in areas most at risk moved away from plate boundaries (San Francisco to Denver or Wellington to Auckland). In Australia the difference in assessed hazard varies only marginally throughout the country and an earthquake could occur anywhere. We can do nothing

[1] Australian Seismological Centre, Bureau of Mineral Resources, Geology & Geophysics, GPO Box 378, Canberra ACT 2601
[2] Sutton Institute of Earthquake Physics, South Australian Department of Mines & Energy, PO Box 151, Eastwood SA 5063
[3] As given earlier in the report, this presumably should be Friday.

about earthquake hazard, but we can reduce the subsequent risk of injury or loss of life according to how much we are prepared to pay for better earthquake resistance in our structures and better building codes.

Acknowledgements

Peter Gregson provided extracts on the fatal accident in the Great Boulder Mine from early Western Australian newspapers. Cynthia Hunter found and drew to our attention the extract from the *Maitland Mercury* of 30 June 1868.

References

Doyle, H.A., 1991 — Earthquake fatalities in Australia. *BMR Journal of Australian Geology & Geophysics*, 12(3), 263.

Everingham, I.B., 1968 — Seismicity of Western Australia. *Bureau of Mineral Resources, Australia, Report* 132.

Everingham, I.B., McEwin, A.J. & Denham, D., 1982 —Atlas of isoseismal maps of Australian earthquakes. *Bureau of Mineral Resources, Australia, Bulletin* 214.

McCue, K.F., 1975 — Seismicity and seismic risk in South Australia. *University of Adelaide*, Report ADP 137.

McCue, K., Wesson, V., & Gibson, G., 1990 — The Newcastle, New South Wales, earthquake of 28 December 1989. *BMR Journal of Australian Geology & Geophysics*, 10, 253—259.

BOOK REVIEWS

Selected papers on hydrogeology

Edited by Eugene S. Simpson & John M. Sharp
Hydrogeology, Selected Papers, Vol. 1; *International Association of Hydrogeologists,* xvi + 506 pp, 1990
Price US $59

This volume contains 37 papers selected from more than 200 presented on hydrogeology at the 28th International Geological Congress in Washington DC, U.S.A. in July 1989. It is the first in a new series issued occasionally by the International Association of Hydrogeologists under this general title. The papers are grouped in seven sections. They cover 17 different countries and diverse hydrogeological environments.

An avant-propos paper discusses deficiencies in the practice and teaching of hydrogeology and environmental and engineering geology. It points to an underemphasis on basic field skills and overemphasis on mathematical modelling and laboratory experiment. It is only two years since similar arguments led to a move back to systematic regional geological mapping in Australia.

Ten papers on carbonate systems follow. The first summarises the rapid transport and poor attenuation of chemical contaminants in groundwater in karst. By contrast another paper highlights the importance of karst in promoting high recharge for water supply in Saudi Arabia. Three papers provide contrasting views on geochemical reactions within the Cretaceous Edwards aquifer in Texas, U.S.A.

A third section contains six papers on geochemistry and isotope hydrology. One documents ultrabasic (pH 11.7) groundwater of an ultramafic massif in Yugoslavia.

Of five papers on wetlands, the first describes the use of a wetland in St Joseph, Minnesota as a cost-effective alternative to tertiary treatment of storm water and sewage for a growing number of small rural communities. A major drawback, however, is a reduction in vegetation diversity from trees and grasses to a reed monoculture.

There are four papers on fractured rock. Two by the same author are on a laboratory study of a single fracture. They show that transmissivity decreases as rock stress increases and flow becomes more channelled in the fracture.

Of five papers on water management, three are on wellhead and well protection zones, highlighting the change in emphasis today from proving new water supplies to protecting what we have.

Six papers on miscellaneous topics range from overflow thermal springs in Italy to storage in the saprolite above fractured basement in central Africa. Together with the other papers in this volume, they demonstrate hydrogeology's growing integration with other disciplines.

This series is a real step forward for the International Association of Hydrogeologists, bringing conference publications to the same standard as those of the existing series *International Contributions to Hydrogeology* and the new journal *Applied Hydrogeology*. The idea of publishing only selected papers for wider distribution is a good one. Clear print, white paper and standard size really do increase their readability. A quibble with this first volume is that figures are not distributed through the text and there are too many landscaped figures and tables.

Libbie Lau

Groundwater recharge — a guide to understanding and estimating natural recharge

David Lerner, Arie Issar & Ian Simmers
International Contributions to Hydrogeology Vol. 8; *International Association of Hydrogeologists, Hannover:Heise,* 345 pp., 1990
Price US $45

This book defines its intentions early in the Preface, and adheres to its objectives rigorously throughout. To paraphrase,

This book is a manual of practice on the estimation of natural groundwater recharge, and is an output of a much broader UNESCO International Hydrogeology Program. The book focuses on the semi-arid and arid regions of the world where techniques of this type are most needed. It is not intended as a 'cookbook', but offers guidance to the practitioner engaged in arid and semi-arid water resources exploration and development. The volume is in four parts:

- overview of study framework and theoretical discussion of concepts relevant to the text and the problem of translation of point measurements to regional recharge estimates;
- development of a series of typical hydrogeological conceptual models;
- detailed analysis of estimation techniques;
- illustration of a variety of techniques through case studies.'

I found the book to be a very honest account of a specialised subject: the book 'does not, therefore, relieve the reader of the need for independent thought on a specific problem, but should be considered as a source of information to facilitate a logical and structured approach to the steps involved'. Throughout the text references are given for supplementary reading. This means a minimum level of understanding of a variety of disciplines is required to make sense of the text.

The impetus for the manual is the knowledge that about half the countries of the world are affected by problems of aridity, and about 30% of the globe is subject to arid and semi-arid climates. All the easily developed land has been developed, and population pressures are forcing land managers to turn their attention to the more arid areas for human survival. At the same time, pressure for the sustainable development of natural resources is increasing. With the limited soil and water resources of arid and semi-arid regions, and surface water supplies usually unreliable, groundwater use is of fundamental importance. Development of groundwater resources in these regions creates a host of problems, since abundantly available groundwater may have only a small recharge, and can be treated as a non-renewable resource. This resource requires careful management. A key to careful management is the quantification of the current rate of natural groundwater recharge in any particular area. Unfortunately, this rate is one of the most difficult parameters to derive in hydrogeological studies.

Though a very useful and timely addition to the literature on groundwater resource management, the book has one major shortcoming: it tries to characterise a multitude of hydrogeological occurrences and conditions in its 345 pages. I believe this to be an impossible task. For instance, in its characterisations of key hydrogeological provinces for the world it fails to mention fractured rock terrains. In Australia, 60% of the continent is underlain by such terrain and groundwater supplies won from these aquifers are critical to population settlement. Whilst it may not be necessary to produce a water resource plan for each remote station water bore, in some parts of the country considerable effort is being spent on recharge characterisation for regional fractured rock aquifers.

I found the text easy to read, though the style of printing and selection of fonts did not suit my eyes. Some of the figure reproduction was not of a high standard, detail being lost in the reduction process. The layout of the book was excellent, with an introduction to each of the four major sections providing a useful overview. The book is rounded by the inclusion of a comprehensive bibliography, indicating that the authors have fully researched their particular topics.

A good and useful book for the practitioner, but definitely not for the general reader unless accompanied by a thorough reference library.

W.R. Evans

BMR
GEOLOGY AND
GEOPHYSICS
AUSTRALIA

CONTENTS

9 780644 249065

B92/21084 Cat. No. 92 1732 5